

**PROTON EXCHANGE MEMBRANE FUEL CELL  
SYSTEMS BASED ON AROMATIC HYDROCARBON and  
PARTIALLY FLUORINATED DISULFONATED  
POLY(ARYLENE ETHER) COPOLYMERS**

*by*

Mehmet SANKIR

Dissertation Submitted to the Faculty of the  
Virginia Polytechnic Institute and State University  
in partial fulfillment of the requirements for the degree of  
Doctor of Philosophy  
in  
Macromolecular Science and Engineering

APPROVED:

Dr. James E. McGrath, Chairman

Dr. Judy S. Riffle

Dr. Garth L. Wilkes

Dr. Sean G. Corcoran

Dr. John J. Lesko

December 6, 2005

Blacksburg, Virginia

Keywords: Fuel Cell, Proton Exchange Membrane, Sulfonation,  
Fluorination, Poly(arylene ether sulfone), poly(arylene ether benzonitrile)

Copyright 2005, Mehmet SANKIR

# **PROTON EXCHANGE MEMBRANE FUEL CELL SYSTEMS BASED ON AROMATIC HYDROCARBON and PARTIALLY FLUORINATED DISULFONATED POLY(ARYLENE ETHER) COPOLYMERS**

by

Mehmet SANKIR

## **ABSTRACT**

This dissertation describes the past and recent progress in proton exchange membranes (PEM) for fuel cells. In particular the synthesis and characterization of materials for advanced alternative PEM were studied with an emphasis on structure-property and structure-property-performance relationships. The focus has included firstly a one-step synthesis and characterization of 3,3'-disulfonated 4,4'-dichlorodiphenyl sulfone comonomer. The procedure developed is adaptable for industrial-scale commercialization efforts. Secondly, the synthesis of aromatic nitrile containing poly(arylene ether sulfone) random copolymers was demonstrated. Various levels of disulfonation allowed the membrane characteristics to be investigated as a function of the membrane ion exchange capacity. The results favorably compare with the current state-of-the-art (Nafion™), particularly for direct methanol systems (DMFC). Thirdly, the mechanically and thermooxidatively stable copolymer membranes were blended with heteropolyacids producing nanocomposites which have potential in higher temperature fuel cell applications. Lastly, the basic PEM parameters such as water uptake, proton conductivity, and methanol permeabilities were controlled and presented as tunable

properties as a function of molecular structure. This was achieved by in-situ control of chemical composition. The direct methanol fuel cell performance (DMFC) was much better than Nafion™. Hydrophobic surface properties of the membranes were improved by partial fluorination which made the Nafion™ bonded electrodes more compatible with the partially fluorinated copolymer membranes. The influence of surface enrichment had two important roles in increasing both initial and long term performance tests. The surface fluorine provided lower contact resistance and lower water uptake. The former was important for the initial tests and the latter provides for better long term performances. A delamination failure mechanism was proposed for the hydrocarbon membrane electrode assemblies (MEA) due to the large difference between water uptake of the catalyst layer and membrane and this was verified by a reduction in high frequency resistance (HFR) for the partially fluorinated systems. This thesis has generated the structure-property and structure-property-performance relationships which will provide direction for the development of next generation (PEM) materials.

## ACKNOWLEDGEMENTS

I would like to express my sincere gratitude and appreciation to my primary advisor, Professor Jim McGrath for providing me with the unique opportunity to work in his group and also his support, guidance and encouragement over the past years. I must thank Professor McGrath also for enhancing my knowledge in polymer science.

I am also grateful to members of my advisory committee, Dr. Judy Riffle, Dr. Garth Wilkes, Dr. Sean Corcoran, and Dr. Jack Lesko for their time, guidance and suggestions and their contributions to my education in polymer science and engineering.

I would like to thank Dr. Bhanu , Dr. Ghassemi and Dr. Harrison for their suggestions and valuable discussions.

I especially thank Dr. Yu Seung Kim and Dr. Brian Pivovar from Los Alamos National Lab. for their great assistance, suggestions and discussions during my research.

I would like to thank Mr. Tom Glass (NMR), Mr. Frank Kromer (XPS) and Mr. Steve McCartney (Microscopy) for their time and valuable assistance.

I would like to thank ladies in the Material Research Institute, Laurie Good and Millie Ryan for their friendship and help with various tasks.

I would like to express my thankful to all my family my mom, Saadet, my sister, Derya and my brothers Tufan and Hasan for their love and prayers. I would like to dedicate this job to my dad, Late Mumin Sankir.

I can not thank my wife, Nurdan enough for her love and patience throughout all these years.

## TABLE OF CONTENTS

Abstract.....	ii
Acknowledgements.....	iv
Table of Contents.....	v
List of Figures.....	x
List of Tables.....	xviii
CHAPTER 1.....	1
CHAPTER 2.....	3
Literature Review.....	3
2.1 The First Fuel Cell; The Gaseous Voltaic Battery.....	3
2.2 Fuel Cells.....	4
2.3 Types of Fuel Cells.....	7
2.3.1 Alkaline Fuel Cells (AFC).....	7
2.3.2 Phosphoric Acid Fuel Cells (PAFC).....	9
2.3.3 Molten Carbonate Fuel Cells (MCFC).....	10
2.3.4 Solid Oxide Fuel Cells (SOFC).....	11
2.3.5 Proton Exchange Membrane Fuel Cell (PEMFC).....	12
2.3.5.1 Electrodes for PEMFC and MEA Fabrication.....	14
2.3.5.2 MEA fabrication Method, The Los Alamos National Lab Approach.....	21
2.3.5.3 The Proton Exchange Membrane Fuel Cell Hardware.....	23
2.3.5.4 PEMFC Stacks.....	26
2.4 Proton Exchange Membranes (PEM).....	28
2.4.1 Perfluorinated Copolymers.....	29
2.4.2 Styrene Based Proton Exchange Membranes (PEM).....	33
2.4.3 Poly (arylene ether)s.....	40
2.4.3.1 Post Sulfonation.....	41
2.4.3.2 Direct Copolymerization of Sulfonated Monomers.....	47
2.4.3.3 Direct Copolymerization of Sulfonated Polyimides.....	53
2.4.3.4 Direct Copolymerization of Sulfonated Poly(arylene ether ketone)s.....	57

2.4.3.5 Direct Copolymerization of Sulfonated Poly(arylene ether phenyl phosphine oxide)s .....	59
2.4.3.6 Direct Copolymerization of Sulfonated Poly(arylene sulfide sulfones)s .....	61
2.4.3.7 Direct Copolymerization of Sulfonated Poly(arylene ether benzonitrile)s.....	63
2.5 Membrane Preparation and Basic Membrane Characteristics of Directly Synthesized Disulfonated Poly(arylene ether sulfone) (BPS) Copolymers .....	65
2.6 Solid State Inorganic Proton Conductors and Composites .....	80
2.7 Basic Consideration of Real Cell Potential and Fuel Cell Performance.....	85
2.8 Major Synthetic Methods to Synthesize Poly(arylene ether sulfones) .....	89
2.8.1 The Ullman Reaction .....	89
2.8.2 Metal Coupling Reactions.....	91
2.8.3 Electrophilic Aromatic Substitution .....	92
2.8.4 Nucleophilic Aromatic Substitution Reaction ( $S_NAr$ ) .....	94
2.8.4.1 Strong Base Approach .....	99
2.8.4.2 Weak Base Approach.....	100
2.9 Structures, Morphological Models and Applications of Ionomers.....	104
CHAPTER 3 .....	118
Synthesis and Characterization of 3,3'- disulfonated 4,4'- dichlorodiphenyl sulfone (SDCDPS) Monomer for Proton Exchange Membranes (PEM) in Fuel Cell Applications .....	118
3.1 Abstract.....	119
3.2 Introduction.....	120
3.3 Experimental.....	123
3.3.1 Reagents.....	123
3.3.2 Disulfonation of DCDPS .....	124
3.3.3 Characterization Methods.....	124
3.3.3.1 Monomer Characterization .....	124
3.3.3.2 Model Copolymerization .....	125
3.4 Results and Discussion .....	126
3.5 Conclusions.....	138
3.6 Acknowledgements.....	138

CHAPTER 4 .....	139
Synthesis of Disulfonated Poly (arylene ether benzonitrile) Statistical Copolymers (PAEB) for Proton Exchange Membrane Fuel Cells (PEMFC) .....	139
4.1 Abstract .....	140
4.2 Introduction .....	141
4.2.1 Hydrocarbon versus Perfluorinated Ionomers .....	146
4.3 Experimental .....	150
4.3.1 Reagents .....	150
4.3.2 Synthesis of 3,3'-disulfonated-4,4'-dichlorodiphenyl sulfone .....	150
4.3.3 Synthesis of Disulfonated Poly (arylene ether benzonitrile) Copolymers .....	153
4.3.4 Film Casting and Membrane Acidification .....	154
4.3.5 Characterization .....	156
4.4 Results and Discussions .....	160
4.5 Conclusions .....	185
4.6 Acknowledgements .....	185
CHAPTER 5 .....	186
Proton Exchange Membrane for DMFC and H <sub>2</sub> /Air Fuel Cells: Synthesis and Characterization of Partially Fluorinated Disulfonated Poly(arylene ether benzonitrile) Copolymers .....	186
5.1 Abstract .....	187
5.2 Introduction .....	188
5.2.1 Basic Membrane Characteristics and Influence of Ion Exchange Capacity .....	190
5.2.2 Fuel Cell Performance Characteristics .....	196
5.2.3 Electrochemical Properties of the Membranes .....	199
5.2.3.1 Electro-osmotic Drag Coefficient .....	199
5.2.3.2 Methanol Crossover and Limiting Current .....	202
5.3 Experimental .....	205
5.3.1 Reagents .....	205
5.3.2 Synthesis of Partially Fluorinated Disulfonated Poly (arylene ether benzonitrile) .....	205
5.3.3 Film Casting and Membrane Acidification .....	206

5.3.4 Characterization .....	207
5.3.4.1 Membrane characterization.....	208
5.3.4.1.1 Methanol Crossover.....	208
5.3.4.1.2 Cell Resistance and DMFC Performance.....	209
5.3.4.1.3 High Frequency Resistance.....	209
5.4 Results and Discussion .....	211
5.4.1 Membrane Properties of a Series of Partially Fluorinated Copolymers .....	218
5.4.1.1 Water Uptake of the Copolymer Membranes .....	218
5.4.1.2 Ion Exchange Capacities of the Copolymer Membranes.....	220
5.4.1.3 Proton Conductivity of the Copolymer Membranes.....	222
5.4.1.4 Lambda Number .....	224
5.4.1.5 Surface Characteristics and XPS Data.....	225
5.4.2 MEA Characteristics.....	227
5.4.3 Fuel Cell Tests .....	228
5.4.3.1 Initial Direct Methanol Fuel Cell Tests .....	228
5.4.3.2 Long Term Direct Methanol Fuel Cell Tests.....	233
5.4.4 Volume-based Proton Exchange Membrane Characteristics.....	237
5.4.4.1 Volume based water uptake.....	239
5.4.4.2 Volume based ion exchange capacity.....	241
5.4.4.3 Selectivity and Relative Selectivity of the Membrane Electrode Assembly.....	242
5.5 Conclusions.....	247
5.6 Acknowledgements.....	247
CHAPTER 6 .....	248
Structure-Property-Performance Relationships of Sulfonated Poly(Arylene Ether Sulfone)s as a Polymer Electrolyte for Fuel Cell Applications.....	248
6.1 Abstract.....	249
6.2 Introduction.....	250
6.3 Experimental.....	254
6.4 Results and Discussion .....	259
6.4.1 Effect of Disulfonation Level .....	259

6.4.2 Effect of Fluorine Moiety .....	259
6.4.3 Effect of Polar Functional Group.....	267
6.4.4 Impact on Fuel Cell Performance .....	273
6.5 Conclusions.....	283
6.6 Acknowledgments.....	283
CHAPTER 7 .....	284
Overall Conclusions.....	284
CHAPTER 8 .....	286
Suggested Future Research.....	286
Vita.....	288

## LIST OF FIGURES

Figure 2.1 The first fuel cell: Introduced by William R. Grove, a set of connected cells was used to produce electricity to electrolyze water .....	4
Figure 2.2 Schematics of a typical fuel cell: Electrochemical reactions at each electrode scales with the energy and sum produces the total energy, which is collected externally from the system .....	5
Figure 2.3 Anode, cathode and overall cell reaction in alkaline fuel cells. ....	8
Figure 2.4 Anode, cathode and overall cell reaction in phosphoric acid fuel cells .....	9
Figure 2.5 Anode, cathode and overall cell reaction in molten carbonate fuel cells .....	10
Figure 2.6 Anode, cathode and overall cell reaction in solid oxide fuel cells .....	11
Figure 2.7 Anode, cathode and overall cell reaction in hydrogen gas powered proton exchange membrane fuel cells .....	13
Figure 2.8 Anode, cathode and overall cell reaction in direct methanol proton exchange membrane fuel cells .....	14
Figure 2.9 Hydrogen gas oxidation on a platinum electrode .....	15
Figure 2.10 Methanol oxidation on a platinum electrode .....	15
Figure 2.11 A typical demonstration of a membrane electrode assembly: Platinum catalyst is adsorbed on carbon black in order to prevent platinum aggregation which decreases the active surface area and the whole system is dispersed in polymer matrix in order to provide mechanical strength and adhesion to the membrane.....	22
Figure 2.12 Membrane electrode assembly with backing layer as anode and cathode substrates: The porous structure in the backing layer act as tiny channels which carry fuel and oxidant to the catalyst layers.....	23
Figure 2.13 Two different flow fields: a) Parallel flow field, b) Serpentine flow field.....	25
Figure 2.14 A more complete depiction of a fuel cell includes flow field (current collector), backing layer and MEA .....	27
Figure 2.15 A fuel cell stack made by combining three cells via bipolar plates: The stack was capped with an endplate .....	27

Figure 2.16 Chemical structures of commercially available sulfonated perfluoro copolymers .....	31
Figure 2.17 Chemical structure of various Ballard Advanced Materials (BAM) copolymers .....	35
Figure 2.18 Chemical structure of styrene/ethylene-butene/styrene triblock Copolymers.....	36
Figure 2.19 Chemical structure of polystyrene-graft-polystyrenesulfonic acid copolymers. ....	38
Figure 2.20 Some of radiation grafted copolymers .....	40
Figure 2.21 Chemical structure of poly(arylene ether sulfone)s : Various random copolymers are possible by a one step copolymerization reaction.....	41
Figure 2.22 Post sulfonation of poly(arylene ether sulfone)s: a. Backbone of poly (arylene ether sulfone), b. and c. Most probable sulfonic acid attachment to a poly(arylene ether sulfone).....	43
Figure 2.23 Chemical structure of sulfonated and unsulfonated poly(ether ether ketone) PEEK .....	45
Figure 2.24 Metalation route to sulfonated polysulfone.....	46
Figure 2.25 Disulfonation of activated and deactivated ring .....	48
Figure 2.26 Direct copolymerization to form disulfonated poly(arylene ether sulfone) (BPSH).....	50
Figure 2.27 Six-membered sulfonated polyimides includes two successive polymerization steps .....	54
Figure 2.28 Sulfonated diamines for direct synthesis of sulfonated polyimides .....	56
Figure 2.29 Directly copolymerized sulfonated poly(arylene ether ketone) .....	58
Figure 2.30 Directly copolymerized sulfonated poly(arylene ether phosphine oxide).....	60
Figure 2.31 Directly copolymerized sulfonated poly(arylene sulfide sulfone) .....	62
Figure 2.32 Directly copolymerized sulfonated poly(arylene ether benzonitrile).....	64
Figure 2.33 a. Chemical structure of four different bisphenols used in copolymerization b. Ion exchange capacity values for four different types of BPSH.....	68
Figure 2.34 Percent water uptake as a function of the degree of disulfonation (Method 1) .....	70

Figure 2.35 Percent water uptake as a function of the degree of disulfonation (Method 2) .....	71
Figure 2.36 Proton conductivity of BPSH membranes acidified with method 1 and method 2.....	72
Figure 2.37 Proton conductivity of BPSH and Nafion™ membranes as a function of water treating (hydrothermal treatment) temperatures.....	74
Figure 2.38 Methanol permeability at 25 °C of BPSH and Nafion™ membranes acidified with method 1 and method 2.....	75
Figure 2.39 Composition of each state of water for BPSH and Nafion™ membranes .....	77
Figure 2.40 a. Direct methanol fuel cell performances of BPSH and Nafion™ membrane b. Degree of methanol permeability from cross over current .....	79
Figure 2.41 Arrhenius plot of some water containing proton conductors .....	81
Figure 2.42 Proton conductivities of Nafion™ and BPSH-40, 30 weight percent HPA containing BPSH-40/HPA composites at different saturated water vapor temperature .....	83
Figure 2.43 A schematic representation of diffusion path of protons through the ZrPPh lamellae .....	84
Figure 2.44 Influence of polarization on cell potential.....	88
Figure 2.45 The Ullman type reaction to synthesize poly(arylene ether)s .....	90
Figure 2.46 Nickel coupling reaction; synthesis of poly(2,5-benzophenone) .....	91
Figure 2.47 Mechanism of sulfonylation which generates sulfonylium cation .....	93
Figure 2.48 a. Addition step, rate determining step, is slow, b. Elimination step is fast: Intermediate formed in first step loses halide .....	96
Figure 2.49 Resonance forms of 4,4'-dichlorodiphenylsulfone.....	98
Figure 2.50 Synthesis of the disodium salt of a bisphenol .....	99
Figure 2.51 Synthesis of poly(arylene ether sulfone) by the strong base approach .....	100
Figure 2.52 Synthesis of poly(arylene ether sulfone)s by the weak base approach .....	102
Figure 2.53 Potassium carbonate decomposes during the reaction and produces water which must be removed by a dehydrating agent such as toluene or xylene ..	103

Figure 2.54 Various possible structural architecture for ionomers a. Monochelic, b. Monochelic block copolymer, c. Telechelic, d. Zwitterionic telechelic, e. star, f. AB diblock, g. ABA triblock, h. (AB) <sub>n</sub> multiblock, i. Star block, j. ABA triblock ionomer, and k. Ionic dendrimer attached to non-ionic chain .....	105
Figure 2.55 a. Ion dipole formation, b. Ion dipole cluster formation .....	108
Figure 2.56 Four states of ionic hydrate association (1) completely dissociated hydrated ion pairs, (2) ion pairs at the contact of undisturbed primary hydration shells, (3) outer sphere complexes, (4) inner sphere complexes ...	109
Figure 2.57 Cluster network model; Ionic clusters with connected short ion channels ....	110
Figure 2.58 Restricted mobility region surrounding the multiplet for a poly(styrene-co-sodium methacrylate ionomer) .....	113
Figure 3.1 Synthesis of “BPSH” via the direct copolymerization route .....	122
Figure 3.2 Effect of reactant ratio on the disulfonation reaction .....	127
Figure 3.3 TGA of SDCDPS monomer dried at 160 °C for 24h indicates <0.5 weight percent water .....	129
Figure 3.4 <sup>1</sup> H NMR spectrum of starting material DCDPS (I), crude SDCDPS monomer (II) and recrystallized SDCDPS monomer (III) .....	132
Figure 3.5 HPLC chromatograms for crude SDCDPS monomer, recrystallized SDCDPS monomer and the starting material DCDPS .....	133
Figure 3.6 UV absorbance spectra of crude SDCDPS monomer, recrystallized SDCDPS monomer and the starting material DCDPS and mixture when a deficient amount of SO <sub>3</sub> was used .....	134
Figure 3.7 <sup>1</sup> H NMR spectra of a disulfonated poly(arylene ether sulfone) copolymer synthesized with SDCDPS using the current process .....	137
Figure 4.1 Chemical structure of Nafion™, where x and y represents molar compositions .....	142
Figure 4.2 Incorporation of proton conducting sites; Post sulfonation or direct copolymerization (monomer sulfonation) methods .....	145

Figure 4.3 Proton NMR confirmed the chemical structure of 3,3'-disulfonated-4,4'-dichlorodiphenyl sulfone monomer; I. Proton NMR for starting material (4,4'-dichlorodiphenyl sulfone ) and II. disulfonated product (3,3'-disulfonated-4,4'-dichlorodiphenyl sulfone).....	152
Figure 4.4 Disulfonated poly(arylene ether benzonitrile) is a random copolymer having a controlled amount of hydrophobic and hydrophilic subunits .....	155
Figure 4.5 The Teflon™ cell to measure proton conductivity.....	159
Figure 4.6 Chemical structures of poly (arylene ether sulfone) and poly (arylene ether benzonitrile) homopolymers.....	160
Figure 4.7 Differential Scanning Calorimeter (DSC) thermogram for poly(arylene ether benzonitrile) from 4,4'-biphenol and 2,6-dichlorobenzonitrile (BP/DCBN) and 4,4'-hexafluoroisopropylidene diphenol and 2,6-dichlorobenzonitrile (6F/DCBN).....	162
Figure 4.8 Synthesis of disulfonated poly(arylene ether benzonitrile) copolymers .....	164
Figure 4.9 Proton NMR spectrum for disulfonated PAEB series: 1. PAEB 10, 2. PAEB 20, 3. PAEB 35, 4. PAEB45, 5. PAEB 60.....	166
Figure 4.10 FTIR bands showing incorporation of sodium sulfonate moieties into copolymer structure .....	168
Figure 4.11The TGA thermogram for acid and salt form of PAEB copolymers .....	169
Figure 4.12 Influence of the degree of disulfonation on TGA weight loss in the acid form of PAEB copolymers (10 °C/min in 50ml/min air ).....	171
Figure 4.13 Storage modulus of disulfonated poly(arylene ether benzonitrile copolymers) at various level of disulfonation compared with Nafion™ 117 .....	173
Figure 4.14 The influence of the degree of disulfonation on water uptake of copolymers acidified with method 1: “I” shows the percolation threshold for water uptake at 45 mol percent sulfonation.....	175
Figure 4.15 The influence of the degree of disulfonation on water uptake of copolymers acidified with method 2 indicates higher swelling compared to copolymers acidified with method 1: “i” represents the percolation threshold, after “ii” point hydrogel formation occurs .....	176

Figure 4.16 Scanning electron micrographs (SEM) of fractured surfaces a. PAEB control (BP/DCBN), b. PAEB 35, c. PAEB 45, d. PAEB 60 .....	178
Figure 4.17 The water uptake of the acid and potassium salt form of the poly(arylene ether benzonitrile) copolymers at various mol percent disulfonation.....	179
Figure 4.18 AFM images for a. Salt form of poly(arylene ether benzonitrile copolymer) at 35 mol percent disulfonation, b. Acid form of copolymers at 35 mol percent disulfonation.....	180
Figure 4.19 The influence of the degree of disulfonation on proton conductivities of copolymers acidified with method 1 and method 2 .....	181
Figure 4.20 a. Influence of the degree of disulfonation on ion exchange capacities (copolymers acidified with method 2) b. Influence of ion exchange capacities on proton conductivities (copolymers acidified with method 2).....	183
Figure 4.21 Normalized proton conductivities with IEC shows a linear relation with the increasing degree of disulfonation .....	184
Figure 5.1 Cross sectional morphology of a membrane electrode assembly (MEAs).....	189
Figure 5.2 Some possible disulfonated poly(arylene ether sulfone)s .....	191
Figure 5.3 Ion exchange capacity of disulfonated poly(arylene ether sulfone) copolymers using various different bisphenols.....	193
Figure 5.4 Proton conductivity, methanol permeability and water uptake of disulfonated poly(arylene ether sulfone) copolymer .....	195
Figure 5.5 Typical fuel cell performance curve as an electrochemical cell where actual performance decayed due to the polarization, activation, ohmic and concentration terms.....	198
Figure 5.6 Sources of water at the cathode; 1. Water from humidification bottle, 2. Product water from the cell current, 3. Water produced by crossover methanol oxidation, 4. Water which has fluxed across the membrane.....	200
Figure 5.7 Limiting current measurement of methanol (transported) oxidation at the fuel cell cathode .....	204
Figure 5.8 The components of the membrane electrode assemblies .....	210

Figure 5.9 Chemical structure of (a) 35 mol percent disulfonated poly(arylene ether benzonitrile) and (b) 35 mol percent disulfonated partially fluorinated poly(arylene ether benzonitrile) .....	212
Figure 5.10 Synthesis of partially fluorinated disulfonated poly(arylene ether benzonitrile) statistical copolymers.....	213
Figure 5.11 Proton NMR of partially fluorinated copolymer series.....	216
Figure 5.12 Influence of partial fluorination on thermooxidative stability of acid form of PAEB copolymers (10 °C/min in air).....	217
Figure 5.13 Water uptake (weight percent) for a series of partially fluorinated disulfonated poly(arylene ether benzonitrile) statistical copolymers .....	219
Figure 5.14 The ion exchange capacity of a series of partially fluorinated disulfonated poly(arylene ether benzonitrile) statistical copolymers .....	221
Figure 5.15 The proton conductivities of a series of partially fluorinated disulfonated poly(arylene ether benzonitrile) statistical copolymers .....	222
Figure 5.16 Surface fluorine enrichment of the series of partially fluorinated copolymers and Nafion™ 112 .....	225
Figure 5.17 Cell resistance was lowered and stabilized with partial fluorination .....	227
Figure 5.18 Initial cell performances were improved with partial fluorination.....	229
Figure 5.19 Methanol permeabilities of stiff hydrocarbon type copolymer series .....	230
Figure 5.20 Several important terms which directly affect the initial direct methanol fuel cell performances.....	231
Figure 5.21 Proposed interfacial delamination mechanism under continuous operation ...	233
Figure 5.22 a. Initial and 200 h DMFC performances of copolymer membrane series (for PAEB 35, 6F25CN35, 6F50CN35).....	234
Figure 5.22 b. Initial and 200 h DMFC performances of copolymer membrane series (for 6F75CN35, 6FCN35).....	235
Figure 5.23 The important terms which directly affect the long term direct methanol fuel cell performances.....	236
Figure 5.24 Volume based membrane parameters might better reflect the structure-property relationship than weight based parameters .....	238

Figure 5.25 a. Relative selectivity of the membranes, b. Water uptake corrected relative selectivity which better correlates structure-property-performance .....	246
Figure 6.1 Chemical structure of disulfonated poly(arylene ether sulfone) copolymers ...	255
Figure 6.2 Effect of fluorine incorporation on membrane water uptake .....	262
Figure 6.3 Effect of fluorine incorporation on proton conductivity as a function of $IEC_V$ (wet) .....	265
Figure 6.4 Effect of fluorine incorporation on conductivity at a fixed $IEC_V$ (wet) .....	266
Figure 6.5 Effect of (a) benzonitrile and (b) PPO polar group incorporation on membrane water uptake .....	269
Figure 6.6 Effect of (a) benzonitrile and (b) PPO polar group incorporation on membrane proton conductivity .....	270
Figure 6.7 Effect of PPO incorporation on proton conductivity at a fixed $IEC_V$ (wet) .....	271
Figure 6.8 Effect of (a) fluorine and (b) PPO incorporation on $H_2$ /air fuel cell performance at 80 °C; $IEC_V$ (wet) values of membranes for (a) and (b) were fixed at 1.25 and 1.35 meq/cm <sup>3</sup> , respectively .....	274
Figure 6.9 Effect of PPO incorporations on high methanol concentration feed (5 M) DMFC performance at 80 °C; $IEC_V$ (wet) value of membranes was fixed at 1.35 meq/cm <sup>3</sup> .....	277

## LIST OF TABLES

Table 2.1 Membrane electrode assembly (MEA) fabrication concept includes two modes .....	18
Table 2.2 Various possible architecture for ionomers .....	106
Table 2.3 Several commercial ionomers.....	115
Table 2.4 Various possible applications of ionomers .....	117
Table 3.1 Proton NMR of the disulfonation reaction after 6h reaction at 1:3.3 DCDPS:SO <sub>3</sub> stoichiometry .....	128
Table 3.2 Intrinsic viscosity and mole percent disulfonation of the BPS copolymers .....	130
Table 3.3 Two fragmentation characteristics of the disulfonated monomer .....	135
Table 4.1 Several thermal properties of two different poly(arylene ether benzonitrile) copolymers where T <sub>g</sub> is the glass transition temperature, T <sub>m</sub> is the melting temperature and T <sub>d</sub> is the decomposition temperature .....	163
Table 4.2 Degree of disulfonation calculated by proton NMR.....	167
Table 4.3 Thermal characterization of the control homopolymer and PAEB copolymers.....	170
Table 5.1 Intrinsic viscosity and 5 weight percent weight loss temperatures series of partially fluorinated copolymers at 35 mol percent disulfonation.....	214
Table 5.2 The basic membrane characteristics were demonstrated as tunable membrane parameters .....	223
Table 5.3 Lambda numbers for the non fluorinated partially fluorinated copolymer series and Nafion™ ionomer .....	224
Table 5.4 Surface fluorine atomic percentages of the partially fluorinated acid form copolymer series compared with Nafion™ .....	226
Table 5.5 Volume based water uptakes of copolymer series (compared with Nafion™) ..	240
Table 5.6 Volume based ion exchange capacities of the copolymer series .....	241
Table 5.7 Several MEA properties of copolymer series which were compared with Nafion™ .....	243
Table 5.8 Selectivity, relative selectivity and water uptake corrected selectivity of MEA s based on our copolymer series and Nafion™ ionomer .....	245

Table 6.1 Effect of the degree of disulfonation on density, IEC, water uptake and proton conductivity .....	279
Table 6.2 Effect of fluorine moiety on density, IEC, water uptake and proton conductivity.....	280
Table 6.3 Effect of polar group on density, IEC <sub>w</sub> , water uptake and proton conductivity.....	281
Table 6.4 Methanol permeability and selectivity of selected copolymers.....	282

---

# CHAPTER 1

## Introduction

---

Environmental concerns such as increasing amount of toxic emissions into the atmosphere when fossil fuels are used to produce electricity and gasoline for vehicles has led to extensive research and development on renewable alternative energy sources. Fuel cells have been proposed to have potential to provide reliable future energy sources.

Proton exchange membrane (PEM) fuel cells are very promising due to their, high power density and high efficiency. Proton exchange membrane fuel cells are favored for use as commercial products in automobiles, residential homes and in portable devices such as laptops and cell phones.

The proton exchange membranes in these fuel cells consist of copolymer materials which include proton conductor units. Usually sulfonic acid groups are utilized. The current state of art for proton exchange membranes is Nafion<sup>TM</sup> (perfluorinated ionomer). Nafion<sup>TM</sup>'s poly(perfluorosulfonic acid) structure imparts exceptional oxidative and chemical stability, which is also important in fuel cell

applications. Moreover, Nafion™ shows high proton conductivity. However, it suffers from high methanol permeability and also relatively low glass transition temperatures.

Our group has emphasized hydrocarbon fully aromatic thermally, mechanically and acid-base stable disulfonated poly(arylene ether sulfone) random copolymers as proton exchange membranes. Direct copolymerizations where the disulfonated monomer is copolymerized with other suitable comonomers to synthesize disulfonated copolymers has been developed<sup>1</sup>.

A crucial precursor for the synthesis of these disulfonated copolymers is the disulfonated monomer, 3,3'-disulfonated 4,4'-dichlorodiphenyl sulfone. The synthesis and characterization of this monomer and detailed characterization was demonstrated in our laboratories. The synthesis and characterization of disulfonated poly(arylene ether sulfone) copolymers from the disulfonated monomer have been extensively studied. In this dissertation, a one-step synthesis of the disulfonated monomer in quantitative yield, adoptable to industrial large scale applications has been demonstrated. Secondly, the nitrile-functional copolymer series (disulfonated poly(arylene ether benzonitrile) were introduced for DMFC and H<sub>2</sub>/air fuel cells. Heteropolyacid nanocomposites of this copolymer for higher temperature fuel cell application were also demonstrated. The disulfonated poly(arylene etherbenzonitrile) copolymers were partially fluorinated using the 6F bisphenol comonomer to fine tune the basic membrane properties.

---

<sup>1</sup> Hickner, M.A.; Ghassemi, H.; Kim, Y.S.; Einsla, B.R.; McGrath, J.E., *Chemical Reviews* 2004, 104, 4587

---

# CHAPTER 2

## Literature Review

---

### 2.1 The First Fuel Cell; The Gaseous Voltaic Battery

The first fuel cell, initially described as the “gaseous voltaic battery” was discovered by William Robert Grove and reported in 1839<sup>1</sup>. The invention was based on the idea that the electrolysis of water requires some energy to produce the hydrogen and oxygen gas. Grove introduced the first hydrogen-oxygen gas fuel cell using sulfuric acid electrolyte and a platinum electrode. The experimental set up of Grove included the cells containing gaseous hydrogen and oxygen to produce the electron flow to upper cell. Hence, the energy produced from bottom cell was used for the electrolysis of water producing gaseous hydrogen and oxygen (Figure 2.1).

The National Aeronautics and Space Administration (NASA) used the hydrogen fuel cell in the Gemini space mission, which was the first mission with the fuel cell producing the electricity and also water for the crew.<sup>2</sup> The need for using fuel cells in space and also low power applications for daily life triggered extensive research to reduce cost and make size effective fuel cells available in mass markets. Hence,

---

<sup>1</sup> Sharon Thomas and Marcia Zalowitz, Fuel Cells-Green Power, Los Alamos National Laboratory, 1999

<sup>2</sup> Oster, E.A.; In *Proceedings of the 16<sup>th</sup> Annual Power Sources Conference*, New Jersey, 1962, p. 22

industrial and academic research has targeted the commercialization and technological improvement of proton exchange membrane (PEM) fuel cells.

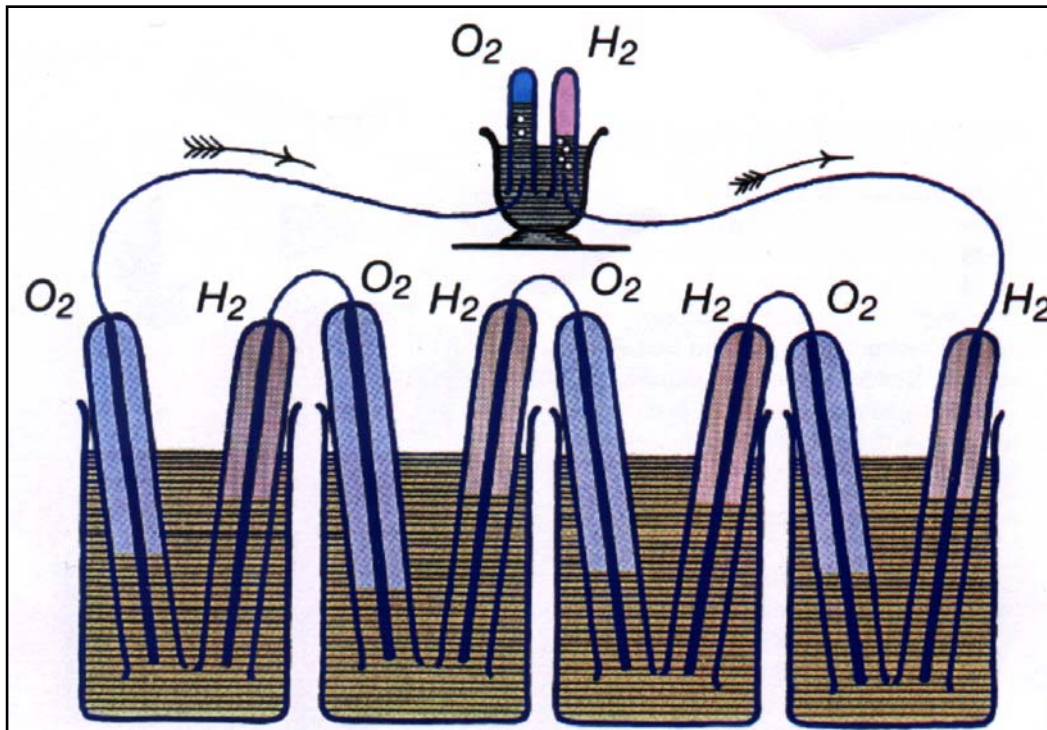


**Figure 2.1**<sup>1</sup> The first fuel cell: Introduced by William R. Grove, a set of connected cells was used to produce electricity to electrolyze water

## 2.2 Fuel Cells

Fuel cells are electrochemical devices that generate direct current (DC) electricity by converting the chemical energy of fuel and oxidant to electrical energy. The basic set up of a fuel cell consists of three compartments, which are the anode, cathode and electrolyte. In a fuel cell, the fuel is oxidized at the anode, while the oxidant is reduced at

the cathode. Ions are produced and travel through from one electrode to another with the help of an electrolyte, which are basically charge carriers. A cell produces DC voltage when the electron transfer occurs and is collected via an external circuit. Typical schematics of a fuel cell can be seen in Figure 2.2.

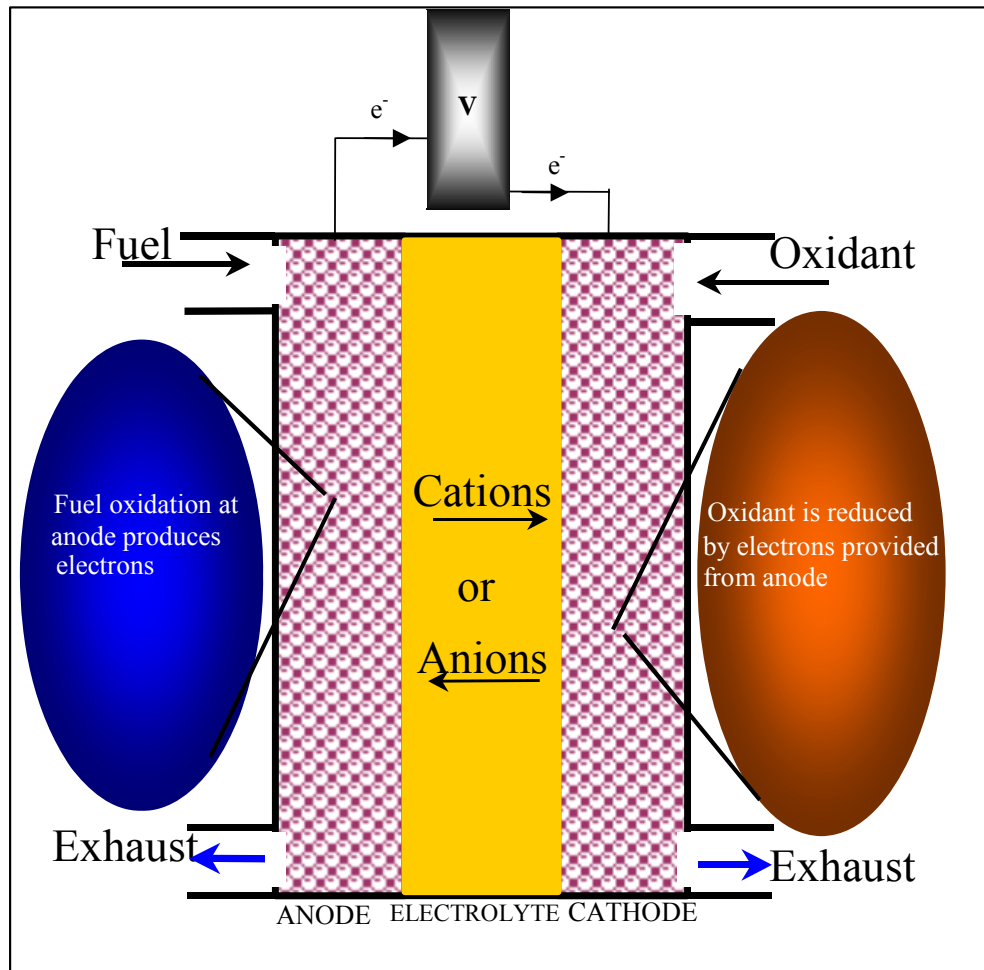


**Figure 2.2** Schematics of a typical fuel cell: Electrochemical reactions at each electrode scales with the energy and sum produces the total energy, which is collected externally from the system

Fuel cells have some similarities to batteries as a way of producing electricity. The limited lifetime of batteries, or need for the external energy to recharge them makes batteries an energy storage device. However, fuel cells are, in contrast, continuous energy conversion devices, if the fuel is supplied externally. The pollution free energy conversion, higher efficiency, design variability, flexibility of fuel, etc., makes fuel cells very attractive. Fuel cells are promising for a wide variety of applications both in the low power area (laptops, cell phones, etc.) and high power area (stationary for buildings and transportation for automobiles). There are several different types of fuel cells based on electrolyte and fuel types. The classification might be more specific by relating the fuel cells to their operating temperatures. In this review, fuel cells are classified as alkaline, phosphoric acid, sulfuric acid, molten carbonate, solid oxide, protonic ceramic and proton exchange membrane fuel cells based on their electrolyte. Each of these fuel cells has distinct applications and operating conditions, which will be discussed in the following section. Our group has focused on developing proton exchange membranes and their structural and electrochemical characterizations for application of proton exchange membrane fuel cells. The different types of proton exchange membranes are classified as perfluorinated, partially fluorinated and hydrocarbon based. Our approach has been to synthesize the proton exchange membrane and to also generate membrane electrode assemblies (MEA).

The electrochemical reactions at the anode and the cathode are called half-cell reactions. In each half-cell reaction, electrons are consumed or generated which display electrochemical energies related to standard electrode potential. The standard electrode

potential is a relative quantity and it is defined as the potential of an electrochemical cell of a standard hydrogen electrode, whose potential arbitrarily is chosen as 0 V. Hence, the sum of both anode and cathode half-cell reaction potentials yields the cell potential. However, the value calculated is also called the open cell potential. In real operating conditions this value decreases due to the several parameters and this detailed information will be provided in Chapter 5.

## **2.3 Types of Fuel Cells**

### **2.3.1 Alkaline Fuel Cells (AFC)**

Alkaline fuel cells were arguably the first type of the fuel cell that had some success especially in space applications<sup>3</sup>. Alkaline fuel cells use potassium hydroxide (KOH) solution (30-45 wt. %) as the electrolyte and operate on compressed hydrogen and oxygen to complete the electrochemical cycle<sup>4</sup>. The efficiency of the alkaline fuel cells is strongly dependent on the purity of the fuel. Higher operating temperatures were used for the earlier types of the alkaline fuel cells. A nickel anode and lithiated nickel oxide cathode and usually 30 weight percent potassium hydroxide (KOH) were used in first types of alkaline fuel cells, where operating temperatures and pressures were 200-230 °C and 5Mpa respectively, in order to increase the oxygen reduction kinetics<sup>5</sup>. The KOH solution was circulated through the fuel cell to provide a better barrier against the gas

---

<sup>3</sup> Broeck, Hugo Van Den, In *Fuel Cell Systems*, Blomen, L.J.M.J; Mugerwa, M.N., Eds., Plenum Press: New York, 1993, p. 245

<sup>4</sup> Bockris. J.O.M., Appleby, A.J., *Energy* 1986, 11, 95

<sup>5</sup> Chen E.; In *Fuel Cell Technology Handbook*, Hoogers, G, Ed. CRC Press: New York, 2003

leakage. It was also used as a coolant for the cell stacks. The alkaline fuel cells are now used at lower temperatures (lower than 100 °C), compared to earlier versions.

Alkaline fuel cells are classified as high cost fuel cells. Since very high platinum loading has been needed for high power application. Their performances are very sensitive to carbon dioxide reaction with the potassium hydroxide<sup>6,7</sup>. This reaction produces potassium carbonate which degrades the electrolyte and decreases the efficiency of the electrodes. Circulation of the electrolyte decreases the destructive effect of carbonate formation. The attainable power from an alkaline fuel cell is between 5 and 150kW<sup>8</sup>. The anode, cathode half-cell reactions and overall cell reaction are summarized below (Figure 2.3).

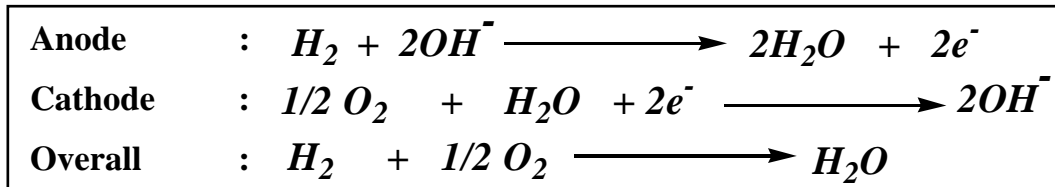


**Figure 2.3** Anode, cathode and overall cell reaction in alkaline fuel cells.

<sup>6</sup> Appleby, A.J.; Foulks, F.R.; *Fuel Cell Handbook*, Van Nostrand Reinhold, New York, 1968

<sup>7</sup> Liebhafsky, H.A.; Cairns, E.J., *Fuel Cells and Fuel Batteries*, John Wiley and Sons, Inc. New York, 1968

<sup>8</sup> Srinivasan, S.; Dave, B.B.; Murugesamoorthi, K.A.; Parthasarathy, A.; Appleby, A.J.; In *Fuel Cell Systems*, Blomen, L.J.M.J; Mugerwa, M.N., Eds., Plenum Press: New York, 1993, p. 37

### 2.3.2 Phosphoric Acid Fuel Cells (PAFC)

Phosphoric acid fuel cells use liquid phosphoric acid, which is quite stable compare to other acids. Generally, a Teflon bonded silicon carbide matrix is used as the electrolyte<sup>9</sup>. The small pore size of the matrix keeps the phosphoric acid from mixing with the fuel. The Pt catalyst dispersed on a carbon-based support is used as the electrode. The amount of Pt in electrodes varies in the electrodes (the cathode may have more Pt than the anode to increase the oxygen reduction kinetics). Phosphoric acid fuel cells show low tolerance to carbon monoxide at high temperatures (150-200 °C), which is generally below, but close to the acid decomposition temperature. At lower temperatures the ionic conductivity decreases and carbon monoxide poisons the platinum catalyst at the anode<sup>10</sup>. Anode and cathode reactions in phosphoric acid fuel cells are given in Figure 2.4. The phosphoric acid fuel cells are the most commercialized of all fuel cells for the present. The realized power of phosphoric acid fuel cells is in the range of 5-20MW<sup>11</sup>.

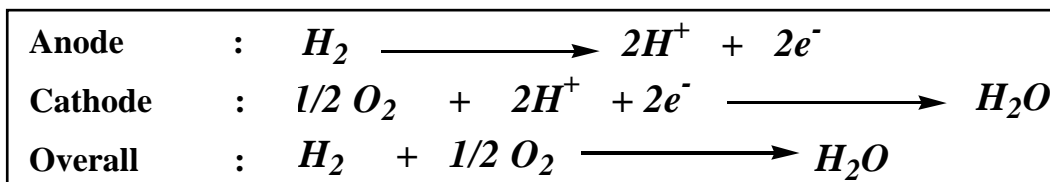


**Figure 2.4** Anode, cathode and overall cell reaction in phosphoric acid fuel cells

<sup>9</sup> Appleby, A.J., Ed. *Fuel Cells: Trends in Research and Applications*; Hemisphere Publishing Corp.: New York, 1987

<sup>10</sup> Horschehofer, J.H.; Stauffer, D.B.; Engleman, R.R., *Fuel Cells: A Handbook for the Department of Energy*; B/T Books: Orinda, CA, 1996; p1-1.

<sup>11</sup> Brenscheidt, T.; Janowitz, K.; Sale, H.J.; Wendt, H.; Brammer, F., *International Journal of Hydrogen Energy* 1998, 23, 53

### 2.3.3 Molten Carbonate Fuel Cells (MCFC)

Molten lithium or potassium carbonate salt matrix or combination of alkali carbonates impregnated in a ceramic matrix is the typical electrolyte in a molten carbonate fuel cell. Nickel catalyst is used which is relatively inexpensive compared to platinum. Molten carbonate fuel cells can extract hydrogen from fuel at 600 to 800 °C where carbonate ions are generated and react with hydrogen to produce carbon dioxide, water and electrons at the anode<sup>12,13</sup> (Figure 2.5). Similarly, produced carbon dioxide is consumed at the cathode. Molten carbonate fuel cells are more tolerable to carbon monoxide poisoning than lower temperature fuel cells. Hydrogen, carbon monoxide, natural gas, propane and coal gasification products can be used as fuel. Molten carbonate fuel cells can be used to build small power plants with a power capacity of 100kW-2MW. However, possible future applications of molten carbonate fuel cells are limited because the molten electrolyte is quite corrosive.

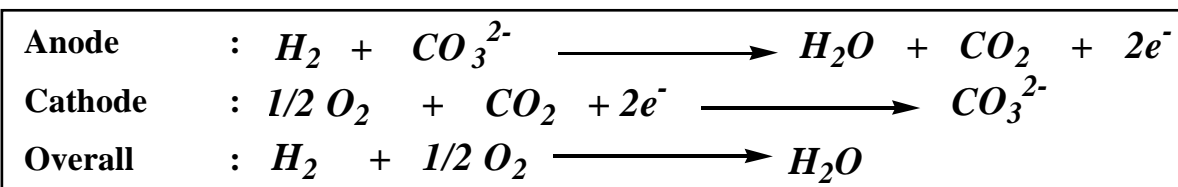


**Figure 2.5** Anode, cathode and overall cell reaction in molten carbonate fuel cells

<sup>12</sup> Minh, N., *Chemtech* 1991, 21, 32

<sup>13</sup> Prabhu, G.; Solaiyan, C.; Dheenadayalan, S.; Chandrasekaran, R.; Pattabiraman, R., *Proceeding of the Indian National Science Academy, Part A: Physical Sciences* 2004, 70, 489

### 2.3.4 Solid Oxide Fuel Cells (SOFC)

Solid oxide fuel cells use non-corrosive non-porous metal oxide ceramics, usually yttria stabilized zirconia, as the electrolyte and operate at 800-1000 °C<sup>5,6</sup>. However, the efficiency of these fuel cells are quite temperature dependent and a decrease in temperature may cause a drop of 10-15 percent of the cell voltage<sup>7</sup>.

Typically the anode is made of cobalt or nickel zirconia while the cathode is strontium or magnesium doped lanthanum manganite<sup>10,11</sup>. Basically, oxygen anions produced at the cathode travels to the anode to oxidize fuel and generate electrons (Figure 2.6). Because of the high operating temperatures internal reforming is needed. The solid oxide fuel cell can extract electrons from hydrocarbon fuels such as coal, natural gas, diesel fuel and alcohols. Moreover, even carbon monoxide can directly be used as fuel.

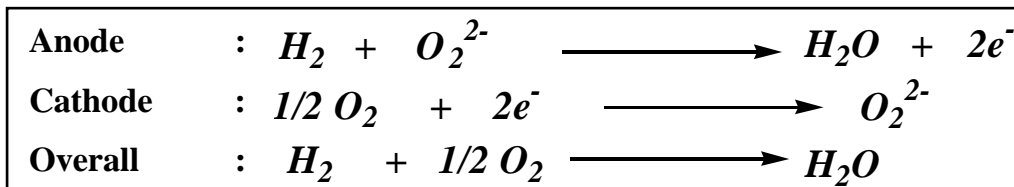


**Figure 2.6** Anode, cathode and overall cell reaction in solid oxide fuel cells

### 2.3.5 Proton Exchange Membrane Fuel Cell (PEMFC)

Proton exchange membrane fuel cells, also called polymer electrolyte fuel cell or solid polymer electrolyte fuel cells use a proton exchange membrane, which acts as a solid electrolyte between the anode and cathode electrodes. Proton exchange membrane fuel cells are favored for use in automobiles, residential power as well as in portable devices such as laptops and cell phones. This preference is due to the reasons listed below<sup>14,15,16,17,18,19</sup>.

1. High power density
2. High efficiency
3. Relatively quick start up
4. Rapid response the varying loads
5. Low operating temperatures
6. Solid non-corrosive electrolyte
7. Insensitive to differential pressures
8. No carbonate formation
9. Long life
10. Potable liquid product water
11. Ease of design and adaptable size

---

<sup>14</sup> Mehta, V.; Cooper, S.C., *Journal of Power Sources* 2003, 114, 32 (Table 2.1 was prepared using this reference with the permission from Elsevier)

<sup>15</sup> Hickner M.A., *Ph.D. Thesis*, VPI&SU, 2003

<sup>16</sup> Zalowitz, N.; Thomas, S.; "Fuel Cells: Green Power", Department of Energy, 1999, LA-UR-99-3231

<sup>17</sup> Dhathathreyan, K.S.; Sridhr, P.; Sasikumar, G.; Ghosh, K.K.; Velayuthan, G.; Rajalakshmi, N.; Subramaniam, C.K.; Raja, M.; Ramya, K., *Int. J. Hydrogen Energy* 1999, 24, 1107

<sup>18</sup> Passalacqua, E.; Lufano, F.; Squadrito, G.; Patti, A.; Giorgi, L., *Electrochimica Acta* 2001, 46, 799

<sup>19</sup> Korges, K.; Simader, G., *Fuel Cells and their Application*, Wiley,-VCH, Weinheim, 1996

However, there are also some disadvantages summarized as follows<sup>13</sup>:

1. High membrane cost
2. High catalyst loading
3. Low quality waste heat
4. Sensitive to carbon monoxide
5. Limited understanding of structure-property-durability-relationships

The McGrath research group at Virginia Tech has been investigating the synthesis of new membranes as well as new catalyst formulations in order to address these problems.

The operating temperature of proton exchange membrane fuel cells has been reported between 60 and 130 °C<sup>20</sup>, but mostly at 80 °C. Both reactions at the anode and cathode and the overall cell reaction for the hydrogen and methanol powered fuel cells are given as below (Figure 2.7 and Figure 2.8).

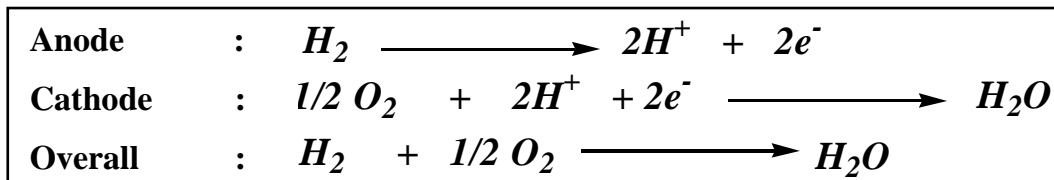


**Figure 2.7** Anode, cathode and overall cell reaction in hydrogen gas powered proton exchange membrane fuel cells

<sup>20</sup> Adjemian, K.T.; Srinivasan. S.; Benziger, J.; Bocarsly, A.B., Journal of Power Sources 2002, 109, 356

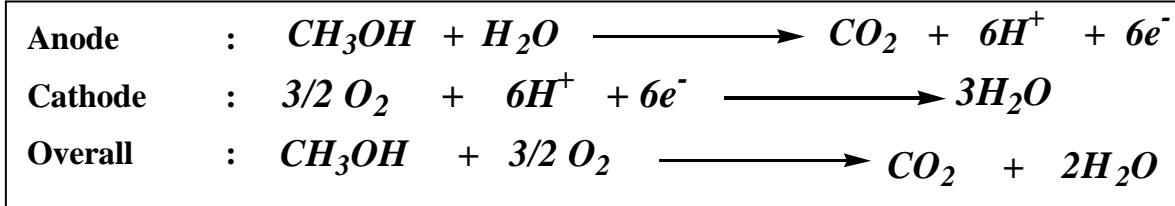


**Figure 2.8** Anode, cathode and overall cell reaction in direct methanol proton exchange membrane fuel cells

The simple single PEM fuel cell consists of backing layer, flow fields or bipolar plates and membrane electrode assembly (MEA). The currently used perfluorinated ionomer membrane is called Nafion™. The Virginia Tech. approach for making proton exchange membranes, MEA fabrication and PEM fuel cell hardware will be discussed in this review.

### 2.3.5.1 Electrodes for PEMFC and MEA Fabrication

The electrodes used in proton exchange membrane fuel cells are micro porous gas diffusion electrodes. The composition of the electrode includes a copolymer matrix (usually Nafion™) impregnated noble metal catalyst (e.g. platinum) which may be supported on carbon black. The oxidation kinetics of the fuel such as pure hydrogen gas with pure platinum catalyst at the anode works well. For instance, the hydrogen oxidation kinetics on platinum catalyst is very fast. Hence, the kinetics is only controlled by mass

transfer. The hydrogen oxidation occurs in several sub-steps including adsorption and dissociation of the molecule into two  $H^+$  ions. The reaction is depicted in Figure 2.9.

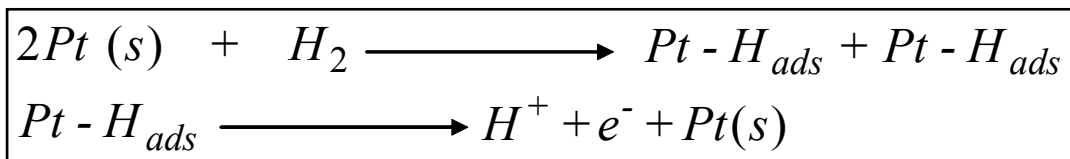


**Figure 2.9** Hydrogen gas oxidation on a platinum electrode

Similarly, the methanol oxidation on platinum catalyst includes adsorption and deprotonation steps. The proposed mechanism<sup>21</sup> of methanol oxidation can be seen in Figure 2.10.

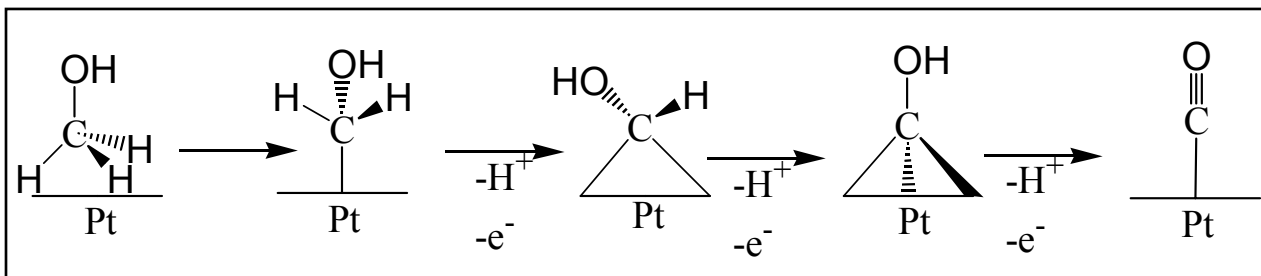


**Figure 2.10** Methanol oxidation on a platinum electrode (*reprinted from reference 21 with permission from Wiley*)

<sup>21</sup> Carrette, L.; Friedrich, K.A.; Stimming, U., *Fuel Cells* 2001,1, 5

However, certain contaminants in hydrogen gas (H<sub>2</sub>) fuels such as carbon monoxide, sulfur, and ammonia poison the catalyst. The carbon monoxide adsorption on active sites of platinum decreases the catalytic activity over time and catalytic activity eventually disappears. Carbon monoxide poisoning can be avoided by fuel reforming or catalyst alloying techniques. Fuel reforming techniques are summarized as selective oxidation, catalysis and hydrogen peroxide addition. Selective oxidation includes mixing the fuel with air or oxygen to oxidize the CO to CO<sub>2</sub><sup>22,23,24</sup>. Among these techniques, catalysis is a gas clean up method by passing fuel and small amount of oxygen over a platinum catalyst. The addition of hydrogen peroxide to the fuel can also minimize the CO<sup>25,26</sup>. The catalyst alloying technique includes platinum alloys of Re, Ru, Os, Rh, Mo, Pb, Bi and Sn have been well studied to oxidize the carbon monoxide to carbon dioxide<sup>27,28,29,30,31,32,33,34,35</sup>.

---

<sup>22</sup> Gottesfeld, S.; Pafford, J.; *Journal of the Electrochemical Society* 1998, 135, 2651

<sup>23</sup> Kolbrecka, K.; Przulski, J.; *Electrochimica Acta* 1994, 39, 1591

<sup>24</sup> Oetjen, H.F.; Schmidt, V.M.; Stimming, U.; *Electrochimica Acta* 1998, 43, 3838

<sup>25</sup> Diviek, J.; Oetjen, H.F.; Peinecke, V.; Schmidt, V.M.; Stimming, U.; *Electrochimica Acta* 1998, 43, 3811

<sup>26</sup> Bellows, R.J.; Marucchi-Soos, E.; Reynolds, R.P.; *Electrochemical and Solid State Letters* 1998, 1, 69

<sup>27</sup> Ogata, N.; Rikukawa, M.; *US Patent* 5, 403, 675, 1995

<sup>28</sup> Iwase, M.; Kawatsu, S., In *Proceeding of the First International Symposium on Proton Conducting Membrane Fuel Cells*, Vol. 1, 1995, p 12

<sup>29</sup> Bauman, J.; Zawodzinski, T.; Rockward, T.; Haridoss, P.; Uribe, F.; Gottesfeld, S., In *Proceeding of the Second International Symposium on Proton Conducting Membrane Fuel Cells*, Vol. 2, 1998, p 200

<sup>30</sup> Chrzanowski, W.; Wieckowski, A., *Langmuir* 1998, 14, 1967

<sup>31</sup> Ley, K.L.; Liu, R.; Pu, C.; Fan, Q.; Leyarowska, N.; Segre, C.; Smotkin, E.S., *Journal of Electrochemical Society* 1997, 144, 1543

<sup>32</sup> Liu, L.; Viswanathan, R.; Liu, R.; Smotkin, E.S., *Electrochemical and Solid State Letters* 1998, 1, 123

<sup>33</sup> Hampson, N.A.; Willars, M.J.; McNiol, B.D.; *Journal of Power Sources* 1979, 4, 191

<sup>34</sup> Arico, A.S.; Poltarzewski, Z.; Kim, H.; Morana, A.; Giordano, N.; Antonucci, V., *Journal of Power Sources* 1995, 55, 159

<sup>35</sup> Gotz, M.; Wendt, H., *Electrochimica Acta* 1998, 43, 3637

The combination of the anode, proton exchange membrane and cathode is known as a membrane electrode assembly (MEA). The MEA design concept is crucial in order to introduce fuel cells into the mass market. Better MEA design producing higher power density may help industry to manufacture smaller, lighter and less expensive fuel cell stacks<sup>36</sup>. MEA can be fabricated by two modes.

Mode I. Fabrication of catalyst layer on directly to backing layer

Mode II. Fabrication of catalyst layer on directly to membrane

The table showed below extracted from the review published by Mehta et al.<sup>14</sup> briefly explains these MEA fabrication methods (Table 2.1).

---

<sup>36</sup>Hoogers, G., In *Fuel Cell Technology Handbook*, CRC Press: New York, 2003

Table 2.1 Membrane electrode assembly (MEA) fabrication concept includes two modes

	<b>Method</b>	<b>Explanation</b>	<b>Ref.</b>
<b>Mode I.</b>	1. Spreading	Catalyzed carbon and PTFE dough spreads on carbon cloth	<sup>37</sup>
	2. Spraying	The electrode is suspended in a mixture of water, alcohol and colloidal PTFE	36
	3. Catalyst Powder Deposition	The components of catalyst (Carbon Black, Vulcan XC-72, PTFE powder and variety of Pt/C loadings) is applied on carbon cloth	38
	4. Ionomer Impregnation	Catalyzed carbon and ionomer (Nafion™) mixture is dispersed with lower aliphatic alcohols, then painted on the backing layer	39
	5. Electro-deposition	Impregnation of the porous carbon with ionomer where cations of the ionomer exchange with a cationic complex of platinum. Platinum in this formulation is electrodeposited on the carbon support.	38,40

<sup>37</sup> Srinivasan, S.; Ferreira, A.; Mosdale, R.; Mukerjee, S.; Kim, J.; Hirano, S.; Lee, S.; Buchi, F.; Appleby, A., In *Proceedings of the Fuel Cell- Program and Abstracts on the Proton Exchange Membrane Fuel Cells for Space and Electric Vehicle Applications*, 1994, p 424

<sup>38</sup> Bevers, D.; Wagner, N.; Bradke, M, *Int. J. Hydrogen energy* 1998, 23, 57

<sup>39</sup> Gottesfeld, S.; Zawodzinski, *Adv. Electrochem. Sci. Eng.* 1997, 5, 195

<sup>40</sup> Taylor, E.; Anderson, E.; Vilambi, N., *J. Electrochem. Soc.* 1992, 139, L45-L46

	<b>Method</b>	<b>Explanation</b>	<b>Ref.</b>
<b>Mode II.</b>	1. Impregnation Reduction	Sodium salt of the ionomer is equilibrated with an aqueous solution of $(\text{NH}_3)_4\text{PtCl}_2$ and a co-solvent of $\text{H}_2\text{O}/\text{CH}_3\text{OH}$ . Following impregnation, vacuum dried PFSA in the $\text{H}^+$ is exposed to aqueous solution of reductant $\text{NaBH}_4$ . <i>(This technique is not being used anymore)</i>	41
	2. Evaporative Deposition	$(\text{NH}_3)_4\text{PtCl}_2$ is evaporatively deposited onto a membrane from an aqueous solution. Metallic platinum is produced by immersion in a solution of $\text{NaBH}_4$	41, 42
	3. Dry Spraying	The mixture of Pt/C, PTFE, PFSA powder are mixed in a knife mill. The mixture then atomized and sprayed on to membrane	43

<sup>41</sup> Foster, S.; Mitchell, P.; Mortimer, R., In *Proceedings of the Fuel Cell-Program and Abstracts on the Development of a Novel Electrode Fabrication Technique for Use in Solid Polymer Fuel Cells*, 1994, p 442

<sup>42</sup> Fedkiw, P.; Her, W., *J. Electrochem. Soc.* 1989, 136, 899

<sup>43</sup> Gulzow, E.; Schulze, M.; Wagner, N.; Kaz, T.; Reissner, R.; Steinhilber, G.; Scheinder, A., *J. Power Sources* 2000, 86, 352

<i>Continued</i>	<b>Method</b>	<b>Explanation</b>	<b>Ref</b>
<b>Mode II.</b>	4. Filtration	PFSA solution is mixed with the catalyst and dried in a vacuum and mixed with PTFE dispersion and calcium carbonate used to form pores and water. The mixture is filtered and the filtrate is formed into a sheet. The calcium carbonate is removed by dipping the sheet in nitric acid. The sheet is dried and the PFSA solution is applied to one side of the sheet and finally it is applied to membrane	44
	5. Catalyst Decaling	Catalyst is mixed with solubilized PFSA. The protonated form of PFSA is converted into tetrabutyl ammonium form. Glycerol is added to this mixture to increase the stability and paintability. The ink is cast on to decal and transferred on to the membrane by hot pressing. The catalyzed membrane is reprotonated by lightly boiling a sulfuric acid solution.	39, 45,46
	6. Painting	Catalyst solution in salt form is prepared as described above. Catalyst solution is directly painted on to membrane and allowed to dry. Then the catalyzed membrane is converted to acid form by immersion in boiling sulfuric acid solution	39, 45, 46

<sup>44</sup> Matsubayashi, T.; Hamada, A.; Taniguchi, S.; Miyake, Y.; Saito, T., In *Proceedings of the Fuel Cell-Program and Abstracts on the Development of a Novel Electrode Fabrication Technique for Use in Solid Polymer Fuel Cells*, 1994, p 581

<sup>45</sup> Gottesfeld, S.; Wilson, M., *J. Electrochem. Soc.*, 1992, 139, L28-L30

<sup>46</sup> Gottesfeld, S.; Wilson, M., *J. Appl. Electrochem.*, 1992, 22, 1

### **2.3.5.2 MEA Fabrication Method, The Los Alamos National Lab Approach<sup>1</sup>**

The fabrication variables of MEA fabrication include the platinum loading, and the thickness of the anode and cathode layers and the proton exchange membrane. The currently used platinum loading is about 0.15- 0.50 mg/cm<sup>2</sup>. The corresponding current obtained from fuel cell performance is from about 0.5 amperes per milligram of platinum to 15 amperes per milligram of platinum. The thickness of the catalyst layers depends on the platinum loading. The thickness is close to 10 microns when the platinum loading is about 0.15 mg platinum/cm<sup>2</sup>. The thickness of the membrane varies with the membrane type and is around 25-200 micron. The typical demonstration of MEA can be seen in Figure 2.11<sup>15</sup>.

The fabrication of the MEA according to the Los Alamos National Laboratory (LANL) includes several steps summarized as below;

1. The catalyst ink is prepared by mixing the proper amount of catalyst which is carbon supported platinum with the solution of the membrane material dissolved or dispersed in alcohols
2. The ink is painted directly onto a dry, solid piece of membrane and heated to dry the catalyst layer-this procedure is then repeated with the other side of the membrane
3. The dried membrane is rehydrated by immersing in lightly boiling dilute acid solution
4. The MEA is washed in distilled water.

Beside the printing method, researchers at Los Alamos National Lab. have applied a catalyst decaling method described in Table 2.1.

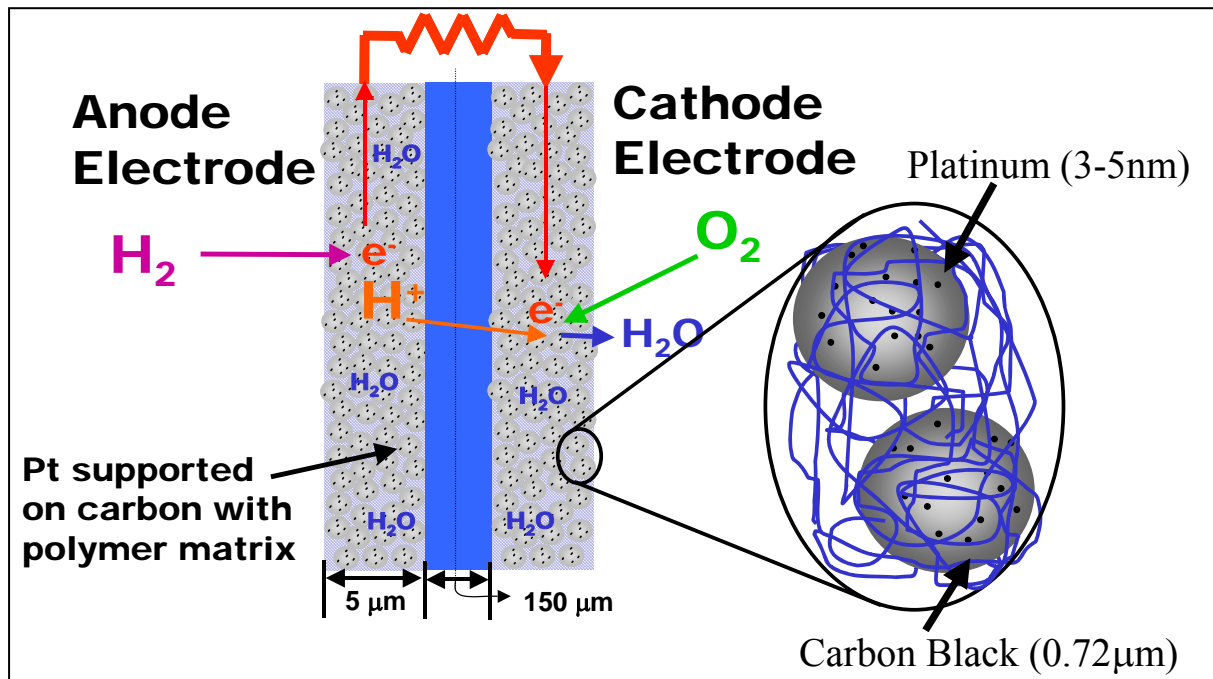


**Figure 2.11**<sup>15</sup> A typical demonstration of a membrane electrode assembly; Platinum catalyst is adsorbed on carbon black in order to prevent platinum aggregation which decreases the active surface area and the whole system is dispersed in polymer matrix in order to provide mechanical strength and adhesion to the membrane

### 2.3.5.3 The Proton Exchange Membrane Fuel Cell Hardware

The proton exchange membrane fuel cell hardware includes backing layers (gas diffusion layer, GDL), flow fields. A schematic of an MEA with backing layer is shown in Figure 2.12<sup>1</sup>. The backing layer is generally made of carbon-based materials such as porous carbon paper or carbon cloth with a thickness of 100-300 microns. The gas diffusion is controlled by the backing layer. The importance of the porous structure of backing layer is to provide continuous diffusion of fuel to the tiny catalyst particles, which are in contact with the backing layer. Moreover, the backing layer should be electrically conductive in order to allow electron transfer from the anode to cathode.

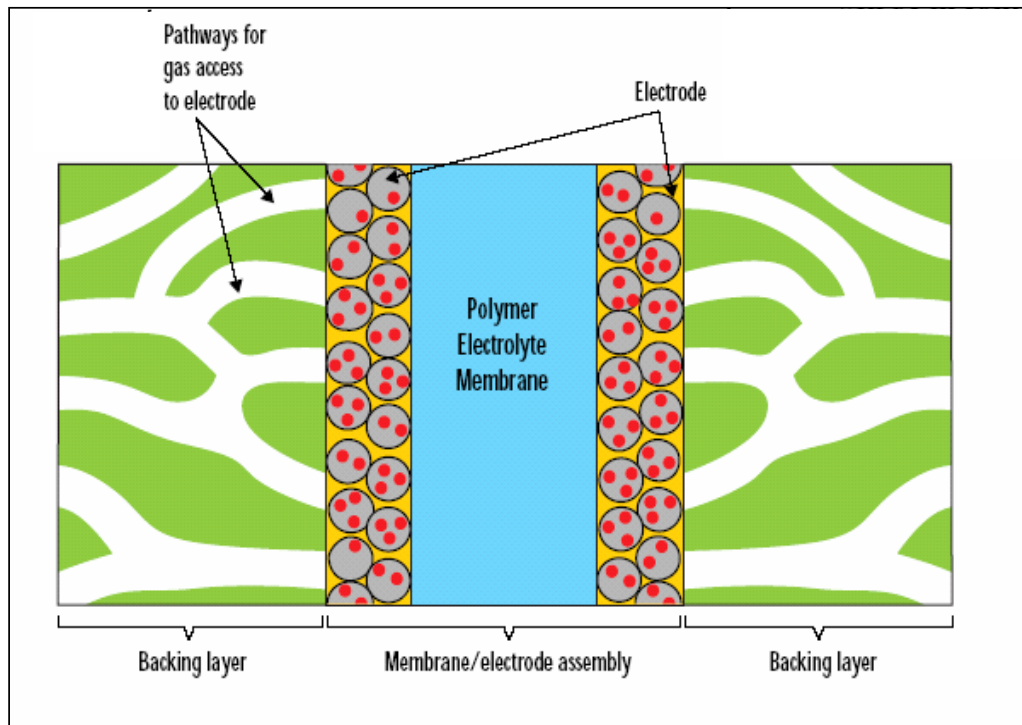


**Figure 2.12<sup>1</sup>** Membrane electrode assembly with backing layer as anode and cathode substrates; The porous structure in the backing layer act as tiny channels which carry fuel and oxidant to the catalyst layers

The backing layer should be sufficiently hydrophobic to prevent the pores of the carbon paper or cloth from flooding. The hydrophobicity can usually be provided by making the backing layer waterproof with PTFE in order to obtain rapid and continuous diffusion of fuel.

Other hardware flow fields may be used in the proton exchange membrane fuel cell to control the fuel and oxidant flow and provide current and heat conductions. Flow fields are made of gas impermeable strong, light-weight plates. In order to achieve these specifications, metals such as aluminum, stainless steel titanium and nickel, or graphite plates are used. Since corrosive environment of the fuel cells, metals are coated with hydrocarbon based coating materials in order to provide corrosion protection. Composites of metal or electrically conductive carbon fiber and graphite are also used while manufacturing flow fields. Baird et al.<sup>47,48</sup> has successfully manufactured fiber-graphite composite flowfields and bipolar plates using rapid wet-lay process which may decrease the manufacturing costs. The plate surface is channel-patterned to ensure that the fuel is evenly distributed into the membrane electrode assembly via the anode. The role of the flow field on the cathode is more complex than that of on the anode. At the cathode, the flow field plays the important role on the removal of product water. The pressure difference between inlet and outlet of the flow field due to the turbulent gas flow require compressive forces to drive the reactants to MEA. However, the pressure drop can be lowered using parallel flow through many channels. Hence, flow field design minimizing the pressure drop may be advantageous, depending on the nature and concentration of the

---

<sup>47</sup> Baird, D.G.; Huang, J.; McGrath, J.E., *Plastic Engineering* 2003, 59,46

<sup>48</sup> a. Huang, J.; Baird, D.G., *Annual Technical Conference-Society of Plastic Engineers* 2003, 61, 2151, b. Huang, J.; Baird, D.G.; McGrath, J.E., *J. Power Sources* 2005, 150, 110

fuel or reactant. There are differently patterned flow fields which aim to transport water out. Among many others, two of well known flow fields are depicted in Figure 2.13<sup>5</sup>. In first design Figure 2.13a, although parallel gas channels lower the pressure difference, product water easily clogged the channels and reactant distribution became inhomogeneous. Since, the reactant is not distributed to any parts of the MEA, and the MEA becomes partially inactive. The serpentine flow fields (Figure 2.13 b) avoid blocking the channels by product water at the expense of the higher pressure difference. Hence, reactant flow rate flows. However, higher reactant flow rate can be obtained by increasing the number of channels in serpentine flow fields.

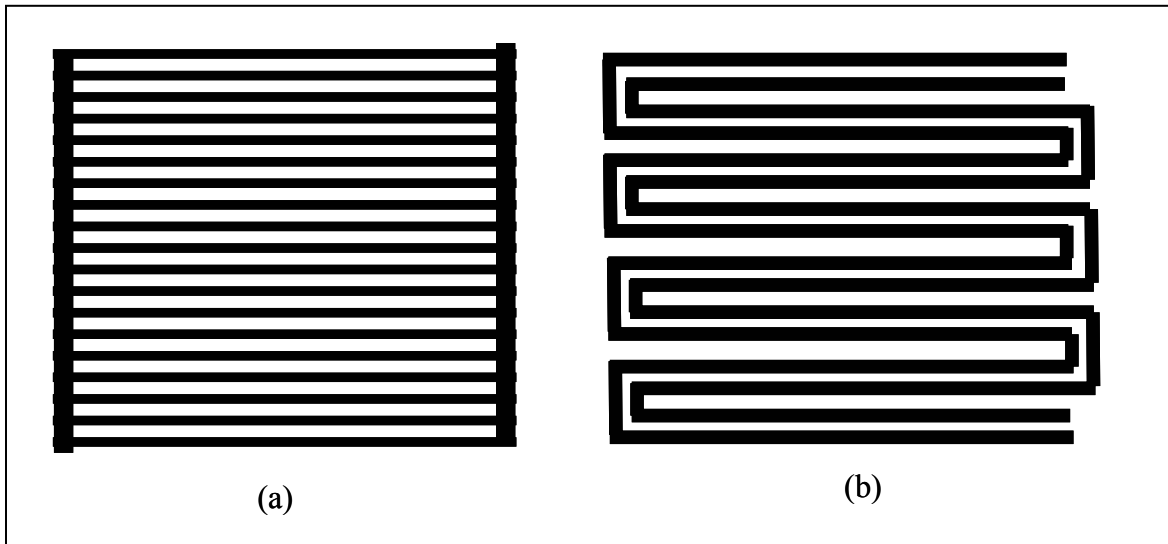


**Figure 2.13** Two different flow fields: a) Parallel flow field, b) Serpentine flow field

#### **2.3.5.4 PEMFC Stacks**

Fuel stacks are essential to get useful power to run effective commercial electric motors, which typically operates at 200-300 volts. Since each cell can only generate about one volt<sup>5-7</sup>, bipolar plates made of electrically conductive, gas-impermeable materials are used to combine each fuel cell into a series of fuel cell stacks. Bipolar plates and flow fields are actually the same material. Bipolar plates in the fuel cell stacks on both sides contain machined flow fields in order to decrease the number of flow fields which decreases the weight and size of the fuel cell stack. Bipolar plates basically separate the one cell from the next and also prevent the mixing of fuel and oxidants of each fuel cell. The produced electrons from each fuel cell are transported through the end plate, which are located at the two ends of the fuel cell stack by bipolar plates. A fuel cell and fuel cell stacks are depicted in Figure 2.14 and Figure 2.15.

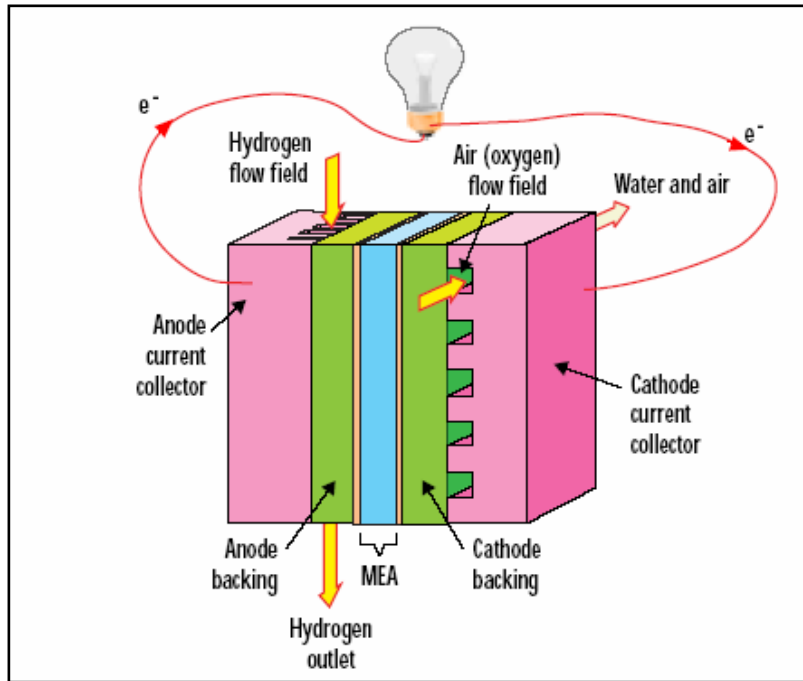


**Figure 2.14**<sup>1</sup> A more complete depiction of a fuel cell includes flow field (current collector), backing layer and MEA

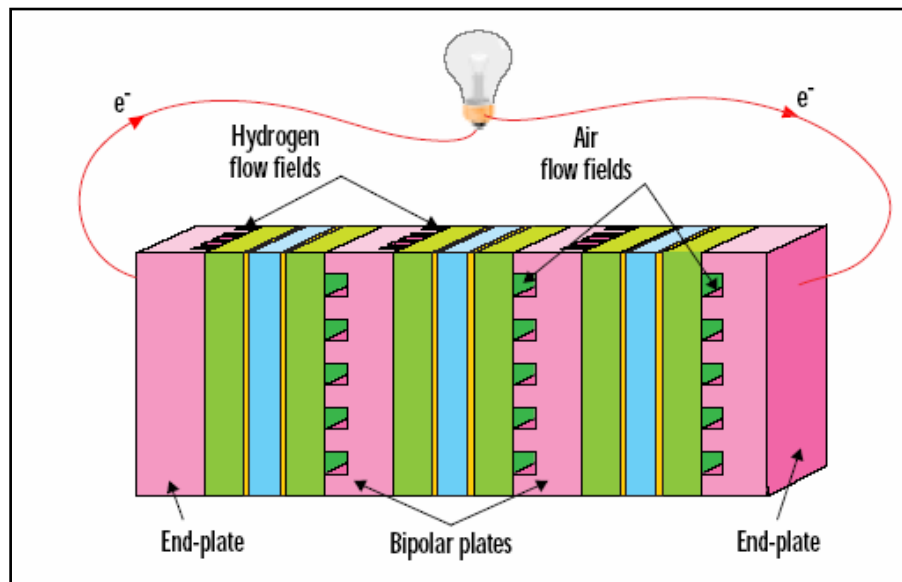


**Figure 2.15**<sup>1</sup> A fuel cell stack made by combining three cells via bipolar plates; The stack was capped with an endplate

## 2.4 Proton Exchange Membranes (PEM)

The proton exchange membranes are solid-electrolytes, which transfer the protons selectively from the anode to the cathode and also act as a solid barrier to prevent the mixing of fuel and oxidants. The desirable properties of proton exchange membranes have been pointed out in literature<sup>49,50</sup>. However, the critical issues to all high performance proton exchange membranes were listed below by McGrath et al.<sup>51</sup> include,

- a) High protonic conductivities
- b) Low electronic conductivity
- c) Low permeability to fuel and oxidants
- d) Low water transport through diffusion and electro-osmosis
- e) Oxidative and hydrolytic stability
- f) Good mechanical properties both in dry and hydrated state
- g) Cost effective
- h) Capable of fabrication into membrane electrode assemblies (MEAs)

Over a last two decades, research groups have been focused on improving the critical issues listed above in order to replace the expensive perfluorinated sulfonated copolymers. Some of these attempts and current state-of-art (Nafion<sup>TM</sup>) will be discussed in this review.

---

<sup>49</sup> Savadogo, O., *J. New Mat. Electrochem. Sys.* 1998, 1, 47.

<sup>50</sup> Appleby, A.J.; Fouelkes, R.L., *Fuel Cell Handbook*, Van Nostrand Reinhold, New York, 1989

<sup>51</sup> Hickner, M.A.; Ghassemi, H.; Kim, Y.S.; Einsla, B.R.; McGrath, J.E., *Chemical Reviews* 2004, 104, 4587

### 2.4.1 Perfluorinated Copolymers

Perfluorinated polymers contain a hydrophobic tetrafluoroethylene backbone and a sulfonated side chains of ether-linked fluoro-carbons<sup>52,53</sup>. The fluorine containing copolymers exhibit very good thermal and oxidative stability. The well-known chemical and thermal stabilities under various conditions including strong bases, strong oxidizing and reducing agents have been extensively reported<sup>54,55</sup>. Since, the strong carbon fluorine bond is quite stable to oxidative conditions found in the fuel cell environment, the development of perfluorinated copolymers increased confidence in the application of proton exchange membrane fuel cells.

Nafion™, Flemion, Aciplex, and the Dow membrane are well known perfluorinated ionomer membranes. Among these membranes Nafion™, produced by Dupont, is the most commercially successful. Nafion™ and related composite systems has the largest body of literature devoted to its study because of industrial importance and availability. A number of review articles emphasizing the structural and physical properties<sup>56,57</sup>, transport properties<sup>58,59</sup> and application<sup>60</sup> of perfluorinated ionomer membranes have been reported. The perfluorosulfonic acid groups provide the proton conductivity, while fluorination provides the better water management, because of the

---

<sup>52</sup> Kordesch, K.; Simader, G., *Fuel Cells and their Applications* 1996, Wiley-VCH, p.72

<sup>53</sup> Eisenberg, A.; Yeager, H.L., *Perfluorinated Ionomer Membranes*; ACS Symposium Series #180:1982

<sup>54</sup> Liebhafsky, H.A.; Cairns, E.J., *Fuel Cells and Fuel Batteries*, John Wiley and Sons, Inc., New York, 1968

<sup>55</sup> Kerr, J.A., *Chem. Rev.* 1996, 66, 465.

<sup>56</sup> Fernandez, R.E.; In *Polymer Data Handbook*; Oxford University Press, 1999; p.233

<sup>57</sup> Mauritz, K.A.; Moore, R.B., *Chem. Rev.* 2004, 104, 4535

<sup>58</sup> Gierke, T.D.; Hsu, W.Y., In *Perfluorinated Ionomer Membranes*; Eisenberg, A.; Yeager, H.L., Eds.: ACS Symposium Series 180, Chapter 13, 1982; p 283

<sup>59</sup> Pourcelly, G.; Gavach, C., In *Proton Conductors, Solids, Membranes, and Gels-Materials and Devices*; Colomban, P., Eds.: Cambridge University Press: Cambridge, UK, 1992

<sup>60</sup> Heitner, W.C., *J. Membr. Sci.* 1996, 120, 1

lower swelling. As has been demonstrated by many similar studies, perfluorinated ionomer membranes have excellent water dependent-proton conductivity and high durability in a fuel cell environment. The proton conductivity of Nafion™ at 80 °C and 100% humidity has been reported to be as high as about 0.2 S/cm. Steck reported that the lifetimes of the Nafion™ membrane could be as high as 60 000 hours where the fuel cell is operated at 80°C<sup>61</sup>.

Proposed chemical structure of commercially available perfluorinated copolymers (Nafion™, Flemion, Aciplex, Dow membrane) are given in Figure 2.16<sup>62</sup>. Nafion™ is produced at different equivalent weights (EW) such as 900, 1100 and 1200. However, the Nafion™ having 1100 equivalent weights with 2, 5 and 7 mils thickness has been commercialized as Nafion™ 112, Nafion™ 115 and Nafion™ 117, respectively.

---

<sup>61</sup> Steck, A., In *Proceedings of the First International Symposium on New Materials for Fuel Cell Systems*: Savadogo, O., Roberge, P.R; Veziroglu, T.N., .Eds., Montreal, 1995, p.74

<sup>62</sup> Rikukawa, M.; Sanui, K., *Prog. Polym. Sci.* 2000, 25, 1463

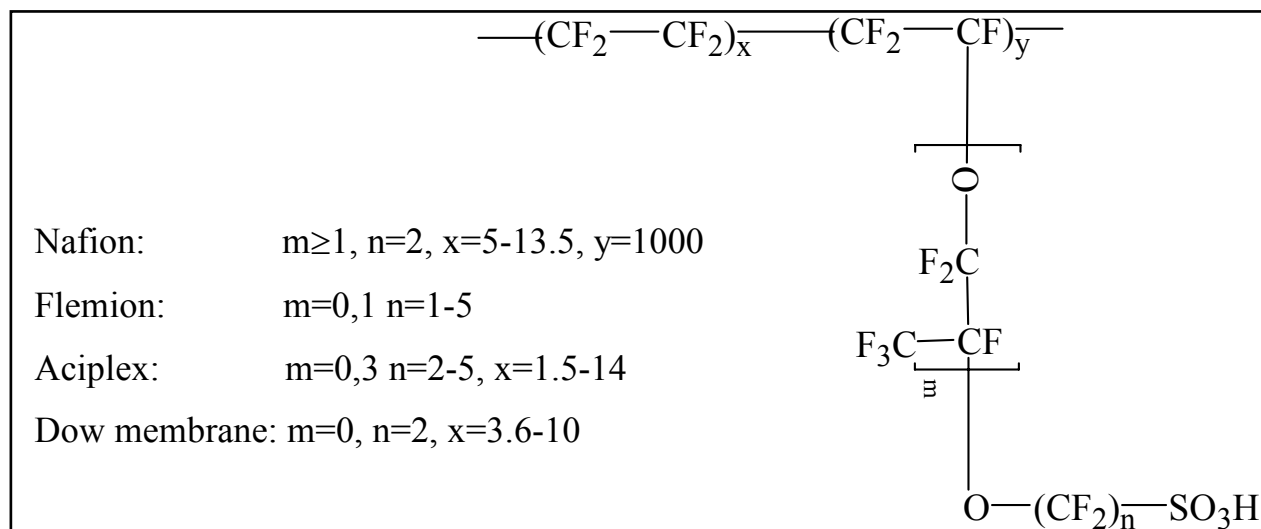


**Figure 2.16** Chemical structures of commercially available sulfonated perfluoro copolymers (*reprinted from reference 62 with permission from Elsevier*)

The Dow Company developed a Nafion™ like perfluorinated polymer (Figure 16) with an equivalent repeat unit molecular weight of this polymer of 800<sup>62</sup>. The Dow polymer has essentially the same backbone structure as the Nafion™ membrane. The major difference between Nafion™ and Dow membrane was lower EW value and smaller thickness of Dow membrane. Dow XUS® membrane was manufactured at 2-mil thickness, while early-commercialized Nafion™ membranes were at about 5-7 mil thicknesses<sup>63,64</sup>. Hence, the Dow copolymer having relatively shorter side chain showed

<sup>63</sup> Wakizoe, M.; Velev, O.A.; Srinivasan, S., *Electrochim. Acta* 1995, 40, 335

<sup>64</sup> Srinivasan, S.; Velev, O.A.; Parthasarthy, A.; Manko, D.J.; Appleby, A.J., *J. Power Science* 1991, 36, 299

better cell performance in direct hydrogen fuel cells with 10000h durability<sup>65,66,67</sup>. The properties of the Dow membrane were probably a major cause for which Dupont decreased the EW and thickness of Nafion™ membranes. However, it is crucial to point out that decreasing the membrane thickness lowers the membrane resistance (ohmic resistance) and improves the hydration of material at the expense of durability of the membrane and fuel crossover which lowers the fuel efficiency and oxygen reduction kinetic. Similarly, Asahi glass company and Asahi Chemical Industry produced Nafion™ like ionomer polymers at varying side chain length, which are named as Flemion and Aciplex<sup>62</sup> (Figure 2.16). However, the Dow membrane is no longer available. The 3M company has reported a similar system<sup>67b</sup>.

However, perfluorinated ionomer membranes suffer serious disadvantages such as poor proton conductivities at low humidities or elevated temperatures, high methanol permeability, high water permeability, relatively low mechanical strength, moderate glass transition temperature and high cost. In addition to these problems, the difficulty in the chemical synthesis of the perfluorinated copolymers due to the safety concerns of tetrafluoroethylene and the cost/availability of the perfluoroether comonomers has introduced new alternative membranes to Nafion™. Poly(oxy-1,4-phenyleneoxy-1,4-phenylenecarbonyl-1,4-phenylene) (PEEK)<sup>68,69</sup>, poly(1,4-phenylene)<sup>70,71</sup>, poly(oxy-1,4-

---

<sup>65</sup> Tant, Martin R.; Darst, Kevin P.; Lee, Katherine D.; Martin, Charles W., Dow Chem. USA, Freeport, TX, USA. ACS Symposium Series, 1989, 395

<sup>66</sup> Eisman, G.A., *Journal of Power Sources* 1990, 29, 389

<sup>67</sup> a. Srinivasan, S., In *Program and Abstracts of Fuel Cell Seminar*, Long Beach, CA, 1988, p 324, b. Hamrock S., ACS: Advances in Materials for Proton Exchange Membrane Fuel Cell Systems, February 2005, Asilomar CA

<sup>68</sup> Bredas, J.L.; Chance, R.R., Silbey, R., *Phys. Rev.* 1982, 26, 5843

<sup>69</sup> Kobayashi, H.; Tomita, H.; Moriyama, H., *J. Am. Chem. Soc.* 1994, 116, 3153

<sup>70</sup> Qi, Z.; Pickup, P.G., *J. Chem. Soc. Chem. Commun* 1998, 15

phenylene)<sup>72</sup>, poly(phenylene sulfide)<sup>73</sup> are some candidate polymers which have been used as a backbone for proton exchange membranes. Of course they have no proton conducting units. One of the new membrane concepts includes replacing the tetrafluoroethylene-based backbones with commercially available, cost effective, easily synthesized styrene and particularly its fluorinated derivatives.

#### 2.4.2 Styrene Based Proton Exchange Membranes (PEM)

The most basic polymer in this class is poly(styrene sulfonic acid). In 1960's, the poly(styrene sulfonic acid), and its derivatives such as phenol sulfonic acid resin and its fluorinated analogous such as poly(trifluorostyrene sulfonic acid) were suggested as proton exchange membrane in fuel cells<sup>62</sup>. One of the first attempts was using crosslinked polystyrene sulfonic acid in the Gemini program by NASA<sup>74</sup>. Since these membranes were not chemically and oxidatively stable in the fuel cell environment, NASA employed the alkaline fuel cell in their subsequent missions<sup>21</sup>. Therefore, all means of synthesis techniques such as crosslinking, grafting were used to improve the chemical and oxidative stability of these polymers<sup>75,76</sup>

Ballard Advanced Materials Corporation introduced a series of sulfonated copolymers of substituted  $\alpha,\beta,\beta$ -trifluorostyrene, named BAM membranes<sup>77</sup>. These membranes, which were one of the most stable polystyrene analogue were reported to

---

<sup>71</sup> Kobayashi, T; Rikukawa, M.; Sanui, K.; Ogata, N.; *Solid State Ionics* 1998, 106, 219

<sup>72</sup> Chalk, A.J.; Hay, A.S., *J. Polym. Sci. A* 1968, 7, 691

<sup>73</sup> Qi, Z.; Lefebvre, M.C.; Pickup, P.G., *J. Electroanal. Chem.* 1998, 459, 9

<sup>74</sup> Watkins, D.S., In *Fuel Cell Systems*; Blomen, L.J.M.J; Mugerwa, M.N., Milenium Press: NewYork, 1993, p 493

<sup>75</sup> Carette, N.; Tricoli, V.; Picchioni, F., *J. Membr. Sci.* 2000, 166,189

<sup>76</sup> Buchi, F.N.; Gupta, B.; Haas, O.; Scherer, G.G., *Electro Chim Acta* 1995, 40, 345

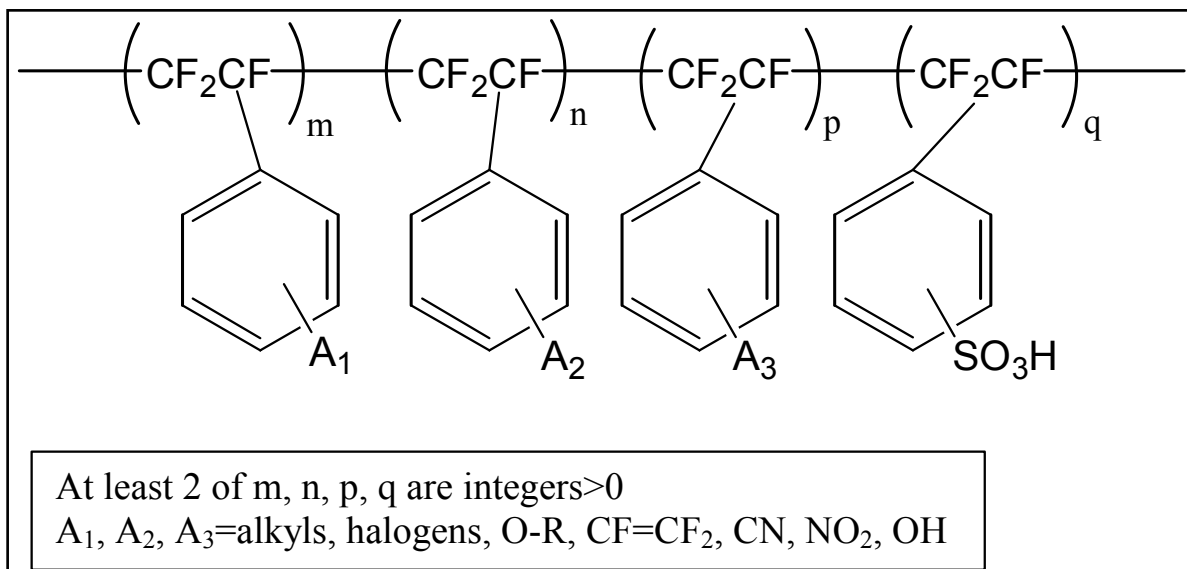
<sup>77</sup> Wei, J.; Stone, C.;Steck, A.E., *U.S. Patent, 5,422,411*, (1995)

exhibit superior performance to both Nafion™ and Dow membranes. The fluorinated backbone provides the long term durability perhaps by reducing the hydroperoxide attack on the benzylic position in the fuel cell environment. It has been reported that  $\alpha,\beta,\beta$ -trifluorostyrene, Ballard's third generation proton exchange membrane (BAM3G) (Figure 2.17) exhibited high proton conductivity, about 0.08 S/cm<sup>78</sup> and high durability, over 100 000h<sup>77</sup>. These membranes with smaller equivalent weights between 375 and 920 show higher water uptake than that of Nafion™ and Dow membranes<sup>79</sup>. Their mechanical properties have not been reported, but it is likely they are brittle.

---

<sup>78</sup> Basura, V.I.; Chuy, C.; Beattie, P.D.; Holdcroft, S., *J. Electroanal. Chem.* 2001, 5011, 77

<sup>79</sup> Wakizoe, M.; Velev, O.A.; Srinivasan, S., *Electrochimica Acta* 1995,40, 335



**Figure 2.17** Chemical structure of various Ballard advanced materials (BAM) copolymers (*reprinted from reference 51 with permission from ACS*)

Styrene/ethylene-butene/styrene triblock copolymers, which were commercialized as Kraton-G by the Shell Company, are well known commercial block copolymers<sup>80</sup>. Dais Analytic developed membranes for proton exchange membrane fuel cells by sulfonating the styrene/ethylene-butene/styrene triblock copolymers. The proposed chemical structure of the copolymer can be seen in Figure 2.18. The conductivities of these membranes, which vary between 0.07 and 0.1 when fully hydrated, are comparable to Nafion™ membranes<sup>81,82,83</sup>. Although these membranes are comparable and they are

<sup>80</sup> Ehrenberg, S.G.; Serpico, J.M.; Wnek, G.E.; Rider, J.N., *U.S. Patent, 5,468,574*, (1995)

<sup>81</sup> Wnek, Gary, Abstract of Papers, 222<sup>nd</sup> ACS National Meeting, Chicago, IL, United States, August 26-30, 2001 (2001)

less expensive than perfluorinated copolymers, the main drawback with these membranes are their lower stability in fuel cell environment since the aliphatic hydrocarbon backbone is oxidatively unstable. Thus, Dais membranes are mostly available for the portable fuel cell power sources of 1kW or less, for which operating temperatures is less than 60 °C.

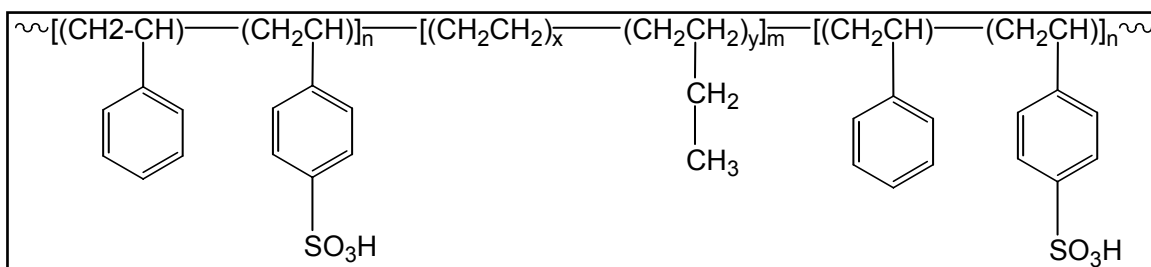


**Figure 2.18** Chemical structure of styrene/ethylene-butene/styrene triblock copolymers  
(reprinted from reference 51 with permission from ACS)

Another approach investigated is the grafting of an ion containing polymers on to a polymer backbone. Holdcroft et al.<sup>84</sup> reported that the length of the graft and the number density of the graft chains could be used as design criteria. Since the length of the graft and number density of the graft chains determine the size of the ionic domains and number of ionic domains per unit volume respectively. Moreover, the degree of connectivity of the ionic domains is controlled by both size and number density of ionic domains.

<sup>82</sup> Kim, J.; Kim, B.; Jung, B., *Journal of Membrane Science* 2002, 207 (1), 129.

<sup>83</sup> Wnek, G.E.; Rider, J.N.; Serpico, J.M.; Einstet, A.G.; Ehrenber, S.G.; Raboin, L.A., *Proceedings-Electrochemical Society* (1995), 95-23 (Proton Conducting Membrane Fuel Cells I), 247-251

<sup>84</sup> Ding, J.; Chuy, C.; Holdcroft, S., *Macromolecules* 2002, 35, 1348

The stable free radical polymerization (SFRP) technique has recently been employed in order to synthesize ionic macromonomers, which are then grafted on to a hydrophobic backbone. Holdcraft et al.<sup>84</sup> reported this class of copolymer consists of styrenic main chain and sodium styrenesulfonate graft chains (PS-*g-mac*PSSNa). The synthetic scheme depicted in Figure 2.19. The same synthetic approach was applied for poly(acrylonitrile) backbone. The membrane properties such as ionic domain morphology, water uptake, proton conductivity, oxygen permeability and solubility can be better controlled by varying the type of backbone and also the length of graft chain. Although the structure property relationship was well established with grafting approach, these membranes are oxidatively instable due to ease of degradation of poly(styrene) backbone or poly(styrene sulfonate) grafts.

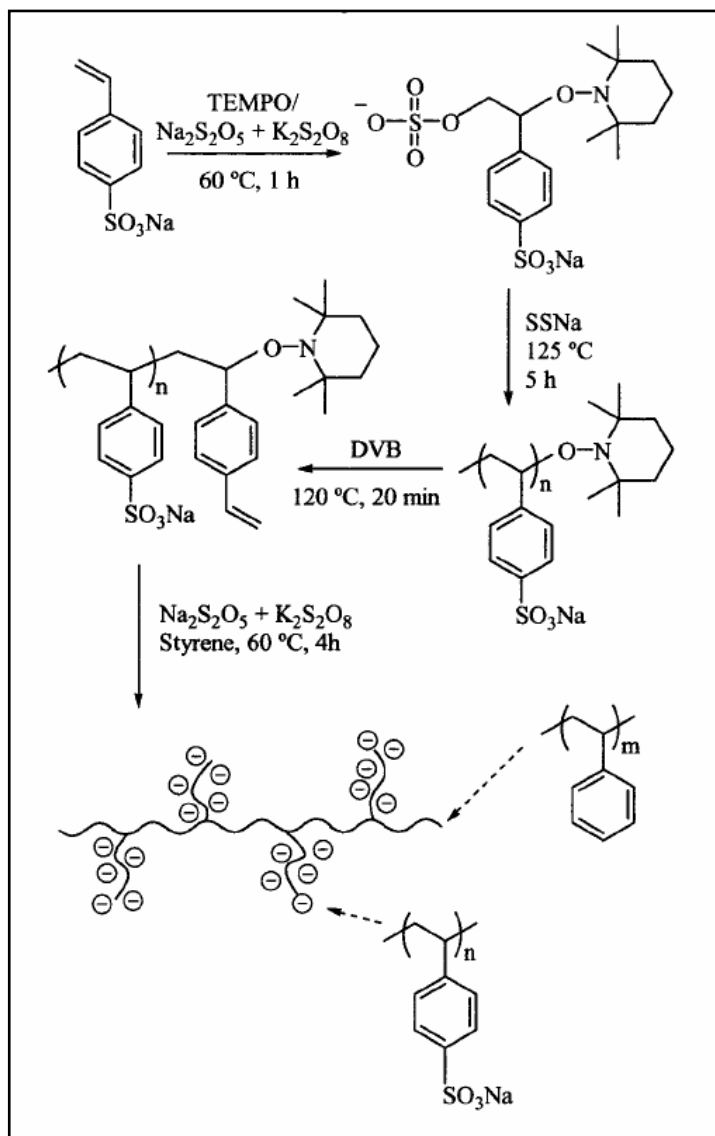


**Figure 2.19** Chemical structure of polystyrene-graft-polystyrenesulfonic acid copolymers (*reprinted from reference 84 with permission from ACS*)

Poly(styrene sulfonic acid) can also be grafted on to partially fluorinated copolymers such as poly(tetrafluoroethylene)<sup>85</sup>, the copolymer of tetrafluoroethylene and perfluoropropylene, poly(tetrafluoroethylene-co-hexafluoropropylene)<sup>76</sup>, poly(ethylene-alt-tetrafluoroethylene) and poly(fluorovinylidene)<sup>86,87</sup> by a radiation grafting technique. This technique includes the irradiating the preformed membranes to produce the reactive species on the backbones of these copolymers. Poly (styrene) is grafted on to these backbones and membranes are then sulfonated by chlorosulfonic acid.

The extent of grafting which determines the resulted membrane properties can be controlled by choice of diluent, grafting temperature, and grafting time. In order to increase the mechanical strength of these membranes and achieve better water management, some of these membranes were crosslinked using divinylbenzene<sup>88,89</sup>. Some of radiation grafted copolymers are depicted in Figure 2.20. Basically, membrane properties of these radiation grafted copolymers as a proton exchange membrane, plus cost of the membranes was better than Nafion™. However, free radicals (.OH) resulted from side reactions when fuel cell operates attack on the polystyrene grafts and lead to loss of poly(styrenesulfonic acid) groups and thus the loss of ion exchange capacity after a short time operating in a fuel cell environment<sup>90</sup>.

---

<sup>85</sup> Guzman-Garcia, A.G.; Pintauro, P.N.; Verbrugge, M.W.; Schneider, E.W., *J. Appl. Electrochem.* 1992, 22, 204

<sup>86</sup> Holmberg, S.; Lehtinen, T.; Nasman, J.; Ostrovskii, D.; Paronen, M.; Serimaa, R.; Sundholm, F.; Sunholm, G.; Torell, L.; Torkkeli, M., *J. Mater. Chem.* 1996, 6, 1309

<sup>87</sup> Flint, S.D.; Slade, R.C.T., *Solid State Ionics* 1997, 97, 299

<sup>88</sup> Gupta, B.; Buchi, F.N.; Scherer, G.G., *J. Polym. Sci., Part A: Polym. Chem.* 1994, 32, 1931

<sup>89</sup> Gupta, B.; Schere, G.G., *Chimia* 1994, 48, 127

<sup>90</sup> Hubner, G.; Roduner, E., *J. Mater. Chem.* 1999, 9, 409

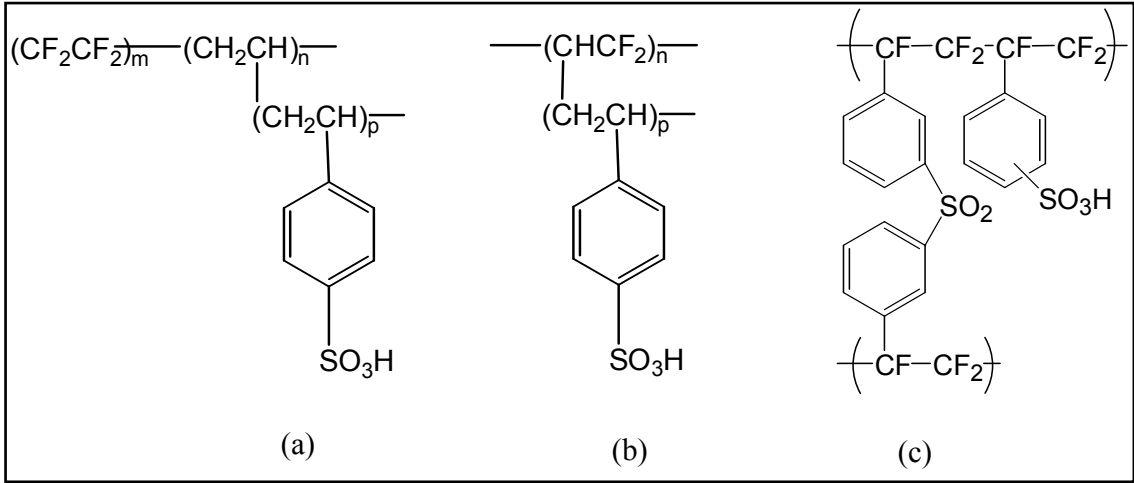


**Figure 2.20** Some of radiation grafted copolymers

### 2.4.3 Poly (arylene ether)s

Hydrocarbon based aromatic polymers have many advantages such as their availability, processability, wide variety of chemical composition and anticipated stability in the fuel cell environment. The poly(arylene ether) family includes poly(arylene ether ether ketones), poly(arylene ether sulfone) and their derivatives which exhibits excellent thermal, hydrolytic and chemical stability against to corrosive environments. The chemical structures of poly(arylene ether)s can be varied by proper molecular design as shown in Figure 2.21.

The stability of these copolymers even with introduction of the proton conductive sites, makes them particularly attractive in PEM fuel cell area. The proton conductivity of the copolymer can be achieved by both a polymer post-modification approach and

direct copolymerization of sulfonated monomers to convert them to their ionomer form to maintain stable proton conduction during fuel cell operation.

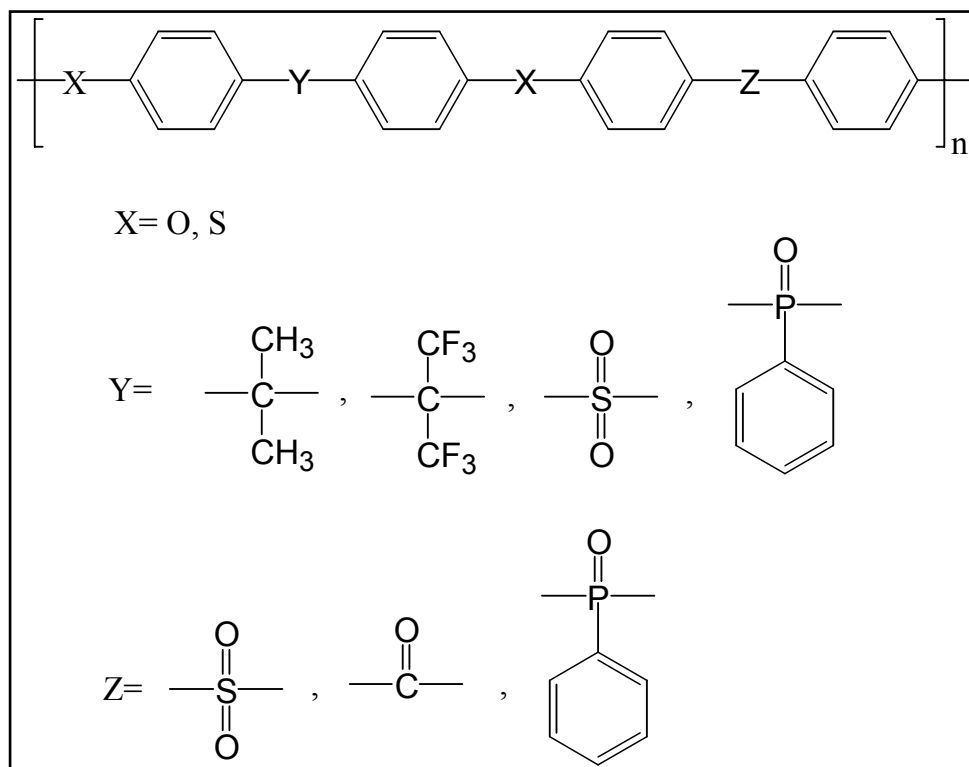


**Figure 2.21** Chemical structure of poly(arylene ether sulfone)s; Various random copolymers are possible by a one step copolymerization reaction (*reprinted from reference 51 with permission from ACS*)

### 2.4.3.1 Post Sulfonation

The post sulfonation of a aromatic ring of a polymer chain to increase the hydrophilicity and introduce the proton conductivity as a PEMs employs an electrophilic aromatic substitution reaction. Various sulfonating reagents such as concentrated sulfuric acid, fuming sulfuric acid, chlorosulfonic acid, or sulfur trioxide can be used to achieve

post modification of the polymers. However, post sulfonation reactions are usually restricted due to the following reasons:

- a. Structural change of postsulfonated polymer: Undesirable chain scission, branching, crosslinking and degradation of polymer backbone occur.
- b. Lack of precise control of degree of sulfonation
- c. Lack of precise control of location of sulfonation: Post sulfonation occurs mostly on the activated side as shown in Figure 2.22.

The most post sulfonated systems are some commercially available polymers such as poly(aryl ether sulfone) (UDEL), polysulfone, poly(ether sulfone) (Vicatex).<sup>91,92,93</sup>

Noshay and Robeson<sup>94</sup> introduced a mild sulfonation procedure where a complex of sulfur trioxide and triethyl phosphate was used to sulfonate a commercially available bisphenol-A- based poly(ether sulfone). Although using the mild conditions prevented the undesired side reactions, the sulfonic acid group is usually restricted to only one sulfonate per activated unit.

---

<sup>91</sup> Kerres, J.; Cui, W.; Eigenberger, G.; Beavers, D.; Schnurnberger, W.; Fischer, A.; Wendt, H., In *Proceeding of the 11<sup>th</sup> Hydrogen Conference*, Veziroglu, T.N.; Winter, C.J.; Baselt, J.P.; Kreysa, G., Eds., Stuttgart, Germany, (1996), p 1951

<sup>92</sup> Nolte, R.; Ledjeff, K.; Bauer, M.; Mulhaupt, R., *J. Membr. Sci.* 1993, 11

<sup>93</sup> Kerres, J.; Cui, W.; Reichle, S, *J. Polym. Sci. Part A Polym. Chem.* 1996, 34, 2421

<sup>94</sup> Noshay, A.; Robeson, L.M., *J. Appl. Polym. Sci.* 1976, 20, 1885

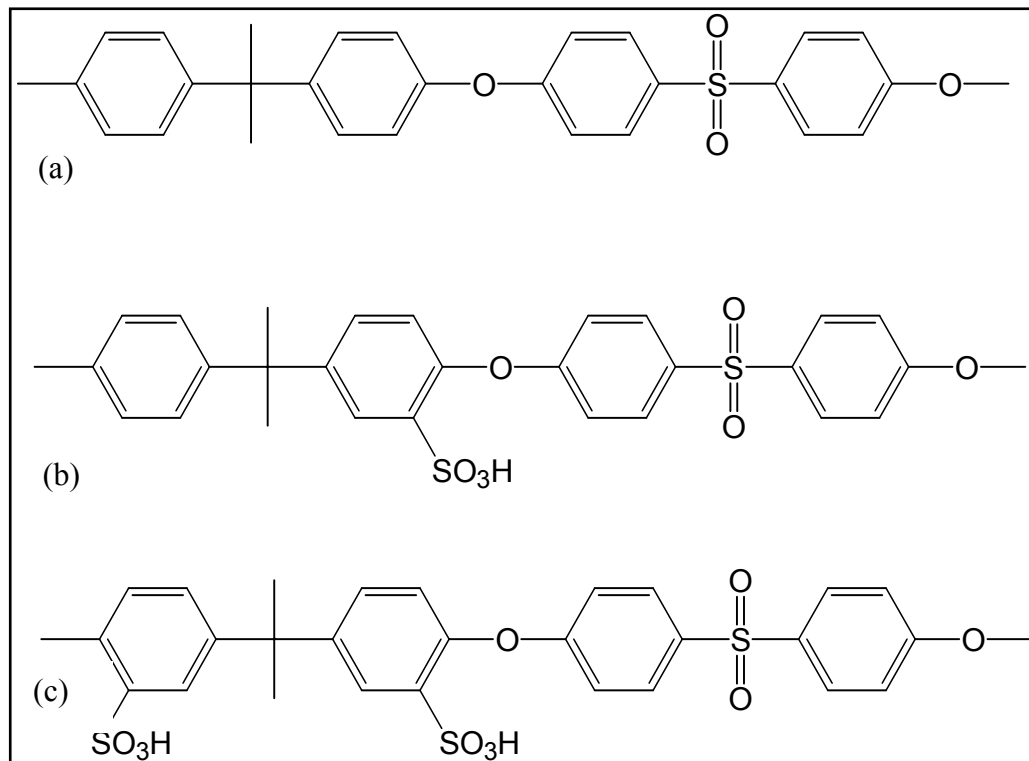


**Figure 2.22** Post sulfonation of poly(arylene ether sulfone)s; a. Backbone of poly(arylene ether sulfone), b. and c. Most probable sulfonic acid attachment to a poly(arylene ether sulfone) (*reprinted from reference 51 with permission from ACS*)

The combination of chloro sulfonic acid ( $\text{ClSO}_3\text{H}$ ) and trimethyl silylchloro sulfonate ( $(\text{CH}_3)_3\text{SiSO}_3\text{Cl}$ ) was employed to sulfonate bisphenol-A-based polymer by Genova-Dimitrova et al.<sup>95</sup> The authors indicated that strong sulfonating agent, chlorosulfonic acid, is the reason for the inhomogeneous reaction. Using a small amount of dimethyl formamide as a co-solvent makes the reaction homogenous. Although this milder sulfonation technique prevented the crosslinking and chain degradation,

<sup>95</sup> Genova-Dimitrova, P.; Baradie, B.; Foscallo, D.; Poinsignon, C.; Sanchez, J.Y., *Journal of Membrane Science* 2001, 185, 59

sulfonation efficiency of the reaction was lower for short reaction times, and longer the reaction times would increase the sulfonation efficiency at the expense of introducing some side reactions, which probably causes main chain degradation.

The poly(ether ether ketone) PEEK exhibits good thermal stability, chemical resistance, and electrical and mechanical properties. This high performance, semicrystalline polymer with both ether and ketone linkages shows limited solubility due to the crystallinity. Sulfonation of PEEK (Figure 2.23) introduces imperfections over the ordered backbone and lowered the crystallinity and increases the solubility so that these types of copolymers can be characterized. A series of sulfonated PEEKs has been reported<sup>96,97</sup>. Because of the electron attracting nature of the neighbouring carbonyl group, the oxygen-phenyl-carbonyl groups remain unsulfonated, while oxygen-phenyl-oxygen units are sulfonated. The sulfonation reaction is usually achieved by concentrated sulfuric acid because of the undesired side reactions and degradation issues with other sulfonating agents such as chlorosulfonic acid or fuming sulfuric acid.

---

<sup>96</sup> Bauer, N.; Jones, D.J.; Roziere, J.; Tchicaya, L.; Alberti, G.; Casciola, M.; Massinelli, L.; Peraio, A.; Besse, S.; Ramunni, E., *J. NewMater. Electrochem. Sysyt.* 2000, 3, 93

<sup>97</sup> Zaidi, S.M.J.; Mikhailenko, S.D.; Robertsen, G.P.; Guiver, M.D.; Kaliaguine, S., *J. Membr. Sci.* 2000, 173, 17

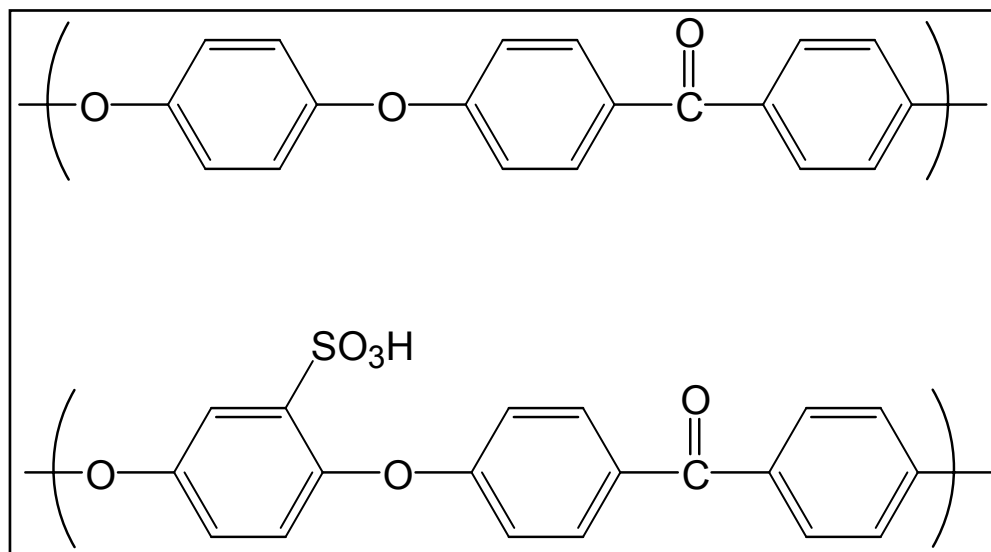


**Figure 2.23** Chemical structure of sulfonated and unsulfonated poly(ether ether ketone) PEEK (reprinted from reference 51 with permission from ACS)

The degree of sulfonation can be controlled by changing the reaction time, temperature, sulfonating agent concentration and as well as the chemical composition of the backbone. Since increasing the proportion of ether groups relative to the carbonyl groups leads to increase the number of available sites for sulfonation.

An interesting, but likely expensive and somewhat lengthy sulfonation process by Kerres et al.<sup>91</sup> includes the metalation of Udel with n-butyl lithium (n-BuLi) at low temperatures (-65 °C), sulfonation of the metallated aromatic ring with sulfur dioxide, and finally oxidation occurs. The challenge in this synthesis is to avoid crosslinking which reduces the number of conductive sites, and reduces also the ion exchange capacity while converting the lithium sulfate to sulfonic acid. In addition to crosslinking reaction, the oxidation step may result in chain degradation, which affects the overall mechanical

properties of the polymer. It was suggested that hydrogen peroxide was the best oxidant for low IEC materials, while potassium permanganate is better to avoid crosslinking or main chain degradation. Conversely, the crosslinking reaction can be considered as a design property which controls the water uptake and gas permeability at the expense of decreasing IEC<sup>98a,98b,99</sup>. The synthetic scheme can be seen in Figure 2.24. It seems doubtful that the isopropylidene group would show good stability under strong acid conditions.

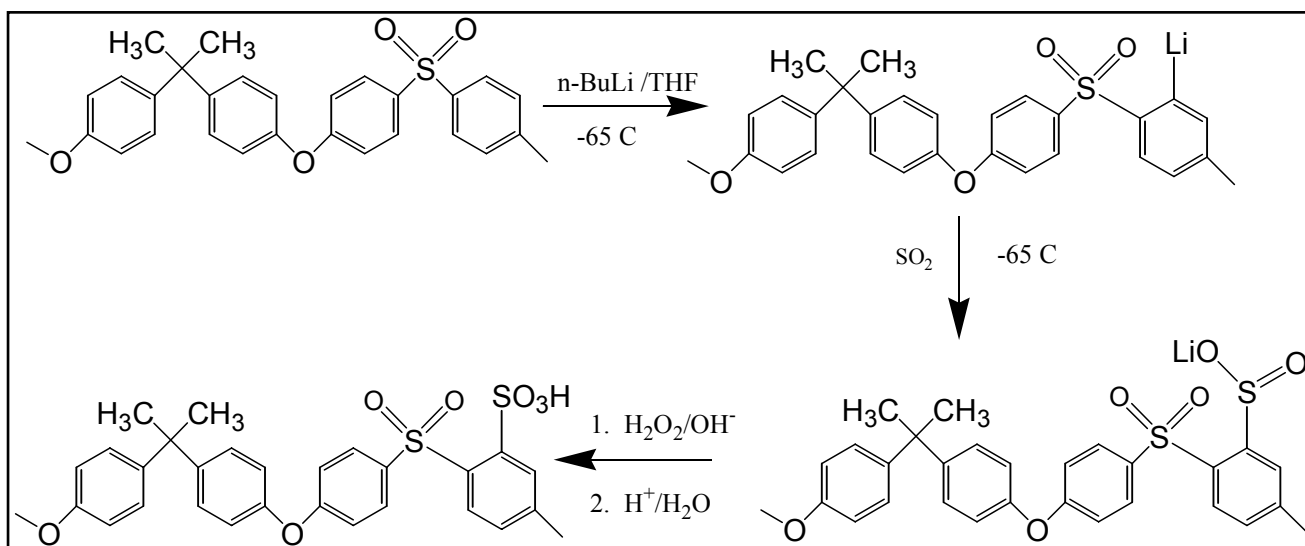


**Figure 2.24** Metalation route to sulfonated polysulfone (reprinted from reference 98b with permission from Wiley)

<sup>98</sup> a. Kerres, J.; Zhang, W.; Cui, W., *J. Polym. Sci.: Part A: Polym. Chem.* 1998, 36, 1441, b. Kerres, J.; Cui, W.; Reichle, S., *J. Polym. Sci.: Part A: Polym. Chem.* 1996, 34, 2421

<sup>99</sup> Kerres, J.; Cui, W.; Junginger, M., *J. Membr. Sci.* 1998, 139, 227

#### **2.4.3.2 Direct Copolymerization of Sulfonated Monomers**

The opportunity of precise control of the degree of sulfonation and the position is possible with monomer sulfonation and subsequent controlled copolymerization. The advantages of direct sulfonation approach over the post sulfonation are summarized as below:

- a. Precise control of degree of sulfonation: Exact control of amount of disulfonation occurs with adjustable molecular weights.
- b. Disulfonation on deactivated ring: Enhanced stability and higher acidity from two sulfonic acid groups (Figure 26) which are attached to an electron deficient aromatic ring rather than one sulfonic acid group bonded to an electron rich aromatic ring as typically occurs in post sulfonation.
- c. One step controlled copolymerization: There are no side reactions, which may cause to backbone degradation, which is one of the most undesired situations with postsulfonation.

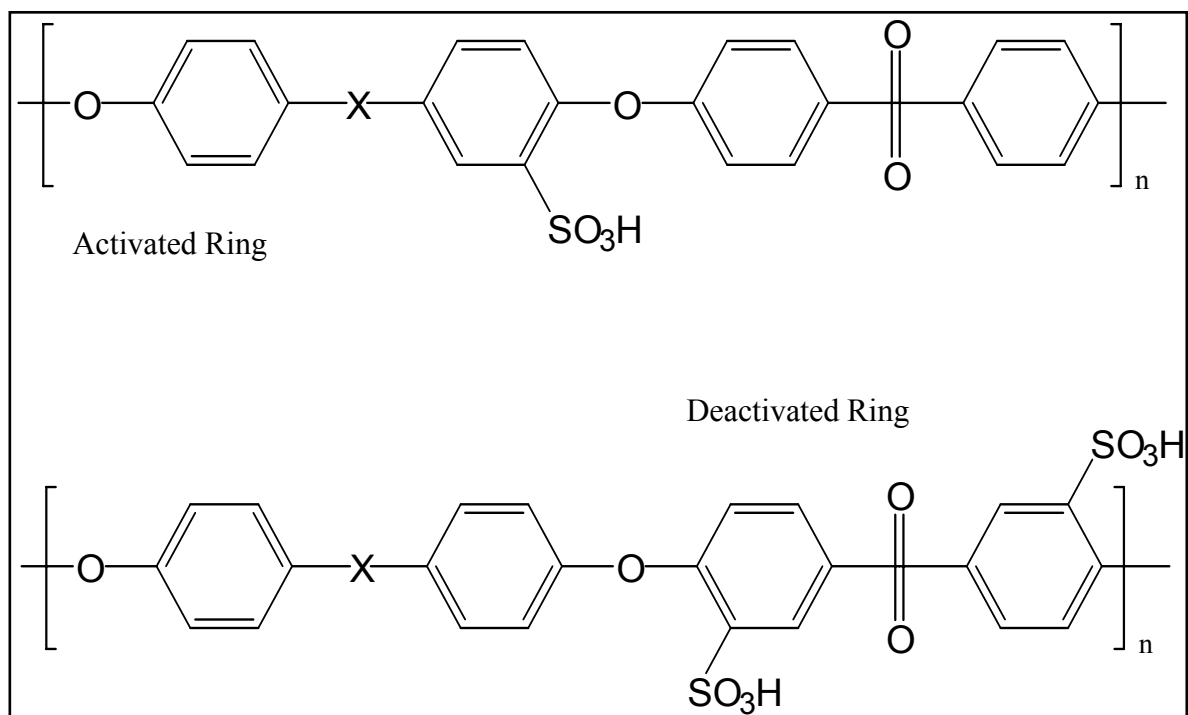


**Figure 2.25** Disulfonation of activated and deactivated ring; Sulfonic acid groups are added to activated rings is more prone to desulfonation. However, more stable behavior is possible with direct copolymerization where sulfonic acid groups are connected to deactivated rings (*reprinted from reference 51 with permission from ACS*)

The first report was from Robeson and Matzner<sup>100</sup> where the sulfonation of 4,4'-dichloro diphenyl sulfone (DCDPS) was demonstrated for the purpose of producing fire retardant materials. Ueda et al.<sup>101</sup> reported the sulfonation of 4,4'-dichlorodiphenyl sulfone and its ability to copolymerize with BPA. The synthesis procedure was further improved in our laboratory<sup>102,103,104</sup>, but has never been investigated in the depth necessary to define several parameters for synthesis of industrial scale quantities. More recently our group defined a novel procedure for the synthesis and analysis of 3,3'-disulfonated 4,4'-dichlorodiphenyl sulfone (SDCDPS) with near quantitative conversion on a kilogram scale. A direct copolymerization route incorporating disulfonated monomers into poly(arylene ether sulfone)s to prepare PEM materials has been reported (Figure 2. 26)<sup>105,106,107</sup>. This approach employs 3,3'-disulfonated, 4,4'-dichlorodiphenyl sulfone (SDCDPS) copolymerized with nonsulfonated activated aromatic dihalides and bisphenols. The stoichiometric ratio of disulfonated to nonsulfonated repeat units can be accurately controlled to tailor the water uptake, conductivities and mechanical properties of these film forming materials.

---

<sup>100</sup> Robeson, L/M; Matzner, M., *U.S. Patent 4,380,598*, 1983

<sup>101</sup> Ueda, M.; Toyota, H.; Ochi, T.; Sugiyama, J.; Yonetake, K.; Masuko, T.; Teramoto, T., *Polym. Sci. Part A: Polym. Chem.* 1993, 31, 85

<sup>102</sup> Wang, F.; Mecham, J.B.; Harrison W.L.; McGrath, J.E.; *Polymer Preprints* 2000, 40(2), 1401

<sup>103</sup> Wang, F.; Hickner, M.H.; Ji, Q.; Harrison W.L.; Mecham, J.B.; Zawodzinski, TA; McGrath, J.E.; *Macromol. Symp.* 2001, 175(1). 387

<sup>104</sup> Sankir M.; Bhanu, V.A.; Harrison, W.; Ghassemi, H.; Wiles, K.B.; Glass, T.E.; Brink, A.E.; Brink, M.H.; McGrath, J.E., *J. Appl. Poly. Sci.*, *Accepted 2005*

<sup>105</sup> Harrison, W.L.; Ph.D. Dissertation, Virginia Tech, 2002

<sup>106</sup> Harrison, W.L.; Wang, F.; Mecham, J.B.; Bhanu, V.A.; Hill M.; Kim, Y.S.; McGrath J.E.; *J. of Polymer Science: Part A Polymer Chemistry* 2003, 41, 2264

<sup>107</sup> Wang, F.; Hickner, M; Kim YS; Zawodzinski, TA; McGrath J.E.; *J. Membrane Science* 2002, 197, 231

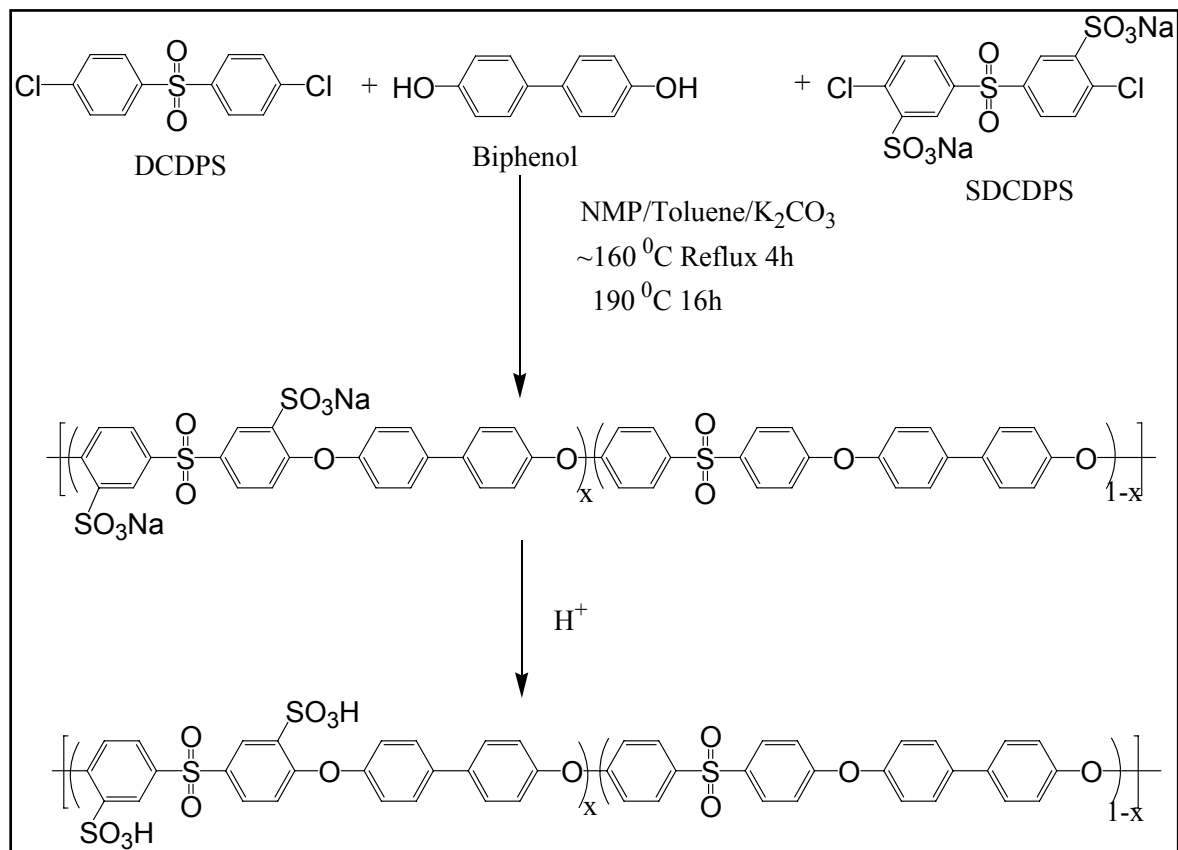


**Figure 2.26** Direct copolymerization to form disulfonated poly(arylene ether sulfone) (BPSH)

The synthesis and characterization of the sulfonated poly(arylene ether sulfone) random copolymers and their membrane characteristics such as proton conductivities, water uptake, methanol permeabilities, ion exchange capacities have been extensively studied<sup>102-107</sup>. The proton conductivities and water uptakes of this copolymers scale with

the degree of disulfonation. However, there is a threshold degree of disulfonation, usually around 50 mol percent, beyond which both water uptake and also conductivity of membranes jumps and increasing degree of disulfonation results with hydrogel formation which lower the mechanical properties. Hence, the balance between conductivity with other physical properties is essential. The water dependency of proton conductivity of these copolymers especially at higher temperatures (higher than 100 ° C) and lower relative humidity conditions (20-40 % RH), makes them relatively ineffective. Hence, McGrath's group has focused on following items in order to decrease the water dependency of the proton conductivity of the membranes

1. Preparing nanocomposites of these thermally stable, high molecular weight copolymers with inorganic particles: Strong hydrogen bonds incorporated inorganic particles such as hetero poly acids and more interestingly zirconium based inorganic compounds may provide water independent proton conductivity due to the lower activation energy (higher mobility) over the path way of the proton conductivity

2. Synthesizing the multi-block copolymers at compositions where lamella morphology is obtained: Sulfonic acid moieties or proton conductive sites in lamella morphology are better aggregated along one dimensional order. Hence, copolymers having lamella morphology might be beneficial for the higher temperature operations at lower humidities. An example of mutiblock copolymer ionomer membranes has already been published<sup>108</sup>.

---

<sup>108</sup> Ghassemi, H.; Ndip, G.; McGrath, J.E., *Polymer* 2004, 45, 5855

Several examples of direct copolymerization of different sulfonated monomers obtained in the McGrath research lab will be given in following part of this review. These sulfonated random copolymers possess similar thermal and mechanical properties of their high performance engineering thermoplastic analogues. The increase in the degree of sulfonation of these copolymers usually results in increase in glass transition temperature, enhanced membrane hydrophilicity and also intrinsic viscosity. The acid forms of these copolymers are prepared by treating the salt form of the membrane with dilute sulfuric acid.

### 2.4.3.3 Direct Copolymerization of Sulfonated Polyimides

Polyimides are high performance materials which are characterized by their excellent thermal and mechanical properties<sup>109,110</sup>. The hydrolytic stability of sulfonated polyimides in fuel cell environment depends on the type of dianhydride structure used during polymerization. The phthalic dianhydrides yields five-membered ring sulfonated polyimides which quickly degrade in fuel cell environment<sup>111</sup>. However, six-membered sulfonated polyimides from naphthalenic dianhydrides were much more stable to hydrolysis<sup>112</sup>. The typical synthesis of six-membered ring sulfonated polyimides by Genies et al.<sup>113</sup> is depicted in Figure 2.27.

---

<sup>109</sup> Feger, C.; Khojasteh, M.M.; McGrath, J.E., *Polyimides: Materials, Chemistry and Characterization*, Elsevier, Amsterdam, 1989

<sup>110</sup> Mittal, K.L., *Polyimides: Synthesis, Characterization and Applications*, Vol. 1&2, Plenum Press, New York, 1984

<sup>111</sup> Gebel, G.; Aldebert, P.; Pineri, M., *Polymer* 1993, 34, 333

<sup>112</sup> Savadogo, O., *J. New Mater. Electrochem. Syst.* 1998, 1, 47

<sup>113</sup> Genies, C.; Mercier R.; Sillion B.; Cornet, N.; Gebel, G.; Pineri, M., *Polymer* 2001, 42, 359

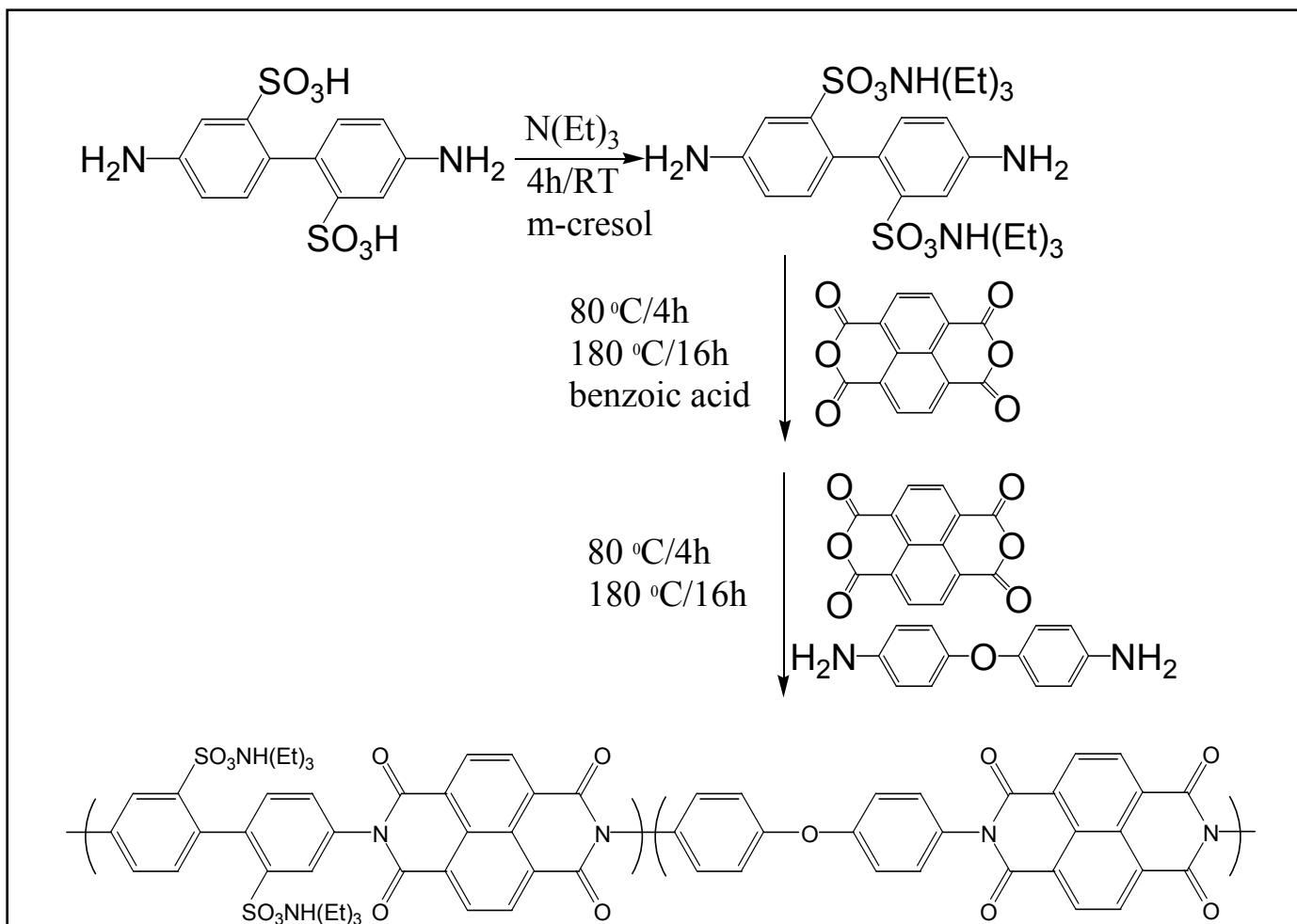


**Figure 2.27** Six-membered sulfonated polyimides includes two successive polymerization steps; First step is the condensation reaction of 4,4'-diamino-2,2'-biphenyl disulfonic acid (BDA) with 1,4,5,8-tetracarboxylic dianhydride which results with a chain with different length of the sulfonated sequence depending on the feed ratio of the monomers. Then, a calculated amount of BDA and 4,4'-oxydianiline (ODA) in SPI is used to control the degree of sulfonation (*reprinted from reference 51 with permission from ACS*)

The sulfonated polyimides from the commercially available sulfonated diamine monomer has been extensively studied mainly by French researchers<sup>114,115,116,117</sup>. In addition to commercially available sulfonated diamine (Figure 2.28a), several novel disulfonated diamines have been prepared by Gunduz et al.<sup>118,119,120</sup> (Figure 2.28 a-d) and Okamoto et al.<sup>121,122,123,124</sup>

---

<sup>114</sup> Faure, S.; Mercier, R.; Aldbert, P.; Pineri, M.; Sillion, B., *French Patent*, 96 05707, 1996

<sup>115</sup> Gebel, G.; Aldebert, P.; Pineri, M., *Polymer* 1993, 34, 333

<sup>116</sup> Genies, C.; Mercier, R.; Sillion, B.; Cornet, N.; Gebel, G.; Pineri, M., *Polymer* 2001, 42, 5097

<sup>117</sup> Vallejo, E.; Pourcelly, G.; Gavach, C.; Mercier, R.; Pineri, M., *J. Membr. Sci.* 1999, 160, 127

<sup>118</sup> Gunduz, N.; McGrath, J.E., *Polymer Preprints* 2000, 41, 180

<sup>119</sup> a. Gunduz, N.; Synthesis and Characterization of Sulfonated Polyimides as Proton Exchange Membranes Fuel Cells, Ph.D. Thesis, VPI&SU, 2001, b. Einsla, B.R.; Hong, Y.T.; Kim, Y.S.; Gunduz, N.; Wang, F.; McGrath, J.E., *J. Polymer Science, Part A: Polymer Chemistry* 2004, 42, 862, c. Einsla, B.R.; McGrath, J.E., *J. Memb. Sci.* 2005, 255, 141

<sup>120</sup> Gunduz, N.; McGrath, J.E., *Polymer Preprints* 2000, 41, 1565

<sup>121</sup> Zhou, W.; Watari, T.; Kita, H.; Okamoto, K.-I., *Chem. Lett.* 2002, 5, 534

<sup>122</sup> Fang, J.; Guo, X.; Harada, S.; Watari, T.; Tanaka, K.; Kita, H.; Okamoto, K.-I., *Macromolecules* 2002, 35, 9022

<sup>123</sup> Guo, X.; Fang, J.; Watari, T.; Tanaka, K.; Kita, H.; Okamoto, K.-I., *Macromolecules* 2002, 35, 6707

<sup>124</sup> Yin, Y.; Fang, J.; Cui, Y.; Tanaka, K.; Kita, H.; Okamoto, K.-I., *Polymer* 2003, 44, 4509

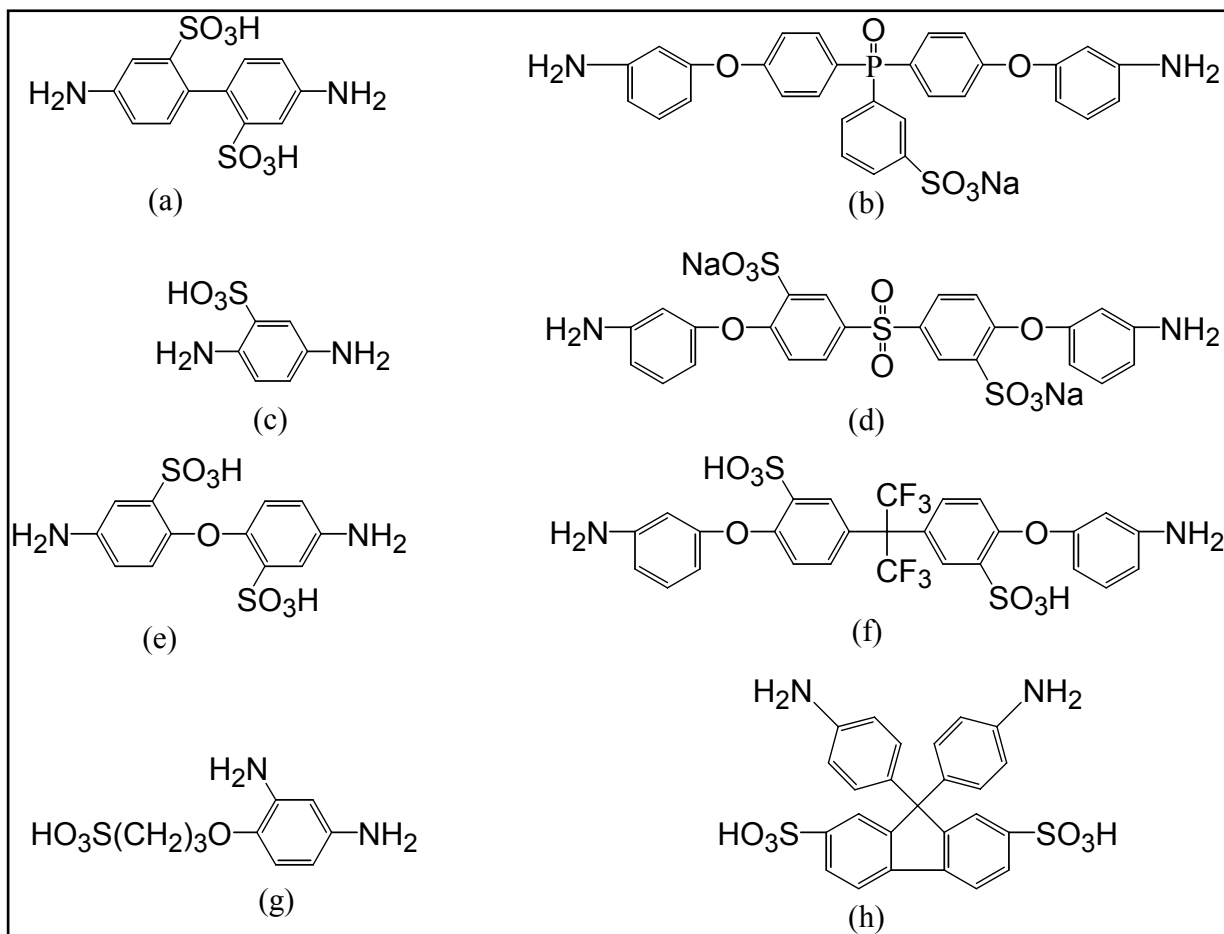


**Figure 2.28** Sulfonated diamines for direct synthesis of sulfonated polyimides; a. 4,4'-diamino-2,2'-biphenyldisulfonic acid (BDA), b. Sulfonated bis(3-aminophenoxy) phenyl phosphine oxide (s-BAPPO), c. 1,4-diaminobenzene sulfonic acid (pPDA-SO<sub>3</sub>H), d. Disulfonated 4,4'-bis(3-aminophenoxy)phenyl sulfone (s-DADPS), e. 4,4'-diamino diphenylether-2,2'-disulfonic acid, f. 2,2-bis[4-(4-aminophenoxy)phenyl] hexafluoropropane disulfonic acid, g. (2',4'-diaminophenoxy)propane sulfonic acid, h. 9,9'-bis(4-aminophenyl)fluorine-2,7-disulfonic acid (*reprinted from reference 51 with permission from ACS*)

#### 2.4.3.4 Direct Copolymerization of Sulfonated Poly(arylene ether ketone)s

Directly copolymerized sulfonated poly(arylene ether ketone) copolymers were first demonstrated by Wang et al.<sup>125,126,127</sup> using 3,3'-disulfonated 4,4'-difluorodiphenyl ketone. The chemical structure of disulfonated monomer and also a typical polymerization scheme of a disulfonated poly(arylene ether ketone) copolymer is given in Figure 2.29. High molecular weight disulfonated poly(arylene ether ketone) copolymers with good thermal stabilities were reported. However, a sulfonated poly(arylene ether ketone) copolymer from hexafluoro isopropylidene bisphenol A (6F) has yielded more thermally stable sulfonated copolymer and had a conductivity of 0.08 S/cm in liquid water at 30 °C<sup>128,129</sup>.

---

<sup>125</sup> Wang, F.; Chen, T.; Xu, J., *Macromolecular Chem. And Phys.* 1998, 199, 1421

<sup>126</sup> Wang, F.; Li, J.; Chen, T.; Xu, J., *Polymer* 1999, 40, 795

<sup>127</sup> Wang, F.; Qi, Y.H.; Chen, T.L.; Xing, Y.; Lin, Y.H.; Xu, J.P., *Acta Crystallographica Section C-Crystal Structure Comm.* 1999, 55, 871

<sup>128</sup> Hopp, R.; Wang, F.; McGrath, J.E., 2001 Summer Undergraduate Research Program, Virginia Tech, August 2001

<sup>129</sup> a. Wang, F; Hopp, R.; Kim, Y.S.; Hickner, M; Zawodzinski, T.; McGrath J.E., *Electrochemical Society Proceedings*, Philadelphia, PA, 2002, b. Yanxiang, L.; Mukundan, T.; Harrison, W.; Hill, M.; Sankir, M.; Yang, J.; McGrath, J.E., *Preprints of Symposia, ACS*, 2004, 49, 536

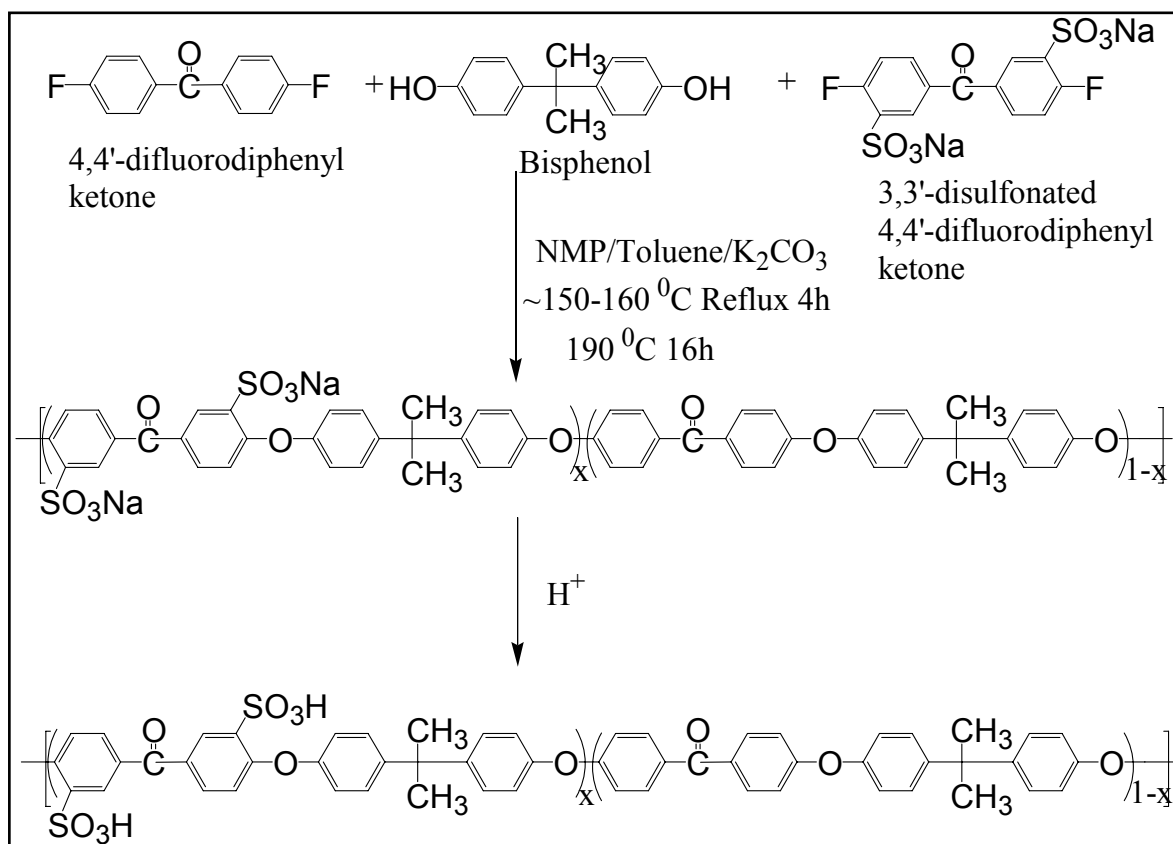


**Figure 2.29** Directly copolymerized sulfonated poly(arylene ether ketone); One step copolymerization yields sulfonated copolymer which is then acidified to utilize the copolymer as proton exchange membrane (*reprinted from reference 125 with permission from Wiley*)

#### 2.4.3.5 Direct Copolymerization of Sulfonated Poly(arylene ether phenyl phosphine oxide)s

The poly(arylene ether phosphine oxide)s are thermally quite stable high performance polymers have been extensively reported as flame retardant materials<sup>130,131,132</sup>. The sulfonation of phosphine oxide monomer to utilize in direct copolymerization reaction was achieved using fuming sulfuric acid. The resulted mono, di and tri sulfonated product preferentially purified to yield monosulfonated monomer<sup>133</sup>. The direct copolymerization reaction using 4,4'-bis(flurophenyl)phenylphosphine oxide, biphenol and monosulfonated 4,4'-bis(flurophenyl)phenylphosphine oxide is depicted in Figure 2.30. The proton conductivities of sulfonated poly(arylene ether phosphine oxide) copolymer membranes yielded lower proton conductivity compare to their poly(arylene ether sulfone) and poly(arylene ether ketone) analogs. It is believed that either mono sulfonation and/or strong hydrogen bonding between the sulfonic acid groups and phosphine oxide groups reduced the proton conductivity.

---

<sup>130</sup> Hergenrother, P.M., *Angew. Chem. Int. Ed. Engl.* 1990, 29, 34

<sup>131</sup> Smith, C.D.; Grubbs, H.J.; Webster, H.F.; Gungor, A.; Whightman, J.P.; McGrath, J.E., *High. Perf. Polym.* 1991, 4, 211

<sup>132</sup> Riley, D.J.; Gungor, A.; Srinivasan, S.A.; Sanakarapandian, M.; Tchatchoua, C.; Muggli, M.W.; Ward, T.C.; McGrath, J.E., *Polym. Eng. Sci* 1997, 37, 1501

<sup>133</sup> Shobha, H.K.; Smalley, G.R.; Sankarpandian, M.; McGrath, J.E., *ACS Polymer Preprints*, 2000, 41, 180

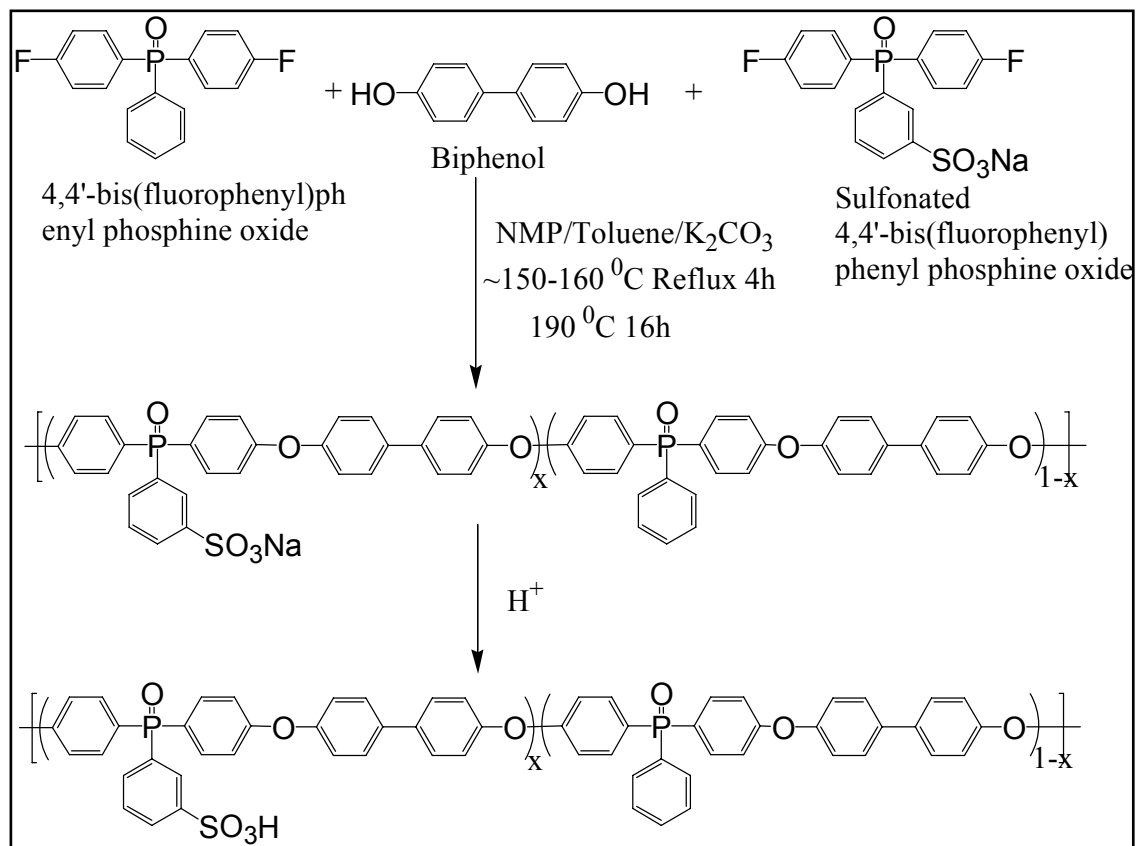


**Figure 2.30**<sup>133</sup> Directly copolymerized sulfonated poly(arylene ether phosphine oxide)

#### 2.4.3.6 Direct Copolymerization of Sulfonated Poly(arylene sulfide sulfone)s

Similar to copolymers mentioned above, poly(arylene sulfide sulfone)s are high performance engineering thermoplastic materials which have usually high glass transition temperatures, good mechanical, thermal properties and chemical resistance. The more practical method over the traditional high pressure route for preparing of poly(arylene sulfide sulfone)s has been reported by the McGrath research group<sup>134</sup>. The new A-A or A-B type thiol functional monomers such as bis-(4-mercaptophenyl) sulfone, 4-chloro-4-mercaptophenyl sulfone were used to synthesize poly(arylene ether sulfone). The disulfonated poly(arylene sulfide sulfone) copolymers were synthesized using 3,3'-disulfonated 4,4'-diflorodiphenylsulfone (SDFDPS), bis-(4-mercaptophenyl sulfone) and 4,4'-diflorodiphenylsulfone (DFDPS) by Fang et al.<sup>135</sup> to utilize them a potential membrane in proton exchange membrane fuel cells (Figure 2.31). The dithiol monomer, bis-(4-mercaptophenyl sulfone), (commercially as 4,4'-thiobisbenzenethiol) were synthesized according to procedure by Liu et al.<sup>134</sup> A series of sulfonated poly(arylene sulfide sulfone) copolymers were synthesized and membrane properties of these copolymers and fuel cell performances have been extensively studied by Wiles et al.<sup>136</sup>

---

<sup>134</sup> Liu, Y., *Ph.D. Thesis*, VPI&SU, 1998

<sup>135</sup> Wang, F.; Mecham, J.B.; Harrison, W.; McGrath, J.E., *Polymer Preprints*, 2000, 40, 180

<sup>136</sup> a. Wiles, K.B., Bhanu, V.A.; Wang, F.; Hickner, M.A.; McGrath, J.E., *Polymer Preprints*, 2003, 44, 1089, b. Wiles, K.B.; McGrath, J.E., *J.Poly. Sci, Polym. Chem* 2005,43, 2964

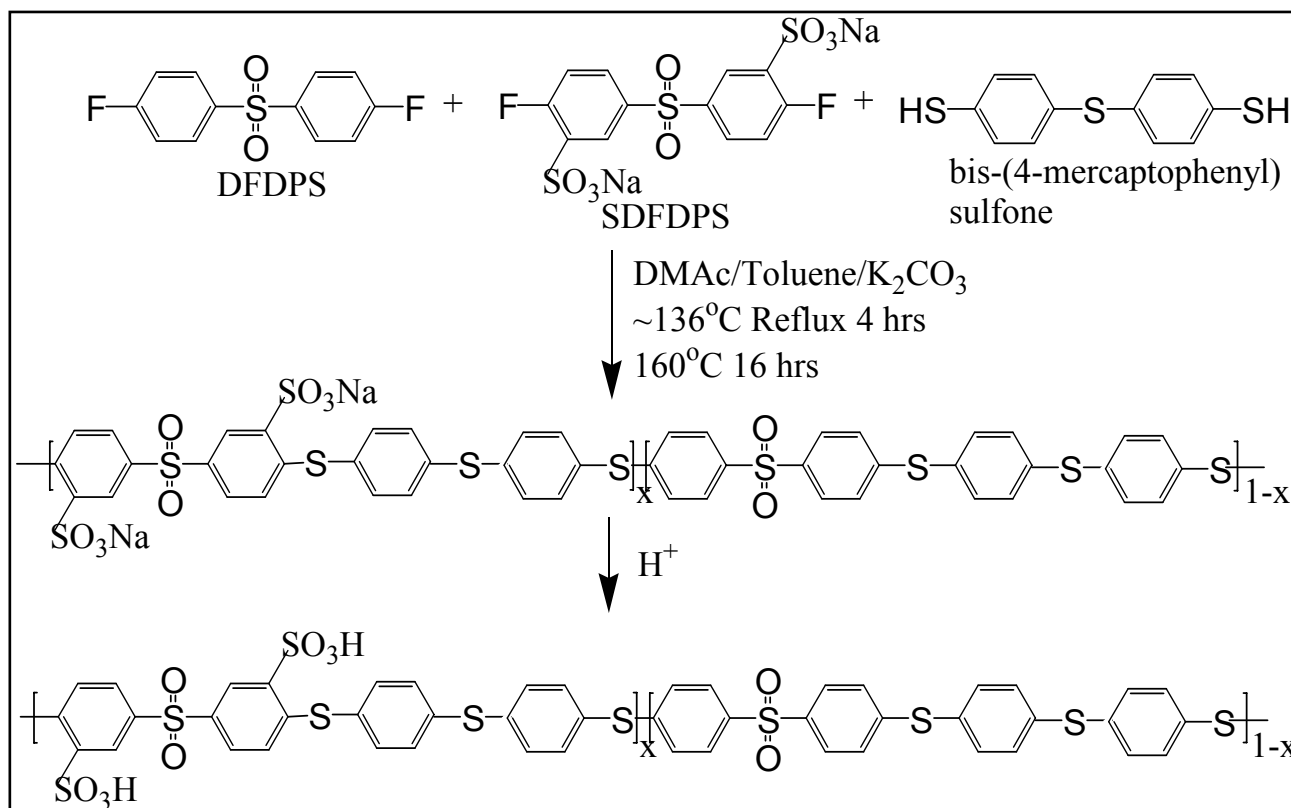


**Figure 2.31**<sup>135</sup> Directly copolymerized sulfonated poly(arylene sulfide sulfone); Later, Wiles et al.<sup>136</sup> has synthesized high molecular weight sulfonated poly(arylene sulfide sulfone) copolymers at various degree of sulfonation using commercially available 4,4'-thiobisbenzenethiol monomer in NMP for use as proton exchange membranes.

#### 2.4.3.7 Direct Copolymerization of Sulfonated Poly(arylene ether benzonitrile)s

The series of high molecular weight, nitrile-functional, disulfonated poly(arylene ether benzonitrile) copolymers were synthesized by directly copolymerizing 3,3'-disulfonated 4,4'-dichlorodiphenylsulfone (SDCDPS), hexafluoroisopropylidene diphenol (6F) and 4,4'-dichlorodiphenylsulfone (DCDPS)<sup>137</sup>. The direct copolymerization reaction is depicted in Figure 2.32. The copolymer from nitrile-activated aryl halide monomers produced membranes having lower water uptake values compared to disulfonated poly(arylene ether sulfone) or poly(arylene ether ketone) copolymers due to the hydrophobic nature of 6F monomer. However, the proton conductivity values of the disulfonated PAEB copolymers were comparable to its disulfonated poly(arylene ether sulfone) or poly(arylene ether ketone) analogous.

---

<sup>137</sup> Sumner, M.J.; Harrison, W.L.; Weyers, R.M.; Kim, Y.S.; McGrath, J.E.; Riffle, J.S.; Brink, A.; Brink, M.H., *J. Membrane Science* 2004, 239, 199

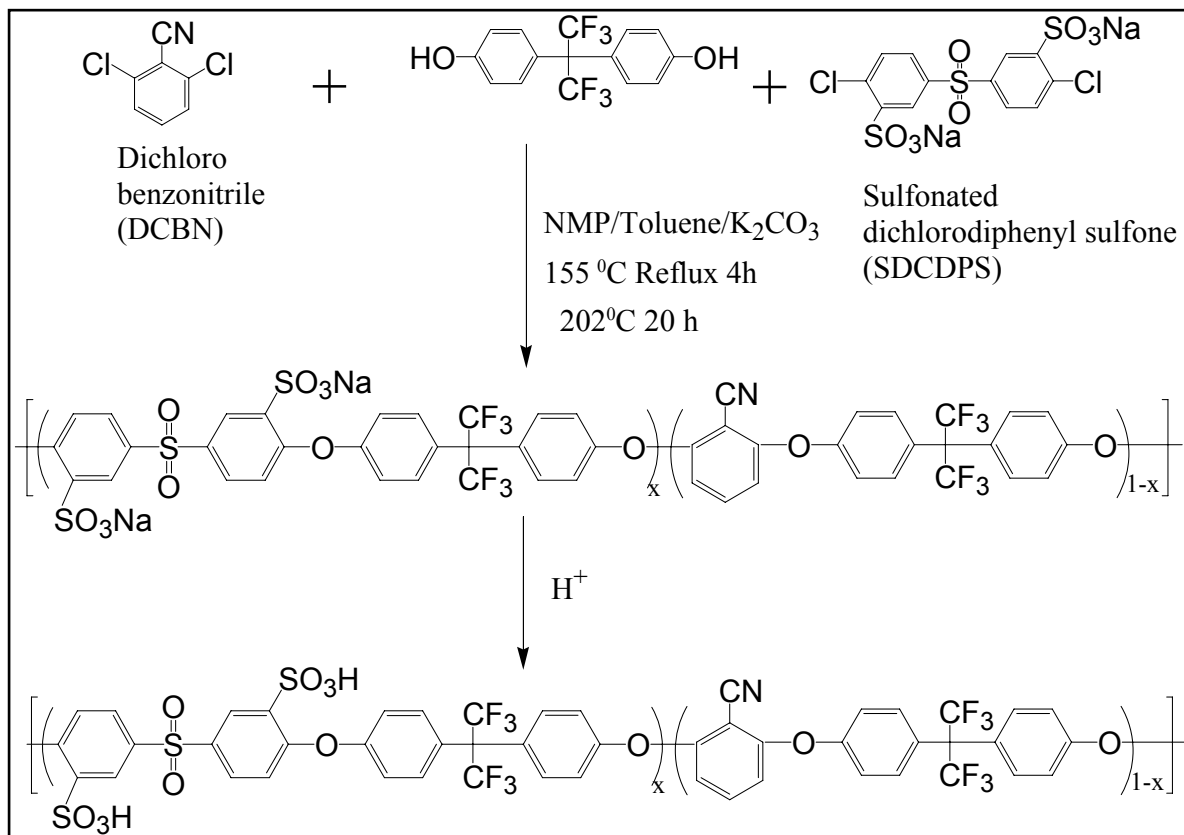


**Figure 2.32** Directly copolymerized sulfonated poly(arylene ether benzonitrile); Partially fluorinated disulfonated copolymers had reduced to water uptake by 10-15 weight percent compared to disulfonated poly(arylene ether sulfone) copolymers having similar ion exchange capacities

## 2.5 Membrane Preparation and Basic Membrane Characteristics of Directly Synthesized Disulfonated Poly(arylene ether sulfone) (BPS) Copolymers

Membranes in the potassium sulfonate form were prepared by first redissolving the copolymer in DMAc as 5-10% (w/v) copolymer solutions, which were then filtered using a syringe filter (0.45  $\mu\text{m}$ ) and were cast onto clean glass substrates. The transparent solutions were carefully dried with infrared heat at gradually increasing temperatures (up to  $\sim 60$   $^{\circ}\text{C}$ ) under a nitrogen flow, until the film was nearly dry; a further drying step was applied in vacuum oven at 140-150 $^{\circ}\text{C}$  for 24 hours. The sulfonated poly(arylene ether sulfone) copolymer films were converted to their acid form (BPSH) using two different methods as described below<sup>138</sup>;

### I. Method 1 (M1) :

The membranes were placed in 1.5M aqueous sulfuric acid solution at 30 $^{\circ}\text{C}$  for 24 hours and then washed with deionized water several times. They were again placed in deionized water at 30 $^{\circ}\text{C}$  for 24 hours and finally rewashed and stored in deionized water.

### II. Method 2 (M2) :

The membranes were boiled in 0.5M aqueous sulfuric acid solution for 2 hours, then washed with deionized water several times, and then were boiled in deionized water for 2 hours, rewashed with deionized water and stored in deionized water.

All films were stored in deionized H<sub>2</sub>O for at least 2 days before any tests were performed

---

<sup>138</sup> Kim, Y.S.; Dong, L.; Hickner, M.A.; Pivovar, B.S.; McGrath; J.E., *Polymer* 2003, 44, 5729

Most of the membrane properties rely heavily on the concentration of ion conducting units (most commonly sulfonic acid units) in the polymer membrane. The ion content is characterized by the molar equivalents of ion conductor per mass of dry membrane and is expressed as equivalent weight (EW) with units of milliequivalents per gram ( mequiv/g or mmol/g) of polymer ( $EW=1000/IEC$ ). Systematic results were derived by the copolymerization of four different bisphenol with SDCDPS were presented by McGrath et al.<sup>106</sup> The chemical structure of bisphenols can be seen in Figure 2.33a. The reported ion exchange capacity values<sup>106</sup> of BPSH (disulfonated poly(arylene ether sulfone)) copolymers as a function of various degree of disulfonation (10 to 60 mol percent) were plotted for four different bisphenols (Figure 2.33b). The ion exchange capacities can be easily controlled by varying the degree of disulfonation and also the type of bisphenol used in copolymerization. Higher degree of disulfonation and/or smaller molecular weight of bisphenols used in copolymerization resulted with higher ion exchange capacity values. The ion exchange capacities of BPSH copolymers after 30 mol percent disulfonation were much higher than Nafion™ ionomer which is given as a dotted line in the Figure 2.33b. Varying the ion content of the membrane can control both its proton conductivity and water uptake. While it is desirable to maximize the conductivity of the membrane by increasing its ion content (decreasing equivalent weight), other physical properties must be considered. Hence ion exchange capacity of the membrane should carefully be chosen to balance the water uptake and also proton conductivity of the membrane. Water uptake is usually reported as a mass fraction, mass percent, or  $\lambda$  value where  $\lambda$  equals to number of water molecules per acid site. Water uptake is also important in determining the ultimate performance of proton exchange

membrane materials. In essentially all current polymeric materials, water is needed as the mobile phase to facilitate proton conductivity. However, absorbed water also affects the mechanical properties membrane by acting as a plasticizer, lowering the glass transition temperature and modulus of the membrane. Careful control of water uptake is critical for reducing adverse effects of swelling and degradation of the mechanical properties of the membrane in humid environments, as well as inducing stresses between the membrane and the electrodes.

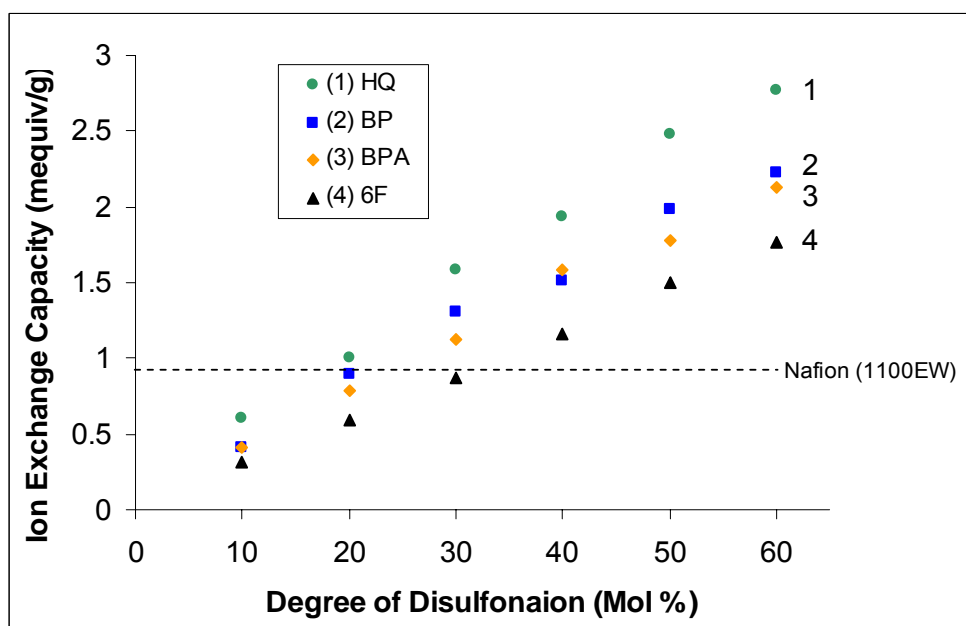
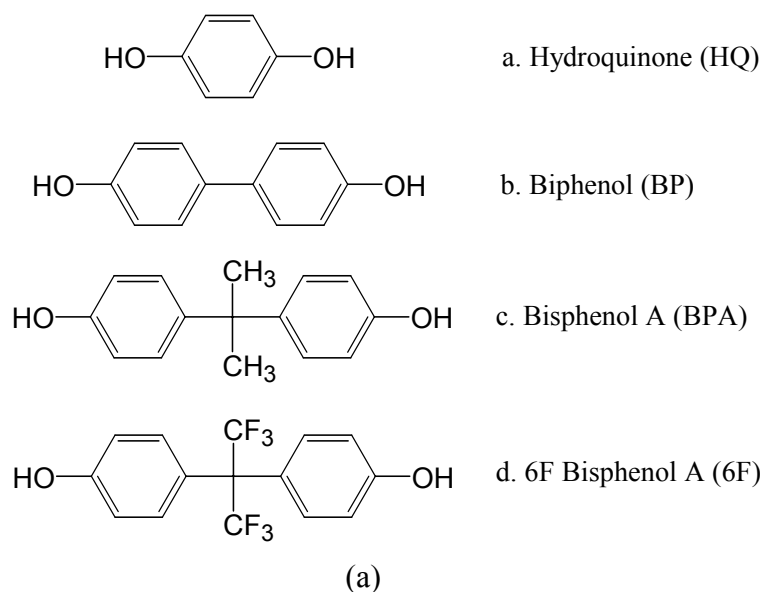


**Figure 2.33** a. Chemical structure of four different bisphenols used in copolymerization

b. Ion exchange capacity values for four different types of BPSH

The influence of degree of disulfonation on water uptake and morphology of BPSH membrane after method 1 and method 2 acidification treatment has been studied by McGrath et al.<sup>139</sup>. The water uptake of BPSH membranes acidified with method 1 (room temperature acidification) linearly increased over the range of disulfonation from 20 to 50 mol percent and then increased dramatically after 50 mol percent (Figure 2.34). The dramatic increase in water uptake was explained by using AFM images of corresponding BPSH membranes. The BPSH copolymers with a low degree of disulfonation showed a closed domain structure and named as regime 1, where isolated hydrophobic domains were surrounded by a hydrophobic matrix. Conversely, higher degree of disulfonation produced more open or continuous hydrophilic domain structure, named as regime 2, where cocontinuous domains were observed (Figure 2.35). The composition where the morphology transfer (discontinuous to cocontinuous) occurred was denoted as percolation threshold.

---

<sup>139</sup> Kim, Y.S.; Hickner, M.A.; Dong, L.; Pivovar, B.S.; McGrath, J.E., *Journal of Membrane Science* 2004, 243, 317

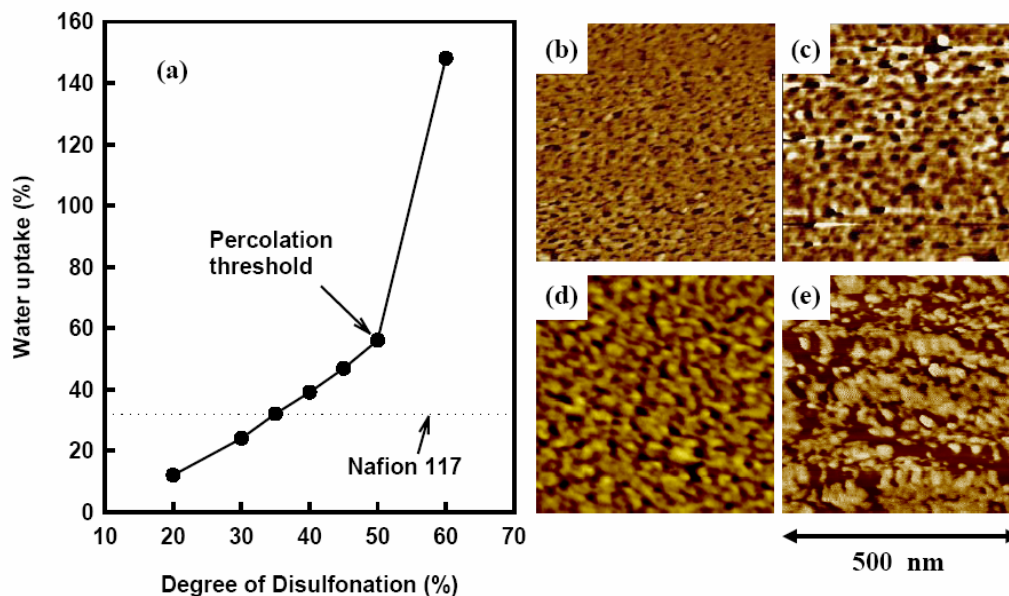


**Figure 2.34** a. Percent water uptake as a function of the degree of disulfonation (compared with Nafion<sup>TM</sup>), b-e. Morphology (AFM at 25 °C) of BPSH membranes acidified with method 1; b. BPSH-20, c. BPSH-40, d. BPSH-50, e. BPSH-60 (*reprinted from reference 139 with permission from Elsevier*)

The morphology of BPSH copolymers strongly depended on the degree of disulfonation and method for acidification. Method 2 acidification (acidification by boiling) followed similar linear behavior observed for method 1. However, the percolation threshold was shifted to a lower degree of disulfonation. As a result, more cocontinuous structure for lower percent degree of disulfonation of BPSH membranes acidified with method 2 were reported (Figure 2.35). It was also noted that the membrane processing conditions strongly affected the membrane characteristics<sup>139</sup>.

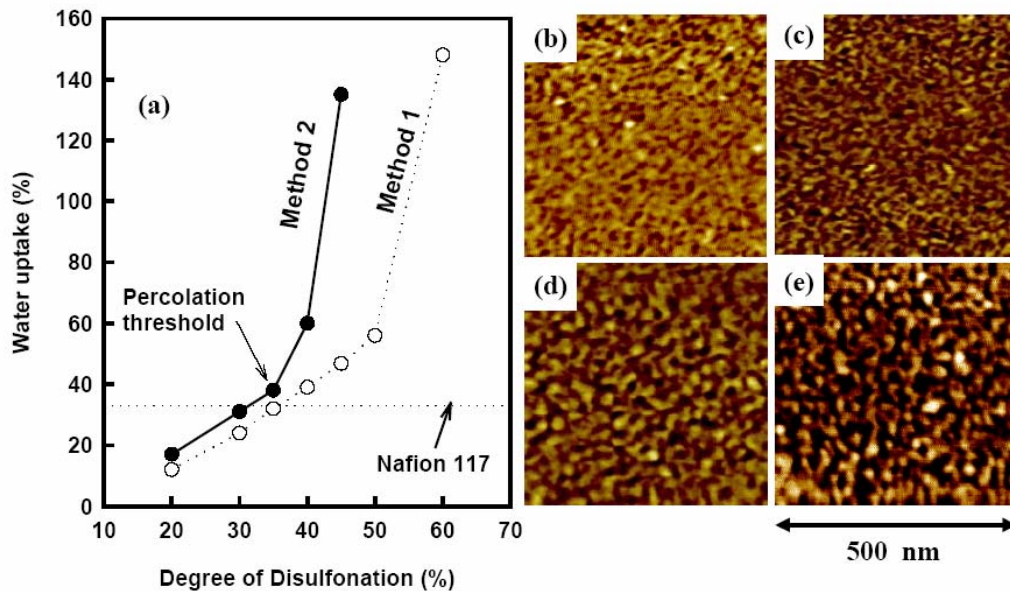


**Figure 2.35** a. Percent water uptake as a function of the degree of disulfonation (compared with Nafion™), b-e. Morphology (AFM at 25 °C) of BPSH membranes acidified with method 2; b. BPSH-30, c. BPSH-35, d. BPSH-40, e. BPSH-45 (*reprinted from reference 139 with permission from Elsevier*)

Proton conductivity of both method 1 and method 2 acidified BPSH membranes in their fully hydrated forms at 30 °C as a function of degree of disulfonation were plotted using the reported data given in reference (Figure 2.36)<sup>107</sup>. Method 2 consistently produced greater proton conductivity than method 1 and the proton conductivity difference increased as degree of disulfonation increased. The influence of hydrothermal treatment on membrane properties of BPSH copolymers were reported by McGrath et al.<sup>138</sup> It was also stated that low temperature treatment of the membrane in water favors

a closed hydrophilic domain structure, while higher temperature treatment in water produces more open structure which enhances proton conductivity. Hence, the hydrothermal treatment was another factor affecting hydrophilic/hydrophobic domain structure.

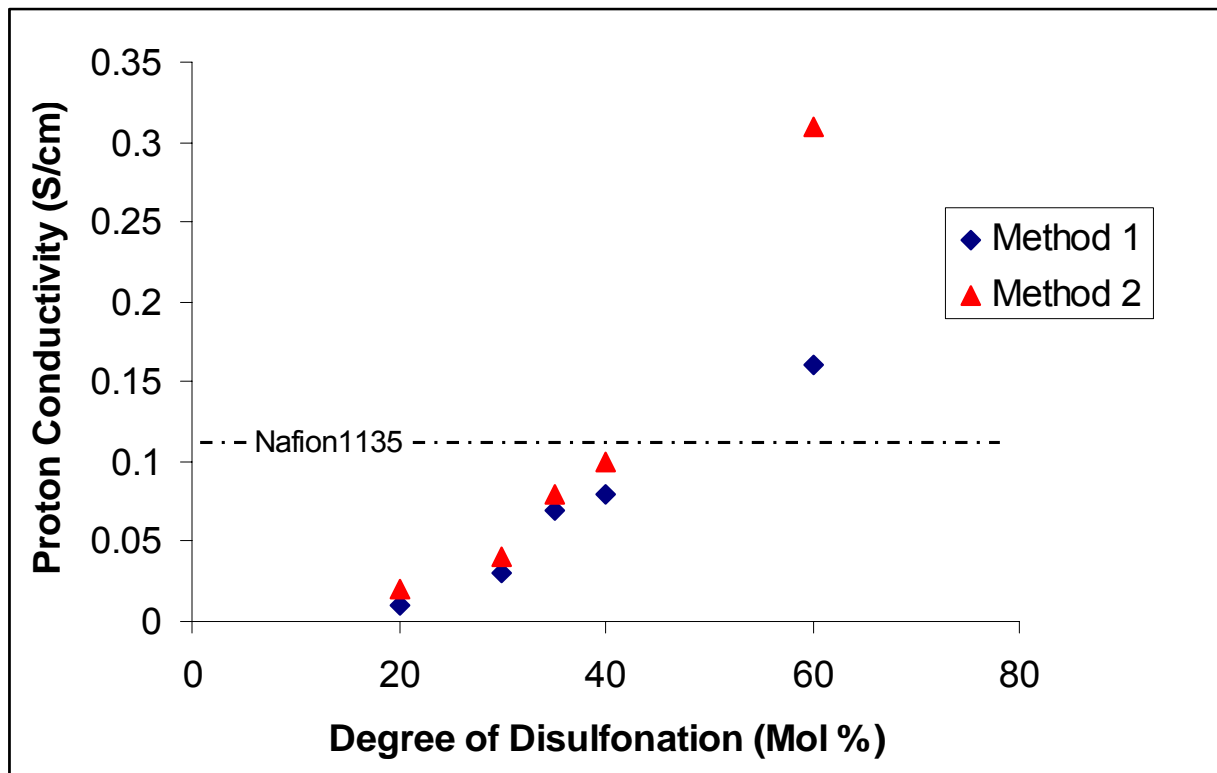


**Figure 2.36** Proton conductivity of BPSH membranes acidified with method 1 and method 2 as a function of degree of disulfonation (compared with Nafion™)

Proton conductivity of the method 1 acidified BPSH and Nafion™ membranes at 30 °C as a function of hydrothermal treatment temperature can be seen in Figure 2.37<sup>138</sup>. Figure 2.37 showed that hydrothermal treatment increased the proton conductivity as hydrothermal treatment temperature increased due to the morphology transfer mentioned above. However, only a little improvement was observed for Nafion™ membrane which may be due to the retardation of morphological reorganization by its small amount of semicrystallinity. At higher hydrothermal treatment temperatures, proton conductivities were decreased due to the morphological relaxation or destruction of the hydrophilic domain structure. However, percolation temperature (120-140 °C) of BPSH membranes (20-35 mol percent disulfonation) where conductivity started to drop was higher than that of Nafion™ membrane (100 °C). The morphological relaxation temperatures were associated with the hydrated glass transition temperature which was higher for BPSH membranes compared to Nafion™. It was stated that the concept of hydrated glass transition temperature beside dehydration was thus a key consideration for producing membranes available for higher temperature (120-150 °C) applications.

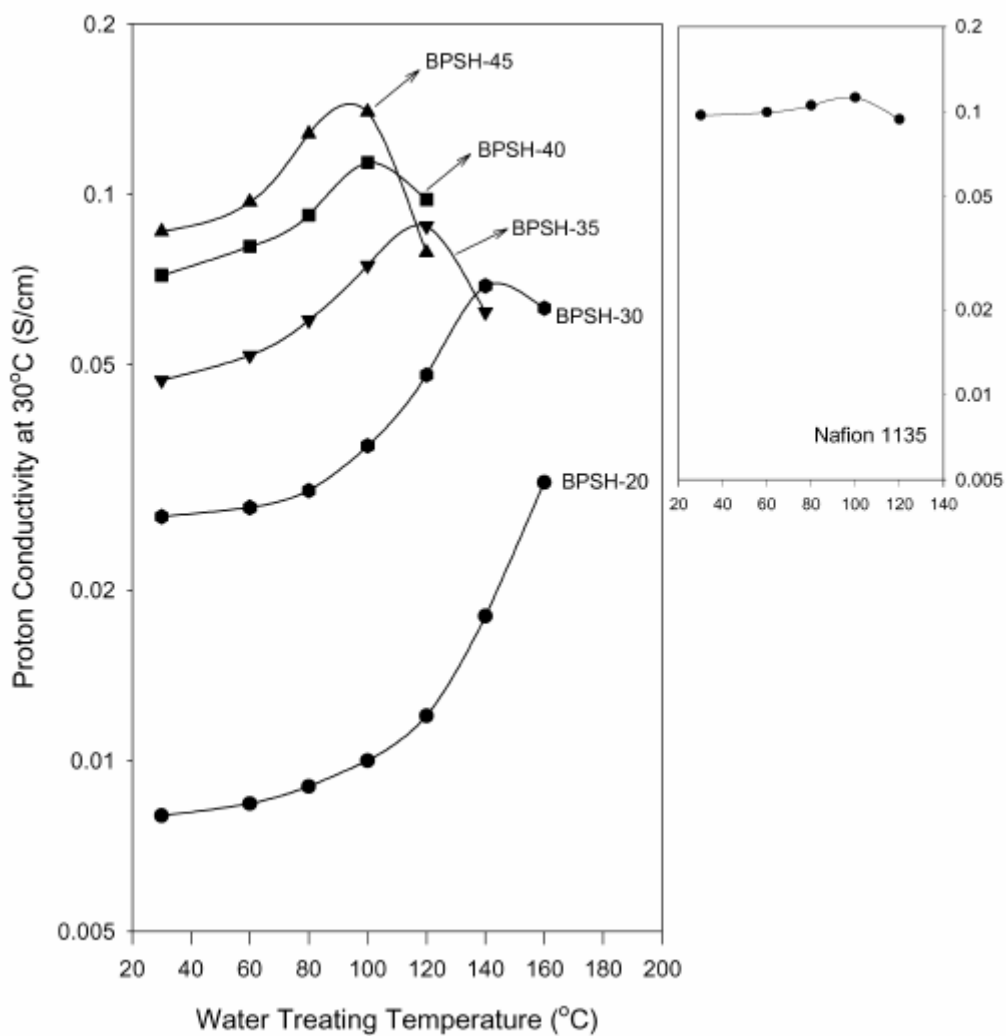


**Figure 2.37** Proton conductivity of BPSH and Nafion™ membranes as a function of water treating (Hydrothermal Treatment) temperatures (*reprinted from reference 138 with permission from Elsevier*)

Another membrane characteristic was its transport properties such as methanol permeability for the DMFC operations. The influence of the degree of disulfonation, acidification method and temperature on methanol permeability has been studied by McGrath et al.<sup>139</sup> It has been reported that the methanol permeability increased with

degree of disulfonation and was always smaller than Nafion™. A dramatic increase in methanol permeability was observed after 45 mol percent disulfonation (percolation threshold) for method 1 acidified membranes, while percolation threshold was observed at 30 percent disulfonation for the membranes acidified with method 2 (Figure 2.38). Similar to the water uptake behavior, the significant increases in methanol permeability was attributed to the morphology change.

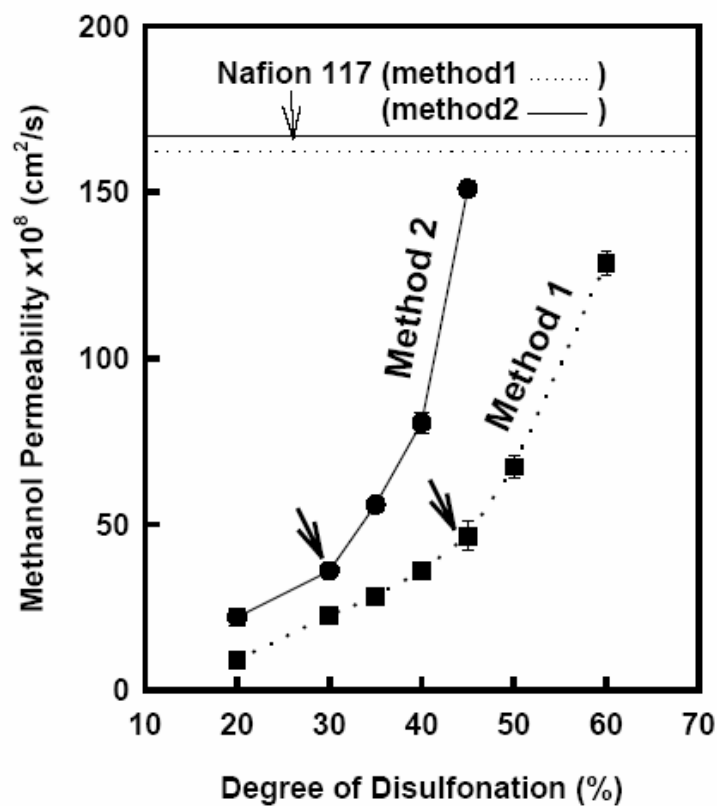


**Figure 2.38** Methanol permeability at 25 °C of BPSH and Nafion™ membranes acidified with method 1 and method 2; (arrows shows percolation thresholds) (*reprinted from reference 139 with permission from Elsevier*)

McGrath et al. proposed that the state of water in the membrane plays a more significant role in membrane transport properties than previously suggested<sup>140</sup>. The state of water in hydrated copolymers, mainly in the context of hydrogels has been extensively studied and defined as<sup>140, 141</sup>;

1. Non-freezing water: Water that is strongly bound to the polymer chain and has a role in effective glass transition reduction (plasticization)
2. Freezable loosely bound water: Water that is weakly bound to the polymer chain or interacts weakly with nonfreezing water and displays relatively broad melting endotherms
3. Free water: Water that is not intimately bound to the polymer chain and behaves like bulk water showing sharp melting point at 0 °C

The quantitative analysis of the state of water were done using pressurized differential scanning calorimeter (DSC) and proton pulse NMR techniques. DSC measurements showed the depression of glass transition temperature, caused by nonfreezing strongly bound water, while the spin-spin relaxation time,  $T_2$ , measurements by proton pulse NMR was used to calculate the distribution of the each state of the water in BPSH and Nafion™ membranes. The amount of each state of water was plotted (Figure 2.39) as a function of degree of disulfonation for BPSH membranes and also for the Nafion™ membrane using the data in reference 140. The amount free water in

---

<sup>140</sup> Kim, Y.S.; Dong, L.; Hickner, M.A.; Glass, T.E.; Webb, V.; McGrath, J.E., *Macromolecules* 2003, 36,6281

<sup>141</sup> (a) Quinn, F.X.; Kampff, E.; Smyth, G.; McBrierty, V.J., *Macromolecules* 1988, 21, 3191. (b) Smyth, G.; Quinn, F.X.; McBrierty, V.J., *Macromolecules* 1988, 21, 3198. (c) Hodge, R.M.; Bastow, T.J.; Edward, G.H.; Simon, G.P.; Hill, A.J., *Macromolecules* 1996, 29, 8137. (d) F.X, Quinn; Kampff, E.; Smyth, G.; McBrierty, V.J., *Macromolecules* 1988, 21, 3192. (e) Lafitte, B.; Karlsson, L.E.; Jannasch, P., *Macromol. Rapid Commun.* 2002, 23, 896.

Nafion™ membrane was higher than in BPSH membrane. It was then concluded that a relatively large fraction of water in BPSH membranes exists in a bound state, which can hinder transport.

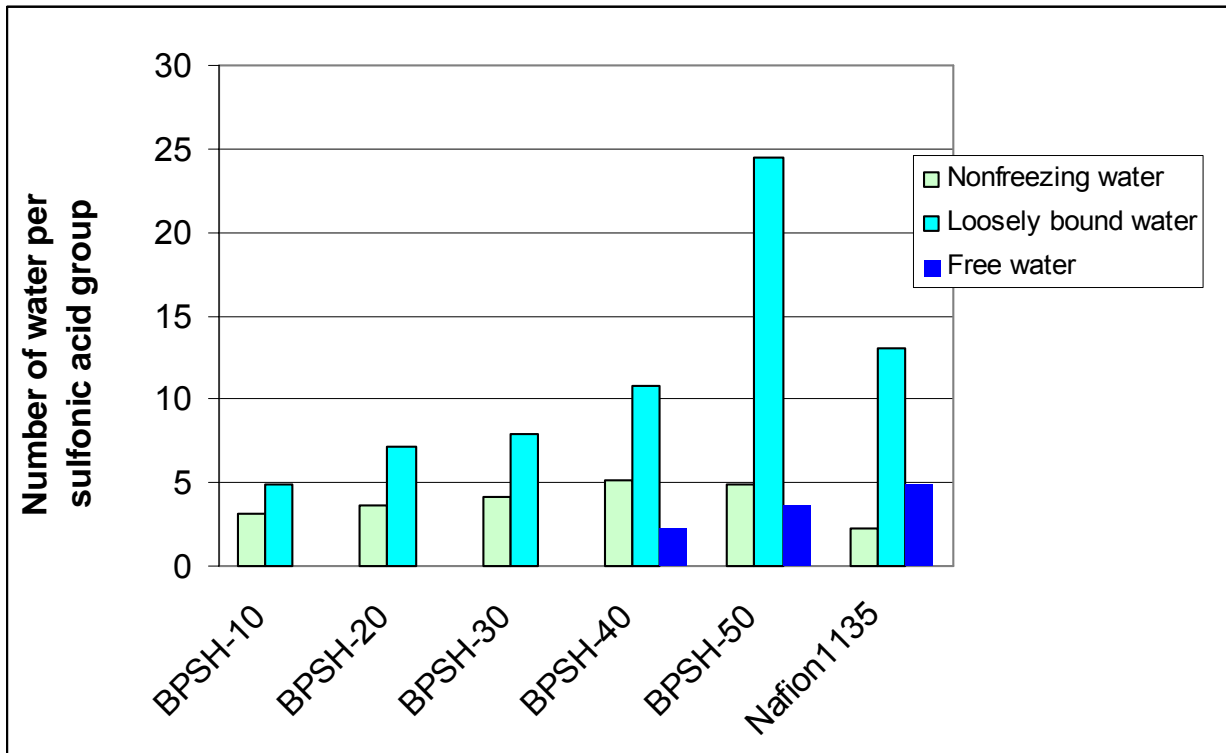
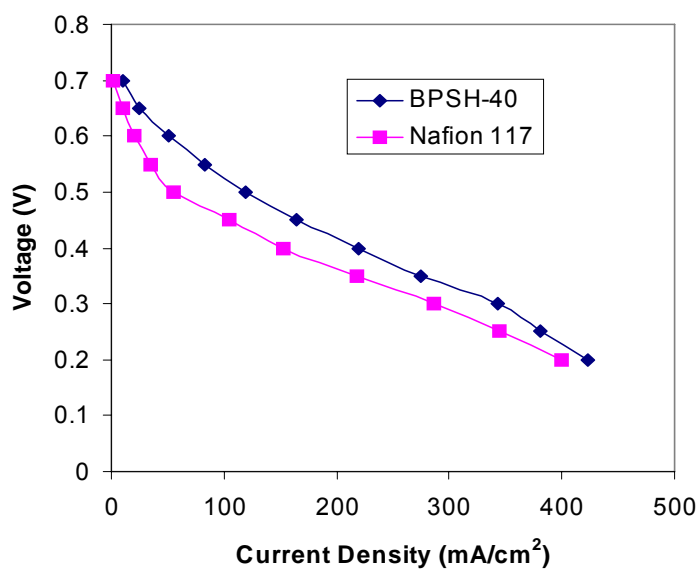


**Figure 2.39** Composition of each state of water for BPSH and Nafion™ membranes; No free water were reported for 10, 20, 30 mol percent disulfonations. (plotted using the data in reference 140)

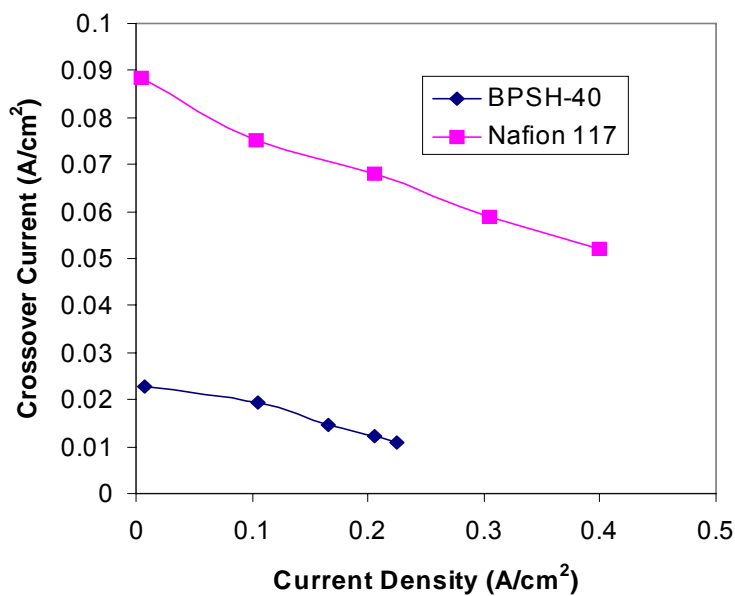
It was demonstrated that BPSH and Nafion™ membranes exhibited similar direct methanol fuel cell performances (DMFC) (Figure 2.40). Since, directly synthesized poly(arylene ether sulfone) copolymer membranes (BPSH) has comparable proton conductivity, but lower methanol permeability than Nafion™ membrane. Other related systems were also reported; partially fluorinated BPS copolymer membranes showed better DMFC performances than Nafion™ membrane<sup>142</sup>. The influence of fluorination on membrane properties and DMFC and Hydrogen (H<sub>2</sub>/Air) fuel cell performances will be a main part of this dissertation.

---

<sup>142</sup> Kim, Y.S.; Sumner, M.J.; Harrison, W.L.; Riffle, J.S.; McGrath, J.E.; Pivovar, S.P., *Journal of the Electrochemical Society* 2004, 151(12), A2150



(a)



(b)

**Figure 2.40** a. Direct methanol fuel cell performances of BPSH and Nafion<sup>TM</sup> membrane b. Degree of methanol permeability from cross over current; The values of cross over current, methanol oxidation current at cathode instead anode, indicating much lower methanol permeability for BPSH membrane.

## 2.6 Solid State Inorganic Proton Conductors and Composites

Solid state proton conductors can be classified into two groups; water containing systems (low temperature) and anhydrous high temperature proton conductors. The proton conductivity of water containing systems, hydrates, depends on the presence of water which is usually loosely bounded in the structure. Since, the temperatures greater than 100 °C or boiling point of water cause dehydration and proton conductivity disappears<sup>143</sup>. Theoretical consideration such as proton conductivity mechanism of inorganic proton conductors has been extensively studied by Kreuer et al.<sup>144</sup> Some of well known inorganic proton conductors are hydrated oxides (e.g.  $\text{SnO}_2 \cdot 2\text{H}_2\text{O}$ ), heteropolyacids (e.g.  $\text{H}_4\text{SiW}_{12}\text{O}_{40} \cdot 28\text{H}_2\text{O}$  or  $\text{H}_3\text{PW}_{12}\text{O}_{40} \cdot 29\text{H}_2\text{O}$ ) or some other complex inorganic compounds having three dimensional structure (e.g.  $\text{H}_2\text{Sb}_4\text{O}_{11} \cdot 3\text{H}_2\text{O}$ ) or layered structure (e.g.  $\alpha$ -Zr sulfophenylphosphonate,  $\gamma$ -Zr sulfophenylphosphonate)<sup>143,145,145</sup>. Some residual proton conductivity was reported for layered acidic phosphates and phosphonates of zirconium after dehydration<sup>143</sup>. However, the oxoacids and their salts (sulfates, selenates, phosphates, and arsenates) were reported with their useful proton conductivities at elevated temperatures due to their self dissociation in totally anhydrous conditions<sup>143</sup>. The conductivity values as a function of temperature of some water containing solid state proton conductors can be seen in Figure 2.41<sup>146</sup>.

---

<sup>143</sup> Kreuer, K.D.; *Chem. Mater.* 1996, 8, 610

<sup>144</sup> Kreuer, K.D.; Paddison, S.J.; Spohr, E., Schuster, M., *Chem. Rev.* 2004, 104, 4637

<sup>145</sup> Alberti, G.; Boccali, L.; Casciola, M.; Massinelli, L.; Montoneri, E., *Solid State Ionics* 1996, 84, 97

<sup>146</sup> Alberti, G.; Casciola, M., *Solid State Ionics* 2001, 145,3

Although some of these inorganic particles in their fully hydrated form were promising for high temperature applications, the next challenge was making composites from these inorganic filler with a suitable polymer matrix in order to apply them in real fuel cell operations.

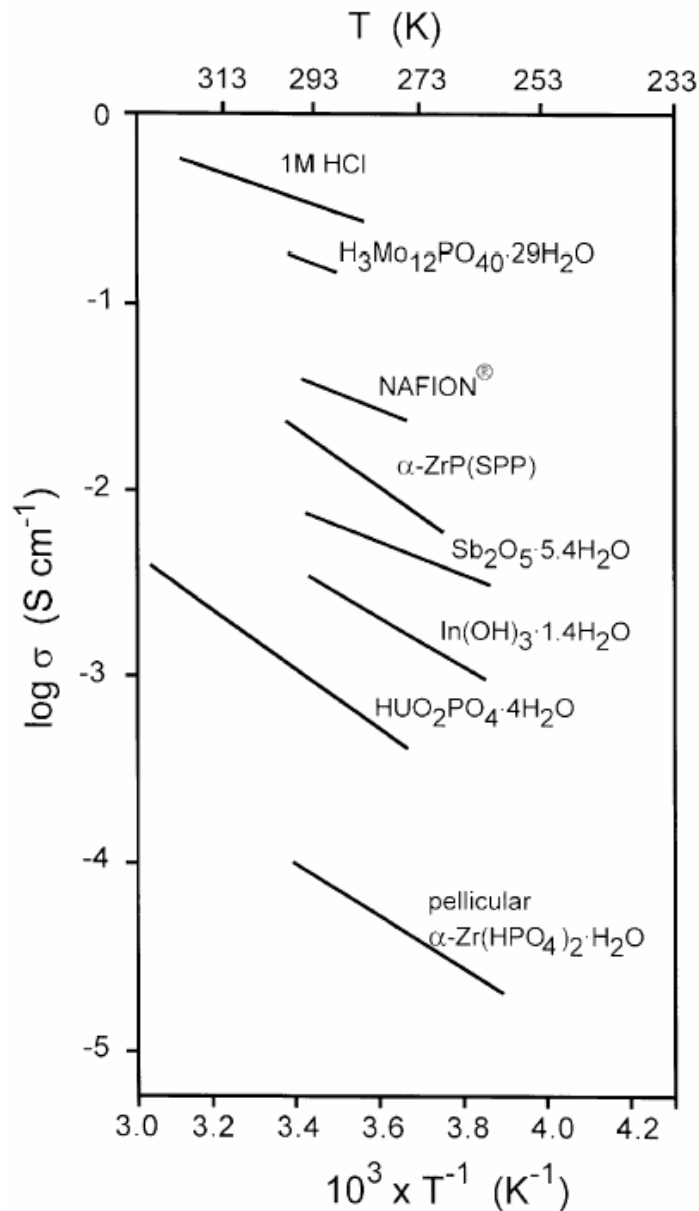


**Figure 2.41** Arrhenius plot of some water containing proton conductors (*reprinted from reference 145 with permission from Elsevier*)

The concept of obtaining improved membrane properties (appreciable proton conductivity, or reduced fuel/oxidant permeability) at lower percent humidity (or totally anhydrous) and higher temperatures (greater than 100 °C) resulted in utilization of nanocomposite proton exchange membranes. For example, Tricoli et al.<sup>147</sup> reported that methanol permeability of Nafion™ membranes dramatically decreased when Nafion™ was doped with cesium ion. Watanabe et al.<sup>148</sup> has presented Pt and/or metal oxides doped Nafion™ membranes which reportedly did not require external humidification. Since generated water by the help of dispersed platinum nano-crystals self humidified the membrane. Other inorganic materials such as silica and zeolites were also investigated as additives in composite membranes<sup>149, 150</sup>.

Among these inorganic materials, highly conductive and thermally stable crystalline heteropolyacids (HPA) are one of the most attractive dopant. Heteropolyacids were also utilized in directly disulfonated statistical poly(arylene ether sulfone) copolymers. McGrath et al.<sup>151</sup> reported higher proton conductivity values for phosphotungstic acid ( $H_3PW_{12}O_{40}$ ) / BPSH composites about 0.15 S/cm at 140 °C under pressure than Nafion™ composites (Figure 2.42). The well dispersed transparent, ductile BPSH/HPA nano-composites showed also better mechanical properties compare to Nafion™ at elevated temperatures.

---

<sup>147</sup> Tricoli, V. *J.Electrochem.* 1998, 145, 3798

<sup>148</sup> Watanabe, M.; Uchida, H.; Seki, Y.; Emori, M.; Stonehart, P., *J.Electrochem.* 1996, 143, 3847

<sup>149</sup> Poltarzewski, Z.; Wieczorek, W.; Przulski, J.; Antonucci, V., *Solid State Ionic* 1999, 119, 301

<sup>150</sup> Antonucci, P.L.; Arico, A.S.; Creti, P.; Ramunni, E.; Antonucci, V., *Solid State Ionic* 1999, 125, 431

<sup>151</sup> Kim, Y.S.; Wang, F.; Hickner, M.; Zawodonski, T.A.; McGrath, J.E., *Journal of Membrane Science* 2003, 212, 263

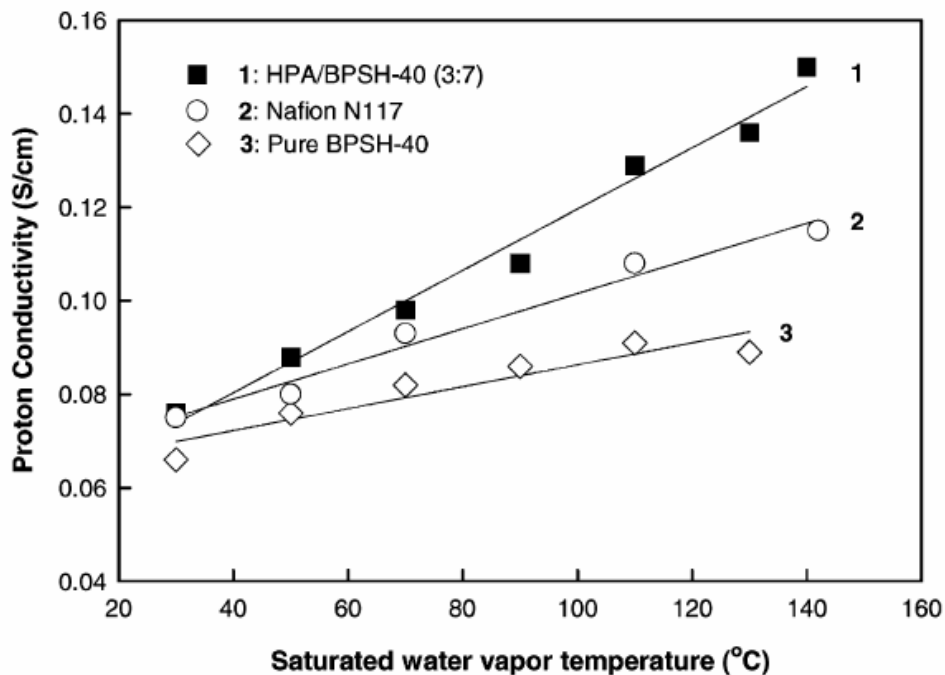


**Figure 2.42** Proton conductivities of Nafion™ and BPSH-40, 30 weight percent HPA containing BPSH-40/HPA composites at different saturated water vapor temperature; However, the main disadvantage of heteropolyacids were their very high solubilities in water which probably makes them less available over the long time of fuel cell operations (*reprinted from reference 151 with permission from Elsevier*)

Alberti et al.<sup>152</sup> reported layered zirconium phosphate or zirconium phenyl phosphonates composites with some proton conducting ionomers ( Nafion™, s-PEK, S-PSU). In-situ incorporation of these inorganic materials and improved fuel cell performance of Nafion™- $\alpha$ -ZrP nano-composite membrane has also been

<sup>152</sup> Alberti, G.; Casciola, M., *Annu. Rev. Mater. Res.* 2003, 33, 129

demonstrated<sup>152</sup>. More interestingly, the proton conductivity of zirconium phenyl phosphonate (ZrPPh)/ Nafion™ composites exhibited results similar to the pure conductivity of zirconium phenyl phosphonate (0.08-0.011 S/cm). This result was attributed to a preferred parallel orientation to the pore surface of the formed lamellar particles (Figure 2.43). Hence, the direct proton conductivity path way was obtained.

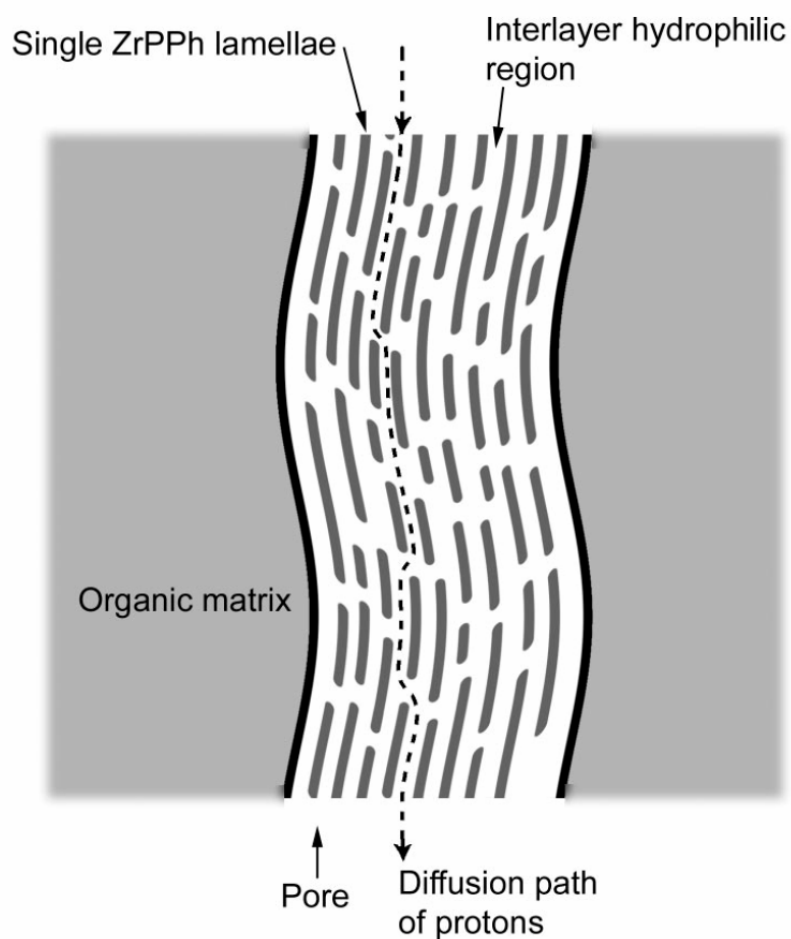


**Figure 2.43** A schematic representation of diffusion path of protons through the ZrPPh lamellae (*reprinted from reference 152 with permission from Annual Reviews, www.annualreviews.org*)

## 2.7 Basic Consideration of Real Cell Potential and Fuel Cell Performance

The equilibrated open cell potential or reversible thermodynamic potential negatively deviates from its equilibrium once irreversible non-equilibrium processes of a practical fuel cell starts. The losses from equilibrium potential are called polarization, or overpotential or overvoltage. In other words, the polarization is difference between the measured potential under working condition and the reversible thermodynamic potential. The source of total polarization includes<sup>5,153,154</sup>

1. Activation Polarization
2. Ohmic Polarization
3. Concentration Polarization

Activation polarization is resulted from the chemical reaction and the physicochemical process associated with the adsorption of molecules on electrode surfaces. The origin of the activation polarization comes from the activation energy of the rate determining step or steps where all other steps depend on this slowest step. The voltage drop due to the activation polarization is expressed by the Tafel equation.

$$\eta = a \log bi$$

Equation 2.1

---

<sup>153</sup> Eisenberg, M., In *Fuel Cells*, Mitchell, W., Ed., Academic Press: New York, 1963, p17

<sup>154</sup> Barendrecht, E., In *Fuel Cell Systems*, Blomen, L.J.M.J; Mugerwa, M.N., Eds., Plenum Press: New York, 1993, p. 73

where a and b are arbitrary constants and other terms are;

$\eta$ : *Activation Polarization*

$i$ : *Current Density*

Concentration polarization occurs due to the fact that the concentration of ions at the electrode is lower than the bulk. In previous derivations with activation polarization, the concentration of ions was assumed an equally concentrated for both electrode surface and the bulk. Because of the mass transfer of ions formed moving a way from the electrode and the species moving to the electrode to react with the ions causes a concentration gradient.

Additional potential loss, resistance polarization, occurs due to the resistance to flow ions in the electrolyte and also resistance to flow of electrode through the electrode. The ohmic polarization term can be shown as below;

$$\eta_{ohmic} = \eta_{ohmic}^{electronic} + \eta_{ohmic}^{proton} = i(R^{electronic} + R^{proton}) \quad \text{Equation 2.2}$$

$$\eta_{ohmic} = iR^{internal} \quad \text{Equation 2.3}$$

$$R^{proton} = r_m \frac{l}{A} \quad \text{Equation 2.4}$$

where  $r_m$  membrane specific resistivity for proton exchange membranes.

The total polarization is sum of activation, concentration and ohmic polarization, expressed by;

$$\eta_T = \eta_{activation} + \eta_{concentration} + \eta_{ohmic} \quad \text{Equation 2.5}$$

Hence, the over all cell potential is the subtraction of total polarization from the thermodynamic reversible potential.

$$E_{cell} = E_r - \eta_T \quad \text{Equation 2.6}$$

The graphical expression of the total effect of polarization and decreasing in reversible thermodynamic potential can be seen in Figure 2.44a. The typical of cell potential versus current diagram for fuel cells illustrates the regions of control by various types of overpotentials (Figure 2.44b)

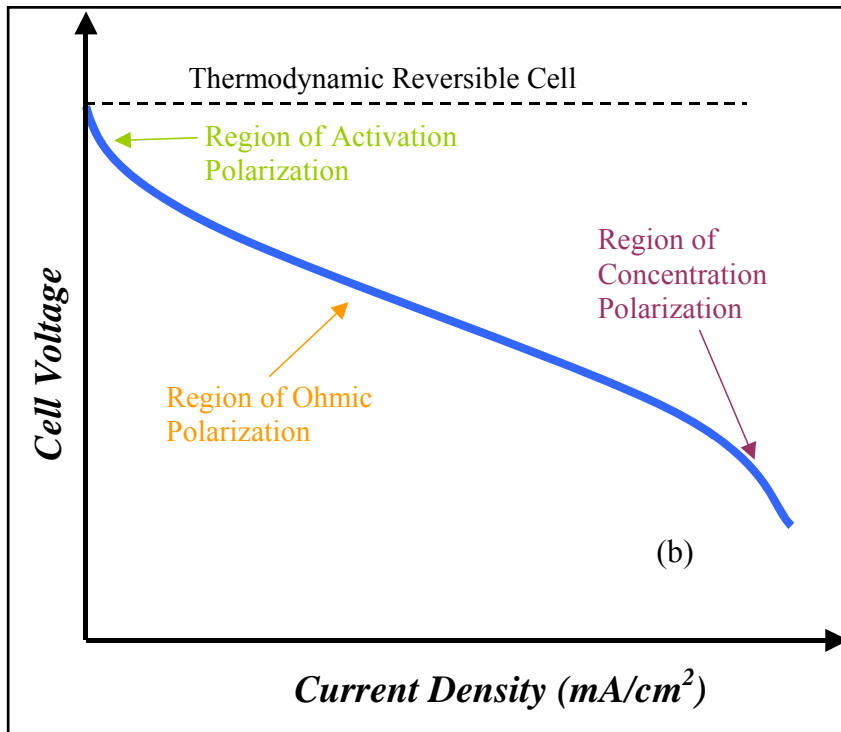
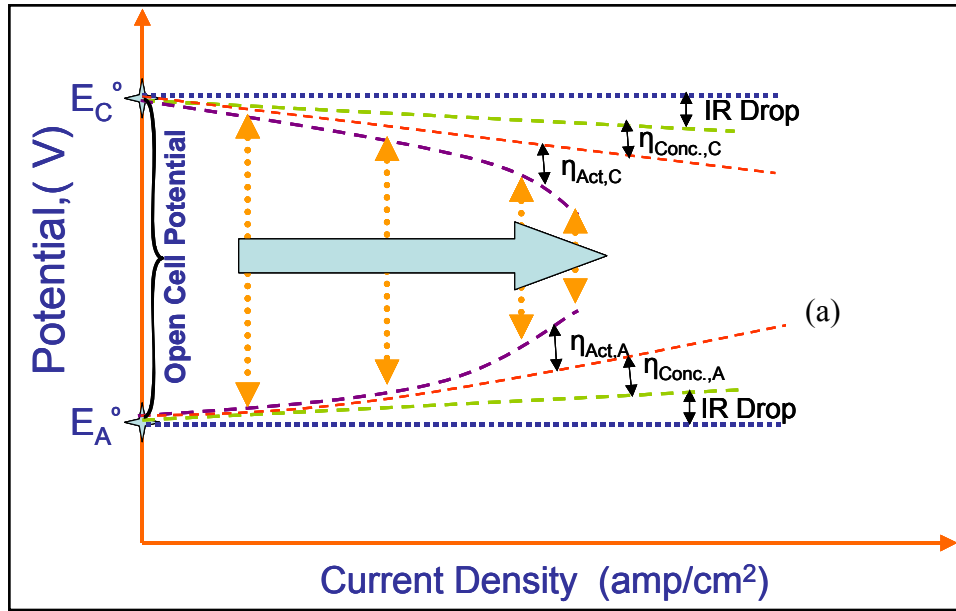


**Figure 2.44** Influence of polarization on cell potential; a. Demonstration of components of polarizations<sup>153</sup>, b. The performance curve characteristics based on polarization regions<sup>8</sup>

## 2.8 Major Synthetic Methods to Synthesize Poly (arylene ether sulfones)

### 2.8.1 The Ullman Reaction

The Ullman reaction was used for synthesis of aromatic ethers and involves the reaction of phenol with unactivated aromatic halides with a suitable catalyst, usually a copper catalyst (e.g.  $\text{Cu}_2\text{O}$ )<sup>155, 156, 157</sup>. While using activated halides was a requirement for nucleophilic aromatic substitution reaction, poly(arylene ether)s from non-activated aromatic halides can be synthesized using Ullman reaction. The halide reactivity is given as;  $\text{I} > \text{Br} > \text{Cl} > \text{F}$ <sup>158</sup>. A synthesis scheme of the Ullman reaction can be seen in Figure 2.45. A typical polymerization reaction is conducted in benzophenone solvent with a cuprous chloride-pyridine complex as the catalyst, a bisphenol, and a dibromoarylene, since bromine compounds were found favorable for the reaction<sup>155-158,159</sup>. Burgoyne et al.<sup>159b</sup> demonstrated synthesis of poly(arylene ethers) from equal molar reaction of a double alkali metal salts of the dihydric 9,9-bis(4-hydroxy phenyl)fluorine and dihydric form of different types of arylene radical and dibromoarylene derivatives in the presence of the cuprous salt. There are several disadvantages which limit the Ullman reaction in polymerization reactions, such as poor reproducibility, the need for brominated monomers and the difficulty of removing copper salts<sup>158</sup>.

---

<sup>155</sup> Farnham, A.G.; Johnson, R.N., US Patent 3,332,909, 1967

<sup>156</sup> Jurek, M.J., Ph.D. Thesis, VPI&SU, 1987

<sup>157</sup> Farnham, A.G.; Robeson, L.M.; McGrath, J.E.; J. Appl. Polym. Sci. Symp. 1975, 26, 373

<sup>158</sup> Wang, S., McGrath, J.E., In: Polyarylene Ethers: A review, in : *Step Polymerization*, Rogers, M., Long, T.E., Eds., Wiley, 2002

<sup>159</sup> Jurek, M.J., McGrath, J.E., *Polym. Prep.* 1987, 28 (1), 180, b. Burgoyne, Jr. et al, US patents 1999 5, 874,516, Nonfunctionolized poly(arylene ethers)

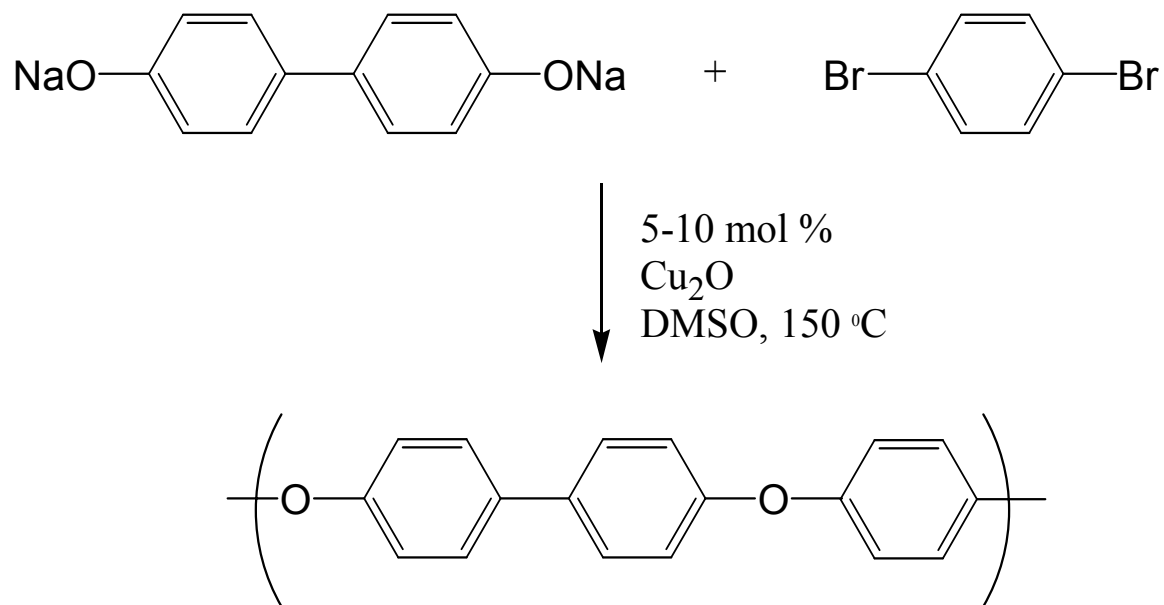


**Figure 2.45** The Ullman type reaction to synthesize poly(arylene ether)s

## 2.8.2 Metal Coupling Reactions

A newer approach for preparing the poly(arylene ether sulfone) is via Nickel coupling reactions which involves the formation of an aromatic carbon-carbon bond<sup>160,161</sup>. Both activated and unactivated dihalides can be utilized in a nickel coupling reactions. In contrast to Ullman reaction which usually works for brominated monomers, nickel coupling reaction eliminates the need for using brominated monomers, so chlorinated monomers could be used in milder reaction conditions.

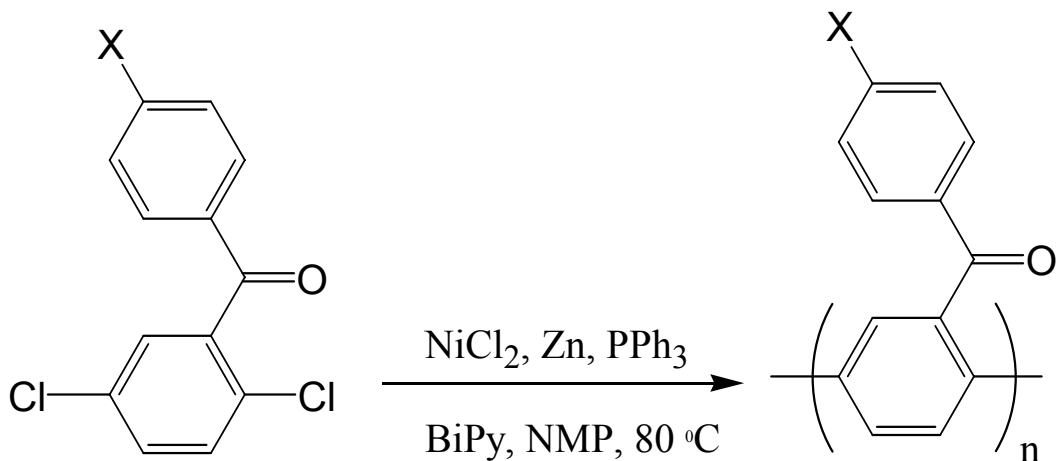


**Figure 2.46** Nickel coupling reaction; synthesis of poly(2,5-benzophenone) (*reprinted from reference 163 with permission from Elsevier*)

<sup>160</sup> Colon, I.; Kwiatkowski, G.T., *J. Polym. Sci., Polym. Chem.* 1990, 28, 367

<sup>161</sup> Colon, I.; Maresca, L.M.; Kwiatkowski, G.T., US. Patents, 4, 263, 466, 1991

Ghassemi and McGrath reported the synthesis of poly(4,4'-diphenylphenylphosphine oxide) which was catalyzed by nickel coupling<sup>162</sup>. A zero valent nickel-triphenylphosphine complex was used to synthesize poly(p-phenylene)s. The typical reaction condition was presented in Figure 2.46<sup>163</sup>.

### 2.8.3 Electrophilic Aromatic Substitution

The sulfone linkages are formed by the reaction of aryl sulfonyl chlorides with aromatic compounds. The reaction is known as Friedel-Crafts sulfonylation which includes two successive steps<sup>164,165,166,167</sup>;

1. Formation of the sulfonylium cation ( $\text{ArSO}_2^+$ ) by Friedel-Crafts catalyst such as  $\text{AlCl}_3$ ,  $\text{AlBr}_3$ ,  $\text{SbCl}_5$ ,  $\text{BF}_3$ , etc.
2. Electrophilic cation attack on the aromatic carbon which generates an intermediate complex, then proton is eliminated which cause to happen the new sulfone linkage (Figure 2.47)

---

<sup>162</sup> a. Ghassemi, H.; McGrath, J.E., *Polymer* 1997, 38, 3139, b. Ghassemi, H.; Ndip, G.; McGrath, J.E., *Polymer* 2004, 45, 5855

<sup>163</sup> Ghassemi, H.; McGrath, J.E., *Polymer* 2004, 45, 5847

<sup>164</sup> Ivin, K.J.; Rose, J.B.; *Advances in Macromolecular Chemistry*, W.M. Pasoka, Ed., Academic Press, London, Vol 1, 1968

<sup>165</sup> Rose, J.B., *Polymer* 1974, 15, 456

<sup>166</sup> Roberts, R.M., In: *Friedel-Crafts Alkylation Chemistry: A Century of Discovery*, Khala, A.A., Ed., New York; M.Dekker, 1984

<sup>167</sup> Suter, C.M., In: *The Organic Chemistry of Sulfur*, New York, 1944, p.670

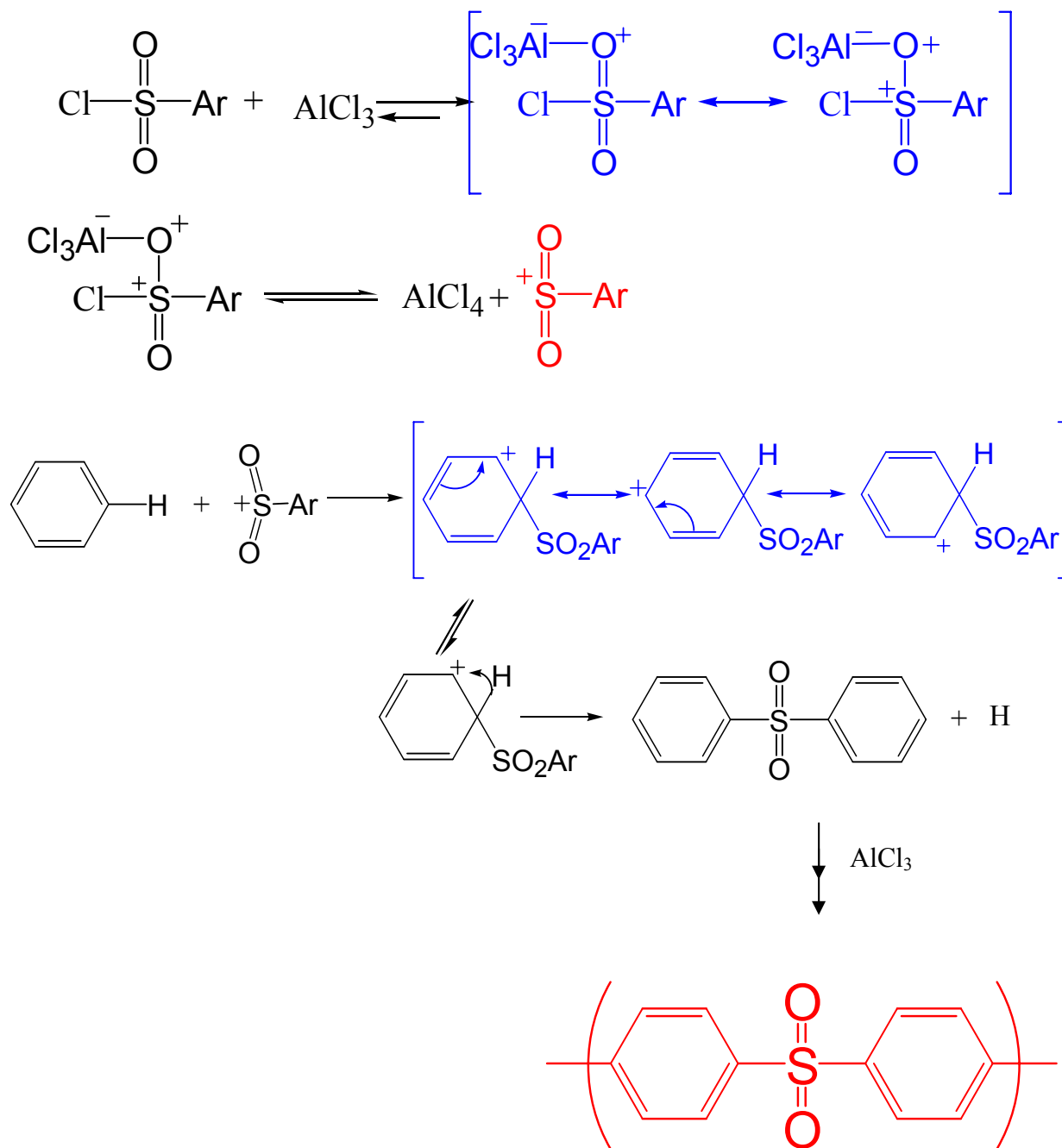


**Figure 2.47** Mechanism of sulfonylation which generates sulfonylium cation (*reprinted from reference 158 with permission from Wiley*)

There are varieties of solvents such as chlorinated biphenyl, nitro benzene and dimethyl sulfone. Electrophilic aromatic substitution reaction requires high catalyst loading. However, it brings a side effect which is the possibility of the substitution of anhydrous metal halides on the aromatic ring. It was noticed that higher reaction temperatures (120-250 °C) eliminates the use of higher catalyst loadings<sup>168, 169</sup>. However, very high temperatures resulted with branched or crosslinked materials. Hence it was agreed that optimum reaction temperature was about 120 °C to obtain linear soluble polymers<sup>170</sup>.

#### 2.8.4 Nucleophilic Aromatic Substitution Reaction (S<sub>N</sub>Ar)

The attack of a nucleophile on the activated carbon halide bond yield resonance stabilized an intermediate called a Meisenheimer complex<sup>171</sup>. This step is the rate determining step. The second step is releasing of leaving group from the Meisenheimer intermediate, which causes decomposition of the intermediate (Figure 2.48). The nucleophilicity order for common nucleophiles is given as: ArS<sup>-</sup>>RO<sup>-</sup>>R<sub>2</sub>NH<sup>-</sup>>ArO<sup>-</sup>>OH<sup>-</sup>>ArNH<sub>2</sub>>NH<sub>3</sub>>I<sup>-</sup>>Br<sup>-</sup>>Cl<sup>-</sup>>H<sub>2</sub>O>ROH<sup>172</sup>. Similarly, the leaving ability of some leaving group is given as F>NO<sub>2</sub>>Cl>Br>OAr>OR>SR<sup>173,174</sup>. Bisphenols as a nucleophile is the commonly used monomer for making poly(arylene ether)s. Because of the reactivity issue bisphenolates from bisphenols are utilized for polymerization reaction.

<sup>168</sup> Jones, M.E.B, British Patent 979,111, 1965

<sup>169</sup> Jennings, B.E.; Jones, M.E.B.; Rose, J.B., *J. Polym. Sci., Part C* 1967, 16, 715

<sup>170</sup> Cudby, M.E.A.; Feasey, R.G.; Jennings, B.E.; Jones, M.E.B.; Rose, J.B.; *Polymer* 1965, 6, 589

<sup>171</sup> Meisenheimer, J.; *Liebigs Ann. Chem.* 1902, 323, 205

<sup>172</sup> Bunnett, J.F.; Zahler, R.E., *Chem. Rev.* 1951, 49, 273

<sup>173</sup> Miller, J.A.; *Aromatic Nucleophilic Substitution*, Elsevier, London, 1968

<sup>174</sup> Beck, J.R., *Tetrahedron* 1978, 34, 2057

Bisphenolates can be prepared using strong or weak base. The bisphenolate obtained by treating a bisphenol with a strong base, e.g., NaOH ( 1:2 mol ratio, respectively) may be reacted with an aromatic dihalide at about 160 °C for 3-5 hours. Unlike the previous example, high molecular weight polymers by nucleophilic aromatic substitution reaction can be synthesized in one-step. A weak base (e.g. potassium carbonate) may also be directly used with a bisphenol and an aromatic dihalide.

Nucleophilic substitution can occur on benzene rings when strong electron-withdrawing groups are ortho or para to the halogen atom. The reaction occurs through an addition-elimination mechanism where a delocalized carbanion (Meisenheimer complex) is an intermediate. The carbanion is stabilized by electron-withdrawing groups in the ortho and para positions

Two step mechanisms were involved during nucleophilic aromatic substitution reaction illustrated in Figure 2.48;

Step 1) Addition Step: Nucleophile attacks aryl halide and bonds to the carbon that bears the halogen (slow-rate determining step-: aromaticity of ring is lost in this step)

Step 2) Elimination Step: Intermediate formed in first step loses halide (fast: aromaticity of ring is restored in this step)

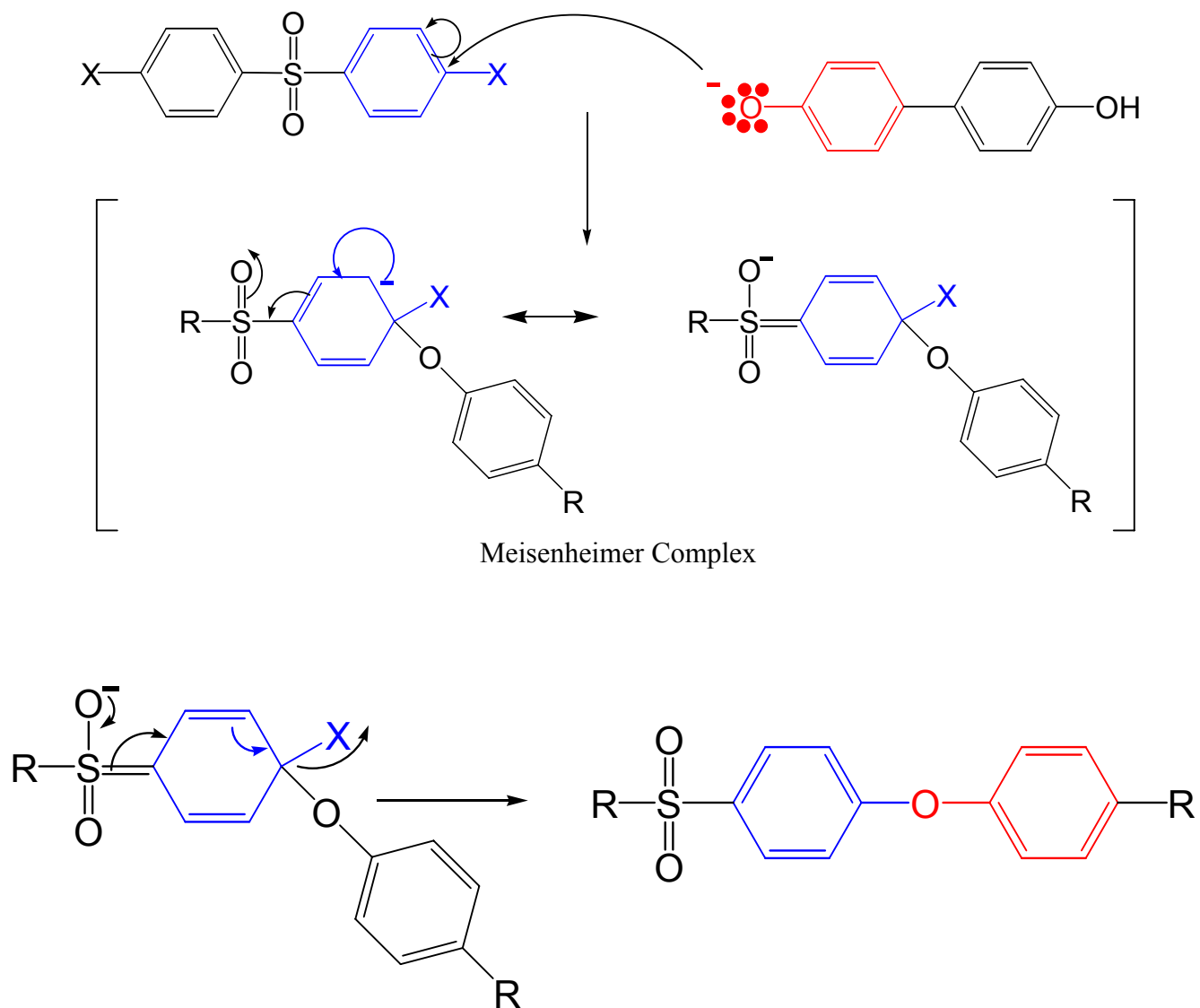


**Figure 2.48** a. Addition step, rate determining step, is slow (where carbanion was stabilized by; 1. Sulfone group, 2. An halide (electronegativity is important!- better stabilization with more electronegative halide), b. Elimination step is fast: Intermediate formed in first step loses halide (fast: aromaticity of ring restored in this step)

Role of the halide in nucleophilic aromatic substitution reaction can be summarized as;

1. Better stabilization of Meisenheimer Complex with highly electronegative halide (Inductive effect) (Figure 2.49)
2. Highly electronegative halide (F) favors the addition step (rate determining step) more than the other halogens by making carbon directly attached to fluorine more electropilic which is more susceptible to nucleophilic attack.

The reaction rate for the S<sub>N</sub>Ar mechanism is;  $F > Cl > Br > I$

It is worthwhile to remember that this was the reverse order for the simple S<sub>N</sub>2 type mechanism which suggests the rate determining is the addition.

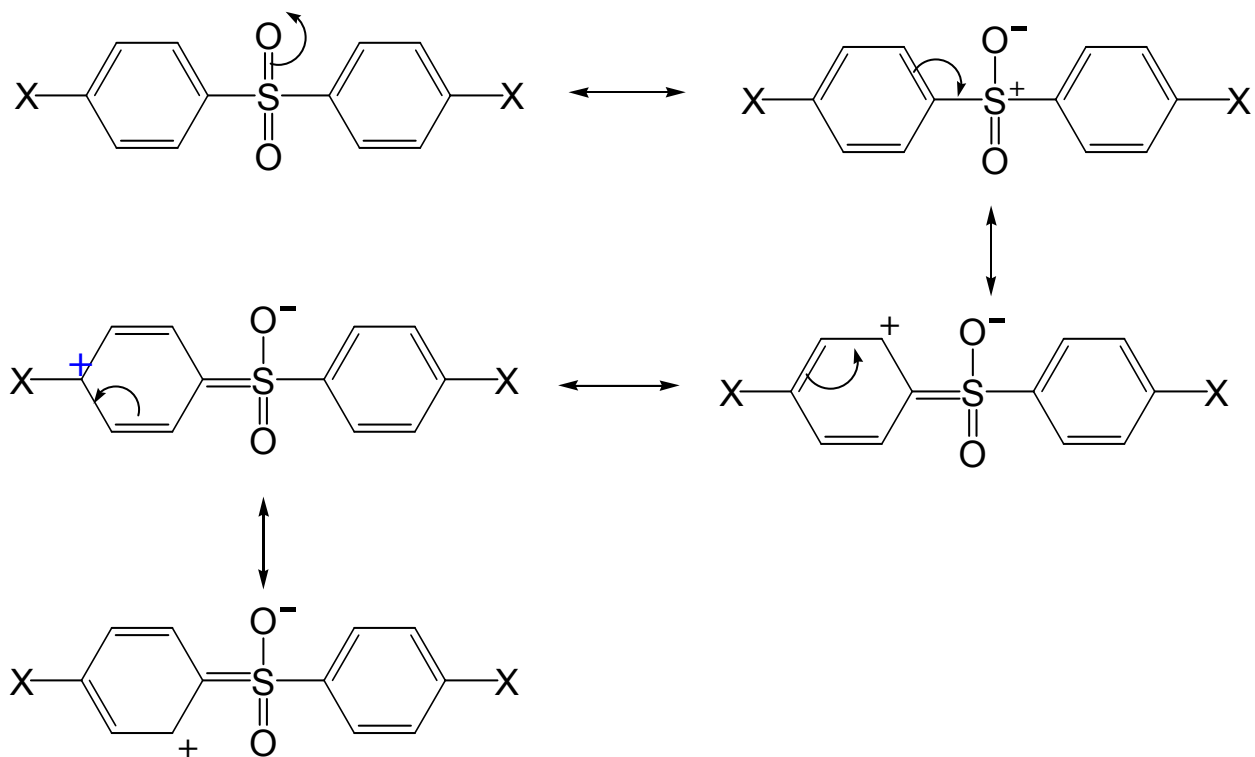


**Figure 2.49** Resonance forms of 4,4'-dichlorodiphenylsulfone; Highly electronegative halide (F) favors the nucleophilic addition step more than the other halogens

### 2.8.4.1 Strong Base Approach

The first successful nucleophilic aromatic route for the synthesis of poly (arylene ether)s was reported by Johnson et al.<sup>175, 176</sup> This route has been also widely used in commercial applications<sup>177</sup>. Johnson et al. investigated a large series of bisphenolates to synthesize poly(arylene ethers)s. The synthesis of bisphenolate from bisphenol A and sodium hydroxide was presented in Figure 2.50. Later, the disodium salt of bisphenolate was reacted with 4,4'-dichlorodiphenyl sulfone at 160 °C for an hour under dry conditions to obtain high molecular weight poly(arylene ether sulfone)s<sup>175,176</sup> (Figure 2.51). The main advantage of the strong base approach was shorter reaction time to afford the high molecular weight, however the trace amount of water side would cause reaction. Another drawback was the solubility problem of many salt forms of bisphenolate (disodium salt of hydroquinone and biphenol). Moreover, strong bases showed the ability of the hydrolyzing the dihalides. This upsets the stoichiometry which prevents obtaining high molecular weight polymer<sup>158</sup>.

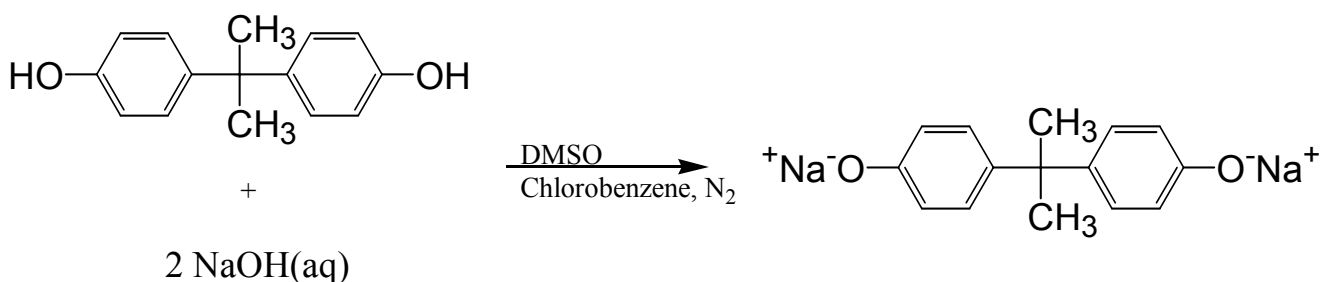


**Figure 2.50** Synthesis of the disodium salt of a bisphenol

<sup>175</sup> Johnson, R.N., In: Encyclopedia of Polymer Science and Technology, N. M. Bikales, (Ed.) Wiley, New York, 1969

<sup>176</sup> Johnson, R.N.; Farnham, A.G.; Clendinning, R.A.; Hale, W.F.; Merriam, C.N., J. Polym. Sci.: Part A-1 1967, 5, 2375

<sup>177</sup> Harris, J.E.; Johnson, R.N.; In. Ency. Poly. Sci. and Eng.; Bikales, N.M., Ed.; John Wiley and Sons: New York, 1988, Vol.13, p96

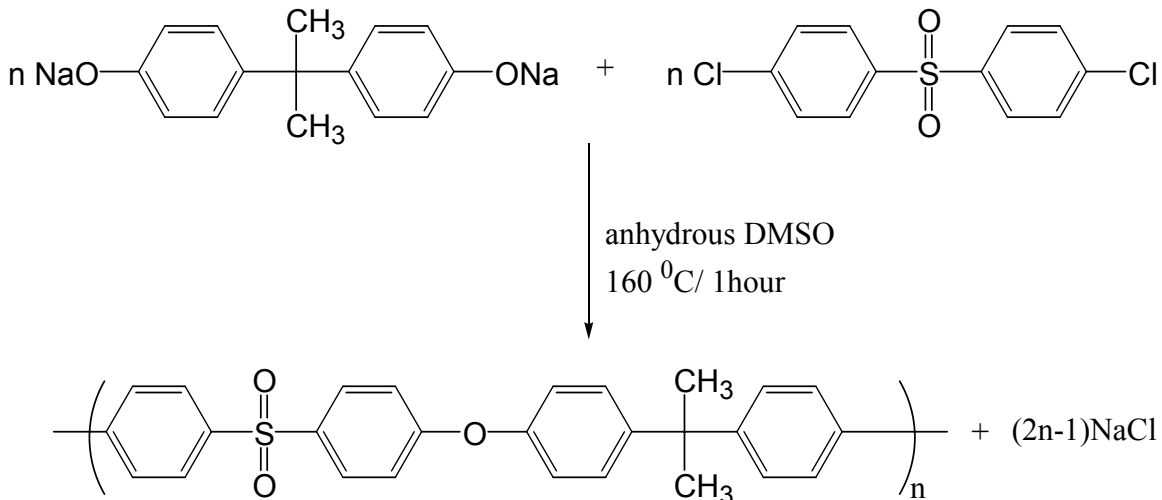


**Figure 2.51** Synthesis of poly(arylene ether sulfone) by the strong base approach

(reprinted from reference 158 with permission from Wiley)

#### 2.8.4.2 Weak Base Approach

Clendinning et al.<sup>178</sup> reported that the potassium carbonate could be used in synthesis of poly(arylene ether sulfone). Some of the first literature published on the weak base method was in the form of a patent. McGrath and coworkers were the first to investigate the weak base method in detail and reported the use of the weak base (potassium carbonate) to synthesize poly(arylene ether sulfone)s in one step<sup>179, 180, 181, 182, 183</sup>. The synthetic approach was shown in Figure 2.52 which includes the

<sup>178</sup> Clendinning, R.A.; Farnham, A.G.; Zutty, N.L.; Priest, D.C., Canada Patent 847, 963, 1970

<sup>179</sup> Viswanathan, R.; McGrath, J.E.; *Polymer Preprints*, 1979, 20, 365

<sup>180</sup> Viswanathan, R.; Johnson, B.C.; McGrath, J.E.; *Polymer* 1984, 25, 1827

<sup>181</sup> Viswanathan, R., Ph.D. Thesis, VPI&SU, Blacksburg, 1981

<sup>182</sup> Hedrick, J.L.; Mohanty, D.K.; Johnson, B.C.; Viswanathan, R.; Hinkley, J.A.; McGrath, J.E., *J. Polym. Sci.: Part A: Polym. Chem.* 1986, 23, 287

<sup>183</sup> Hedrick, J.L.; Dumais, J.J.; Jelinski, L.W.; Patsiga, R.A. McGrath, J.E., *J. Polym. Sci.: Part A: Polym. Chem.* 1987, 25, 2289

formation of phenolate and then polymerization. Potassium carbonate was reported to be better than sodium carbonate due to its higher acidity and higher solubility in the reaction medium. Unlike the strong base method, an excess of potassium carbonate was used in weak base method. Aprotic polar solvents (Dimethyl sulfoxide (DMSO), dimethyl acetaamide (DMAc), dimethyl formamide (DMF), N,N-dimethyl pyrrolidone (NMP), etc) were utilized for the weak base approach. These solvents were good solvents for common monomers. Moreover, the Meisenheimer complex was stabilized by these solvents<sup>158</sup>.

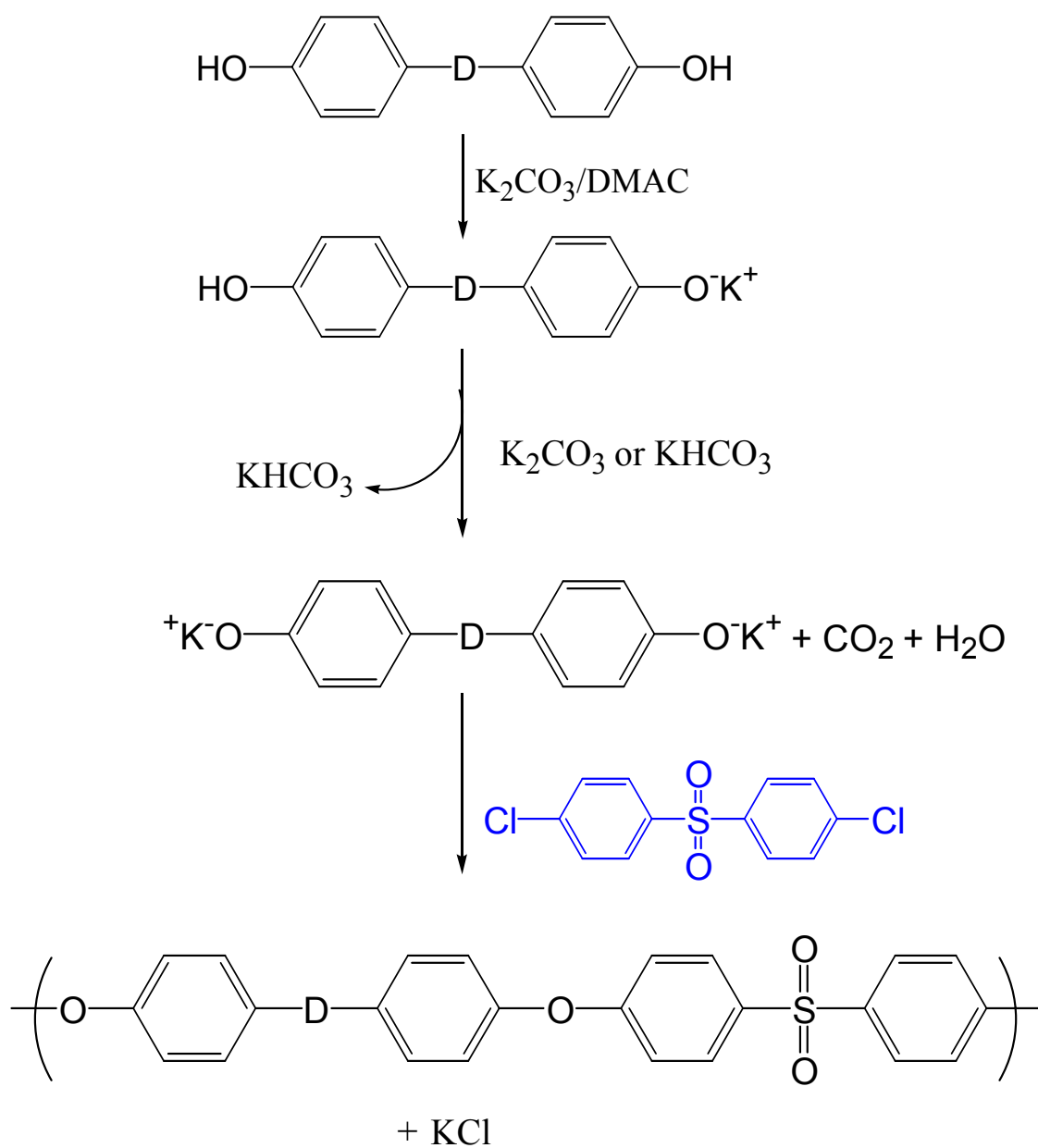


**Figure 2.52** Synthesis of poly(arylene ether sulfone)s by the weak base approach

The synthetic approach used by McGrath et al. utilized the DMAc as dipolar aprotic solvent and toluene as azeotropic agent remove the water which was produced by following process (Figure 2.53). This approach was superior to control the molecular weight of the polymer and also provided the complete removal of water causing side reactions by acting as a nucleophile. This nucleophile reacts with the dihalide and produce an unreactive bisphenol.



**Figure 2.53** Potassium carbonate decomposes during the reaction and produces water which must be removed by a dehydrating agent such as toluene or xylene

## 2.9 Structures, Morphological Models and Applications of Ionomers

Various polymer physical properties such as glass transition temperature, mechanical properties, molecular weight and structure and topology can be tailored by introducing ion containing groups in polymers. This structure property relationship was mainly attributed to significant morphological changes which modifies the physical properties<sup>184</sup>. Ionomers have been defined as ion containing polymers having less than 15 mol percent ion content<sup>185</sup>. However, the definition in terms of physical properties (rather than compositional based) were proposed by Eisenberg and Rinaudo<sup>186</sup>. Hence, ionomers were polymers known as their ionic interaction and aggregates. However, polyelectrolytes was defined as large electrostatic interactions over distances in high dielectric constant solvents<sup>187</sup>. The possible variations of topologies (Figure 2.54) are explained and exemplified in Table 2.2. Other architectures such as random ionomers where ionic groups were randomly distributed, ionene where ionic groups were regularly spaced, comb and graft types of ionomer has been also extensively studied<sup>188</sup>. Among all these architecture a considerable amount of research has been devoted to random ionomers<sup>189</sup>. Hence the morphologies of the random ionomers were of great interest. The multiplet concept was proposed and developed by Eisenberg<sup>190</sup>. The spatial

---

<sup>184</sup> Capek, I., *Advances in Colloid and Interface Science* 2004, 112, 1

<sup>185</sup> *Ionomers: Synthesis, Structure, Properties and Applications*, Tant, M. R., Mauritz, K. A. and Wilkes, G.L., Eds.; 1997, Chapman and Hall: New York.

<sup>186</sup> Eisenberg, A.; Rinaudo, M., *Polymer Bull.* 1990, 24, 671

<sup>187</sup> Eisenberg, A.; Kim, J.S., *Introduction to Ionomers*, 1998, John Wiley and Sons: New York

<sup>188</sup> Weiss, RA; MacKnight, W.J.; Lundberg, R.D.; Mauritz, K.A.; Thies, C.; Brant, D.A., In: *Coulombic Interactions in Macromolecular Systems*, Eisenberg, A.; Bailey, F.E., Ed. , ACS Washington DC, 1986

<sup>189</sup> a. Holliday, L., *Ionic Polymers*, Applied science Publishers: London, 1975, b. Mauritz, K.A.; *J. Macromol. Sci. Rev. Macromol. Chem. Phys.* 1988, C28, 99, c. Tant, M.R.; Wilkes, G.L., *J. Macromol. Sci. Rev. Macromol. Chem. Phys.* 1988, C28, 1

<sup>190</sup> Eisenberg, A., *Macromolecules* 1970, 3, 147

arrangements of the ion pairs in the random type of ionomers known as ion pair aggregation occurs to form quadruplets, sextuplets, and higher aggregates leading to formation of multiplets.

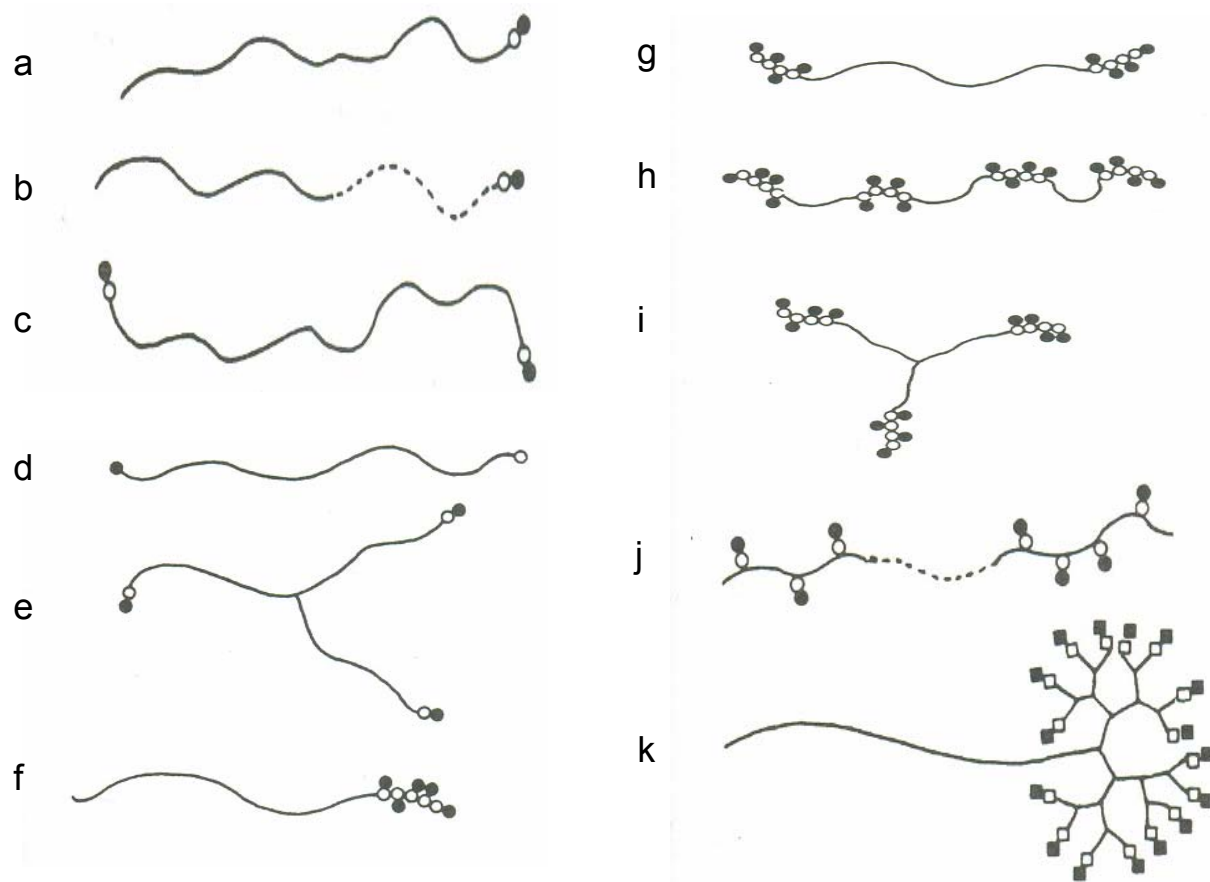


**Figure 2.54** Various possible structural architecture for ionomers a. Monochelic, b. Monochelic block copolymer, c. Telechelic, d. Zwitterionic telechelic, e. Star, f. AB diblock, g. ABA triblock, h.  $(AB)_n$  multiblock, i. Star block, j. ABA triblock ionomer, and k. Ionic dendrimer attached to non-ionic chain (*reprinted from reference 187 with permission from Wiley*)

Table 2.2 Various possible architecture for ionomers

Figure 2. 54	Type	Explanation	Example
A	Monochelic	An ionic group at the one end	Polystyrene containing a terminal carboxylate anion
B	Monochelic Block copolymer	Total one ion at the end of block copolymer	Tertiary amine terminated block copolymer of styrene and isoprene
C	Telechelic	Same type ion at each end of a polymer chain	Dicarboxylate terminated Block copolymer of styrene and isoprene
D	Zwitterionic telechelic	Different type ion at each end of a polymer chain	Tertiary amine and sulfonic acid terminated polyisoprene
E	Star	Three-arm star is tipped at each arm's end	Sulfonic acids terminated polyisobutylene
F	Diblock AB,	AB type block copolymer where one block is nonionic, the other consists of ionic repeat units	Polystyrene (nonionic) block N-methyl-4-vinylpyridinium iodide (ionic)
G	ABA triblock	ABA type triblock copolymer where "A" block is nonionic, the "B" block consists of ionic repeat units	Polystyrene (nonionic) block N-methyl-4-vinylpyridinium iodide (ionic) block polystyrene
H	(AB) <sub>n</sub> mutiblock	Multiblock of AB where "A" block is nonionic, the "B" block consists of ionic repeat units	Multiblock of polyurethane (nonionic) and polyacrylic acid (ionic)
I	Star block	Three-arm star	Three arm star ionomer of polyisobutylene and polymethacrylic acid
J	ABA triblock ionomer	ABA type triblock copolymer where "A" block consists of ionic repeat units, the "B" block is nonionic,	Partially sulfonated styrene block hydrogenated butadiene block partially sulfonated styrene
K	Ionic dendrimer	Ionic dendrimer attached to non-ionic chain	Polystyrene (nonionic) acid functionalized poly(propylene imine) dendrimer

Arrangements of these multiplets were modeled in various different ways. The first model was a multiplet-cluster (or ion-pair cluster model) introduced by Eisenberg<sup>190</sup> which included formation of ion pairs by counter ions when the acid form of the ionomer was neutralized with monovalent ions. The ion pair then serves as a strong dipole-dipole interaction along the polymer backbone which was a driving force to cause association of the ion-pairs into spherical forms of multiplets of two, three, etc with hydration (Figure 2.55 a)<sup>191</sup>. Aggregates can accommodate a maximum number of ion pairs which depends on the the ability of the exclusion of the chain (Figure 2.55 b)<sup>191</sup>. More sophisticated models by Forsman<sup>192</sup>, Dreyfus<sup>193</sup>, Dayte and Taylor<sup>194</sup> based on the same principle of electrostatic (favors the agglomeration) versus elastic forces (opposes the agglomeration). The origin of the elastic deformation was related to energy needed to move chains out of the way of growing agglomeration. Electrostatic interactions between these agglomerates (collective agglomeration of multiplets, Figure 2.55b) cause to formation of phase separated morphology upon hydration<sup>191</sup>. This was energetically favored for the ionomer having critical ionic concentrations.

---

<sup>191</sup> Mauritz, K.A.; Hora, C.J.; Hopfinger, A.J., In: *Ion in Polymers*, Ed. Eisenberg, A.D. ACS Washington DC, 1980

<sup>192</sup> Forsman, W.C., *Macromolecules* 1982, 15, 1032

<sup>193</sup> Dreyfus, B., *Macromolecules* 1985, 18, 284

<sup>194</sup> Datye, V.K.; Taylor, P.L., *Macromolecules* 1985, 18, 1479

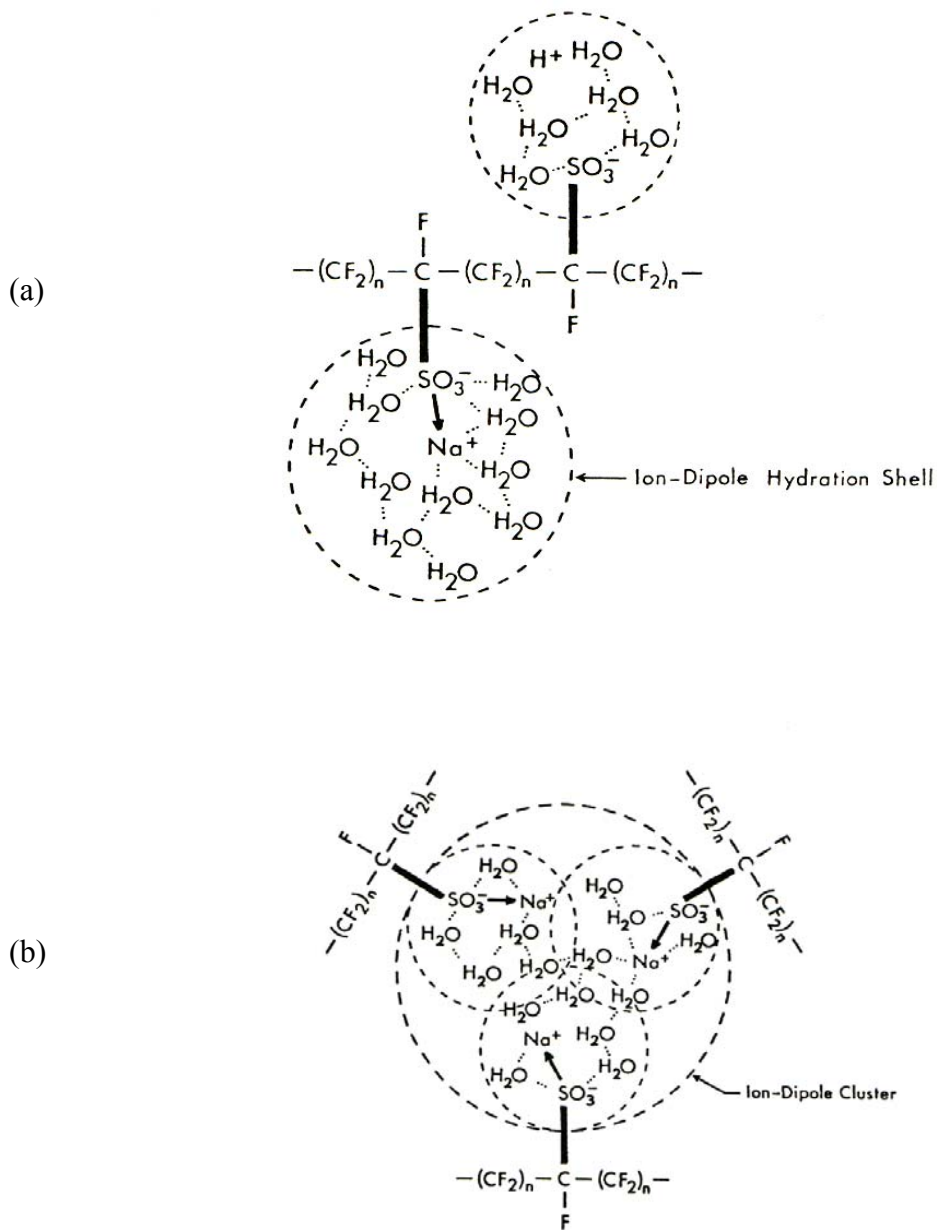


**Figure 2.55** a. Ion dipole formation, b. Ion dipole cluster formation (collective agglomeration of multiplets (*reprinted from reference 191 with permission from ACS*))

Mauritz and Lowry<sup>195</sup> noticed that the mobility of the sodium ions were increased in the Nafion™ ionomer as a function of water content and also reported that not all water was involved for hydration. These types of water behave much like bulk water. Mauritz et al.<sup>196</sup> improved their model by better defining the different possible states of ion-counter ion interactions. The four states of the ion-counter ion association is illustrated in Figure 2.56.

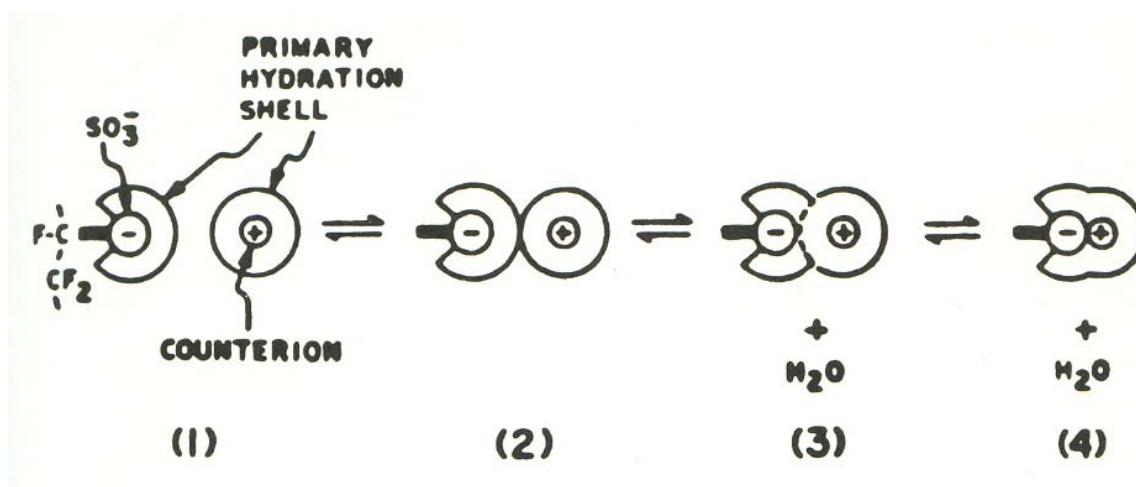


**Figure 2.56** Four states of ionic hydrate association (1) completely dissociated hydrated ion pairs, (2) ion pairs at the contact of undisturbed primary hydration shells, (3) outer sphere complexes, (4) inner sphere complexes (*reprinted from reference 191 with permission from ACS*)

<sup>195</sup> Mauritz, K.A.; Lowry S.R., *Polym. Prepr. ACS* 1978, 19(2), 336

<sup>196</sup> Mauritz, K.A.; Rogers, C.E., *Macromolecules* 1985, 18, 483

The ion-cluster network model was proposed for Nafion™ by Gierke et al.<sup>191</sup> to explain the ion transport in the ionomer (Figure 2.57). It was phenomenological approach that the clusters were connected by short narrows so that ion transports could occur.

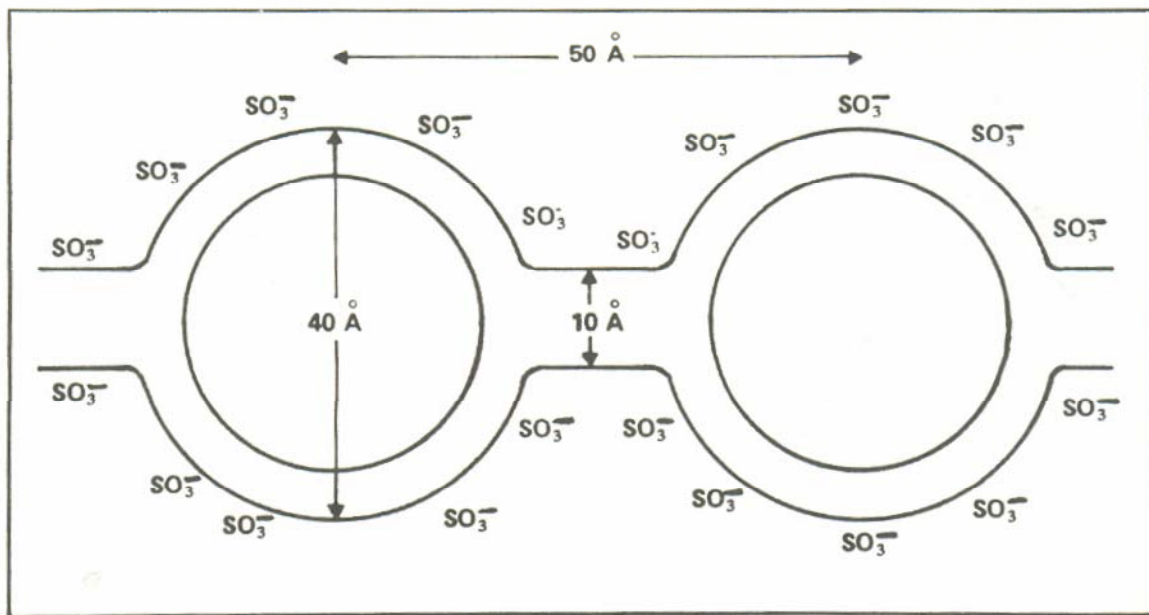


**Figure 2.57** Cluster network model; Ionic clusters with connected short ion channels  
(reprinted from reference 191 with permission from ACS)

The previous theories having potential to demonstrate the phase separation as a favorable thermodynamic process, however it was impractical to define all the interactions contributing to either elastic or electrostatic forces. Gierke et al.<sup>197</sup> defined a lesser number of interactions which was necessary to calculate the equilibrium cluster diameter by minimizing the total free energy of the system.

<sup>197</sup> Hsu, W.Y.; Gierke, T.D., *Macromolecules* 1982, 15, 101

A number of other methods were applied to describe morphological possibilities due to the collective aggregation of the ion dipoles upon hydration. However, none of the previous models were totally consistent with all of the available experimental data based on structure-property relations<sup>185</sup>. The over all problems associated with the previous models were summarized as<sup>185,187,191</sup>.

The cluster behaved as a separate phase having its own glass transition temperature. Previous models also did not predict well the mechanical properties of the ionomers. At relatively low ion content, the aggregates behaved as physical crosslinking points. However, the modulus value increased rapidly (an order of magnitude higher than theoretical calculation based on rubber elasticity theory) at higher ion content. Increasing modulus with increasing ion content suggested the phase inversion of the high glass transition phase which became continuous after a critical concentration. However, the SAXS profile of these ionomers showed that the dimension of aggregates were too small, amounting no more than septimers even at relatively high ion contents. This was inconsistent to two phase behaviour of the ionomers. Since the interparticle scattering distance was smaller than the ionic cluster dimension. For example, in order to observe a second T<sub>g</sub>, the domains must have minimum dimension of 50-100 °A, however, the size of the lattice from SAXS was only about 30 °A. Eisenberg, Hird and Moore (EHM)<sup>198</sup> proposed a model which was consistent to wide range of experimental observations.

---

<sup>198</sup> Eisenberg, A.; Hird, B.; Moore, R.B., *Macromolecules* 1990, 23, 4098

EHM model was based on the formation of the multiplets. The multiplets formation depends on several criteria described below<sup>198</sup>

1. The electrostatic interactions between ion pairs should be strong enough to overcome the elastic forces of the chains to which they are attached
2. The ion pair concentration should not be too dilute. If the ion pairs are too away from each other, they would not tend to aggregate
3. The characteristics of the host polymer (chains which ion pairs are attached) are also important. Ionic aggregation is favored for low T<sub>g</sub>, and low dielectric constant host polymers, whereas it is restricted for the high T<sub>g</sub>, high dielectric constant host polymers.
4. Steric factors determine the size of the multiplets; if the host polymer is rigid, then the multiplets are postulated as small and rigid. For example, telechelics produces large and flexible multiplets
5. Each ion pair in the multiplet anchors the chain. Hence the mobility of chain in this conformation is decreased compare to their bulk conformation. The mobility of the chain increases gradually as the chain become distant to multiplet. Rigid multiplet requires higher electrostatic interactions and restrict the mobility more than flexible ones.

The so called restricted chain mobility (or skin) region was illustrated in Figure 2.58.

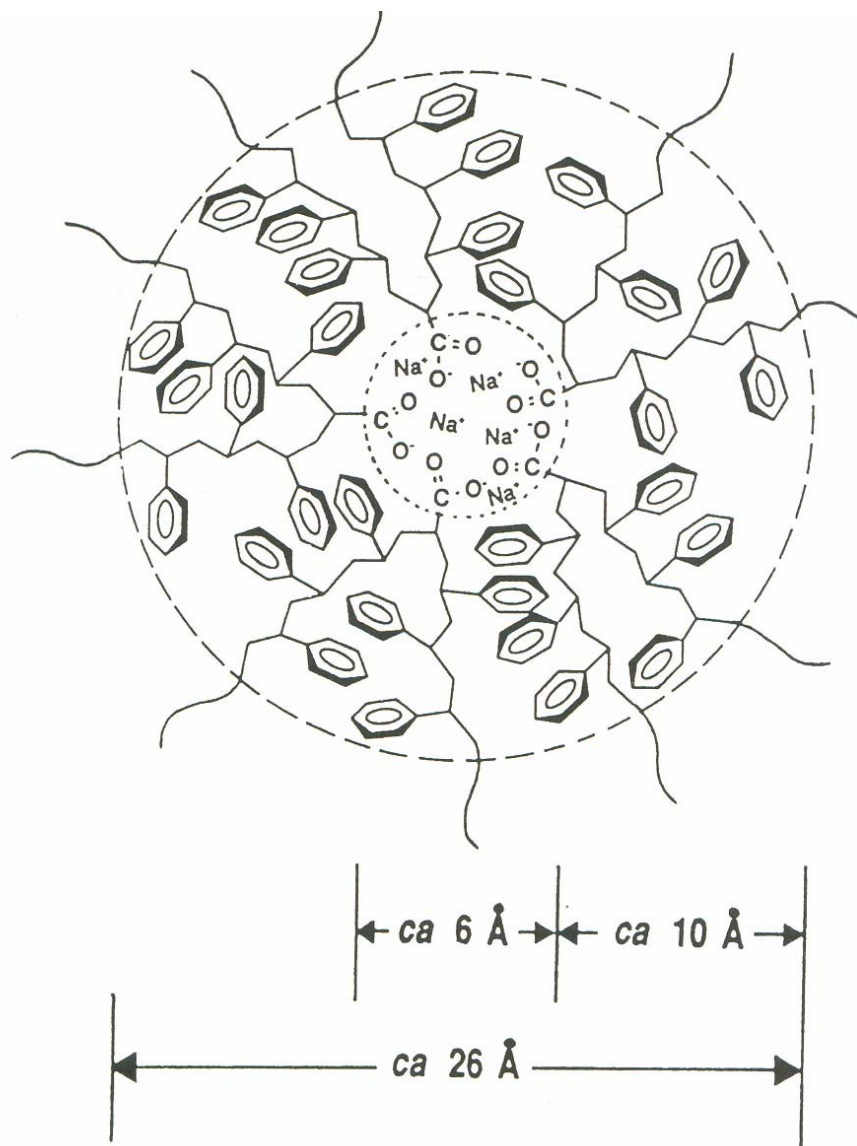


**Figure 2.58** Restricted mobility region surrounding the multiplet for a poly(styrene-co-sodium methacrylate ionomer) (reprinted from reference 198 with permission from ACS)

It was stated that the restricted mobility region surrounding by isolated multiplet would be too small to have its own glass transition temperature. However it can act as large crosslinking point increasing Tg.

As the ion content increases, number of multiplet increases and the distance between multiplets decreases. Hence the substantial amount of overlap occurs in the regions of restricted mobility. As the ion content increases the overlapping regions increases. When such a region becomes large enough ( 50-100 °A), it behaves as an independent phase exhibiting its own glass transition temperature.

Ionomers have wide range of applications with increasing commercial interest. One of the most known applications of ionomers has been as a membrane in the chlor-alkali process, fuel cells and reverse-osmosis<sup>185, 187</sup>. Weiss et al.<sup>188</sup> classified various commercial ionomers and according to their application areas given in Table 2.3.

Table 2.3 Several commercial ionomers (*reprinted from reference 188 with permission from ACS*)

Polymer system	Commercial Name	Applications
Poly(ethylene-comethacrylic acid)	Surlyn	Flexible thermoplastics
Poly( butadiene-co-acrylic acid)	Hycar	Elastomer
Telechelic carboxylate elastomers	Hycar	Specialty uses
Chlorosulfonated polyethylene	Hypalon	Elastomeric Sheeting
Sulfonated ethylene-propylene diene terpolymer	Ionic Elastomer	Thermoplastic Elastomer
Persulfonate Ionomers	Nafion™	Multiple membrane uses
Perfluorocarboxylate Ionomers	Flexion	Chloralkali Membrane

Ionomers as plastics due to the ionic aggregation produce high T<sub>g</sub> tough materials. Ionomers as elastomers showed very interesting features. For example, EPDM terpolymer with zinc counter ion was used as self-vulcanizing rubber. The ionic interactions between multiplets could be disappeared, which reduced the viscosity in the melt and allowed injection molding. Upon cooling, the interactions between mutiplets were reestablished which provided crosslinking points to give the material desirable rubber properties<sup>187</sup>.

Perfluorinated ionomers were successfully applied in the chlor-alkali process. This process includes the production of hydrogen and chlorine from NaCl solution at the anode and cathode, respectively. The role of the membrane is to keep apart the produced gases apart and allowing sodium hydroxide in high purity to collect at the cathode.

Fuel cells are energy converting devices uses ionomers as separator for the fuel and oxidants and also act as proton conductor. Hence the ionomers are solid electrolytes in the proton exchange membrane fuel cells. Reverse osmosis and ultrafiltration is another major application area. In the reverse osmosis process a system forces water to pass through a semipermeable barrier (ionomer) allowing selective transfer of particular species such as water. However this barrier partially or completely holds the solutes such as sodium chloride. Chemical potential difference across the membrane provides driving force for the transport. Other well-known applications of ionomers were presented in Table 2.4.

**Table 2.4** Various possible applications of ionomers

Application	Types	Example	Reference
Membrane	Chloro-alkali	Perfluorinated ionomers	185,187,199
	Fuel Cell		185,187, 199, 200
	Reverse Osmosis		185,201
	Energy storage (batteries)		185, 187,189
Packaging	Oil and chemical resistance ionomers	Ethylene ionomers	185,187, 189,202
Magnetic Recording Media	Aqueous dispersion form	Polyurethane ionomers	187,203
Imaging	electrophotography	Styrene-n-butyl methacrylate-potassium methacrylate terpolymer	187, 203

<sup>199</sup> *Perfluorinated Ionomer Membranes*, Eisenberg, A.; Yeager, H.L., Eds; ACS symposium Series 180, ACS Washington DC, 1982

<sup>200</sup> *Ionomers, Characterization, Theory and Application*, Schlick, S. Ed. ; CRC: Boca Raton, FL, 1996,

<sup>201</sup> Tsuru, T.; Urairi, M.; Nakao, S.; Kimura, S., *J. Chem. Eng. Japan* 1991 24, 518

<sup>202</sup> Statz, R.J.; *Polym. Prep., ACS* 1989, 29, 435

<sup>203</sup> Tan, J.S. in: *Structure and Properties of Ionomers*; Pineri, M.; Eisenberg, A., Ed., NATO ASI Series C: Mathematical and Physical Sciences, 198; Reidel: Dordrecht, 1987

---

## CHAPTER 3

### **Synthesis and Characterization of 3,3' - disulfonated 4,4'-dichlorodiphenyl sulfone (SDCDPS) Monomer for Proton Exchange Membranes (PEM) in Fuel Cell Applications**

---

Taken from :

1. Sankir, M.; Bhanu, V. A.; Ghassemi, H.; Wiles, K. B.; Hill, M. L.; Harrison, W.; Sumner, M.; Glass, T. E.; Riffle, J. S.; McGrath, J. E. Systematic study of the synthesis and characterization of 3,3'-sulfonylbis(6-chlorobenzenesulfonic acid) disodium salt monomer for proton conducting polymeric membranes in fuel cell applications. **Polymer Preprints (American Chemical Society, Division of Polymer Chemistry) (2003), 44(1), 1079-1080. Presented at the National ACS Conference in New Orleans.**
2. Sankir, M.; Bhanu, V.A.; Harrison, W.L.; Ghassemi, H.; Wiles, K.B.; Glass, T.E.; Brink, A.E., Brink, M.H. and J.E. McGrath et al. Synthesis and Characterization of 3,3' - disulfonated 4,4'- dichlorodiphenyl sulfone (SDCDPS) Monomer for Proton Exchange Membranes (PEM) in Fuel Cell Applications. **Accepted in J. Applied Polymer Sci., 2006.**

### 3.1 Abstract

A systematic study of the synthesis and characterization of 3,3'-disulfonated 4,4'-dichlorodiphenyl sulfone (SDCDPS) monomer was conducted by varying reactant stoichiometries (molar ratios of 4,4'- dichlorodiphenyl sulfone (DCDPS) to SO<sub>3</sub> 1:2.2, 1:2.9 and 1:3.3), reaction temperature (90-120 °C) and reaction time (4-6 hours). The optimum synthesis batch process variables were 1:3.3 reactant molar ratio (DCDPS: SO<sub>3</sub>) at 110 °C for 6h. In earlier studies, recrystallization of the “crude” disulfonated monomer from alcohol/water mixture was necessary to remove the mono sulfonated and DCDPS impurities which lowered yield. However, in the current research, SDCDPS was successfully synthesized at nearly 100 % conversion which effectively eliminated the need for recrystallization. Recrystallization of SDCDPS from several alcohol-water mixtures (methanol, ethanol and isopropanol water mixtures) was investigated to compare product purities. Several characterization methods including proton NMR, HPLC, UV-Visible, and fast atom bombardment mass spectroscopy (FAB) confirmed that the crude SDCDPS was completely disulfonated, without having any mono sulfonated and/or starting material DCDPS impurities. Hence, it was demonstrated that the crude SDCDPS monomer by the current one step process and the recrystallized SDCDPS monomer were identical. This optimized monomer synthesis has been used to scale up the SDCDPS and poly(arylene ether sulfone) random and statistical copolymers at controlled disulfonation (35 and 45 mol %) levels which were then used to fabricate proton exchange membranes for fuel cell applications. The intrinsic viscosity data confirmed that high molecular weight film forming copolymers were synthesized. The calculated degree of

disulfonations by proton NMR was in close agreement with target disulfonations. One concludes that this optimized SDCDPS synthesis eliminates the need for recrystallization which would be expected to improve process economics.

### 3.2 Introduction

Sulfonated high performance ion containing polymer “ionomers” can be produced by post-sulfonating polymeric precursors such as poly(arylene ether sulfone)s<sup>1</sup>, poly(benzimidazole)s<sup>2</sup>, and polyether ketones<sup>3</sup>. These materials display phase-separated morphologies, which make them suitable for water desalination, gas separations, and demanding applications requiring enhanced mechanical properties<sup>4,5,6</sup>. The sulfonation reactions proceed by electrophilic aromatic substitution of the aromatic rings, using reagents such as SO<sub>3</sub> or chlorosulfonic acid. It is well recognized that another potential application for sulfonated aromatic copolymers is in proton exchange membrane (PEM) fuel cells. Nafion™, a perfluorinated sulfonic acid copolymer, is currently the state of art for such applications<sup>7,8,9</sup>. Sulfonated aromatic copolymers may have several advantages such as higher mechanical strength, improved durabilities at higher temperatures in the fuel cell environment, and lower cost. These materials may be particularly advantageous

---

<sup>1</sup> Quentin, J.P. Sulfonated poly(arylene ether sulfones), U.S. Patent 3, 709,841, Rhone-Poulenc, January 9, 1973

<sup>2</sup> Alberti, G.; Casciola, M.; Massinelli, L.; Bauer, B.; *J. Membrane Science* 2001, 185, 73

<sup>3</sup> Glipa, X.; Haddad, M.E.; Jones, D.; Roziere, J.; *J. Solid State Ionics* 1997, 97, 33

<sup>4</sup> Lundberg, R.D. Encyclopedia of Polymer Science and Technology, 1987, vol.8, 393

<sup>5</sup> Fitzgerald, J.J., Weiss, R.A., *J. of Macromolecular Science, Reviews in Macromolecular Chemistry and Physics* 1998, C28(1), 99

<sup>6</sup> Hajadost, S and Yarwood, J.; *J. Cem. Soc. Faraday Trans.* 1997, 93, 1613

<sup>7</sup> Jones, D.J.; Roziere, J.; *J. Membrane Science* 2001, 185, 41

<sup>8</sup> Kerres, J.A.; *J. Membrane Science* 2001, 185, 3

<sup>9</sup> Jorissen, L.; Gogel, V.; *J. Power Sources* 2002, 105, 267

in direct methanol fuel cells (DMFC) due to the lower methanol permeability compared to Nafion™.

We have recently described a direct statistical copolymerization route incorporating disulfonated activated aromatic halide monomers into poly(arylene ether sulfone)s to prepare PEM materials<sup>10,11</sup> (Figure 3.1). This approach employs 3,3'-disulfonated, 4,4'-dichlorodiphenyl sulfone (SDCDPS) copolymerized with nonsulfonated activated aromatic dihalides and bisphenols. The stoichiometric ratio of disulfonated to nonsulfonated repeat units can be accurately controlled to tailor the water uptake, conductivities and mechanical properties of these film forming materials.<sup>10,12</sup> The synthesis of SDCDPS was first reported by Robeson and Matzner<sup>13</sup> and was later studied by Ueda et al<sup>14</sup>. The synthesis procedure was further improved in our laboratory<sup>15,16,17</sup>, but has never been investigated in the depth necessary to define several critical parameters required for the synthesis of larger scale quantities.

---

<sup>10</sup> Harrison, W.L.; Ph.D. Dissertation, Virginia Tech, 2002

<sup>11</sup> Harrison, W.L.; Wang, F.; Mecham, J.B.; Bhanu, V.A.; Hill M.; Kim, Y.S.; McGrath J.E.; *J. of Polymer Science: Part A Polymer Chemistry* 2003, 41, 2264

<sup>12</sup> Wang, F.Hickner; M, Kim YS; Zawodzinski, TA; McGrath J.E.; *J. Membrane Science* 2002, 197, 231

<sup>13</sup> Robeson, L.M; Matzner, M.; U.S. Patent 4,380, 598, Flame Retardant Polyarylate Compositions, Union Carbide, April 19, 1983

<sup>14</sup> Ueda, M.; Toyota, H.; Ouchi, T.; Sugiyama, J.; Yonetake, K.; Masuko, T. and Teramoto, T.J.; *Polym. Sci. Part A: Polymer Chemistry* 1993, 31, 853

<sup>15</sup> Hickner, M.A.; Ghassemi, H.; Kim, Y.S.; Einsla, B.R.; McGrath, J.E, *J.E. Chem. Rev.* 2004, 104, 4587-4612

<sup>16</sup> Wang, F.; Hickner, M.A.; Ji, Q.; Harrison W.L.; Mecham, J.B.; Zawodzinski, TA; McGrath, J.E.; *Macromol. Symp.* 2001, 175(1), 387

<sup>17</sup> Sankir M.; Bhanu, V.A.; Ghassemi, H.; Wiles, K.B.; Hill, M.H.; Harrison, W.; Sumner, M.; Glass, T.E.; Riffle, J.S.; McGrath, J.E.; *Polymer Preprints*, 2003, 44(1),

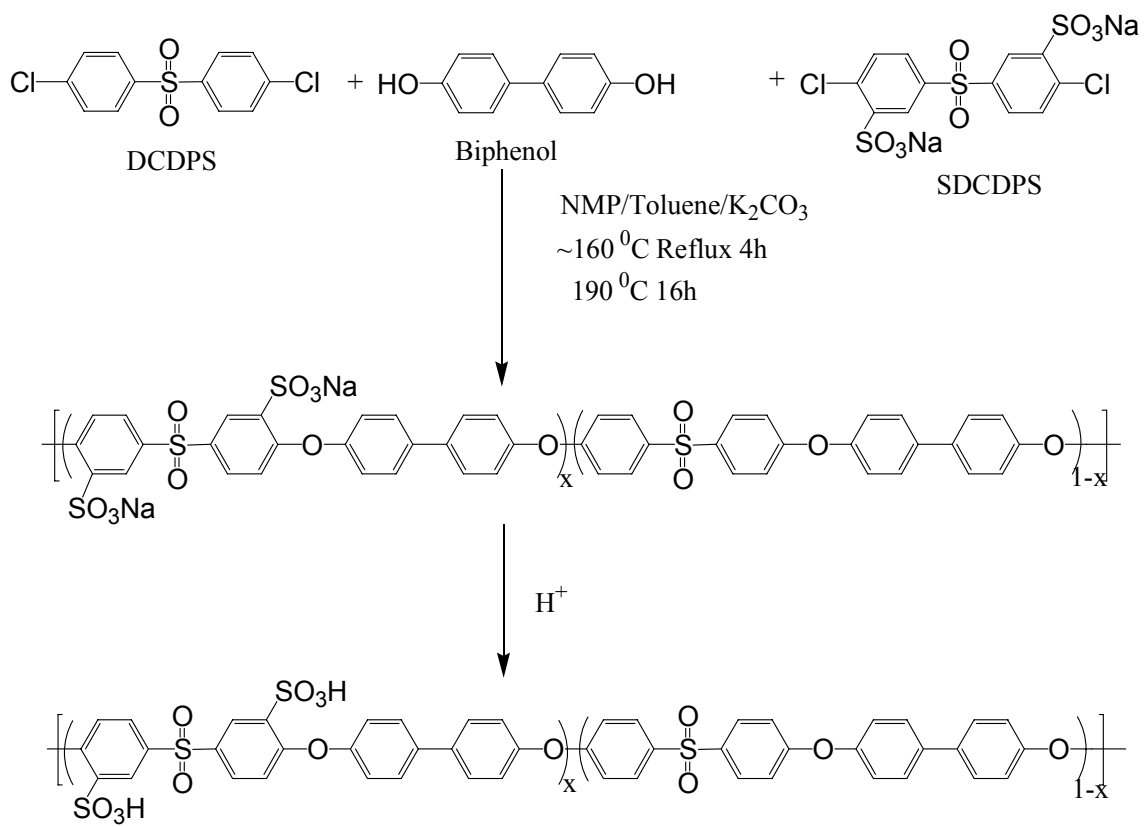


**Figure 3.1** Synthesis of BPSH via the direct copolymerization route

This paper describes: (1) a novel procedure for the synthesis and analysis of 3,3'-disulfonated 4,4'- dichlorodiphenyl sulfone (SDCDPS) with near quantitative conversion useful on a kilogram (or larger) scale, (2) identification of the impurities formed in the disulfonation reaction, and (3) demonstration of the synthesis of high molecular weight poly(arylene ether sulfone) copolymers using the disulfonated monomer prepared by this process.

### **3.3 Experimental**

#### **3.3.1 Reagents**

Fuming sulfuric acid with a measured 27-33 wt % of sulfur trioxide (SO<sub>3</sub>), sodium chloride, sodium hydroxide pellets, potassium carbonate and toluene were obtained from Aldrich and used as received. Solvay Advanced Polymers Inc provided high purity 4,4'-dichlorodiphenyl sulfone (DCDPS) monomer. The 4,4'-isopropylidenebiphenol (Bisphenol A) (Dow chemical) was recrystallized from toluene and dried under vacuum. N-Methyl-2-pyrrolidinone (NMP) (Fisher) was vacuum distilled from calcium hydride onto molecular sieves under vacuum, then stored under nitrogen.

### **3.3.2 Disulfonation of DCDPS**

The 4,4'-dichlorodiphenyl sulfone (10g, 0.0348 mol) and fuming sulfuric acid ( $\text{SO}_3$  to DCDPS molar ratio were 1:2.2, 1:2.9 and 1:3.3. The amount of the electrophilic  $\text{SO}_3$  in fuming sulfuric acid was determined by titration using 0.01 N sodium hydroxide. The reagents were added to a 100-mL three-necked flask fitted with an overhead mechanical stirrer and nitrogen inlet and outlet, and purged with nitrogen for several minutes. The purge was then stopped during the reaction to minimize  $\text{SO}_3$  losses. Disulfonation reactions were performed as a function of reaction time (4-6 h), temperature, (room temperature and 90-120 °C) and stoichiometries of the reactants. The reaction product was dissolved into a mixture of 50 g of ice and 50 g of water. The sodium chloride (25 g) was dissolved with stirring into the solution when the solution temperature was about 65 °C. The mixture was stirred, cooled to room temperature and filtered. The product was redissolved in deionized water (100 g) and the pH of the solution was adjusted to 7 with 10 N sodium hydroxide. The product was salted out by adding the sodium chloride (25 g) at about 65 °C and filtered at room temperature. Finally, it was dried under vacuum at 160 °C for 24 h.

### **3.3.3 Characterization Methods**

#### **3.3.3.1 Monomer Characterization**

Chemical structures of both the SDCDPS monomer and the disulfonated copolymers were confirmed by proton NMR using a Varian Unity 400 spectrometer. All spectra were obtained from a 10% solution (w/v) in dimethylsulfoxide- $d_6$  solution at room temperature. High performance liquid chromatography for the disulfonated

monomers was conducted on a Beckman SystemGold chromatograph. The reversed phase column was obtained from the Restek Corporation. Chromatograms were obtained by injecting 10  $\mu$ L samples, which were prepared by first dissolving the samples in methyl alcohol. The mobile phase was acetonitrile-water (4:1 v/v). Further purity studies of the SDCDPS monomer were conducted using a Shimadzu Model UV-1601 UV-Visible spectrometer. The samples were dissolved in methanol to maintain several ppm solutions and absorbance data was generated. Fast atom bombardment mass spectroscopy (FAB<sup>-</sup>MS) in negative ion mode was obtained using JEOL-JMS HX110 dual focusing mass spectrometer. The low freezing point liquid matrix was 3-nitrobenzyl alcohol. Thermogravimetric analysis (TGA) was performed on a TA Instruments TGA Q 500. Dried SDCDPS monomer (5-10 mg) was evaluated over the range of 25 to 190 °C at a heating rate of 10 °C/min in air.

Copolymer Characterization: Intrinsic viscosity measurements for were performed in NMP at 25 °C using a Cannon Ubbelohde viscometer. The proton NMR spectra were obtained as described above for the monomer characterization.

### **3.3.3.2 Model Copolymerization**

Disulfonated poly(arylene ether sulfone) copolymers were achieved with various degrees of disulfonation (35-45 mol % SDCDPS) via direct copolymerization of 3,3'-disulfonated 4,4'-dichlorodiphenyl sulfone (SDCDPS), 4,4'-dichlorodiphenyl sulfone and 4,4'-biphenol (BP) as reported Sankir (17). The DCDPS (2.5866 g, 0.0090 mol), SDCDPS (2.3826 g, 0.0049 mol) and BP (2.5804 g, 0.0139 mol ) and potassium

carbonate (15% excess, 2.2025 g) were transferred to a 3-neck flask equipped with a mechanical stirrer, a nitrogen inlet and a Dean Stark trap. Dry NMP (15mL) was introduced to provide 35% (w/v) solid concentration and ratio of NMP to toluene (v/v), an azeotroping agent, was 2:1. The reaction mixture was refluxed for 4 hours at 150 °C to complete the dehydration process. The reaction temperature slowly was increased to 190 °C for 16 hours, after gradual removal of the toluene. The viscous reaction product was cooled and diluted with NMP (10 ml) and precipitated in deionized water (500 mL) as swollen fibers. After being washed several times with deionized water, the precipitated copolymer was transferred to boiling deionized water where the salts were extracted for 4 hours. The copolymer was then washed several times with deionized water and dried in a vacuum oven at 120 °C for 24 hours.

### **3.4 Results and Discussion**

The disulfonation reaction was found to be mostly affected by the reactant stoichiometries, reaction temperature and time. The desired amount of fuming sulfuric acid based on the actual titrated measurement of the SO<sub>3</sub> content in fuming sulfuric acid was the most important optimization variable. It was observed that the crude disulfonated product salted out with some monosulfonated impurity and starting material with the low reactant ratios, e.g., moles of DCDPS to SO<sub>3</sub> were 2.2 and 2.9. Theoretically, these ratios were enough for complete disulfonation. However, experimentally, this was only achieved when the reactant ratio were about 3.3. It was obvious that stoichiometry was easily upset by SO<sub>3</sub> loss during the earliest conducted reaction and possibly also be material transfer including weighing step prior to reaction. However, use of 1.3-mole

excess of  $\text{SO}_3$  containing fuming sulfuric acid produced products of essentially 100 % conversion. The  $^1\text{H}$  NMR spectra, as a function of reactant ratios confirming this are provided in Figure 3.2.

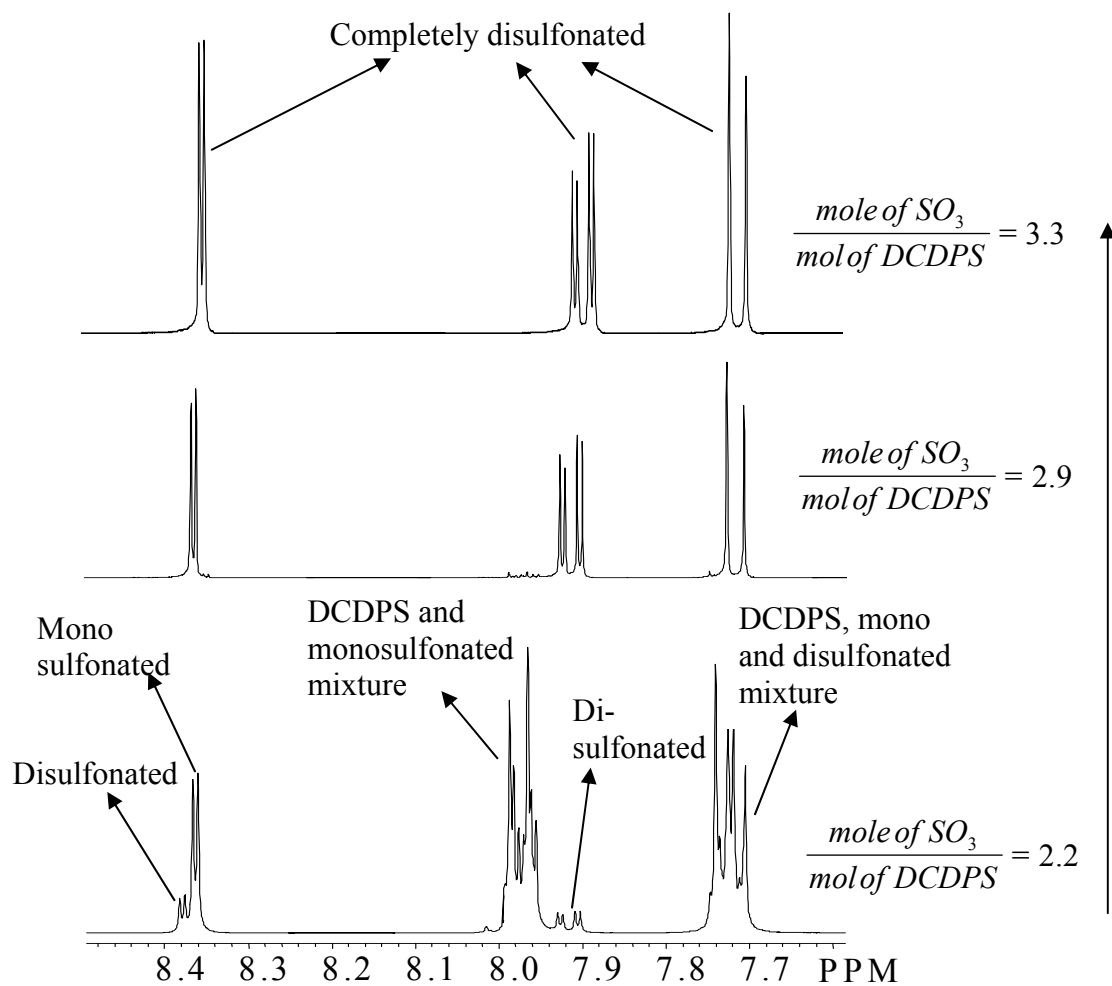


**Figure 3.2** Effect of reactant ratio on the disulfonation reaction; Mixture of monosulfonated ,disulfonated product and starting material disappear gradually with increasing reactant ratio

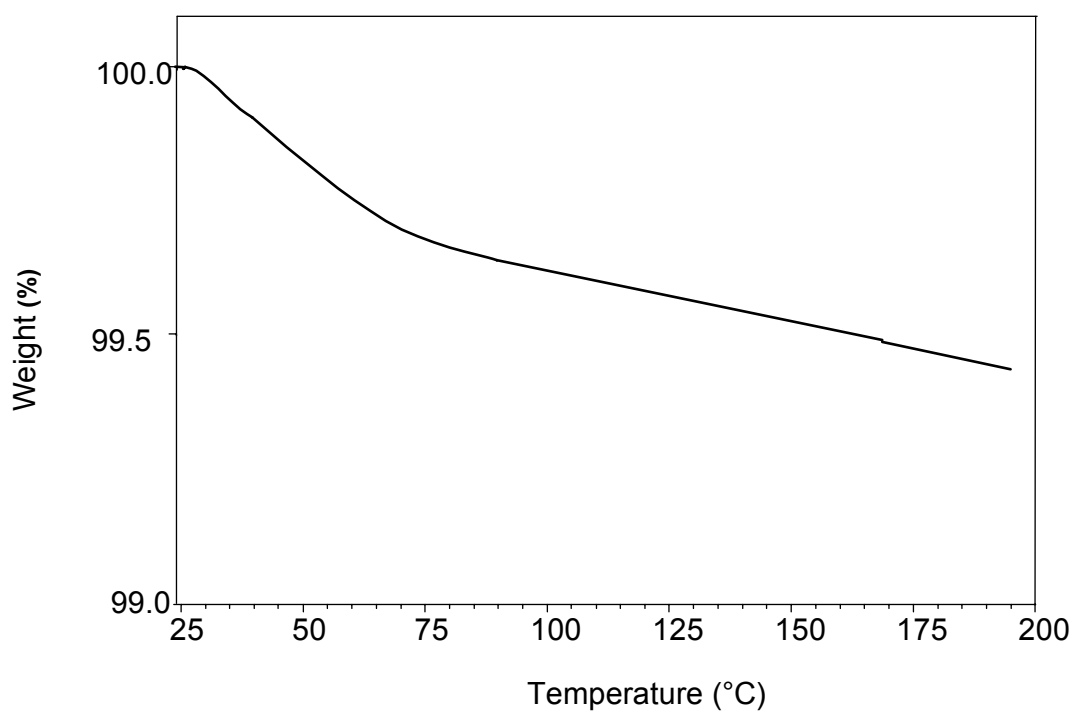
The reaction temperature was another optimization variable. Based on literature literature and our earlier studies, it was generally varied in the range of 90- 120 °C. Later, some experiments were conducted at room temperature, with the optimized reactant molar ratio of 1:3.3 (DCDPS: SO<sub>3</sub>). The reaction progress was monitored and the results were summarized in Table 3.1 in terms of the observed impurities by <sup>1</sup>H NMR. Subsequently, all disulfonation reactions were conducted at 110 °C. The disulfonation reaction at 110 °C with 1:3.3 reactant mol ratio was repeated for 4-6 hours and always produced only disulfonated product. Therefore, one may conclude that the best conditions for the disulfonation reaction were at 110 °C with 1:3.3 reactant ratio for 6 hours.

Table 3.1 Proton NMR of the disulfonation reaction after 6h reaction at 1:3.3 DCDPS:SO<sub>3</sub> stoichiometry

Reaction Temperature °C	Starting material DCDPS	Mono sulfonated DCDPS	Disulfonated DCDPS
25-28	MP	O	O
90	O	O	O
100	NO	O	O
110	NO	NO	DP
120	NO	NO	DP

MP: Major product, O: Observed, NO: Not observed, DP: Desired product

The sulfonic acid moieties were converted to their sodium salt form after the disulfonation reaction to isolate the product. The excess acid in the isolated product was titrated slowly with sodium hydroxide until the product salted out. The final SDCDPS was dried for 24 hours at 160 °C to remove all of the water. TGA after this drying treatment shows only about 0.5 % loss, which indicates that almost all of the water was removed by the drying step (Figure 3.3).



**Figure 3.3** TGA of SDCDPS monomer dried at 160 °C for 24h indicates <0.5 weight percent water

Recrystallization of the “crude” disulfonated monomer from various alcohol/water mixtures was earlier performed to remove the mono sulfonated and DCDPS impurities. However, under the condition described above one does not observe monosulfonated product or starting material. Recrystallization was performed to compare the polymerizability of the recrystallized and crude products. The major drawback with the recrystallization is that yield decreases markedly to about 50-70 % percent for various alcohol-water mixtures such as methanol-water, ethanol-water and isopropanol-water. The chemical structure of the disulfonated monomer was confirmed and compared with its recrystallized form by fast atom bombardment mass spectroscopy (FAB<sup>-</sup>-MS) in the negative ion mode, proton NMR, HPLC and UV spectroscopy.

Table 3.2 Intrinsic viscosity and mole percent disulfonation of the BPS copolymers, which indicate high molecular weight copolymers were achieved

Copolymer	$[\eta]_{25^{\circ}\text{C}}^{\text{NMP}}$ (dL/g)	Mole Percent Sulfonation ( <sup>1</sup> H NMR)
BPS-35	1.1	34.9
BPS-45	1.2	44.5

The proton NMR for both the crude and recrystallized monomer and starting material is shown in Figure 3.4. The new peak (Hd) incorporated at around 8.3 ppm indicates the proton next to the SO<sub>3</sub>Na and confirms the disulfonation. The meta proton with respect to chlorine (Hb) atom was not affected much from sulfonation and remained in same position as in the DCDPS structure. However, the proton labelled as Hc was affected by the SO<sub>3</sub>Na moieties and shifted from about 8 ppm to 7.85 ppm. It should be pointed out that all these characteristic peaks were observed for both one step and recrystallized products.

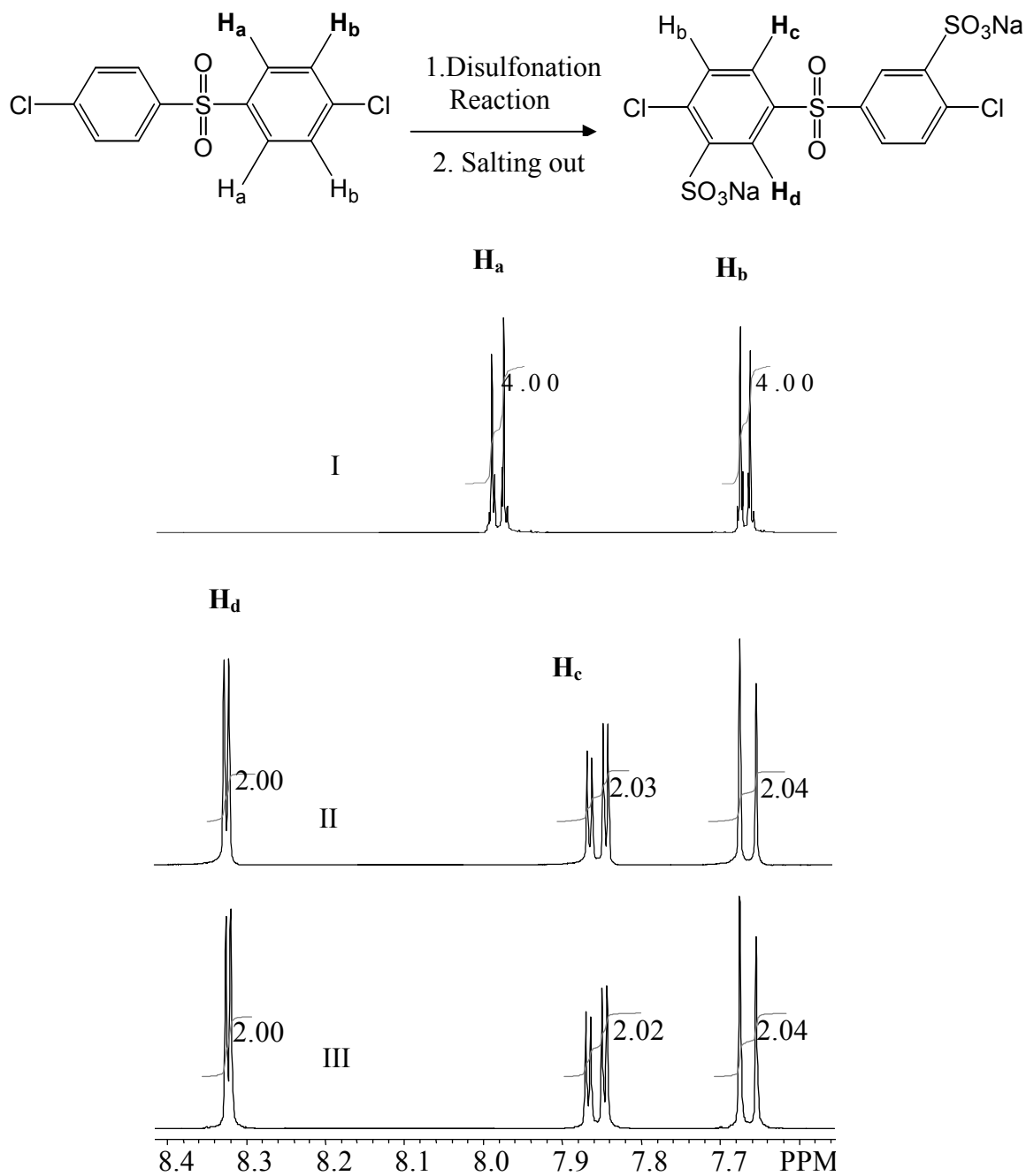


**Figure 3.4** <sup>1</sup>H NMR spectrum of starting material DCDPS (I), crude SDCDPS monomer (II) and recrystallized SDCDPS monomer (III) : The peak incorporated at about 8.32 ppm and integration values confirm disulfonation

Reversed phase HPLC in which the stationary phase is nonpolar and mobile phase is relatively polar was used to measure the retention times of the crude SDCDPS, recrystallized SDCDPS and starting material DCDPS. The most polar components among these materials eluted first and were either the crude or recrystallized SDCDPS. The least polar component, the starting material DCDPS eluted last (Figure 3.5). The crude and recrystallized SDCDPS showed exactly same retention time. However, crude SDCDPS peak was slightly broader than that of recrystallized SDCDPS. This may be due to the some associated excess sodium chloride from the salting out step, which relatively decreased during the recrystallization step.

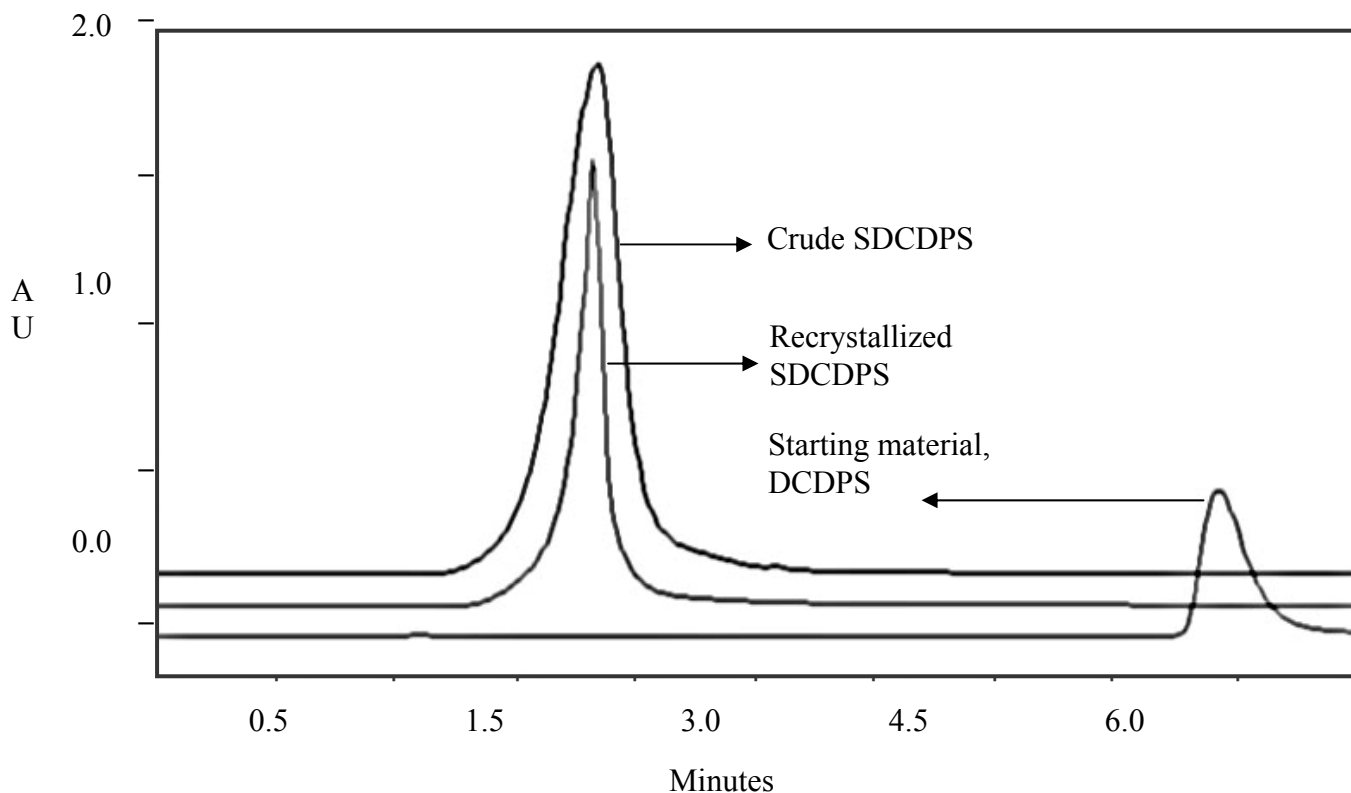


**Figure 3.5** HPLC chromatograms for crude SDCDPS monomer, recrystallized SDCDPS monomer and the starting material DCDPS

A blue shift due to the disulfonation was observed by UV spectroscopy. The UV spectrometric determination of crude SDCDPS, recrystallized SDCDPS and the starting DCDPS is shown in Figure 3.6. One notes that both crude and recrystallized SDCDPS show exactly the same UV absorption characteristics.

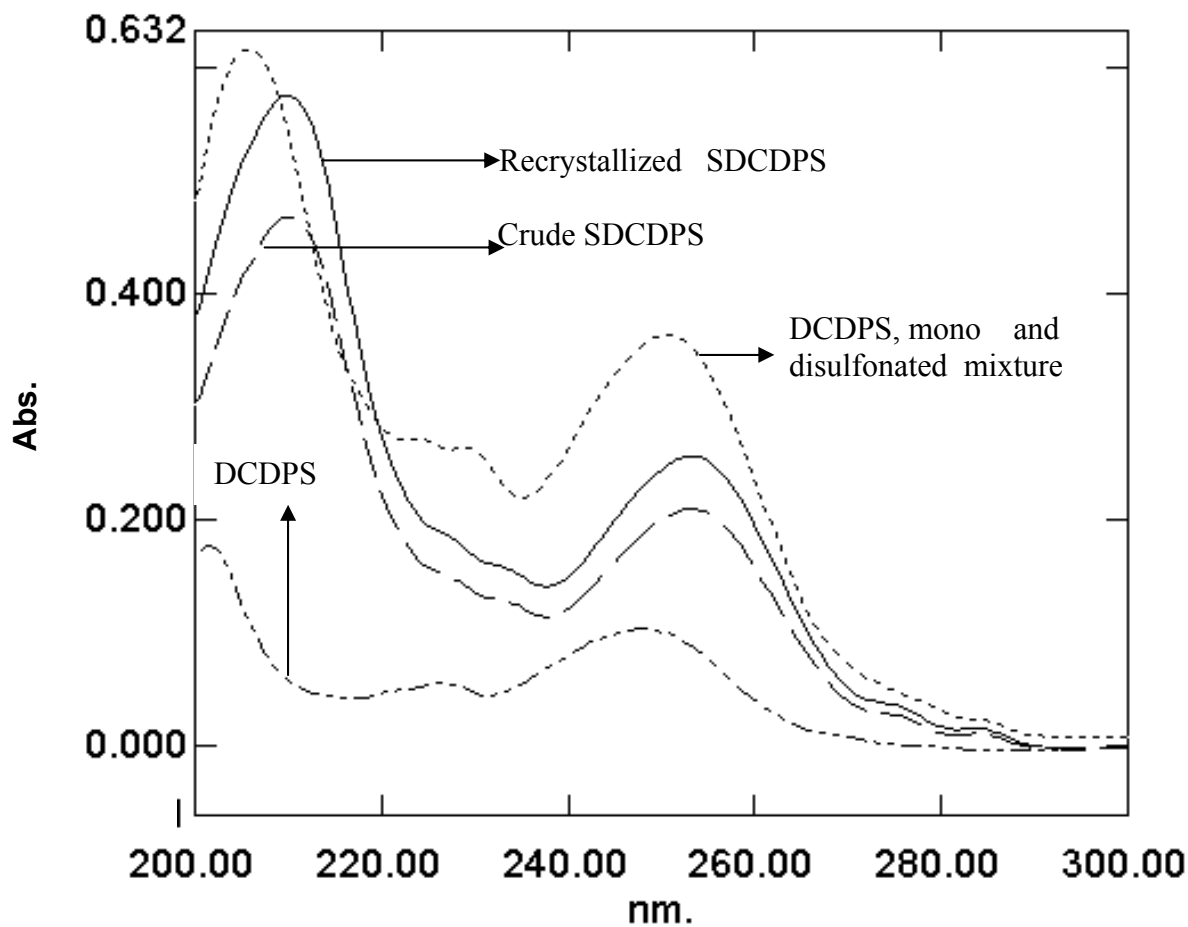


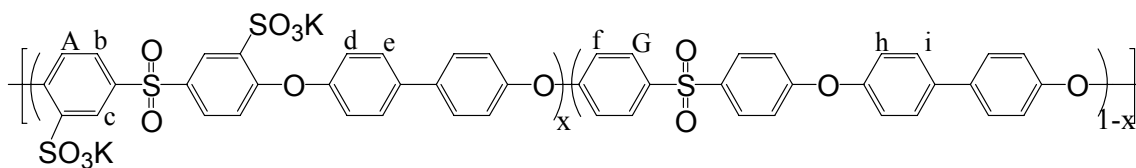
**Figure 3.6** UV absorbance spectra of crude SDCDPS monomer, recrystallized SDCDPS monomer and the starting material DCDPS and mixture when a deficient amount of  $\text{SO}_3$  was used

Fast atom bombardment mass spectroscopy is a soft ionization method for polar and labile materials. The disulfonated monomer has two sulfonated moieties which afforded two major minus charged fragmentations. The results are summarized in Table 3.3. The first fragmentation labeled as  $[M-1Na]^-$  was due to the loss of one sodium atom from entire monomer structure. Another characteristic fragmentation with the loss of two sodium atoms and incorporation of a proton, which maintains the minus one charge ( $[M-2Na+H]^-$ ). Both the crude and recrystallized disulfonated monomers showed the same characteristics indicating that the crude and recrystallized monomers have same chemical structure. Otherwise, the possible impurities such as monosulfonated monomer and starting material DCDPS would result in deviation in the obtained molecular weight of disulfonated monomer from fast atom bombardment mass spectroscopy. However, the two fragmentation patterns showed an exact agreement with the calculated molar mass of the disulfonated monomer.

**Table 3.3 Two fragmentation characteristics of the disulfonated monomer**

SDCDPS (M)	Fragmentation I	Fragmentation II
$C_{12}H_6Cl_2Na_2O_8S_3$ MW: 491.2542 g/mol	$(M - 1Na)^-$	$(M - 2Na + 1H)^-$
Molecular Weights from FAB <sup>-</sup> MS	468.2631	446.2814

The disulfonated monomer process described above was successfully scaled up at Hydrosize Inc to kilogram quantities. The optimized monomer has been used to scale up poly(arylene ether sulfone) copolymers to which are of interest as proton exchange membranes for fuel cell applications. The proton NMR spectrum of the copolymer is shown in Figure 3.7. The intrinsic viscosities confirmed that high molecular weight film forming copolymers were synthesized (Table 3.2)



$$\text{Mole percent of sulfonation} = (A/2) * 100 / (A/2 + G/4) = 34.9 \%$$

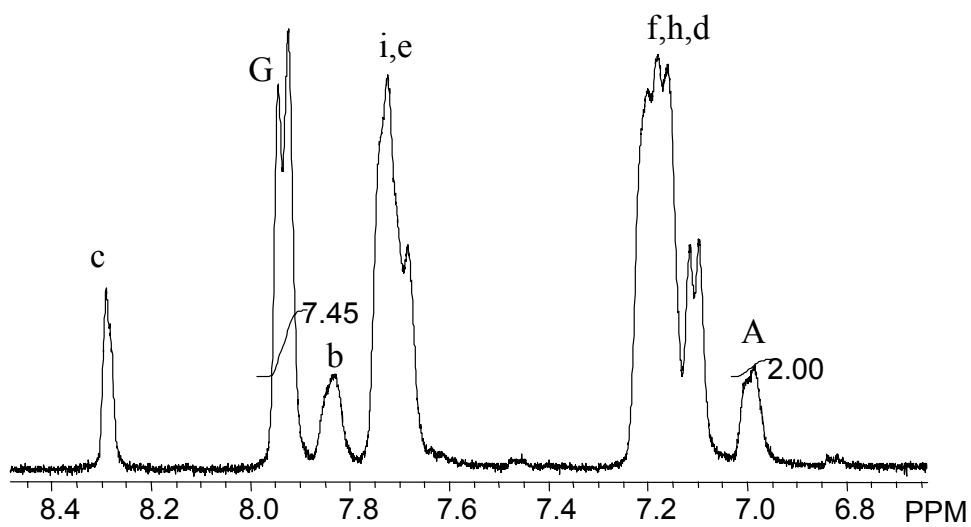


**Figure 3.7**  $^1\text{H}$  NMR spectra of a disulfonated poly(arylene ether sulfone) copolymer synthesized with SDCDPS using the current process

### **3.5 Conclusions**

Synthesis conditions for generating SDCDPS from DCDPS and fuming sulfuric acid were systematically studied and optimized. The best disulfonation reaction was achieved using a 1:3.3 reactant mol ratio (DCDPS: SO<sub>3</sub>) at 110 °C for 6h. The salted out product was isolated always in disulfonated form without having any mono sulfonated and/or starting material DCDPS impurities. Several characterization methods confirmed that crude SDCDPS monomer and recrystallized SDCDPS monomer were identical. Successful scale up of the SDCDPS monomer and high molecular weight disulfonated poly(arylene ether sulfone copolymer) for making proton exchange membrane in fuel cell applications at kilogram quantities has been demonstrated. The disulfonation reaction product is of polymerization purity without the need for a recrystallization step, which one may conclude is important for process economics.

### **3.6 Acknowledgements**

We would like to thank the National Science Foundation Partnership for Innovation (HER-009556) and Department of Energy (DOE-FC36-01G0186) for support of this research.

---

## CHAPTER 4

### **Synthesis of Disulfonated Poly (arylene ether benzonitrile) Statistical Copolymers (PAEB) for Proton Exchange Membrane Fuel Cells (PEMFC)**

---

Taken from:

1. **Sankir, Mehmet; Harrison, William L.; Wiles, Kent B.; Li, Yanxiang; McGrath, James E.,** Proton exchange membrane fuel cells: I. Synthesis and characterization of disulfonated poly (arylene ether benzonitrile) copolymers. **Preprints of Symposia - American Chemical Society, Division of Fuel Chemistry (2004), 49(2), 526-527. Presented at the National ACS Conference in Philadelphia.**
2. **Sankir, Mehmet, McGrath, James E,** Synthesis of Disulfonated Poly (Arylene Ether Benzonitrile) Statistical Copolymers (PAEB) for Proton Exchange Membrane Fuel Cells (PEMFC), **Submitted to Journal of Membrane Science 2006.**

## 4.1 Abstract

Poly (arylene ether benzonitrile) homo and statistical copolymers were synthesized by nucleophilic step polymerization from 4,4'-biphenol (BP) and/or 4,4'-hexafluoroisopropylidene diphenol (6F) and 2,6-dichlorobenzonitrile (DCBN). The BP homopolymer showed some solvent induced crystallinity but the 6F homopolymer was completely amorphous. Three monomers, 4,4'-biphenol, 2,6-dichlorobenzonitrile and 3,3'-disulfonated 4,4'-dichlorodiphenyl sulfone (SDCDPS) were copolymerized to produce ductile, novel disulfonated copolymers with various degrees of disulfonation (0-60 mol% SDCDPS), which afforded ion exchange capacities (IEC's) up to 2.02 mmol/g. NMR and FTIR analysis coupled with titration of sulfonated moieties confirmed both chemical structure and copolymer composition. Intrinsic viscosity analysis in NMP, or preferably NMP containing 0.05 M lithium bromide indicated that high molecular weight copolymers were synthesized. Good thermoxidative stabilities were demonstrated by dynamic TGA. The influence of the acidification conditions on the several membrane properties such as proton conductivity, water uptake and ion exchange capacity were investigated. These multiphase ionomeric materials show an inversion of the continuous phase from hydrophobic to hydrophilic as observed from FE-SEM images when the degree of disulfonation was increased from 45 to 60 mol percent. This phase inversion dramatically increased water uptake and proton conductivity values, but hydrogel type

mechanical behavior was also produced. The copolymers produced ductile films when the hydrophobic phase at least cocontinuous, with thin film conductivities reaching 0.12 S/cm, suggesting they are good candidates for proton exchange membranes in fuel cells. The proton conductivity values were normalized with ion exchange capacity and a linear relation was obtained between the normalized proton conductivities and degree of disulfonation.

## 4.2 Introduction

Proton exchange membranes for fuel cells have number of requirements including high protonic conductivities, low electronic conductivity, and low permeability to fuel and oxidants, low water transport through diffusion and electro-osmosis, oxidative and hydrolytic stability, good mechanical properties both in dry and hydrated state, cost effective, and capable of fabrication into membrane electrode assemblies (MEAs)<sup>1</sup>. The current state of art for proton exchange membrane is the Dupont product Nafion™ which is a statistical copolymer ionomer. Nafion™ is a perfluorinated sulfonic acid copolymer which has a Teflon® like (~87 %) backbone with a sulfonated side chain (~13 %) (IEC 0.91 mequiv/g) of fluoro etherlinked comonomer<sup>2</sup> (Figure 4.1).

---

<sup>1</sup> Hickner, M.A.; Ghassemi, H.; Kim, Y.S.; Einsla, B.R.; McGrath, J.E, *J.E. Chem. Rev.* 2004, 104, 4587-4612

<sup>2</sup> Mauritz; K.A., Moore; R.B., *Chem. Rev.* 2004, 104, 4535

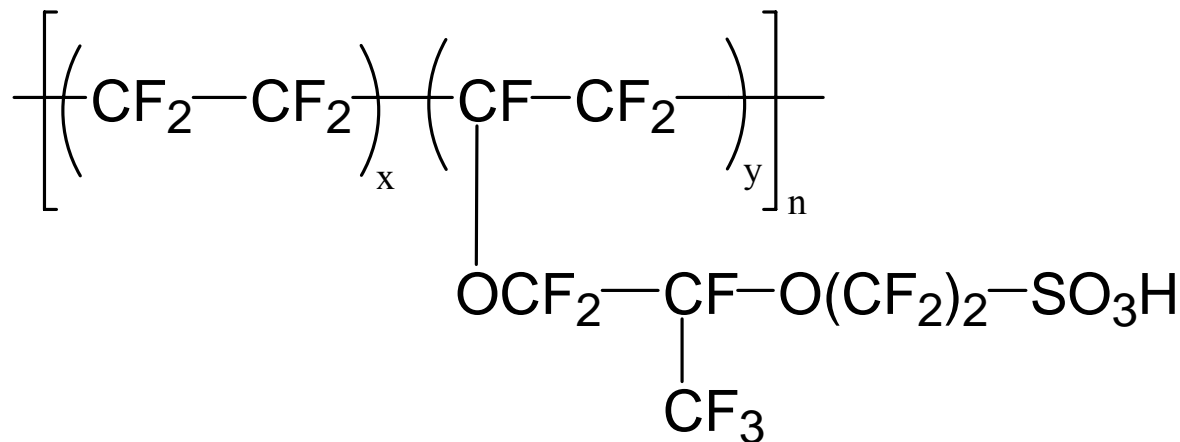


**Figure 4.1** Chemical structure of Nafion™, where x and y represents molar compositions

The excellent proton conductivity, good mechanical properties and long term stability in a fuel cell environment has been demonstrated. However, Nafion™ suffers from several limitations including high cost, loss of transport and mechanical properties at elevated temperatures (greater than 80 °C) and high permeabilities to fuel/reactant<sup>1,3,4</sup>. Alternative PEMs have often been based on post-sulfonated aromatic engineering polymers, such as poly ether sulfones and poly ether ketones<sup>5,6</sup>. In contrast, our approach has been to use nucleophilic step polymerization<sup>7,8,9</sup> and to control the ion exchange capacity by utilizing a disulfonated comonomer. It has also been demonstrated that control of sulfonation sequences is much better via direct copolymerization versus post-

<sup>3</sup> Jones, D.J., Roziere; J., *J. Membrane Science* 2001, 185, 41

<sup>4</sup> Kerres, J.A.; *J. Membrane Science* 2001, 185, 3

<sup>5</sup> Jorrisen, L.; Gogel, V.; *J. Power Sources* 2002, 105, 267

<sup>6</sup> Harrison, W.L., Ph.D. Dissertation, Virginia Tech, 2002

<sup>7</sup> Wang; S., McGrath; J.E., in *Synthetic Methods in Step Growth Polymers*, Rogers; M.E., Long; T.E., Eds., John Wiley and Sons Inc: Hoboken, N.J., 2003, p.327-374

<sup>8</sup> Cotter; R.J., *Engineering Plastics: A handbook of polyarylethers*, Basel, Switzerland : Gordon and Breach, 1995

<sup>9</sup> Johnson; R.N., Farnham; A.G., *Journal of Polymer Science Part A-1: Polymer Chemistry* 1967, 5, 2415

sulfonation. This has been shown by titration and NMR studies<sup>10,11,12</sup>. The direct copolymerization reacts a disulfonated monomer (3,3'-disulfonated 4,4'-dichlorodiphenyl sulfone (SDCDPS)) and biphenol (4,4'-biphenol (BP), or 4,4'-isopropylidene diphenol (BPA), or hydroquinone (HQ), or 4,4'-hexafluoroisopropylidene diphenol (6F)) with a nonsulfonated activated monomer such as 4,4'-dichlorodiphenyl sulfone (DCDPS). The synthesis, characterization and membrane characteristics of these thermally, oxidatively stable high molecular weight copolymers abbreviated as BPS has been previously reported<sup>1,6-12</sup>. The disulfonated monomer required for the direct copolymerization was first synthesized by Robeson and Matzner<sup>13</sup>. Later, Ueda et al.<sup>14</sup> reported the sulfonation of 4,4'-dichlorodiphenyl sulfone. An important study of the synthesis and analysis of 3,3'- disulfonated 4,4'-dichlorodiphenyl sulfone (SDCDPS), with near quantitative conversions useful on a kilogram (or larger) scale including the identification of the impurities formed in the disulfonation reaction has been presented<sup>15</sup>.

Our group is interested in the synthesis and characterization of poly(arylene ether sulfones). The well known (structure–property based) properties of poly(arylene ether sulfone)s has been previously demonstrated<sup>16</sup>. High thermal stability, good stability

---

<sup>10</sup> Harrison, W.L.; Wang, F.; Mecham, J.B.; Bhanu, V.A.; Hill M.; Kim, Y.S.; McGrath J.E.; *J. of Polymer Science: Part A Polymer Chemistry* 2003, 41, 2264

<sup>11</sup> Wang, F.; Hickner, M.; Kim, Y. S.; Zawodzinski, T. A.; McGrath, J. E., *J. Membr. Sci.* 2002, 197, 231

<sup>12</sup> Wang, F.; Hickner, M.; Ji, Q.; Harrison, W.; Mecham, J.; Zawodzinski, T.; McGrath, J. E., *Macromol. Symp.* 2001, 175(1), 387

<sup>13</sup> Robeson, L.M; Matzner, M.; U.S. Patent 4,380, 598, Flame Retardant Polyarylate Compositions, Union Carbide, April 19, 1983

<sup>14</sup> Ueda, M.; Toyota, H.; Ouchi, T.; Sugiyama, J.; Yonetake, K.; Masuko, T. and Teramoto, T.J.; *Polym. Sci. Part A: Polymer Chemistry* 1993, 31, 853

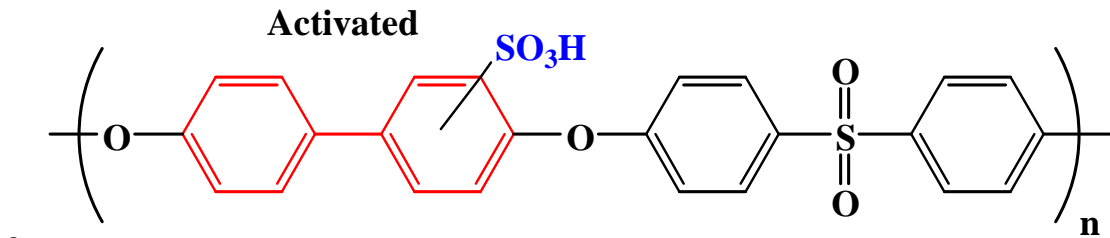
<sup>15</sup> Sankir, M. Bhanu; V.A, Harrison; W.L, Ghassemi; H, Wiles, K.B., Glass; T.E., Brink; A.E., Brink; M.H, McGrath; J.E, *accepted, J. Applied Polymer Sci.* 2005

<sup>16</sup> Hickner M.A., Ph.D. Dissertation, Virginia Tech 2003

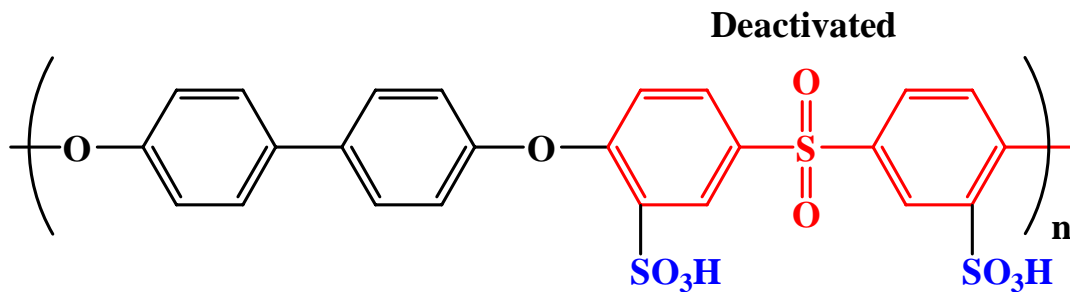
against acid, bases and oxidants, good mechanical properties are among them. Poly(arylene ether sulfones) are film-forming, high-performance thermoplastics, and are melt processible. It is relatively easy to synthesize poly(arylene ether sulfone)s and several monomers are commercially available.

The incorporation of the proton conductive sites was required to use poly(arylene ether sulfone)s as proton exchange membrane in fuel cells. The ionomer formation, the addition of proton conductive sites, has been achieved in either of these two different methods. First method is called as post sulfonation where in the backbone of the polymer chain was sulfonated using a suitable sulfonating agent such as sulfuric acid, sulfur trioxide complexes or chlorosulfonic acid. However, sulfonation occurs on the most reactive, but least stable position which results in easy desulfonation. The other method is known as monomer sulfonation and allows direct copolymerization. In direct copolymerization, the disulfonated monomer (where sulfonation is on the deactivated position) is directly copolymerized with other suitable comonomers. The latter method produces higher proton conductive copolymer membranes. Since there are two sulfonic acid moieties per repeat unit resulted with direct copolymerization, whereas it is one randomly placed per repeat unit for post sulfonation (Figure 4.2). The side reactions which may cause structural imperfections during the post sulfonation reaction are absent in direct copolymerizations. Our approach is to use this direct copolymerization method which includes synthesis of the sulfonated monomer and to copolymerize this monomer with other suitable co-monomers. The advantages of direct copolymerization was reported as ; Precise control of ionic concentration during synthesis, well-defined ion

conductor location; morphology control, high H<sup>+</sup> conductivity, enhanced stability due to deactivated position of -SO<sub>3</sub>H, and ease of very high molecular weight copolymer synthesis.



- Post sulfonation occurs on the most reactive, but least stable, position
- High electron density leads to relatively easy desulfonation



- Monomer sulfonation on the deactivated position
- Enhanced stability due to low electron density

**Figure 4.2** Incorporation of proton conducting sites; Post sulfonation or direct copolymerization (monomer sulfonation) methods

#### 4.2.1 Hydrocarbon versus Perfluorinated Ionomers

Proton exchange membranes (e.g. perfluorinated-based ionomer membranes or hydrocarbon-based ionomer based membranes) have excellent water dependent-proton conductivity as function of temperature. However, when proton exchanges membranes are subjected to temperatures above the 100 °C, their conductivity decreases significantly due to the dehydration and subsequent loss of transport. External pressure helps, however it is not practical in fuel cells due to its loss of reactants and high power requirements for compressors. The high dependence on humidification for Nafion™ limits its functionality well above 80°C in an H<sub>2</sub>/air or DMFC systems. However, there is a strong driving force to operate at higher temperatures. In the H<sub>2</sub>/air, the move to higher temperatures will increase cathode reactivity and will allow the fuel cell to tolerate much higher levels of carbon monoxide which poisonous the catalytic activity<sup>17,18,19,20,21</sup>.

Dehydration is an important transport issue and may be reduced using humidified fuel. However, there is also a structural reason (low T<sub>g</sub>) for decreasing performance over the range of 80-100 °C for Nafion™ type perfluorinated membranes (proton conductivity is usually monitored at various temperature-humidity interval). At higher temperatures, proton conductivities of these membranes are decreased due to the morphological relaxation or destruction of the hydrophilic domain structure. The morphological relaxation temperatures are associated with the hydrated glass transition temperature. If

---

<sup>17</sup> Hoogers; G., *Fuel Cell Technology Hand Book*, CRC Press,; New York, 2003

<sup>18</sup> Eisenberg, M., In *Fuel Cells*, Mitchell, W., Ed., Academic Press: New York, 1963, p17

<sup>19</sup> Hart, A.B.; Womack, G.J., *Fuel cells*, Chapman and Hall : London, 1967, p 21

<sup>20</sup> Hart, A.B.; Womack, G.J., *Fuel cells*, Chapman and Hall : London, 1967, p 49

<sup>21</sup> Barendrecht, E., In *Fuel Cell Systems*, Blomen, L.J.M.J; Mugerwa, M.N.,Eds., Plenum Press: New York, 1993, p.73

the hydrated glass transition temperature is near to the operation temperature, then the membrane performance may be suppressed due to the morphologic relaxation of the ionic clusters. BPSH-disulfonated poly(arylene ether sulfone) copolymers have higher hydrated glass transition temperature so that they may be useful for the temperatures greater than 100 °C. The concept of hydrated glass transition temperature and dehydration was thus a key consideration for producing membranes available for higher temperature (120 °C) applications<sup>22,23</sup>.

Operation of the fuel cell at the temperatures below room temperature, or even below 0 °C (freezing point of free water), is one additional challenge. In order to decide the functional availability of a proton exchange membrane in the range of temperature below zero to above 100 °C, a phenomenon known as the states of the water was investigated.

The state of water in proton exchange membranes plays a more significant role in membrane transport properties than previously suggested. The state of water in hydrated copolymers, such as hydrogels has been extensively studied. They are defined as; 1. Non-freezing water: Water that is strongly bound to the polymer chain and has a role in effective glass transition reduction (plasticization), 2. Freezable loosely bound water: Water that is weakly bound to the polymer chain or

---

<sup>22</sup> Kim; Y.S., Dong; L., Hickner; M.A., Pivovar; B.S., McGrath; J.E. *Polymer* 2003, 44, 5729

<sup>23</sup> Kim, Y.S.; Dong, L.; Hickner, M.A.; Glass, T.E.; Webb, V.; McGrath, J.E., *Macromolecules* 2003, 36,6281

interacts weakly with nonfreezing water and displays relatively broad melting endotherms, 3. Free water: Water that is not intimately bound to the polymer chain and behaves like bulk water showing sharp melting point at 0 °C<sup>23, 24</sup>.

One critical issue is whether one can utilize the non-freezing water to run the fuel cell on very cold days or at temperatures higher than 100 °C. There is a strong evidence (NMR relaxation data) that strongly bound water is retained in the copolymer structure even in these extreme cases<sup>25</sup>. There appear to be non-freezing water connected to the copolymer structure that may provide proton conductivity for the temperatures of minus 20 °C, or even lower. The amount of free water in Nafion™ membrane was higher than in the BPSH membrane. Since, relatively a large fraction of water in the BPSH membranes exists in a bound state, the low temperature behavior may be improved.

One current challenge is to obtain an ideal morphological structure which provides appreciable proton conductivity, or reduced fuel/oxidant permeability at low relative humidities for temperatures greater than 100 °C and below than 0 °C. The hydrocarbon based copolymer membranes may be more promising due to the reasons

---

<sup>24</sup> (a) Quinn, F.X.; Kampff, E.; Smyth, G.; McBrierty, V.J. *Macromolecules*, 1988, 21, 3191. (b) Smyth, G.; Quinn, F.X.; McBrierty, V.J., *Macromolecules* 1988, 21, 3198. (c) Hodge, R.M.; Bastow, T.J.; Edward, G.H.; Simon, G.P.; Hill, A.J., *Macromolecules* 1996, 29, 8137. (d) F.X, Quinn; Kampff, E.; Smyth, G.; McBrierty, V.J., *Macromolecules* 1988, 21, 3192. (e) Lafitte, B.; Karlsson, L.E.; Jannasch, P., *Macromol. Rapid Commun.* 2002, 23, 896.

<sup>25</sup> Roy; A., Hickner; M. A., Glass; T., Li; Y., Einsla; B., Wiles; K. B.; Yu, X., McGrath; J. E., States of water- investigating the water-polymer interactions and transport phenomenon in proton exchange membranes. Preprints of Symposia - American Chemical Society, Division of Fuel Chemistry (2005), 50(2), 699-700

listed above. Our group has focused on developing hydrocarbon-based ionomer copolymers including statistical and multi block systems<sup>26,27,28</sup>.

The synthesis and characterization of disulfonated poly(arylene ether benzonitrile) copolymers from 3,3'-disulfonated 4,4'-dichlorodiphenyl sulfone (SDCDPS), 4,4'-hexafluoroisopropylidene diphenol (6F) and 2,6-dichlorobenzonitrile (DCBN) has been recently jointly reported with the Los Alamos National Lab (LANL)<sup>29,30,31</sup>. The copolymers showed great promise, especially for direct methanol fuel cells (DMFC) to be utilized in portable power applications. The collaborations with LANL are continuing and include studies on copolymers partially or entirely based on 4,4'-biphenol (BP). This bisphenol is generally recognized to be more reactive and less costly than 6F. Moreover, poly(arylene ethers) derived from BP are very oxidatively stable and produce ductile films.

---

<sup>26</sup>Yu; X., Roy; A., McGrath; J.E., Synthesis and characterization of multiblock copolymers for proton exchange membranes. Preprints of Symposia - American Chemical Society, Division of Fuel Chemistry (2005), 50(2), 577-578

<sup>27</sup>Lee; H.S, Einsla; B., McGrath; J.E. Synthesis and characterization of segmented sulfonated poly(arylene ether)-B-polyimide copolymers as proton exchange membranes. Preprints of Symposia - American Chemical Society, Division of Fuel Chemistry (2005), 50(2), 579-580.

<sup>28</sup>Wang; H., McGrath; J.E., Synthesis of (poly(arylene ether sulfone)-substituted poly(P-phenylene)) multiblock copolymers for proton exchange membrane. Preprints of Symposia - American Chemical Society, Division of Fuel Chemistry (2005), 50(2), 581-582

<sup>29</sup> Sumner; M.J., Harrison; W.L., Weyers; R.M., Kim; Y.S., McGrath; J.E., Riffle; J.S., Brink; A.E., Brink; M.H., *J. Membr. Sci.* 2004, 239, 199

<sup>30</sup> Kim; Y.S, Sumner; M.J., Harrison; W.L., Riffle; J.S., McGrath; J.E., Pivovar, B.S., *Journal of The Electrochemical Society* 2004, 151, 12, A2150-A2156

<sup>31</sup> Harrison; W.L, Hickner; M.A., Kim; Y.S., McGrath; J.E., *Fuel Cells* 2005, 5(2), 201

## 4.3 Experimental

### 4.3.1 Reagents

4,4'-biphenol was kindly provided by Eastman Chemical while 2,6-dichlorobenzonitrile was purchased from Aldrich. Both were of high purity and were used without any purification. The disodium salt of 3,3'-disulfonated-4,4'-dichlorodiphenyl sulfone (SDCDPS) was synthesized through the reaction of 4,4'-dichlorodiphenyl sulfone (Solway Advanced Polymers) and fuming sulfuric acid, as described previously<sup>15</sup>. 4,4'-Hexafluoroisopropylidene diphenol (6F), (received from Ciba), was purified by sublimation. All other reagents were obtained from commercial sources and purified, as needed, via common procedures.

### 4.3.2 Synthesis of 3,3'-disulfonated-4,4'-dichlorodiphenyl sulfone

The 4,4'-dichlorodiphenyl sulfone (10g, 0.0348 mol) and fuming sulfuric acid (SO<sub>3</sub> to DCDPS molar ratio was 1:3.3). The amount of the electrophilic SO<sub>3</sub> in fuming sulfuric acid was determined by titration using 0.01 N sodium hydroxide. The reagents were added to a 100-mL three-necked flask fitted with an overhead mechanical stirrer and nitrogen inlet and outlet, and purged with nitrogen for several minutes. The purge was then stopped during the reaction to minimize SO<sub>3</sub> losses. Disulfonation reactions were performed as a function of reaction time (4-6 h), temperature, (room temperature and 90-120 °C) and stoichiometries of the reactants. The reaction product was dissolved into a mixture of 50 g of ice and 50 g of water. The sodium chloride (25 g) was dissolved with stirring into the solution when the solution temperature was about 65 °C. The

mixture was stirred, cooled to room temperature and filtered. The product was redissolved in deionized water (100 g) and the pH of the solution was adjusted to 7 with 10 N sodium hydroxide. The product was salted out by adding the sodium chloride (25 g) at about 65 °C and filtered at room temperature. Finally, it was dried under vacuum at 160 °C for 24 h. The proton NMR of the starting material (4,4'-dichlorodiphenyl sulfone) and disulfonated product (3,3'-disulfonated-4,4'-dichlorodiphenyl sulfone) were presented in Figure 4.3. The sulfonation was confirmed with the peak observed at about 8.3 ppm. The procedure defined here and has been previously defined in Sankir et al<sup>15</sup> always produces near quantitative yields for the disulfonated monomer.

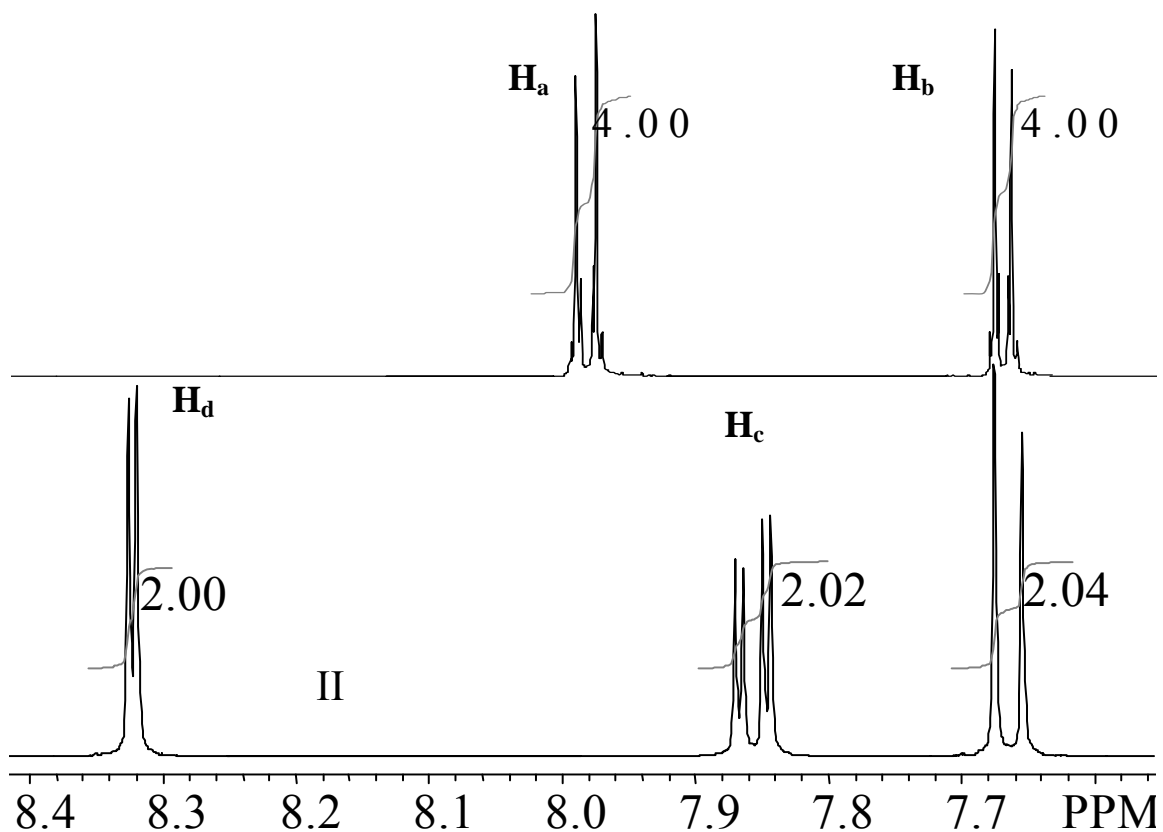
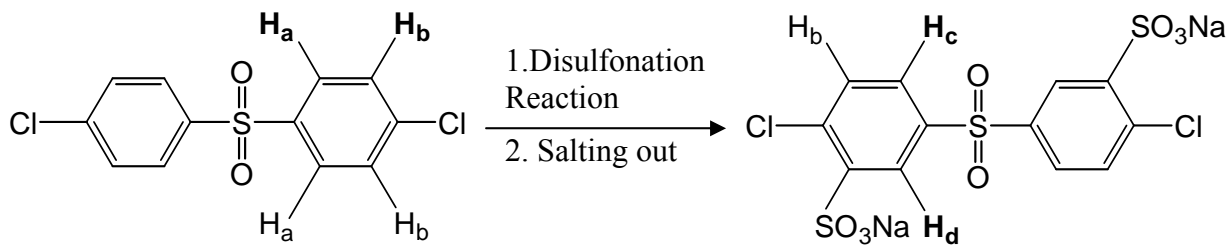


**Figure 4.3** Proton NMR confirmed the chemical structure of 3,3'-disulfonated-4,4'-dichlorodiphenyl sulfone monomer; I. Proton NMR for starting material (4,4'-dichlorodiphenyl sulfone) and II. disulfonated product (3,3'-disulfonated-4,4'-dichlorodiphenyl sulfone)

### 4.3.3 Synthesis of Disulfonated Poly (arylene ether benzonitrile) Copolymers

Sulfonated poly (arylene ether benzonitrile) (PAEB) copolymers were prepared with various degrees of disulfonation (0-60 mol% SDCDPS) via direct copolymerization of 3,3'-disulfonated-4,4'-dichlorodiphenyl sulfone (SDCDPS), 2,6-dichlorobenzonitrile (DCBN) and 4,4'-biphenol (BP). Thus, 2.2609 g (0.0131 mol ) DCBN, 3.4767 g (0.0071mol) SDCDPS and 3.7654 g (0.0202 mol ) BP and 3.2139 g potassium carbonate (15% mol excess) were transferred to 3-neck flask equipped with a mechanical stirrer, a nitrogen inlet and a Dean Stark trap in order to synthesize 35 mol percent SDCDPS containing copolymer, (named PAEB 35). Dry NMP ( 20 mL) was used as the polymerization solvent while toluene (10ml) was the azeotrope. The reaction mixture was refluxed for 4 hours at 150 °C to complete the dehydration process. The reaction temperature slowly increased to 190 °C for 16 hours just after the removing of the toluene gradually. The viscous reaction product was cooled, diluted with NMP and precipitated in deionized water as swollen fibers. After washing several times with deionized water, the precipitated copolymers were boiled in deionized water for 4 hours to further remove the salts. The copolymers were isolated by filtration then dried in vacuum oven at 120 °C for 24 hours.

Several homo and random copolymers were synthesized from BP/DCBN, SDCDPS and hexafluoroisopropylidene diphenol (6F) using same method described above.

#### 4.3.4 Film Casting and Membrane Acidification

Membranes in the potassium sulfonate form were prepared by first redissolving the copolymer in DMAc as 5-10% (w/v) copolymer solutions, which were then filtered using a syringe filter (0.45  $\mu\text{m}$ ) and cast onto clean glass substrates. The transparent solutions were carefully dried with infrared heat at gradually increasing temperatures (up to  $\sim 60$   $^{\circ}\text{C}$ ) under a nitrogen flow, until the film was nearly dry; a further drying step was applied in a vacuum oven at 140-150 $^{\circ}\text{C}$  for 24 hours. The sulfonated poly(arylene ether sulfone) copolymer films were converted to their acid form using two different methods as described below<sup>22</sup>;

The degree of disulfonation can precisely be controlled which allows control of the morphology. Hydrophilic/hydrophobic phase separated morphology is obtained as a function of composition. One may adjust the amount of hydrophilic region concentration from 0 to 60 percent (Figure 4.4). The disulfonated poly(arylene ether benzonitrile) is a statistical copolymer (also known as PAEB). It may be isolated in its salt form, and then converted to acid form to achieve proton conductivity. There are two different methods for acidification, method 1 and method 2. The two procedures produce relatively different morphologies<sup>32</sup>.

---

<sup>32</sup> Kim; Y.S., Wang; F., Hickner; M., McCartney; S., Taik Hong; Y., Harrison; W., Zawodzinski; T.A., McGrath; J.E., *Journal of Polymer Science: Part B: Polymer Physics* 2003, 41, 2816

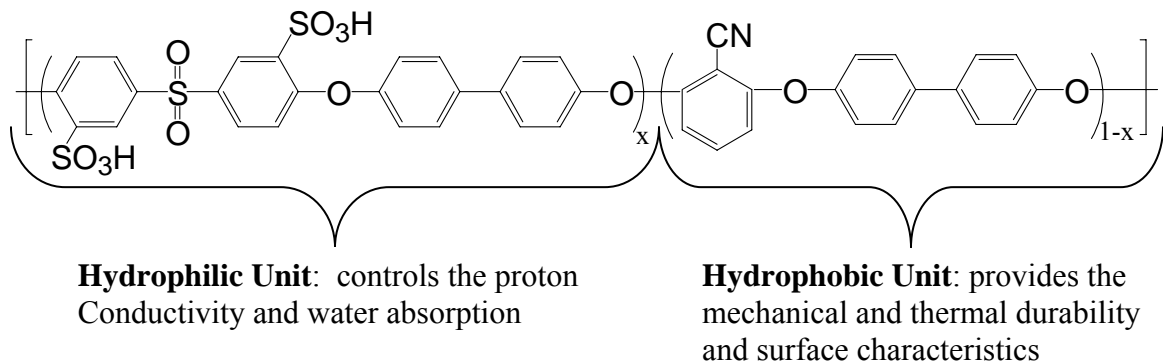


**Figure 4.4** Disulfonated poly(arylene ether benzonitrile) is a random copolymer having a controlled amount of hydrophobic and hydrophilic subunits

*Method 1 (M1) :*

The membranes were placed in 1.5M aqueous sulfuric acid solution at 30°C for 24 hours and then washed with deionized water several times. They were again placed in deionized water at 30°C for 24 hours and finally rewashed and stored in deionized water.

*Method 2 (M2) :*

The membranes were boiled in 0.5M aqueous sulfuric acid solution for 2 hours, then washed with deionized water several times, and then were boiled in deionized water for 2 hours, rewashed with deionized water and stored in deionized water.

All films were stored in deionized H<sub>2</sub>O for at least 2 days before any tests were performed

#### 4.3.5 Characterization

A Nicolet Impact 400 FT-IR spectrometer was utilized on the thin films to confirm the functional groups within the copolymers. Proton ( $^1\text{H}$ ) and carbon ( $^{13}\text{C}$ ) NMR analyses were conducted on a Varian UNITY 400 spectrometer. All spectra were obtained from a 10% solution (w/v) in dimethylsulfoxide- $d_6$  at room temperature. The monomer purity as well as copolymer compositions were analyzed via NMR spectroscopy. Intrinsic viscosities were determined in pure NMP at 25 °C or NMP containing 0.05 M LiBr using an Ubbelohde viscometer. Field emission scanning electron microscopy FE-SEM, Leo 1550 Gemini was operated using an in-lens detector at a low incident beam voltage (7kV) to minimize charging. Samples were fractured under cryogenic conditions and vacuum sputtered at the thin layer of the samples before imaging. Tapping mode atomic force microscopy (AFM, Digital Instruments Dimension 3000) with a micro-fabricated cantilever, with a force constant of approximately 40 N/m was used. Surface phase imaging was obtained with equilibrated samples at 50 % relative humidity. Under those experimental conditions, the small silicon nitride tip was sensitive to local stiffness (phase lag) differences between hydrophobic and hydrophilic domains in the top several nanometers from the outermost surface<sup>33</sup>.

The thermooxidative behavior of both the salt-form (sulfonate) and the acid-form copolymers was performed on a TA Instruments TGA Q 500. Vacuum dried thin films (5 to 10 mg in the potassium salt form) were evaluated over the range of 110 to 600 °C at a heating rate of 10 °C/min in 50ml/min air. Titration of the sulfonic acid groups were

---

<sup>33</sup> Kim; Y.S., Hickner; M.A., Dong; L., Pivovar; B.S., McGrath; J.E., *Journal of Membrane Science* 2004, 243, 317

performed on the acidified membrane samples of known mass by first exchanging with sodium sulfate then back titrating with 0.01M sodium hydroxide with an automatic titrator (Schott TitroLine Easy).

The concentration of the ion conducting units was characterized by the molar equivalents of ion conductor per mass of dry membrane and is expressed as equivalent weight (EW) with units of grams polymer per equivalent, or ion exchange capacity (IEC) with units of milliequivalents per gram (mequiv/g or mmol/g) of polymer (EW)  $1000/IEC$ ).

Ion exchange capacity for disulfonated copolymers is expressed as the formula given below;

$$IEC = \frac{2 \times \text{Mole fraction of disulfonation}}{MW_{\text{nonsulfonated unit}} \times \text{Its mole fraction} + MW_{\text{sulfonated unit}} \times \text{Its mole fraction}}$$

Equation 4.1

One concludes that IEC values depends on the degree of disulfonation as well as the chemical structure of the backbone which varies the molecular weight of both the sulfonated and non sulfonated repeating unit.

The water uptake of each copolymer was determined by according to the formula below;

$$\text{Water Uptake (\%)} = \frac{W_{wet} - W_{dry}}{W_{dry}} \times 100 \quad \text{Equation 4.2}$$

$W_{wet}$  : Weight of membranes after submersion in deionized water at 30 °C for 48 h (excess water removed by blotting with a paper towel.)

$W_{dry}$  : Weight of membranes after drying under vacuum oven at 120 °C for 24 hours.

Thin film conductivity measurements were conducted on acidified membranes while submerged in deionized water using a Hewlett Packard 4129A Impedance/Gain-Phase Analyzer. The data were recorded from 10 MHz to 10 Hz. The experimental apparatus was depicted in Figure 4.5.

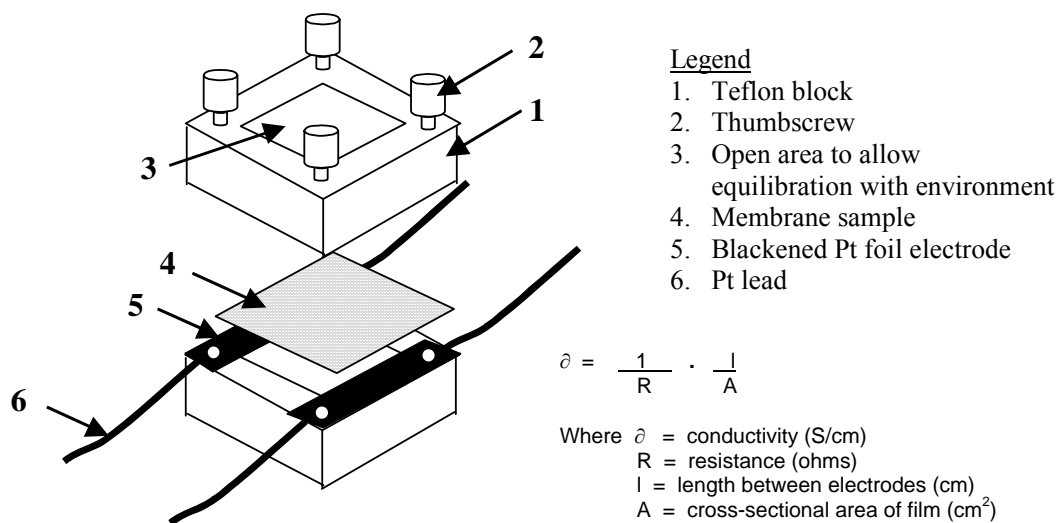


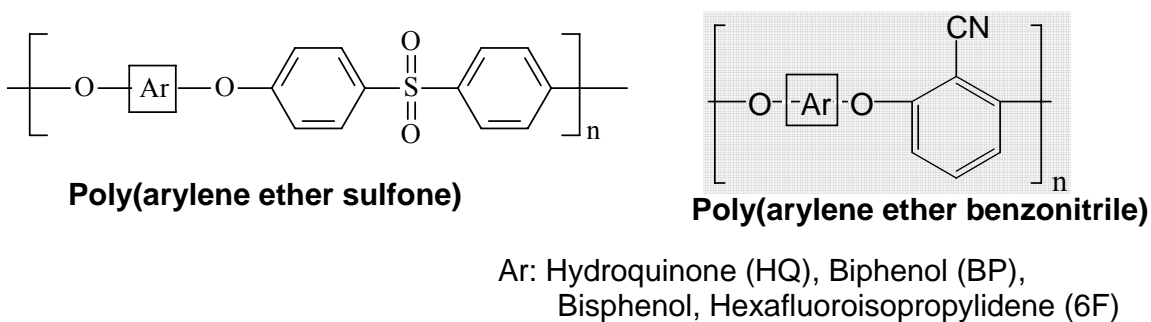
**Figure 4.5** The Teflon™ cell to measure proton conductivity<sup>34</sup>

Storage modulus of membranes in liquid water was measured using dynamic mechanical analysis (DMA, TA Instruments, DMA 2980). DMA was in the tensile mode at a frequency of 1Hz. Temperature was scanned from 35 to 80 °C at a rate of 0.1 °C/min. Films with dimensions of 5x30x0.18 mm were subject to sinusoidal deformation with 20 μm amplitude.

<sup>34</sup> Zawodzinski; T.A, Neeman; M., Sillerud; L. O., Gottesfeld; S *J. Phys. Chem.* 1991, 95, 6040

#### 4.4 Results and Discussions

Poly(arylene ether sulfone) homopolymers are engineering thermoplastics that display very good stability against highly corrosive conditions (acid, bases, oxidants). Poly(arylene ether benzonitrile copolymers) are very similar to poly(arylene ether sulfones) copolymers in many respects. The repeat unit of the poly(arylene ether benzonitrile)s were compared with poly(arylene ether sulfones) in Figure 4.6. It has been reported that the cyano group provides adhesion to many substrates<sup>35</sup> which might be an important parameter while making membrane electrode assemblies (MEA). Cyano groups also provide chemical resistance, mechanical strength and flame retardancy possibly by enhancing inter/intra molecular forces.



- The cyano group on the aromatic ring provides adhesion to many substrates
- Excellent chemical resistance, mechanical strength, flame retardancy
- May be semicrystalline (depends on aryl structure!)

**Figure 4.6** Chemical structures of poly (arylene ether sulfone) and poly (arylene ether benzonitrile) homopolymers

<sup>35</sup> Rao; V.L., Saxena; A., Ninan; K.N., Journal of Macromolecular Science, Part C-polymer Reviews 2002, Vol C42, No.4, p513

The poly(arylene ether benzonitrile) homopolymers could be either amorphous or semicrystalline depending on the biphenol types used in the polymerization. The homopolymer based on 4,4'-biphenol/2,6-dichloro benzonitrile (BP/DCBN) could be generated as a solvent induced semicrystalline polymer having a glass transition temperature of 215 °C and melting point temperature of 349 °C. On the other hand, the poly(arylene ether benzonitrile) from 4,4'-hexafluoroisopropylidene diphenol (6F)/dichlorobenzonitrile (6F/DCBN) was completely amorphous with a glass transition temperature of 185 °C (Figure 4.7).

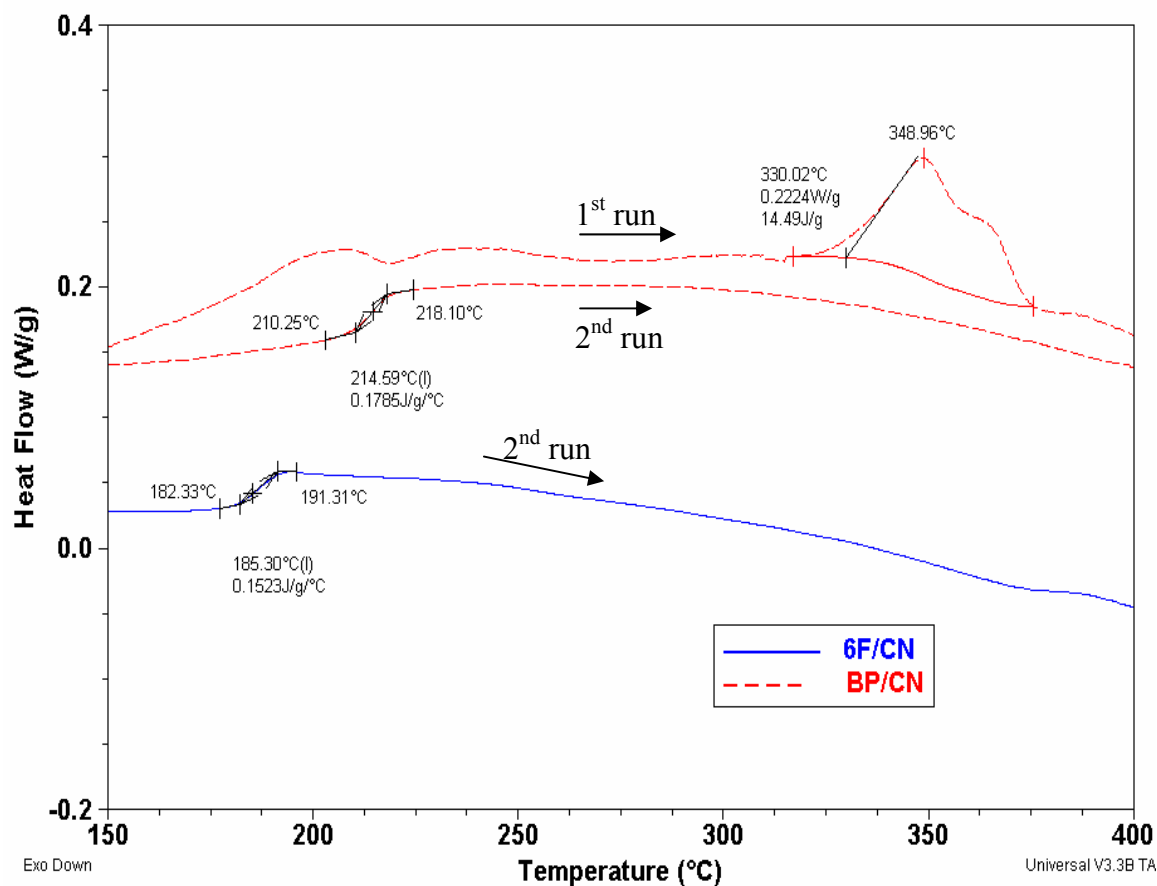


**Figure 4.7** Differential Scanning Calorimeter (DSC) thermogram for poly(arylene ether benzonitrile) from 4,4'-biphenol and 2,6-dichlorobenzonitrile (BP/DCBN) and 4,4'-hexafluoroisopropylidene diphenol and 2,6-dichlorobenzonitrile (6F/DCBN)

The TGA thermal decomposition temperature of BP/DCBN system was comparable to the 6F/DCBN homopolymers. Table 4.1 provides the corresponding DSC results. The homopolymer from BP/DCBN was crystallized after 6-8 hours polymerization reaction in the NMP solvent and the product were only slightly soluble at 190 °C in NMP. The glass transition temperature detected by DSC as 215 °C and

melting point were probably lowered by the solvent. The greater depression in both glass transition and melting temperature widens the crystallization window which results in rapid crystallization at lower temperature in a suitable solvent. This effect is known as solvent induced crystallization. Hence, the melt endotherm at 349 °C was only observed in the first run for already crystallized homopolymer in the solution. There was not enough chain mobility after melting for recrystallization, but this was easily induced by the solvent. Similar DSC characteristics were previously reported<sup>35</sup>.

Table 4.1 Several thermal properties of two different poly(arylene ether benzonitrile) copolymers where T<sub>g</sub> is the glass transition temperature, T<sub>m</sub> is the melting temperature and T<sub>d</sub> is the decomposition temperature which corresponds the 10 percent weight loss temperature by TGA (10 °C/min in air, 50 ml/min)

<b>T (°C)</b>	<b>6F/ DCBN</b>	<b>BP/ DCBN</b>
T <sub>g</sub>	185	215
T <sub>m</sub>	-	349
T <sub>d</sub>	497	512

The poly(arylene ether benzonitrile) copolymers with sulfonic acid proton conductive sites were studied as proton exchange membranes for fuel cells. The direct nucleophilic copolymerization reaction was applied to synthesize several series of high molecular weight copolymers from SDCDPS, BP and DCBN. The procedure reported earlier<sup>1,7-12</sup> includes two successive stages; namely, four hours dehydration, achieved by refluxing toluene at 155 °C and step copolymerization at 190 °C for 16 h. The synthetic route is depicted in Figure 4.8.

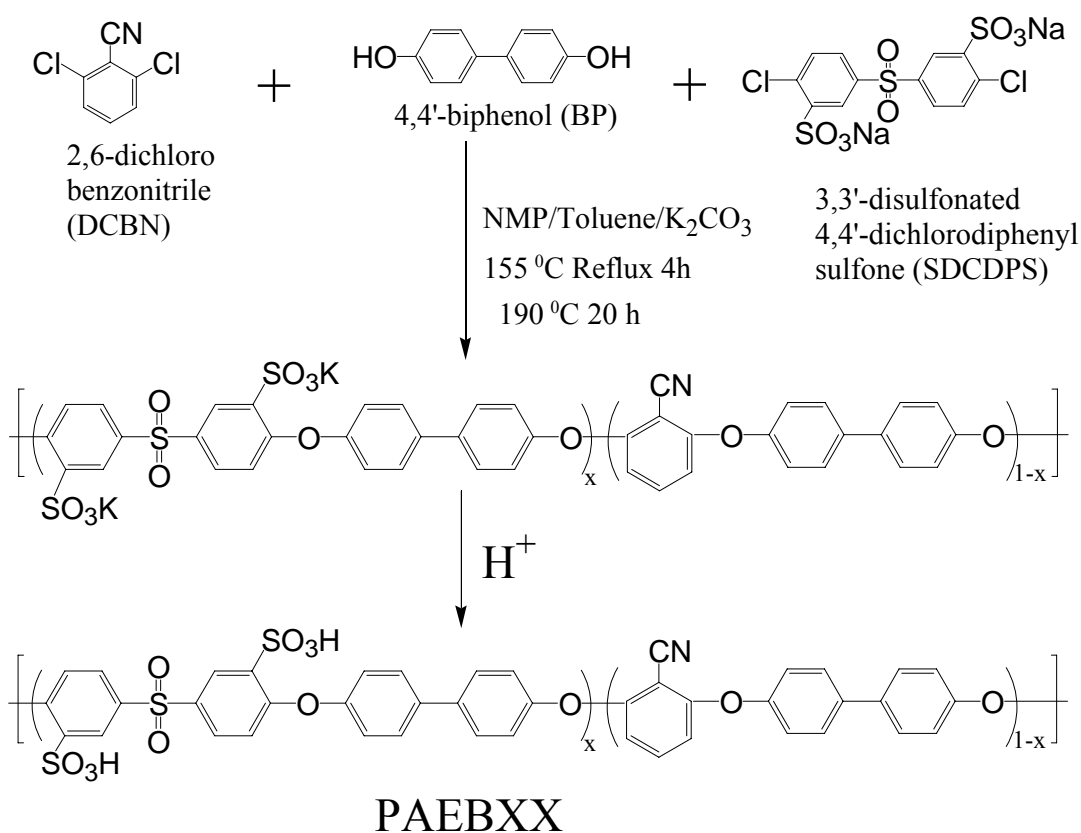
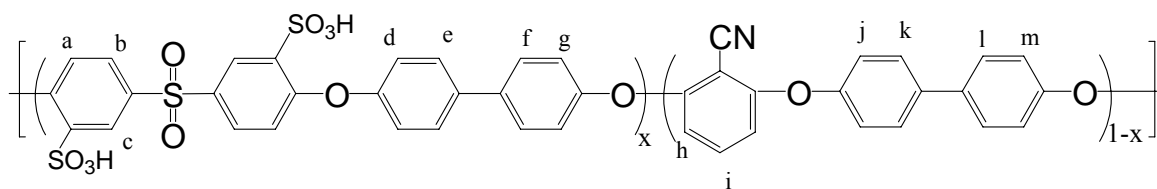


**Figure 4.8** Synthesis of disulfonated poly(arylene ether benzonitrile) copolymers (PAEB XX where XX denotes mol percent of disulfonation) from 4,4'-biphenol, 2,6-dichloro benzonitrile and 3,3'-disulfonated-4,4'-dichlorodiphenyl sulfone

The high molecular weight disulfonated copolymers produced very viscous reaction solutions in NMP and were diluted before being isolated as swollen fibers by precipitation in stirred deionized water. The 60 percent disulfonated copolymer was precipitated in isopropyl alcohol water mixture (50/50; v/v) since its higher hydrophilicity nature made the filtration step in pure water difficult.

High molecular weight disulfonated PAEB copolymers were achieved as suggested by intrinsic viscosity and film ductility. The related data are tabulated in Table 4.2. The  $^1\text{H}$  NMR was used for compositional and structural determinations. Figure 4.9 shows the proton NMR of series of disulfonated PAEB copolymers. The peaks were further assigned using Cosy NMR. The target and actual mole percent disulfonation reported in Table 4.2 were in close agreement.



$$\text{Mole percent disulfonation} = (100/(c/2+i/1)) * (c/2)$$

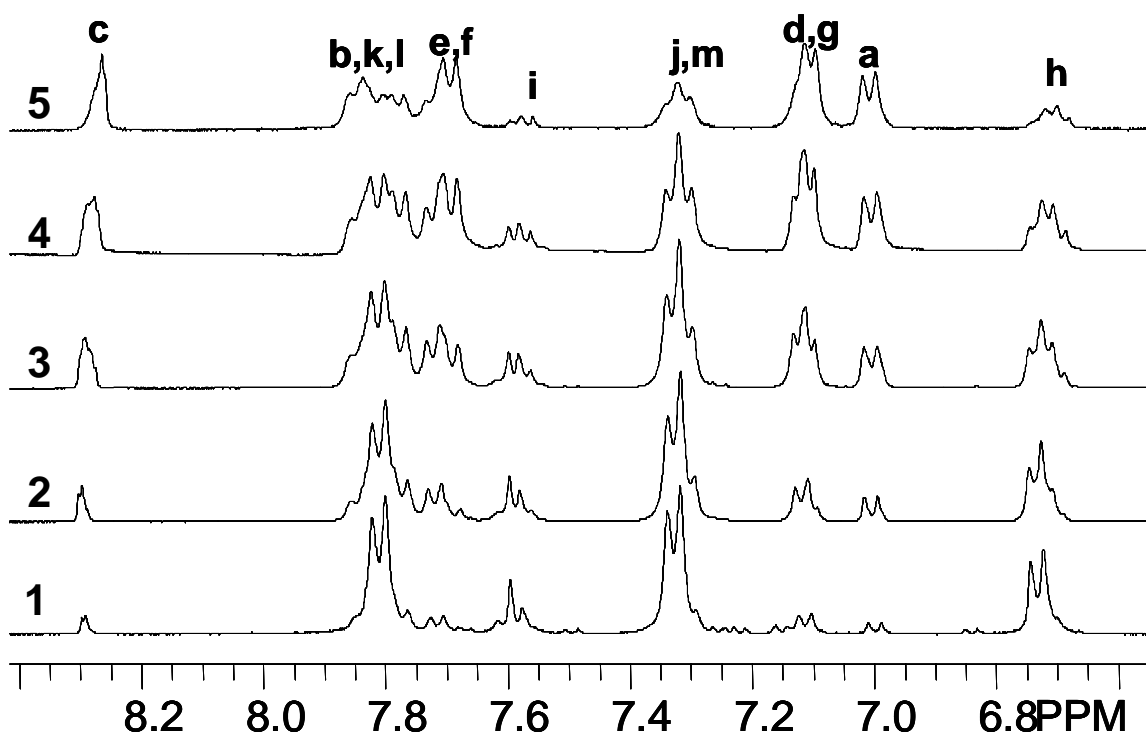


**Figure 4.9** Proton NMR spectrum for disulfonated PAEB series: 1. PAEB 10, 2. PAEB 20, 3. PAEB 35, 4. PAEB45, 5. PAEB 60

Polyelectrolytes (charged macromolecules) behave differently than regular neutral polymers. A neutral polymer possesses random coil conformation in a good solvent, whereas an extended rod transition occurs for polyelectrolytes. Hence the more extended chain shows higher dilute solution viscosity than its neutral form. The simple solution to address this problem was to do the measurements in the presence of a low molar mass salt, which is also known as isoionic dilution. The isoionic dilution keeps the ionic strength of the solution of a series similar and allows intrinsic viscosity values to be obtained.

Table 4.2 Degree of disulfonation was calculated by proton NMR where XX represents the target, high intrinsic viscosity data confirms the high molecular weight as well as desired disulfonation . IV measurements were done in a solution of 0.05M LiBr in NMP

<b>Copolymer PAEB-XX*</b>	<b>Degree of Sulfonation by 1H NMR</b>	<b>IV (dL/g) <math>[\eta]_{25^{\circ}\text{C}}^{\text{NMP}}</math></b>
PAEB10	9.5	1.2
PAEB20	19.7	1.4
PAEB35	34.0	1.2
PAEB45	44.0	1.2
PAEB60	59.1	1.1

Copolymers at various mol percent disulfonation and control without sulfonation were compared using FTIR spectra. The two new peaks resulting from sulfonic acid moieties were observed for the Ar-O-Ar and the salt of sulfonic acid groups at  $1070\text{ cm}^{-1}$  and  $1095\text{ cm}^{-1}$ , respectively (Figure 4.10).

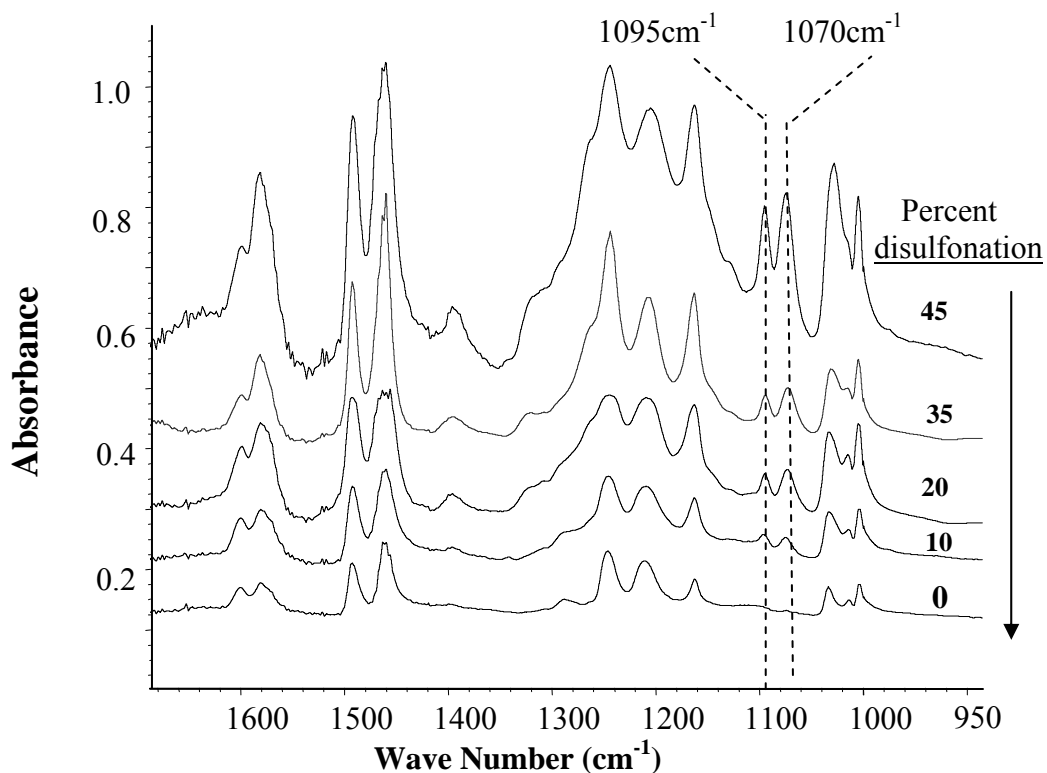


**Figure 4.10** FTIR bands showing incorporation of sodium sulfonate moieties into copolymer structure

The salt form of these disulfonated copolymers showed better thermooxidative stability than their acid forms. Figure 4.11 illustrates the thermal stability of acid and salt forms of poly(arylene ether benzonitrile) copolymers at 20 mol percent sulfonation in air.

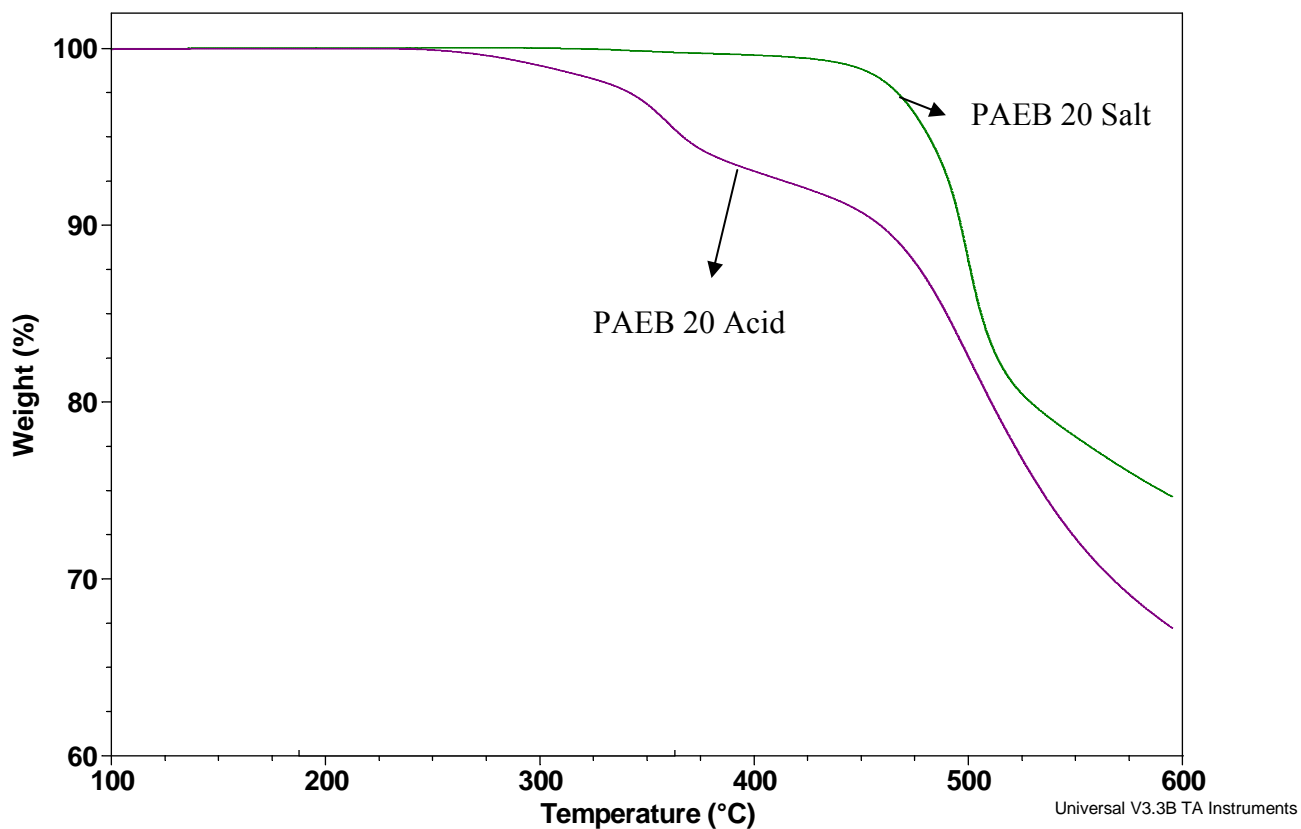


**Figure 4.11** TGA thermogram in air 10 °C/min for the acid and salt forms of PAEB copolymers

The high molecular weight, PAEB and even disulfonated PAEB copolymers at various percent disulfonation up to 60 mol percent showed very good thermal stabilities when investigated by thermogravimetric analysis. The ten percent weight loss temperature of the acid form of copolymers decreased with increasing degree of sulfonation, as expected. However, the values were between 350 and 440 °C, which should be enough for fuel cell applications (operating temperatures lower than 120 °C) (Table 4.3). The thermooxidative behavior of acid forms includes likely first desulfonation and then main chain decomposition as seen in Figure 4.12. Table 4.3 also shows the influence of the degree of disulfonation on the dry glass transition temperatures. The glass transition temperatures were increased with increasing amount of bulky sulfonic acid moieties.

Table 4.3 Thermal characterization of the control homopolymer and PAEB copolymers

<b>Degree of Disulfonation (Mol %)</b>	<b>10% Weight Loss Temperatures (°C) Acid Form</b>	<b>Glass Transition Temperatures (°C) from DSC* Acid Form</b>
10	503	219
20	438	230
35	367	240
45	361	249
60	352	-
Control (BP/DCBN) no acid treatment	512	215

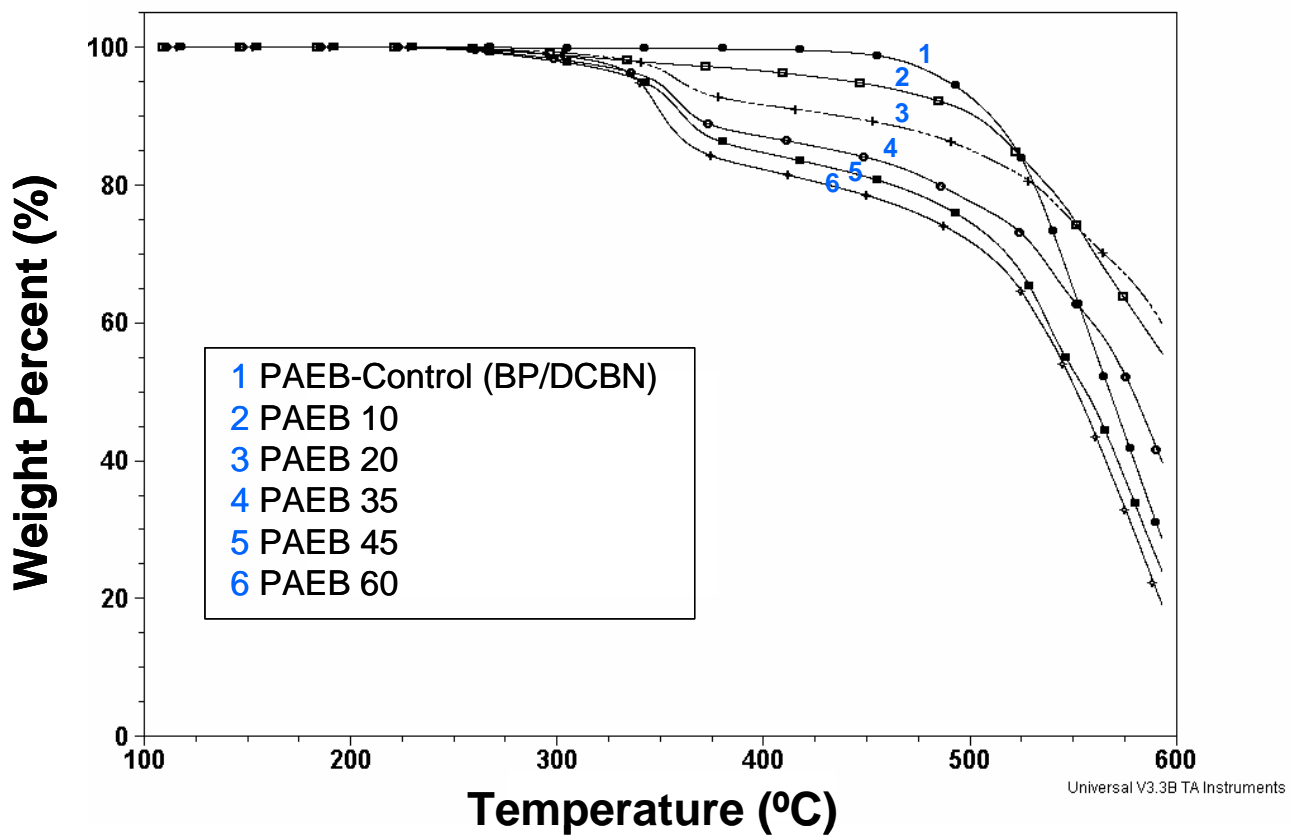


**Figure 4.12** Influence of the degree of disulfonation on TGA weight loss in the acid form of PAEB copolymers (10 °C/min in 50ml/min air )

The thermo-oxidative properties of these copolymers and their mechanical properties in dry and fully hydrated forms are important to understand the durability in a fuel cell environment. Hence dynamic mechanical analysis in the tensile mode was used to help developing this information. The storage modulus data were obtained for a series of disulfonated poly(arylene ether benzonitrile) copolymer membranes with a thickness of 7-mil at different level of sulfonation and at various temperature intervals. This data was compared with the Nafion™ membrane (Nafion™ 117, 7mil) (Figure 4.13).

The storage modulus of sulfonated copolymers was in the range of 0.13 GPa to 1.2GPa. As the sulfonation level increases, the storage modulus was decreased due to the increasing water uptake of the copolymer membrane series. However, it was still about 10 times higher than Nafion™ due to the stiff backbone of the poly(arylene ether benzonitrile)s.

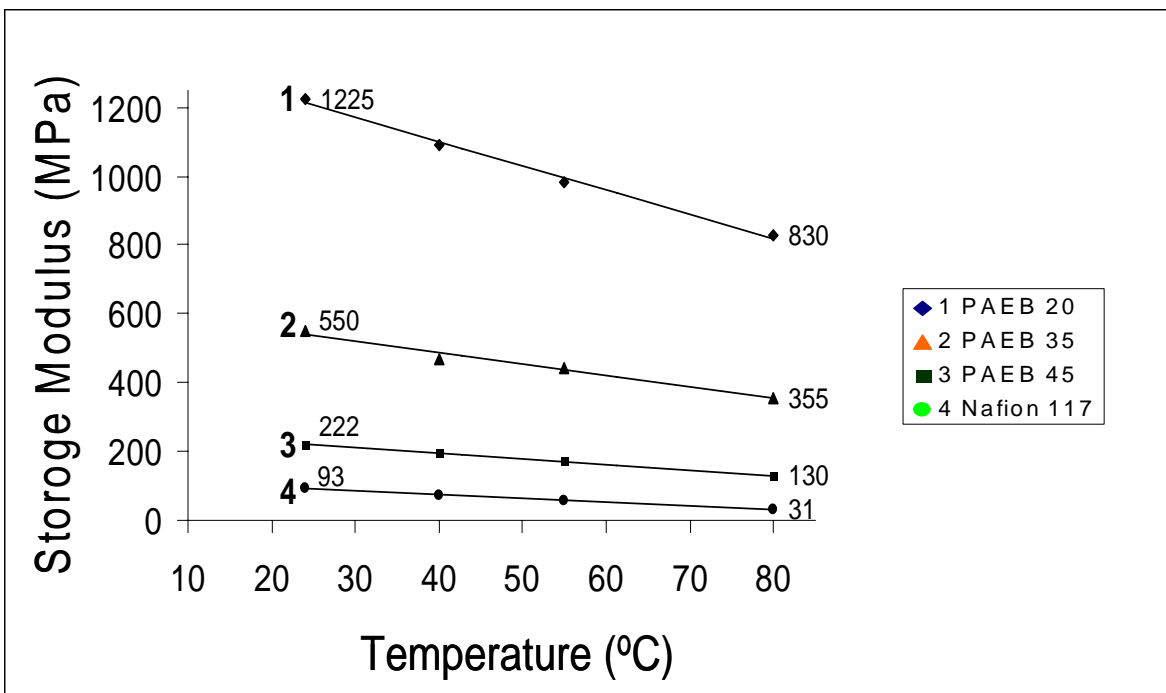


**Figure 4.13** Storage modulus of disulfonated poly(arylene ether benzonitrile copolymers) at various level of disulfonation compared with Nafion™ 117

The water uptake and proton conductivities of the copolymers scales with the degree of disulfonation and as well as the method used for acidification. The water uptakes of the copolymers acidified with method 1, room temperature acidification, linearly increased from 5 to 44 percent with increasing degree of disulfonation from 10 to 45 mol percent. A jump from 44 percent to 150 percent was observed when degree of disulfonation was increased from 45 to 60 percent. This percolation threshold was previously attributed to the morphological development which occurred inversion of continuous phase from hydrophobic to hydrophilic at greater than about 45 mol percent disulfonation<sup>11,22,34,35</sup> (Figure 4.14).

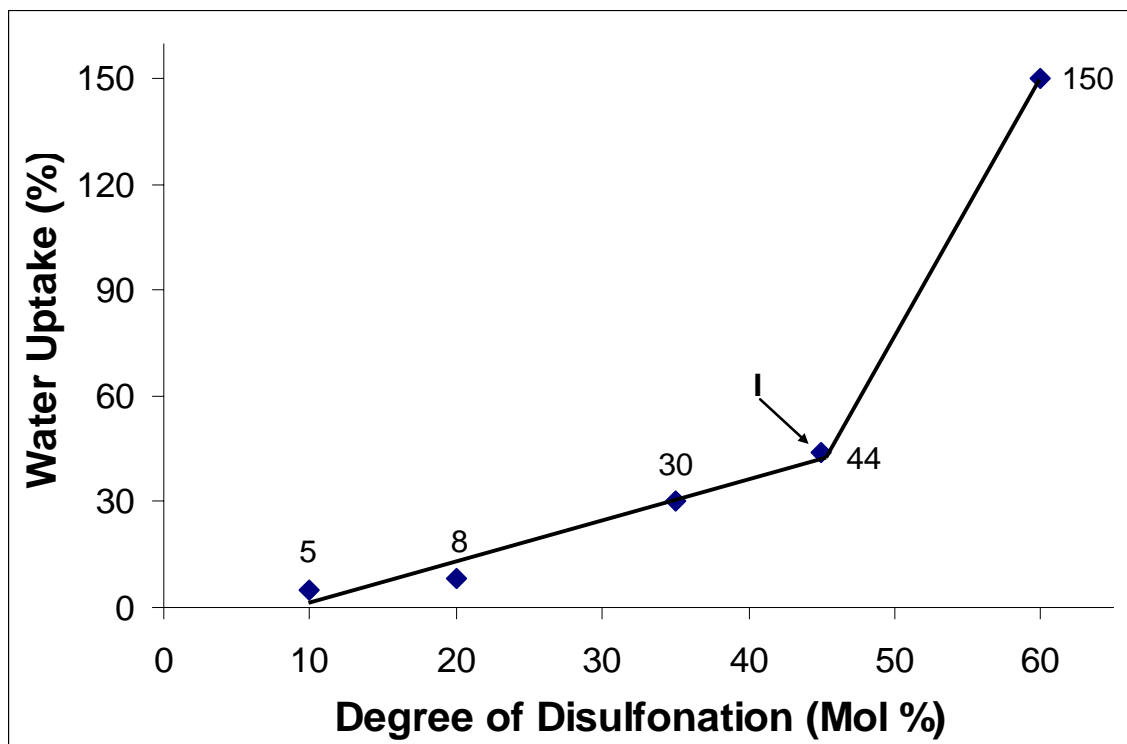


**Figure 4.14** The influence of the degree of disulfonation on water uptake of copolymers acidified with method 1: “I” shows the percolation threshold for water uptake at 45 mol percent sulfonation

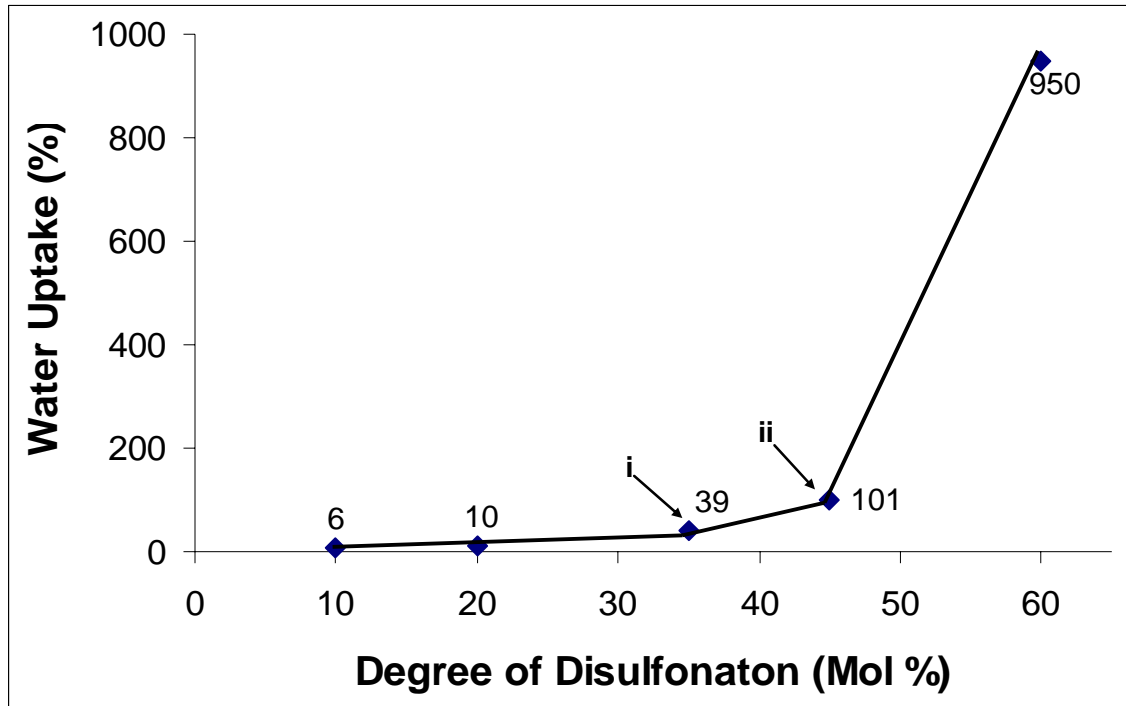


**Figure 4.15** The influence of the degree of disulfonation on water uptake of copolymers acidified with method 2 indicates higher swelling compared to copolymers acidified with method 1: “i” represents the percolation threshold, after “ii” point hydrogel formation occurs

Similarly, water uptake increased linearly at lower degrees of disulfonation ( 10 to 35 mol %) for the copolymers acidified with method 2. However, method 2 acidification produced much higher water uptake compared to method 1. The percolation threshold with method 2 was observed at 35 mol percent disulfonation, while it was 45 mol percent for membranes acidified with method 1. The water uptake increased about 10 times from 100 to 950 percent when the degree of disulfonation varied from 45 to 60 percent (Figure 4.15). The reason for the tremendous amount increases in water uptake is again due to

the phase inversion which result in a hydrogel. Similar phase inversion behaviour was observed with disulfonated poly(arylene ether benzonitrile) (Figure 4.16). As can be seen in the FE-SEM images of the fractured surfaces, the control homopolymer can easily be differentiated from disulfonated copolymers with bigger feature size. However, there is a nano-phase morphology for the disulfonated ionomeric copolymers and the size of the feature increases as disulfonation level increases from 35 to 45 mol percent probably due to the cocontinuity of the phases. Interestingly, the feature size then decreased for 60 mol percent disulfonated copolymer and image of 60 mol percent disulfonated copolymer was similar to that of 35 mol percent disulfonated copolymer. This may show the phase inversion where the hydrophilic domains become continuous, while hydrophobic domains were continuous for 35 mol percent disulfonated copolymers.

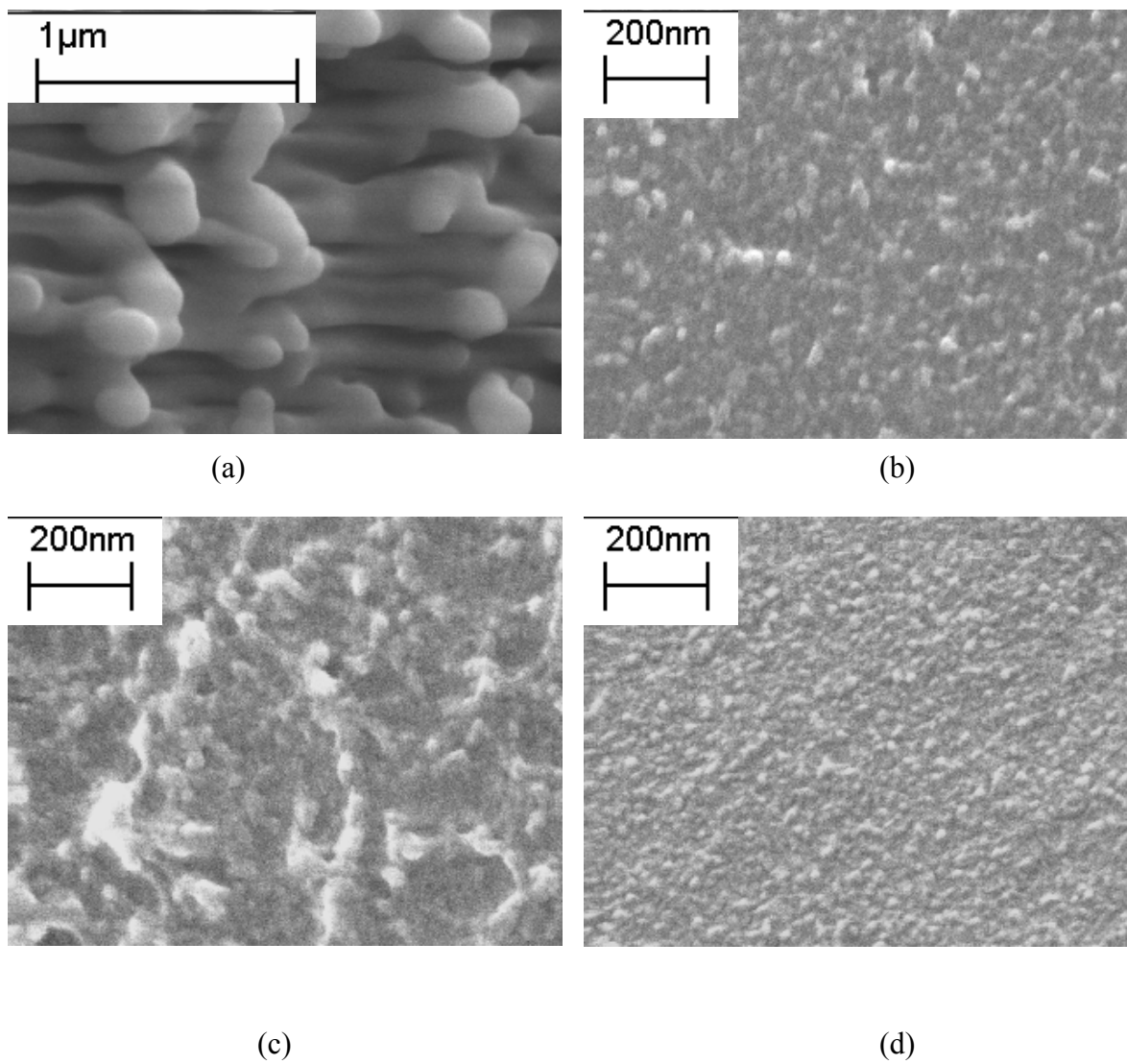


**Figure 4.16** Scanning electron micrographs (SEM) of fractured surfaces a. PAEB control (BP/DCBN), b. PAEB 35, c. PAEB 45, d. PAEB 60

The salt form of these copolymer membranes had also some water uptake. Both the potassium sulfonate and cyano groups are somewhat hydrophilic. The water uptake of both acid and salt forms was similar at lower mol percent disulfonation. However the influence of acidification on water uptake was more dominant for higher mol percent disulfonation (Figure 4.17).

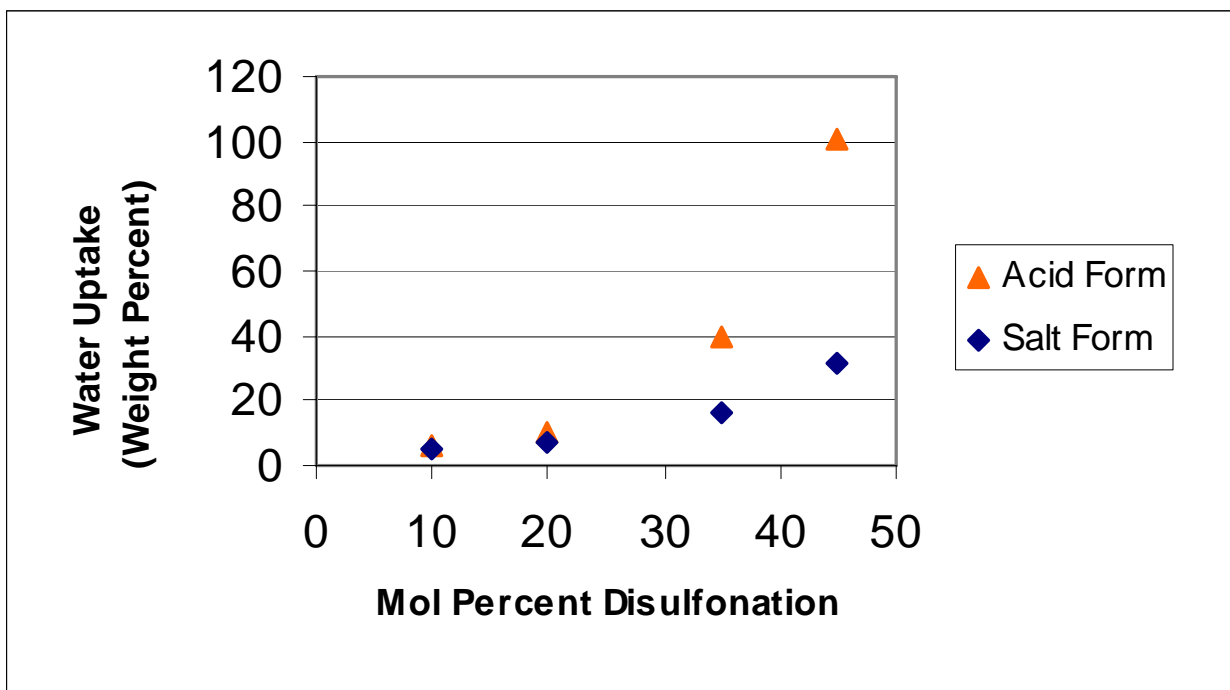


**Figure 4.17** The water uptake of the acid and potassium salt form of the poly(arylene ether benzonitrile) copolymers at various mol percent disulfonation

This influence can be seen in AFM phase images (Figure 4.18). The acid form produces more connectivity between hydrophilic phases; whereas salt form possesses a more close structure which may restrict the water uptake.

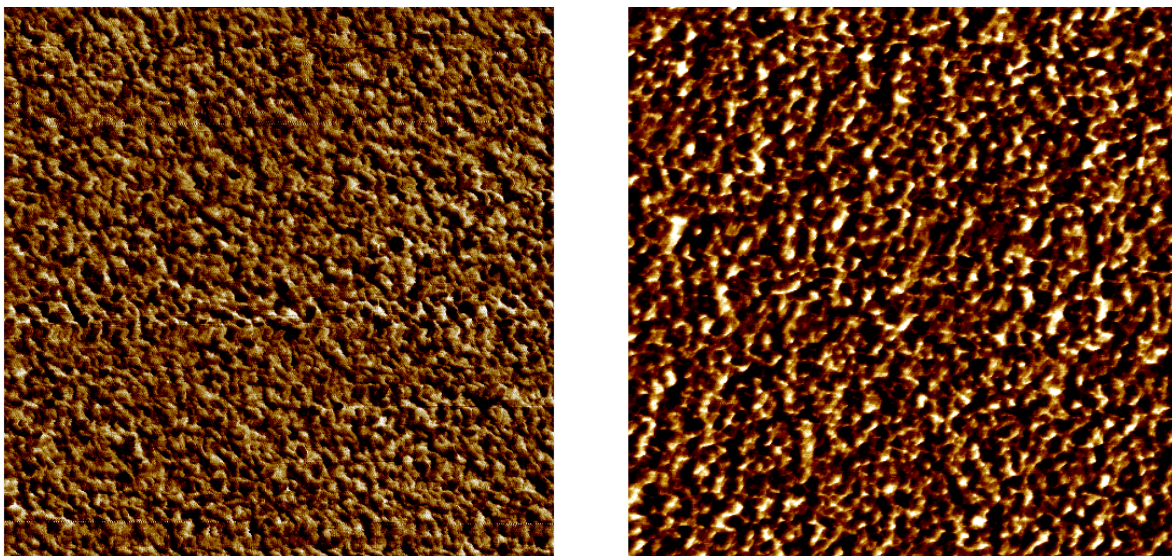


**Figure 4.18** AFM images for a. Salt form of poly(arylene ether benzonitrile copolymer) at 35 mol percent disulfonation, b. Acid form of poly(arylene ether benzonitrile copolymer) at 35 mol percent disulfonation (images are 250x250nm)

Proton conductivities of these copolymers showed similar trends to the water uptake. The proton conductivity depends on the number of conductive sites as well as the mobility of those sites. One can conclude that increasing the amount of hydration increases the mobility as well as conductivity. Membranes acidified with method 2 swells more than membranes acidified with method 1 and yielded higher proton conductivities (Figure 4.19).

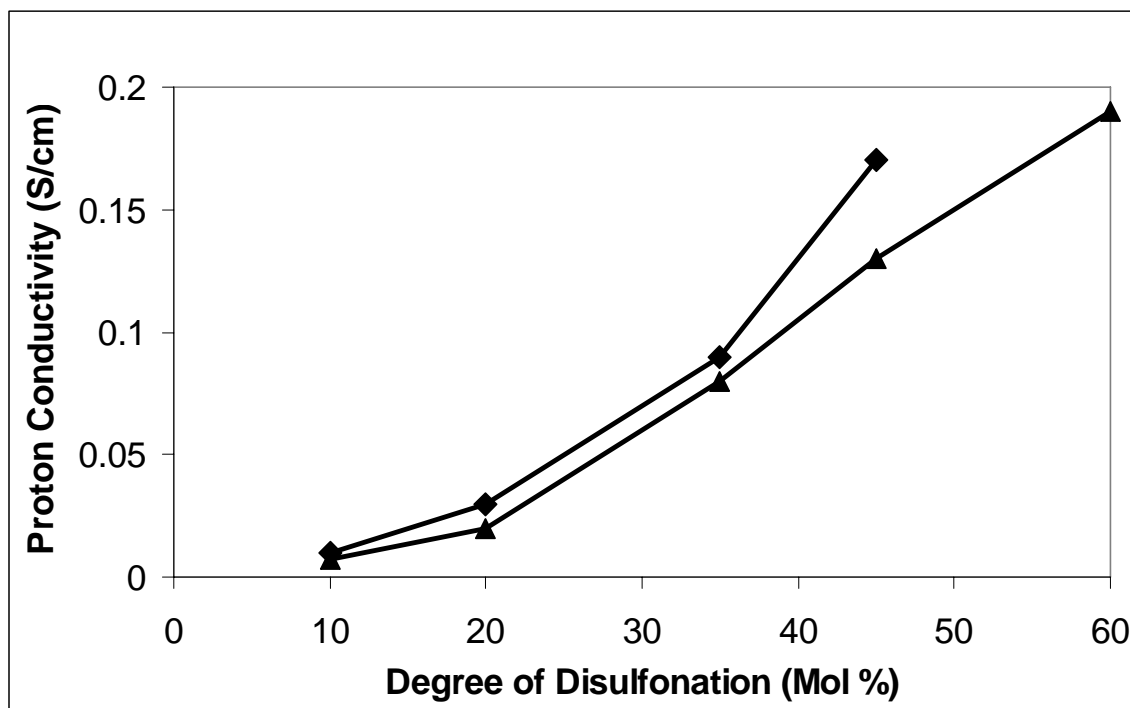


**Figure 4.19** The influence of the degree of disulfonation on proton conductivities of copolymers acidified with method 1 and method 2

The number of ions controls the amount of water uptake and proton conductivity. The ion exchange capacity (IEC) is the molar equivalent of ion content per mass of dry membrane. As expected, the ion exchange capacity linearly increases with an increasing degree of disulfonation (Figure 4.20 a). The influence of ion exchange capacity on proton conductivity can be seen in Figure 4.20 b. Proton conductivity values increased linearly with increasing IEC values. However, a jump in proton conductivity was observed for higher IEC values due to increase in swelling.

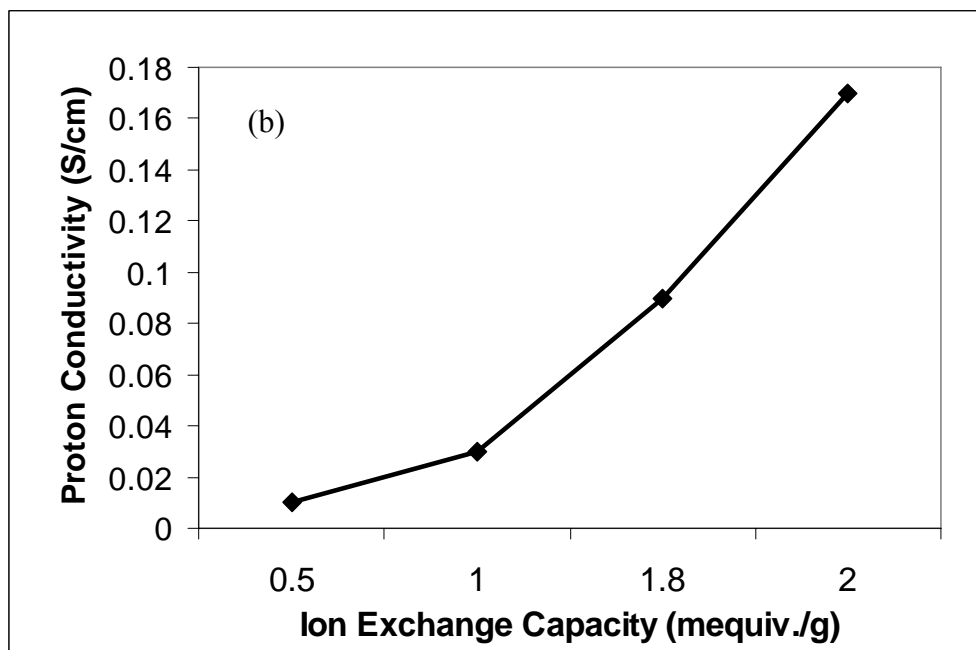
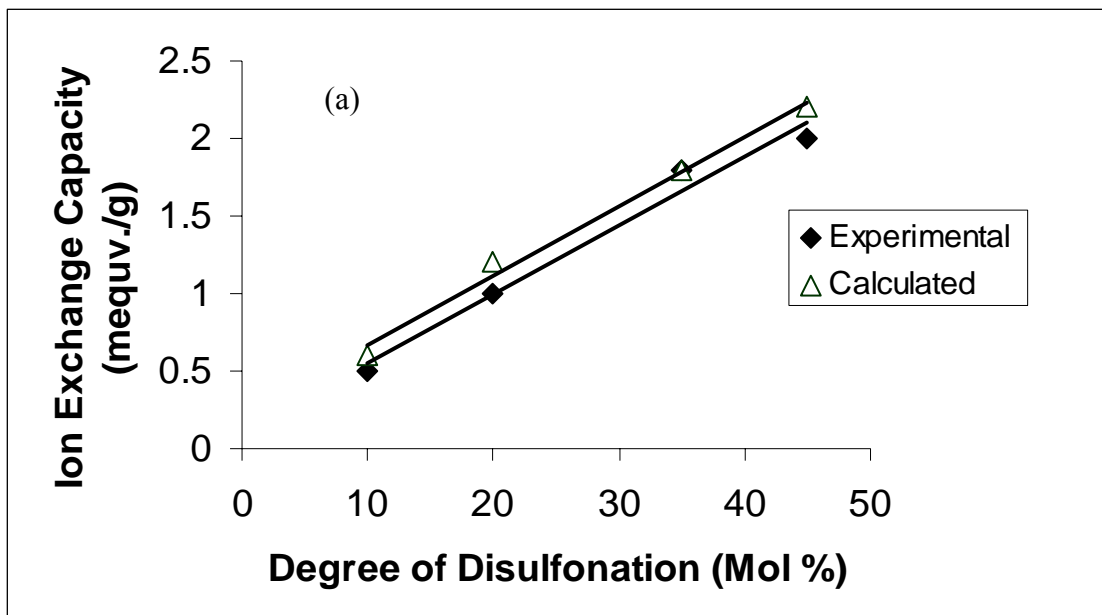


**Figure 4.20** a. Influence of the degree of disulfonation on ion exchange capacities (copolymers were acidified with method 2) b. Influence of ion exchange capacities on proton conductivities (copolymers were acidified with method 2)

The proton conductivity data can be normalized by ion exchange capacity. As can be seen in Figure 4.21, the proton conductivity per IEC values shows a linear relation with degree of disulfonation. Normalization was done for both experimental and calculated values of ion exchange capacities and very little deviation was observed among them.

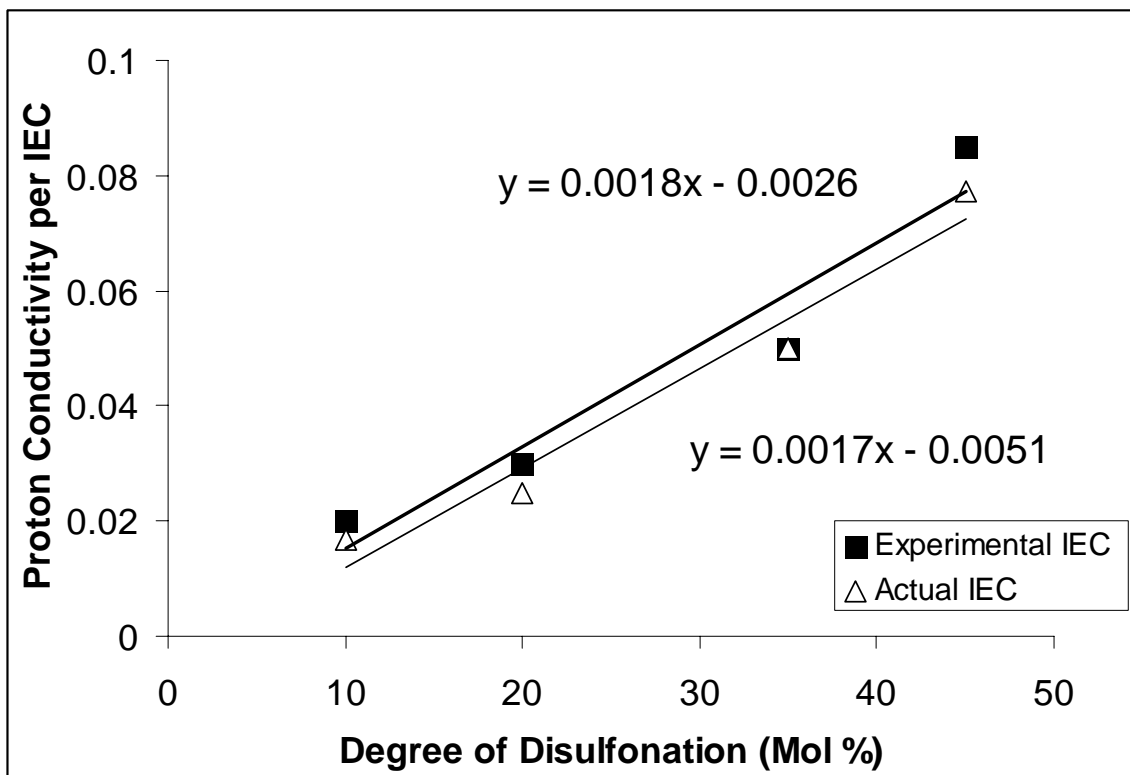


**Figure 4.21** Normalized proton conductivities with IEC shows a linear relation with the increasing degree of disulfonation

## **4.5 Conclusions**

Thermally stable, ductile high molecular weight disulfonated copolymers were successfully synthesized. Structural and compositional characterizations showed that all the starting monomers were well incorporated into the copolymer. Water uptake and proton conductivities were demonstrated to be a function of the degree of disulfonation. Higher water uptake and proton conductivities were obtained with method 2 acidification (boiling method). The disulfonated copolymers with tunable proton conductivity and water uptake are promising candidates for both methanol and hydrogen air proton exchange membrane fuel cells. Moreover, cyano groups could contribute adhesion to the electrode or catalyst layer. The cyano groups can also provide compability to additives such as heteropoly acids to make composites for higher temperature fuel cell applications which will be reported later. The spectrum of the physical properties described here as a function of degree of disulfonation is being used to provide input data while fabricating the proton exchange membranes into membrane electrode assemblies (MEA's) for both H<sub>2</sub>/Air and direct methanol fuel cells (DMFC).for the desired fuel cell applications.

## **4.6 Acknowledgements**

The authors would like to thank the National Science Foundation “Partnership for Innovation” Program (HER-0090556) and the Department of Energy (DE-FC36-01G01086) for support of this research effort.

---

## CHAPTER 5

### **Proton Exchange Membrane for DMFC and H<sub>2</sub>/Air Fuel Cells: Synthesis and Characterization of Partially Fluorinated Disulfonated Poly(arylene ether benzonitrile) Copolymers**

---

Taken from:

1. Sankir, Mehmet; Kim, Yu Seung; Harrison, William L.; Badami, A.S. and McGrath, James E. Proton exchange membrane fuel cells: II. Synthesis and characterization of partially fluorinated disulfonated poly (arylene ether benzonitrile) copolymers. *Preprints of Symposia - American Chemical Society, Division of Fuel Chemistry* (2005), 50(2), 568-570. Presented at the National ACS Conference in Washington DC. (nominated for RA Glenn Award)
2. Sankir, Mehmet; Kim, Yu Seung; Pivovar, Bryan S. and McGrath, James E. Proton Exchange Membrane for DMFC and H<sub>2</sub>/Air Fuel Cells: Synthesis and Characterization of Partially Fluorinated Disulfonated Poly(arylene ether benzonitrile) Copolymers, Submitted to *Journal of the Electrochemical Society* 2006.

## 5.1 Abstract

Partially fluorinated disulfonated poly(arylene ether benzonitrile) copolymers were synthesized by direct nucleophilic substitution copolymerization reactions. The 2,6-dichlorobenzonitrile and 3,3'-disulfonated 4,4'-difluorodiphenyl sulfone (SDFDPS) and controlled amounts of 4,4'-biphenol and hexafluoroisopropylidene diphenol (hexafluorobisphenol A, 6F) were used to produce partially fluorinated disulfonated copolymers with various degrees of fluorination (0-100 mol% 6F). NMR analysis coupled with titration of sulfonated moieties confirmed both chemical structure and copolymer composition. The copolymers produced ductile films and intrinsic viscosity analyses indicated high molecular weight copolymers were synthesized. Several basic PEM parameters such as water uptake, proton conductivity, and methanol permeabilities were controlled and presented as tunable properties which were a function of molecular structure. This was achieved by controlling of the chemical composition. Water uptake of membranes and cell resistance of MEAs were lowered by partial fluorination. The influence of this on desirably improving direct methanol fuel cell (DMFC) performance was demonstrated. A delamination failure mechanism was proposed for the hydrocarbon membrane electrode assemblies (MEA) due to the large difference between water uptake of the catalyst layer and membrane and this was verified by a reduction in high frequency resistance (HFR) for the partially fluorinated systems. A new term defined as water uptake corrected relative selectivity was introduced which better correlated DMFC performance.

## 5.2 Introduction

Proton exchange membrane fuel cells (PEMFC) have excellent potential in automobiles, residential area and as well as in portable devices such as laptops and cell phones. Their well known advantages include; high power density, high efficiency, relatively quick start up, rapid response the varying loads, low operating temperatures, solid non-corrosive electrolyte, insensitive to differential pressures, no carbonate formation, long life, potable liquid product water, ease of design and adaptable size. However there are also some disadvantages such as; high membrane cost, high catalyst loading, low quality waste heat, sensitive to carbon monoxide and limited understanding of structure-property-durability-relationships<sup>1,2,3,4,5,6,7</sup>.

Hydrogen and direct methanol proton exchange membrane fuel cells can be compared and contrasted in following ways: Hydrogen air system produces high power density; DMFC has simpler design but produces lower power. Typically, Hydrogen air fuel cells operate at 80 °C at 100% relative humidity, whereas DMFC operates from room temperature to 80 °C, with usually 0.5 M methanol. A major technical challenge in the hydrogen air area is to increase operation temperature to 100 to 120 °C at low RH. Reducing the methanol cross over is the major challenge for DMFC. A membrane electrode assembly for a typical hydrogen/air system is depicted in Figure 5.1.

---

<sup>1</sup> Mehta, V.; Cooper, S.C., *Journal of Power Sources* 2003, 114, 32

<sup>2</sup> Hickner M.A., *Ph.D. Thesis*, VPI&SU, 2003

<sup>3</sup> Zalowitz, N.; Thomas, S.; "Fuel Cells: Green Power", Department of Energy, 1999, LA-UR-99-3231

<sup>4</sup> Dhathathreyan, K.S.; Sridhr, P.; Sasikumar, G.; Ghosh, K.K.; Velayuthan, G.; Rajalakshmi, N.; Subramaniam, C.K.; Raja, M.; Ramya, K., *Int. J. Hydrogen Energy* 1999, 24, 1107

<sup>5</sup> Passalacqua, E.; Lufrano, F.; Squadrito, G.; Patti, A.; Giorgi, L., *Electrochimica Acta* 2001, 46, 799

<sup>6</sup> Kordesch, K.; Simader, G., *Fuel Cells and their Application*, VCH, New York, 1996

<sup>7</sup> Hickner, M.A.; Ghassemi, H.; Kim, Y.S.; Einsla, B.R.; McGrath, J.E., *Chemical Reviews* 2004 104, 4587

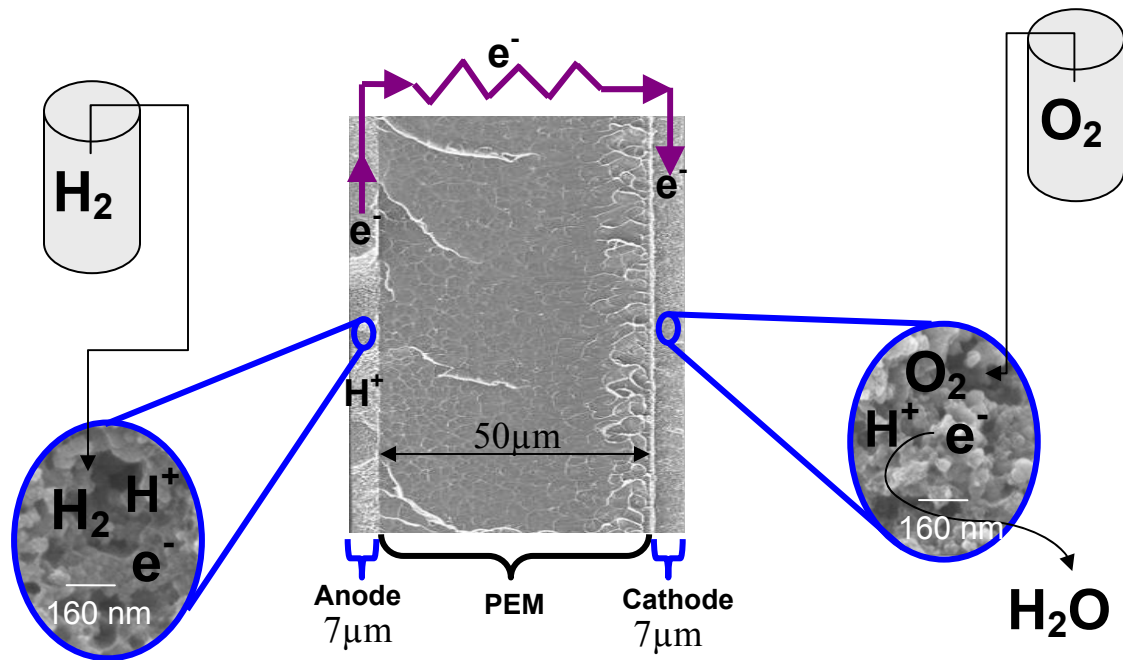


**Figure 5.1** Cross sectional morphology of a membrane electrode assembly (MEAs) where the anode and cathode compartments were fabricated by hot pressing of a decal on to the proton exchange membrane; Hydrogen gas is oxidized at anode and produces protons and electrons. Protons are transported from anode to cathode via the proton exchange membrane. However, electrons are collected via an external circuit. Oxygen provided from the air, electrons and protons combine at cathode and produce water

### 5.2.1 Basic Membrane Characteristics and Influence of Ion Exchange Capacity

The critical issues to all high performance proton exchange membranes by McGrath et al.<sup>7</sup> are listed below including; High protonic conductivities, low electronic conductivity, low permeability to fuel and oxidants, low water transport through diffusion and electro-osmosis, oxidative and hydrolytic stability, good mechanical properties both in dry and hydrated state, cost effective, capable of fabrication into membrane electrode assemblies (MEAs).

The concentration of the ion conducting units is characterized by the molar equivalents of ion conductor per mass of dry membrane and is usually expressed as equivalent weight (EW) with units of grams polymer per equivalent or ion exchange capacity (IEC), or units of milliequivalents per gram (mequiv/g or mmol/g) of polymer (EW=1000/IEC).

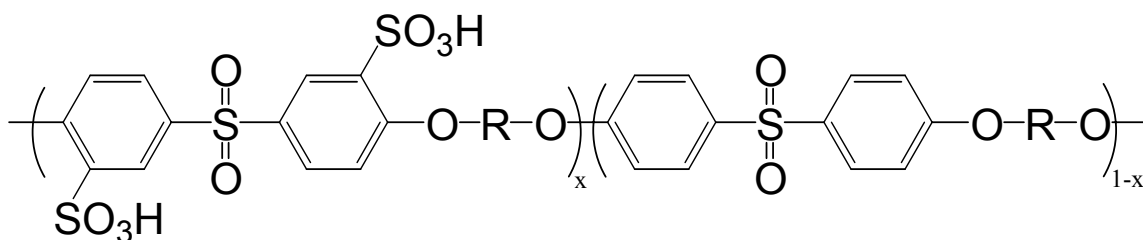
The ion exchange capacity for disulfonated copolymers can be expressed with the equation 5.1.

$$IEC = \frac{2x \text{ Mole fraction of disulfonation}}{MW_{\text{nonsulfonated unit}} \times \text{Its mole fraction} + MW_{\text{sulfonated unit}} \times \text{Its mole fraction}}$$

Equation 5.1

One can conclude that IEC values depends on the degree of disulfonation as well as the chemical structure of the backbone, which varies the molecular weight of both

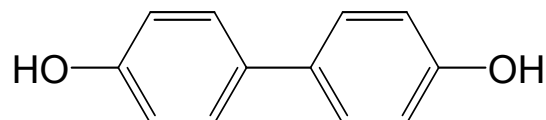
sulfonated and non sulfonated repeating unit. Figure 5.2 shows the general structure of the disulfonated poly(arylene ether sulfones) having different bisphenol units.



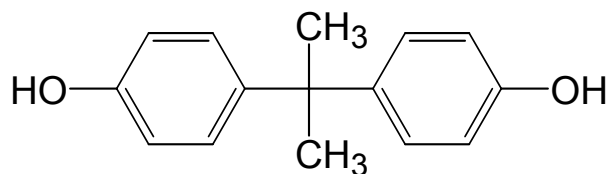
Where R is one of the following bisphenols ;



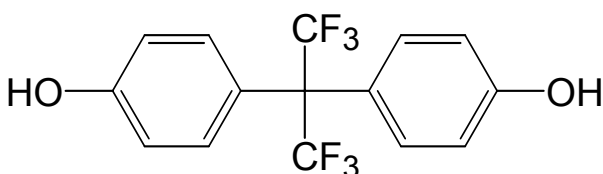
a. Hydroquinone (HQ)



b. Biphenol (BP)



c. Bisphenol A (BPA)



d. 6F Bisphenol A (6F)

**Figure 5.2** Some possible disulfonated poly(arylene ether sulfone)s random copolymers from different bisphenols which permit ion exchange capacities to be varied

Figure 5.3 illustrates the influence of the type of bisphenols used and degree of disulfonation on ion exchange capacity. The molecular weight of bisphenols increases in the order of hydroquinone, biphenol, bisphenol A and 6F bisphenol. The ion exchange capacity is proportional to the mole fraction of degree of disulfonation, but inversely relates to the cross product of molecular weight of the bisphenol and mole fraction of the degree of disulfonation. Hence, the influence of type of bisphenol on ion exchange capacity was not too important at lower mol percent disulfonation. As it reaches to 30 mol percent disulfonation, the ion exchange capacities become more dependent on the type of bisphenols (see the area above the Nafion™ line). This influence becomes more dominant especially for 60 mol percent disulfonation. However, too many ionic groups cause an excessive amount of swelling which usually results in poor mechanical behavior under continuous operations. The ion exchange capacities of these disulfonated poly(arylene ether sulfone) copolymers were also compared with the Nafion™ membrane having 1100 equivalent weight ( Figure 5.3).

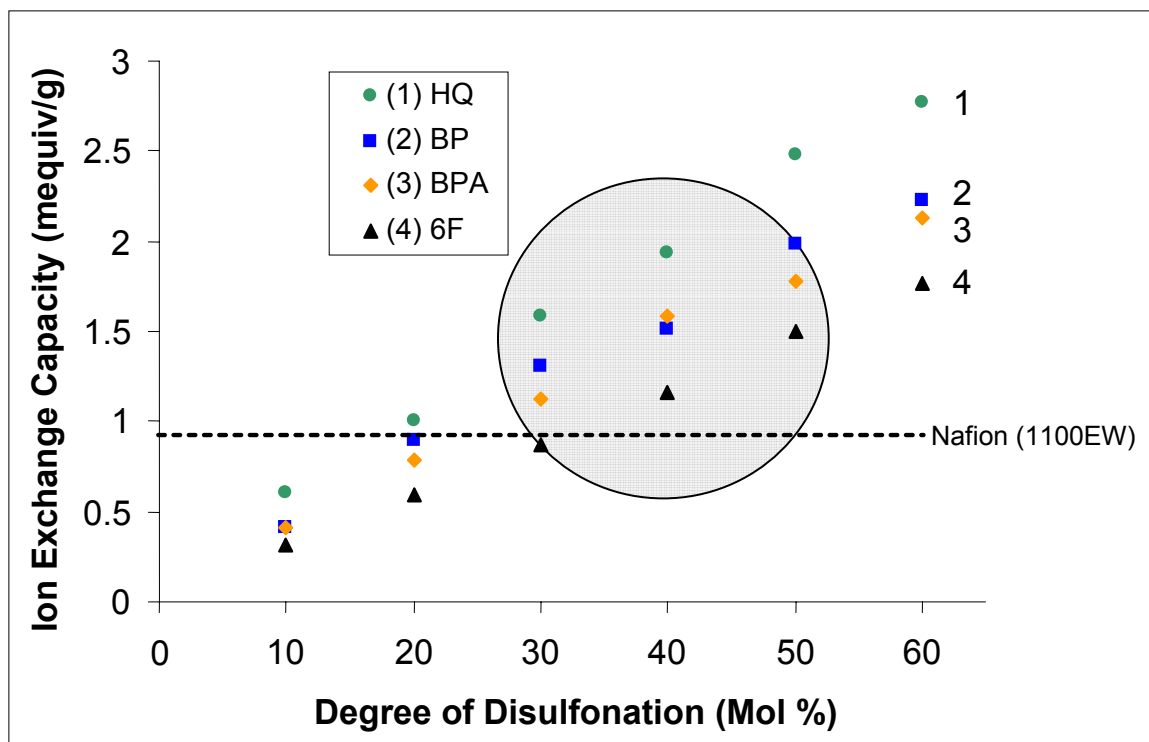


**Figure 5.3** Ion exchange capacity of disulfonated poly(arylene ether sulfone) copolymers using various different bisphenols; The molecular weight of the bisphenols increases from number 1 to number 4 (1. Hydroquinone, 2. Biphenol, 3. Bisphenol A, 4. 6F Bisphenol A). The most used IEC region (when the swelling and proton conductivity was considered, see also Figure 5.4) was illustrated with the shaded circle

The proton conductivity, fuel and oxidant permeability and water uptake of the disulfonated poly(arylene ether sulfone) copolymers scales with ion exchange capacity. Hence one can simply control these properties by varying the ion exchange capacities. It was earlier demonstrated that these basic membrane properties undergoes a transition at a certain ion exchange capacity value, which was assumed to be the percolation threshold<sup>8</sup>. This percolation threshold is depicted as a line in Figure 5.4. Below this line the basic membrane properties linearly increase with increasing IECs. However, just after the percolation, disulfonated copolymers produces morphologically more open structure. Hence, one of the objectives of this study is to control these basic membrane properties in a way favoring better fuel cell performance. Figure 5.4 also demonstrate the most useful working area as a function of the ion exchange capacity. Too low IEC values produces poor membrane transport characteristics, whereas, membranes having higher mole percent disulfonation (around 60 mol percent or higher) generally result in highly swollen hydrogels.

---

<sup>8</sup> Kim; Y.S., Hickner; M.A., Dong; L., Pivovar; B.S., McGrath; J.E., *Journal of Membrane Science* 2004, 243, 317

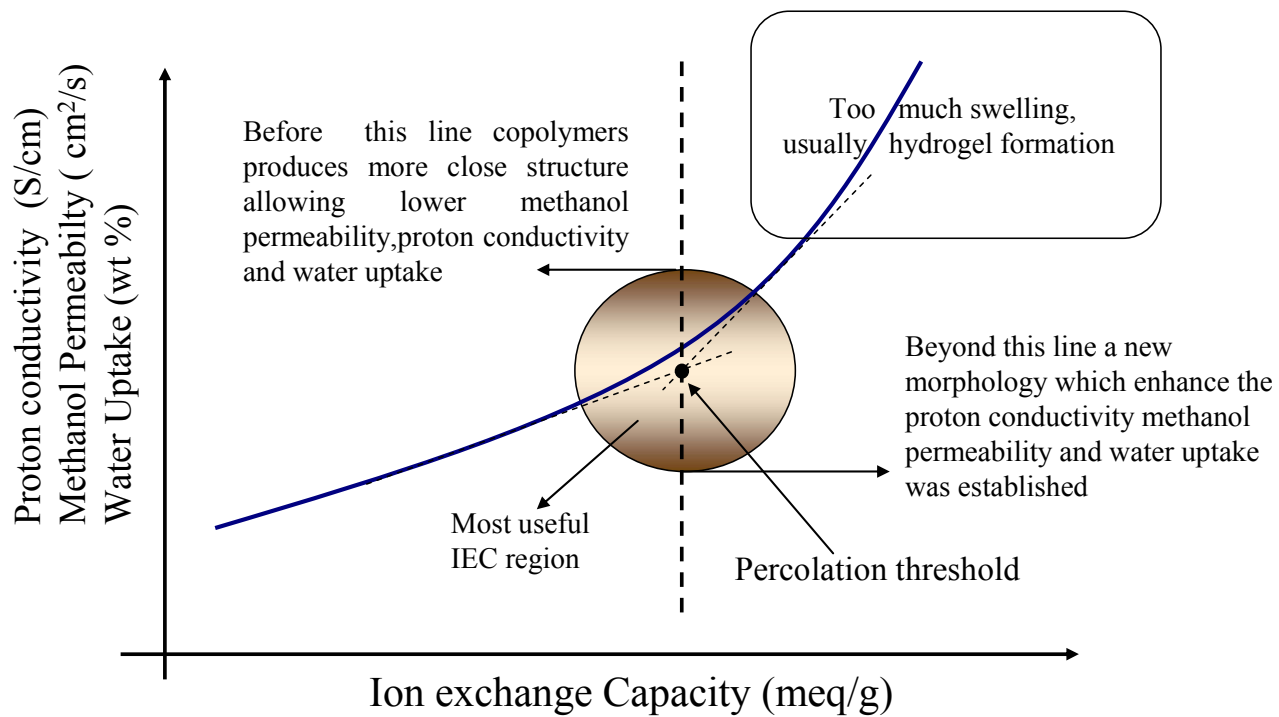


**Figure 5.4** Proton conductivity, methanol permeability and water uptake of disulfonated poly(arylene ether sulfone) copolymer as a function of ion exchange capacity (IEC)

## 5.2.2 Fuel Cell Performance Characteristics

The equilibrated open cell potential or reversible thermodynamic potential negatively deviates from its equilibrium once irreversible non-equilibrium processes of a practical fuel cell starts. The losses from equilibrium potential are called polarization, overpotential or overvoltage. In other words, the polarization is difference between measured potential under working conditions and the reversible thermodynamic potential. The source of total polarization includes<sup>9,10,11</sup>; 1. Activation Polarization, 2. Ohmic Polarization, 3. Concentration Polarization

Activation polarization is resulted from the chemical reaction and the physicochemical process associated with the adsorption of molecules on electrode surfaces. The origin of the activation polarization comes from the activation energy of the rate determining step or steps where all other steps depend on this slowest step. The voltage drop due to the activation polarization is expressed by Tafel equation. Concentration polarization occurs due to the fact that the concentration of ions at the electrodes is lower than the bulk. In previous derivations with activation polarization, the concentration of ions was assumed to be equally concentrated for both electrode surfaces and the bulk. The mass transfer of ions formed moving away from the electrode and the species moving to the electrode to react with the ions causes a concentration gradient. Additional potential loss, resistance polarization, occurs due to the resistance to flow ions

---

<sup>9</sup> Chen E.; In *Fuel Cell Technology Hand Book*, Hoogers, G, Ed., CRC Press: New York, 2003, p.3-26, 4-6, 4-7 2003

<sup>10</sup> Eisenberg, M., In *Fuel Cells*, Mitchell, W., Ed., Academic Press: New York, 1963, p17

<sup>11</sup> Barendrecht, E., In *Fuel Cell Systems*, Blomen, L.J.M.J; Mugerwa, M.N., Eds., Plenum Press: New York, 1993, p. 73

in the electrolyte and also resistance to flow of electrode through the electrode. The ohmic polarization term can be shown as below;

$$\eta_{ohmic} = \eta_{ohmic}^{electronic} + \eta_{ohmic}^{proton} = i(R^{electronic} + R^{proton}) \quad \text{Equation 5.2}$$

$$\eta_{ohmic} = iR^{internal} \quad \text{Equation 5.3}$$

$$R^{proton} = r_m \frac{l}{A} \quad \text{Equation 5.4}$$

where  $r_m$  membrane specific resistivity for proton exchange membranes.

The total polarization is the sum of activation, concentration and ohmic polarization, expressed by;

$$\eta_T = \eta_{activation} + \eta_{concentration} + \eta_{ohmic} \quad \text{Equation 5.5}$$

Hence, the over all cell potential is equal to the subtraction of total polarization from the thermodynamic reversible potential.

$$E_{cell} = E_r - \eta_T \quad \text{Equation 5.6}$$

The typical cell potential versus current diagram for fuel cells illustrates the regions of control by various types of overpotentials. Figure 5.5 shows how the cell performance decays from its initial thermodynamic reversible potential. Hence, besides the basic membrane properties, any improvement can be considered on the basis of these three polarization regions. The same curve was plotted by considering lower fuel cross

over which would produce better performance than any control system having higher fuel crossover.

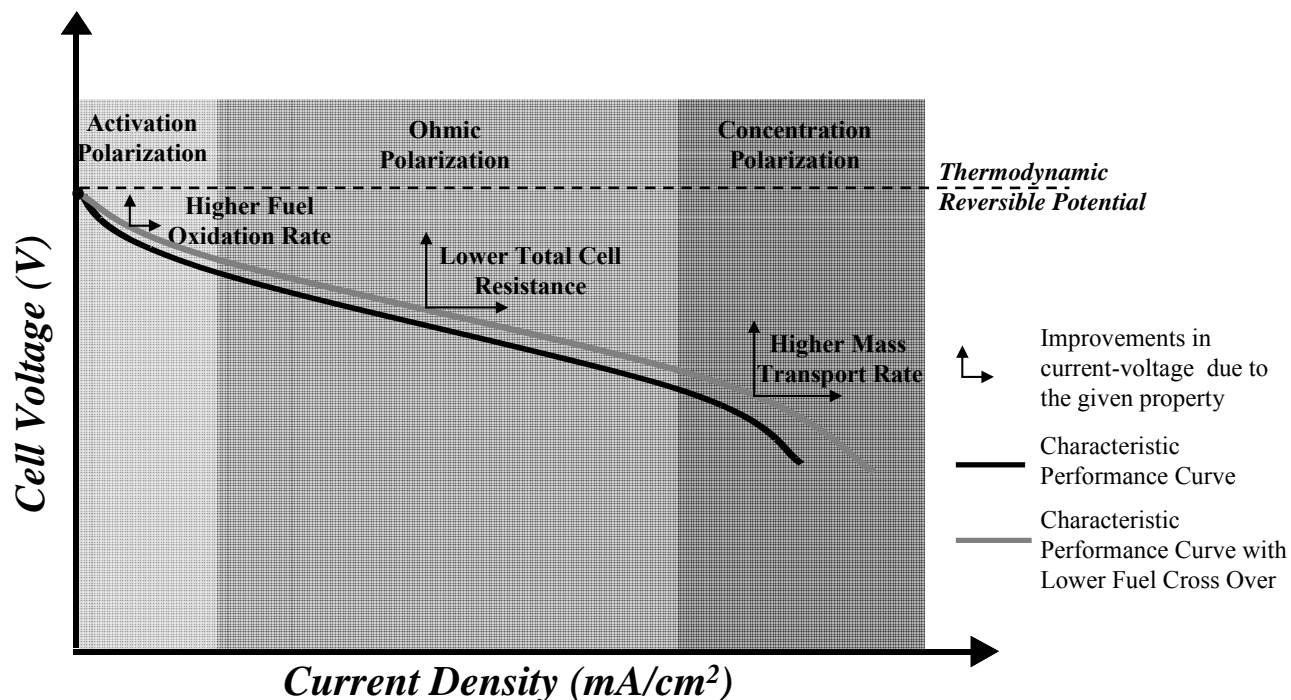


**Figure 5.5** Typical fuel cell performance curve in an electrochemical cell where actual performance decayed due to the polarization, activation, ohmic and concentration terms

The synthesis and characterization of high molecular weight, nitrile-functional copolymers using 3,3'-disulfonated 4,4'-difluorodiphenyl sulfone (SDFDPS), 2,6-dichlorobenzonitrile and 4,4'-hexafluoroisopropylidene diphenol (hexafluorobisphenol A, 6F)<sup>12</sup> and its nonfluorinated analogue<sup>13</sup> have been reported by our group. In this

<sup>12</sup> Sumner, M.J.; Harrison, W.L.; Weyers, R.M.; Kim, Y.S.; McGrath, J.E.; Riffle, J.S.; Brink, A.; Brink, M.H. *J. Membrane Science* 2004, 239, 199

<sup>13</sup> Sankir, M.; Harrison, W. L.; Wiles, K. B.; Li, Y.; McGrath, J. E. Div. of Fuel Chem., Preprints of Symposia ACS (2004), 49(2), 526-527

contribution, we report the synthesis and characterization of partially fluorinated disulfonated poly (arylene ether) copolymers and their direct methanol fuel cell (DMFC) performances.

### 5.2.3 Electrochemical Properties of the Membranes

#### 5.2.3.1 Electro-osmotic Drag Coefficient

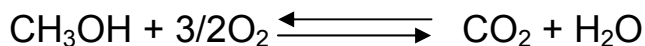
The presence of the water at the cathode occurs in several different ways. Figure 5.6 reveals the sources of the water collected from the cathode stream. There are four different types of water accumulated at cathode. These were labeled previously as<sup>14,15</sup> ;

Water (1) : Water from humidification bottle which is a set value

Water (2) : Produced water which can be calculated from the cell current



Water(3): (For DMFC's) Water produced by crossover methanol oxidation can be calculated flux of carbon dioxide measured in cathode exhaust stream



Water(4): Water flux across the membrane which can be evaluated

Total water effluent from the cathode exhaust ( $W_{\text{total}}$ ) is expressed as below;

$$W_{\text{total}} = \text{Water}(1) + \text{Water}(2) + \text{Water}(3) + \text{Water}(4) \quad \text{Equation 5.7}$$

<sup>14</sup> Ren, X.; Henderson, W.; Gottesfeld, S., *J. Electrochem. Soc.* 1997, 144 (9), L267

<sup>15</sup> Ren, X.; Springer, T.E.; Zawodzinski, T.A.; Gottesfeld, S., *J. Electrochem. Soc.* 2000, 147 (2), 466

So the water flux across the membrane can be calculated using the following equation;

$$\text{Water (4)} = W_{\text{total}} - \text{Water(1)} - \text{Water(2)} - \text{Water(3)} \quad \text{Equation 5.8}$$

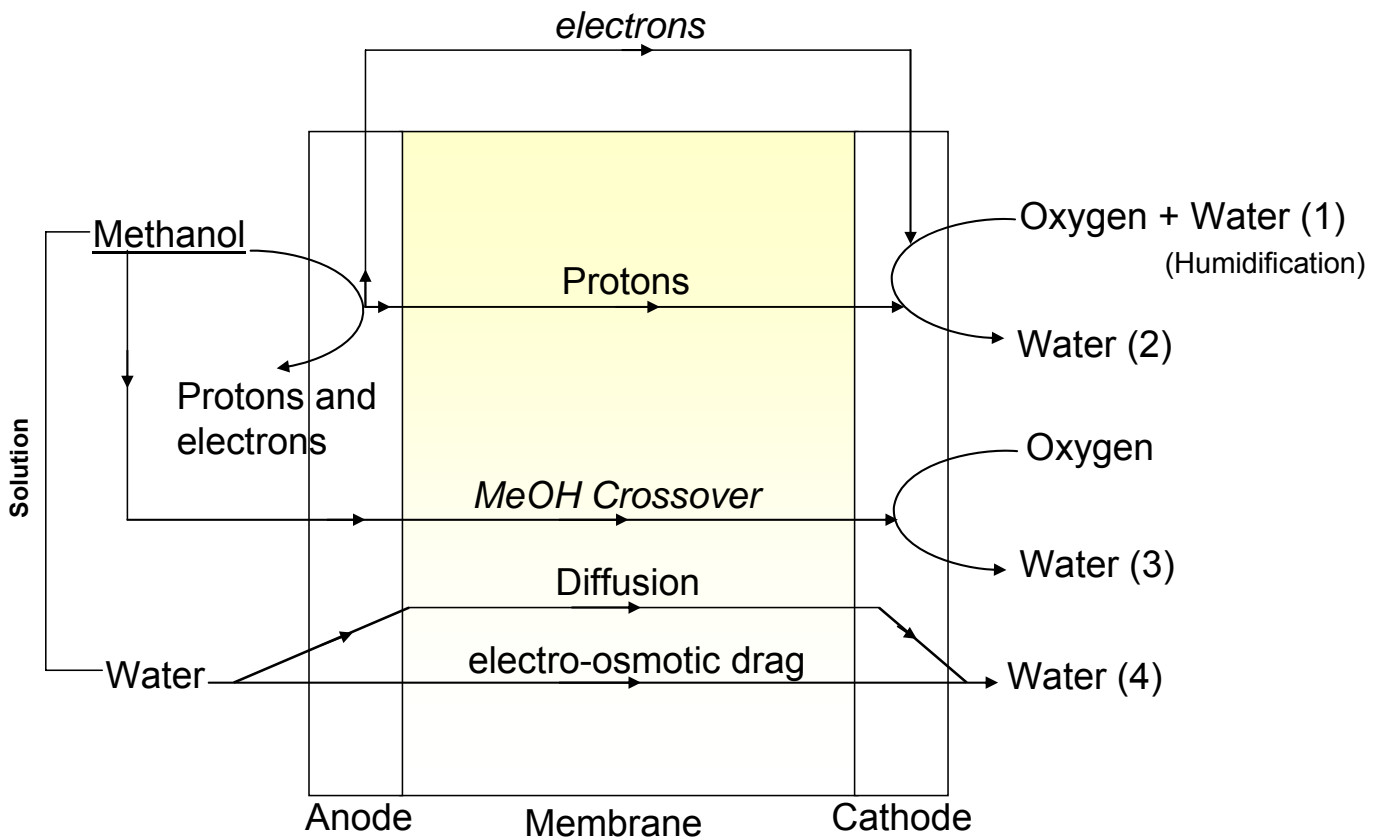


**Figure 5.6** Sources of water at the cathode; 1. Water from humidification bottle, 2. Product water from the cell current, 3. Water produced by crossover methanol oxidation, 4. Water which has fluxed across the membrane

Under the open circuit condition, the water flux from anode to cathode occurs by diffusion and is set by the water activity gradient between anode and cathode sides. However, when the fuel cell operates, water is transported from anode to cathode by diffusion and electro-osmotic drag<sup>14</sup>.

Water transport by diffusion is eliminated at higher current densities due to the electro-osmotic drag and an increase in cathodic activity. As the back pressure increases the water flux decreased due to the compressed gas preventing the water removal from the cathode under open circuit conditions. Electro-osmotic drag becomes the major mechanism for higher current densities and water flux across the membrane as a function of current density, since it linearly increases to yield a line crossing the origin in a water flux versus current density plot. This influence can be seen in water flux versus current density plot. Hence the linear region in the plot resembles the water flux by electro-osmotic drag at various current densities and the slope is called as electro osmotic drag coefficient (or water drag coefficient) which quantified as  $\text{H}_2\text{O}/\text{H}^+$ <sup>15</sup>. Zawodzinski et al. measured a water drag coefficient of 2.5  $\text{H}_2\text{O}/\text{H}^+$  for Nafion™ 117<sup>16</sup>. Kim et al. found that the hydrocarbon type of ionomer membranes has a lower electro osmotic drag coefficient (1.3 vs. 3.3  $\text{H}_2\text{O}/\text{H}^+$  6FCN35 versus Nafion™ respectively) and the 6FCN35 copolymer provided better water management at the cathode<sup>17</sup>. This was attributed to the states of the water where Nafion™ had less bound and more free water.

---

<sup>16</sup> Zawodzinski, T.A.; Springer, T.E.; Davey, J.; Valerio, J.; Gottesfeld, S., *Proceedings-Electrochemical Society* 1991, 91-10, 187

<sup>17</sup> Kim; Y.S, Sumner; M.J., Harrison; W.L., Riffle; J.S., McGrath; J.E., Pivovar, B.S., *Journal of The Electrochemical Society* 2004, 151, 12, A2150-A2156

### 5.2.3.2 Methanol Crossover and Limiting Current

Methanol crossover from anode to cathode causes a drastic reduction of energy efficiency, and of output voltage in terms of loss of fuel, reduced fuel efficiency, reduced cathode voltage and excess thermal load in the cell<sup>18,19</sup>. Methanol permeability of the membrane electrode assembly in the fuel cell can be measured by two common methods which measure carbon dioxide flux in the cathode exhaust and a voltammetric method that measures the methanol cross over current<sup>15,20</sup>.

The methanol permeation flux was determined from the limiting current density resulting from a transport-controlled methanol electro-oxidation at the other side of the cell by using a potential step experiment<sup>20</sup>. Methanol permeability was calculated from equation 5.9;

$$\text{Methanol permeability (cm}^2\text{/s)} = (\xi \times t) / (6F \times c) \quad \text{Equation 5.9}$$

where,  $\xi$  is the methanol crossover limiting current (A/cm<sup>2</sup>);  $t$  is the wet membrane thickness (cm);  $F$  is the Faraday constant (s·A·mol);  $c$  is the methanol feed concentration (mol/cm<sup>3</sup>).

---

<sup>18</sup> Kim, D.W.; Choi, H.S.; Lee, C.; Blumstein; A., Kang, Y., *Electrochimica Acta*, 2004, 50, 659–662

<sup>19</sup> Tricoli, V.; Carretta, N.; Bartolozzi, M. *Journal of The Electrochemical Society* 2000, 147 (4), 1286

<sup>20</sup> Ren, X.; Springer, T.E.; Gottesfeld, S., *J. Electrochem. Soc.* 2000, 147 (1), 92

The electro-osmotic drag causes a counter flux to the methanol transport. For example, since the electro-osmotic drag of Nafion™ membrane was measured as 2.5 H<sub>2</sub>O/H<sup>+</sup>, for each one MeOH molecule was transported, 15 water molecules were transported through opposite way of methanol flow (Figure 5.7).

Hence, the measured cross-over current under open cell condition was higher than the limiting current. The electro-osmotic-drag corrected methanol cross-over current was expressed as;

$$\zeta_{\text{lim},m} = \frac{6 \cdot x_0 \xi \zeta_{\text{lim},c}}{\ln[1 + 6 \cdot x_0 \xi]} \quad \text{Equation 5.10}$$

where  $x_0$  is the molar fraction in the feed aqueous methanol solution,  $\xi$  is the electro-osmotic drag coefficient of protons in the membrane, and  $\zeta_{\text{lim},c}$  is the limiting methanol crossover current for the membrane.

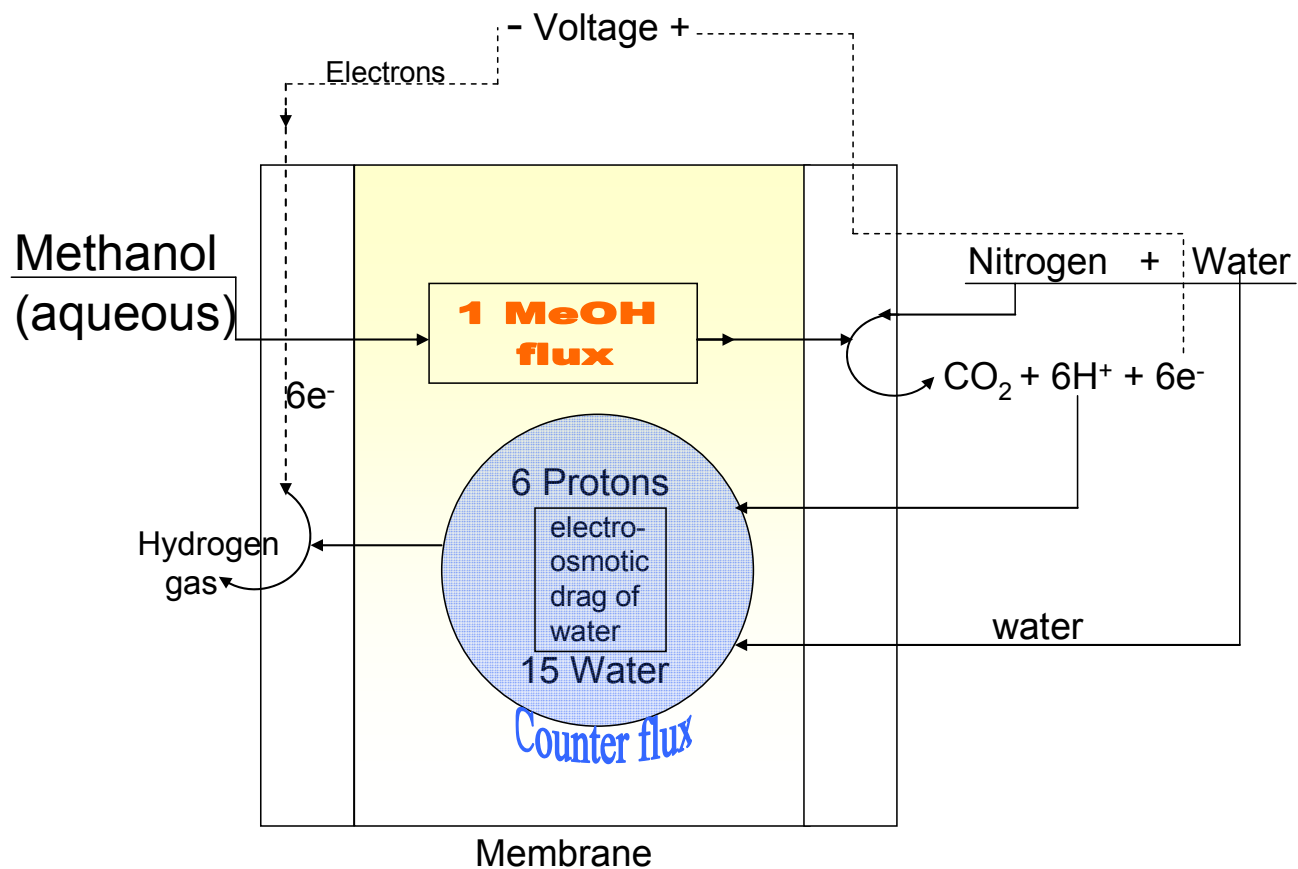


**Figure 5.7** Limiting current measurement of methanol (transported) oxidation at the fuel cell cathode; This process (methanol flux from left to right) is hindered with counter flux (from right to left) due to the electro-osmotic drag

## 5.3 Experimental

### 5.3.1 Reagents

4,4'-biphenol was kindly provided by Eastman Chemical, 2,6-dichlorobenzonitrile was purchased from Aldrich and both were used without any purification. The 4,4'-hexafluoroisopropylidene diphenol (hexafluorobisphenol A), received from Ciba, was purified by sublimation and dried *in vacuo*. The disodium salt of 3,3'-disulfonated 4,4'-dichlorodiphenyl sulfone (SDCDPS) was synthesized through the reaction of 4,4'-difluorodiphenyl sulfone (Solvay Advanced Polymers) and fuming sulfuric acid, as described previously<sup>21</sup>. All other reagents were obtained from commercial sources and purified, as needed, via common procedures.

### 5.3.2 Synthesis of Partially Fluorinated Disulfonated Poly (arylene ether benzonitrile)

Partially fluorinated disulfonated poly(arylene ether benzonitrile) copolymers were prepared at 35 mol percent disulfonation with various degrees of fluorination (0-100 mol% 6F) via direct copolymerization. A typical copolymerization is presented for 25 mol % 6F incorporated in 35 mol percent disulfonated poly(arylene ether benzonitrile). Thus, 2,6-dichlorobenzonitrile (1.3487 g, 7.8 mmol), 3,3'-disulfonated 4,4'-difluorodiphenyl sulfone (SDFDPS) ( 1.9350 g, 4.2 mmol), 4,4'-biphenol (1.6846 g, 9 mmol), 4,4'-hexafluoroisopropylidene diphenol (1.0139 g, 3mmol) and 1.9172 g potassium carbonate (15% mol excess) were transferred to 3-neck flask equipped with a

---

<sup>21</sup> Sankir, M. Bhanu; V.A, Harrison; W.L, Ghassemi; H, Wiles, K.B., Glass; T.E., Brink; A.E., Brink; M.H, McGrath; J.E, *accepted, J. Applied Polymer Sci.* 2005

mechanical stirrer, a nitrogen inlet and a Dean Stark trap. Dry NMP (15 mL) was used as the polymerization solvent while toluene (7.5 ml) was the azeotrope. The reaction mixture was refluxed for 4h at 150 °C to complete the dehydration process. The reaction temperature was slowly increased to 180 °C for 16 h just after removal of the toluene. The viscous reaction product was cooled, diluted with NMP and precipitated in deionized water as swollen fibers. After washing several times with deionized water, the precipitated copolymers were boiled in deionized water for 4 h to remove residual salts. The copolymers were isolated by filtration, then dried in a vacuum oven at 120 °C for 24h.

### 5.3.3 Film Casting and Membrane Acidification

Membranes in the potassium sulfonate form were prepared by first redissolving the copolymer in DMAc to afford 5-10% (w/v). Next, the polymer solutions were filtered, and then cast onto clean glass substrates. The transparent solutions were carefully dried with infrared heat at gradually increasing temperatures (up to ~ 60 °C) under a nitrogen flow, until the film appeared. The sulfonated poly(arylene ether sulfone) copolymer films were converted to their acid form by boiling the cast membranes in 0.5 M sulfuric acid for 2 hours, followed by 2 hours extraction in boiling deionized water, which has been referred to as Method 2<sup>22</sup>.

---

<sup>22</sup> Kim; Y.S., Wang; F., Hickner; M., McCartney; S., Taik Hong; Y., Harrison; W., Zawodzinski; T.A., McGrath; J.E., *Journal of Polymer Science: Part B: Polymer Physics* 2003, 41, 2816

### 5.3.4 Characterization

Intrinsic viscosities were determined in NMP containing 0.05 M LiBr at 30 °C using an Ubbelohde viscometer. The thermo-oxidative behavior of both the salt-form (sulfonate) and the acid-form copolymers was performed on a TA Instruments TGA Q 500. Dried, thin films (5 to 10 mg in the salt form) were evaluated over the range of 30 to 800 °C at a heating rate of 10 °C/min in air. Titration of the sulfonic acid groups was performed on acidified membrane samples of known mass by exchanging with sodium sulfate then back titrating with 0.01M NaOH. Thin film conductivity measurements were conducted on acidified membranes while submerged in deionized water using a Hewlett Packard 4129A Impedance/Gain-Phase Analyzer recorded from 10 MHz to 10 Hz.

MEAs were prepared from standard commercial catalyst inks using unsupported platinum and platinum-ruthenium catalysts. To prepare the catalyst ink mixtures, a 5% Nafion™ dispersion (1100 equivalent weight, Solution Technology, Inc.) was added to the water-wetted catalysts. The anode ink composition was 86 wt % 1:1 platinum ruthenium (Johnson Matthey) and 14 wt % Nafion™, and the cathode ink composition was 90 wt % platinum black (Johnson Matthey) and 10 wt % Nafion™. Catalyst inks were mixed by sonication for about 90 s and then directly transferred to a predried membrane by direct painting at 75°C. The painted MEAs were dried at 75°C for 20 min on a vacuum plate. The geometric active cell area was 5 cm<sup>2</sup>. The anode and cathode catalyst loading was approximately 10 and 6 mg/cm<sup>2</sup>, respectively. Single- and double-

sided hydrophobic carbon cloths (E-TEK, Inc.) were used as anode and cathode gas diffusion layers, respectively. All the MEAs tested were prepared by the same procedures.

#### **5.3.4.1 Membrane Characterization**

Fluorine compositions of the air and glass contacting surfaces of 6FCN-35 and recast Nafion™ were measured by X-ray photoelectron microscopy (XPS, Perkin-Elmer physical electronic model 5400) with a hemispherical electron analyzer and a position sensitive detector. The spectrometer was equipped with a Mg Ka X-ray source operated at 15 kV and 20 mA. The pressure in the sample chamber was maintained at  $\sim 10^{-8}$  Torr during spectra collection. Angle-dependent studies were performed for depth analysis of fluorine content. Takeoff angle used of  $45^\circ$  was approximately corresponding to sampling depths of 4 nm.

##### **5.3.4.1.1 Methanol Crossover**

Limiting methanol crossover currents through the membrane in a cell were measured to estimate the methanol crossover. For the data reported here, 0.5 M methanol solution was fed to one side of the cell, while humidified nitrogen at 500 sccm and ambient pressure was supplied to the other side. The methanol permeation flux was determined from the limiting current density resulting from transport-controlled methanol electrooxidation at the other side of the cell using a potential step experiment described in greater detail elsewhere<sup>15,20</sup>.

#### 5.3.4.1.2 Cell Resistance and DMFC Performance

Cell resistance and polarization curves for single cells were performed using a fuel cell test station (Fuel Cell Technology, Inc.) after 12 h break-in under hydrogen/air conditions at a cell voltage of 0.5 V. For DMFC testing, the cell was held at 80°C; 0.5 M methanol was fed to the anode with a flow rate of 1.8 mL/min; 90°C humidified air was fed at 500 sccm without back pressure (high humidification and stoichiometry were used to minimize cathode effects).

#### 5.3.4.1.3 High-frequency Resistance (HFR)

HFR was measured by applying a sinusoidal wave perturbation at 2 kHz and 30 mV. This frequency was chosen because it was found to minimize capacitive contributions to cell impedance.

The total resistance terms along the whole MEA includes resistance from the bipolar plates,  $\Omega_{bp}$  (metal or composites), fuel diffusion layer for anode,  $\Omega_{AGDL}$  and oxidant diffusion layer for cathode,  $\Omega_{CODL}$  (carbon cloth), both anode,  $\Omega_{ANODE}$  and cathode,  $\Omega_{CATHODE}$  electrodes and membrane,  $\Omega_{MEMBRANE}$  (Figure 5.8). The total resistance is the sum of these resistances and interfacial resistances. The resistance due to bipolar plates, diffusion layers and membrane and the interfacial resistance between electrode layers and carbon cloth become constant. The HFR resistance mainly resembles the interfacial resistance between the membrane and the catalyst layer, which also qualify the adhesion of the electrode to membrane.

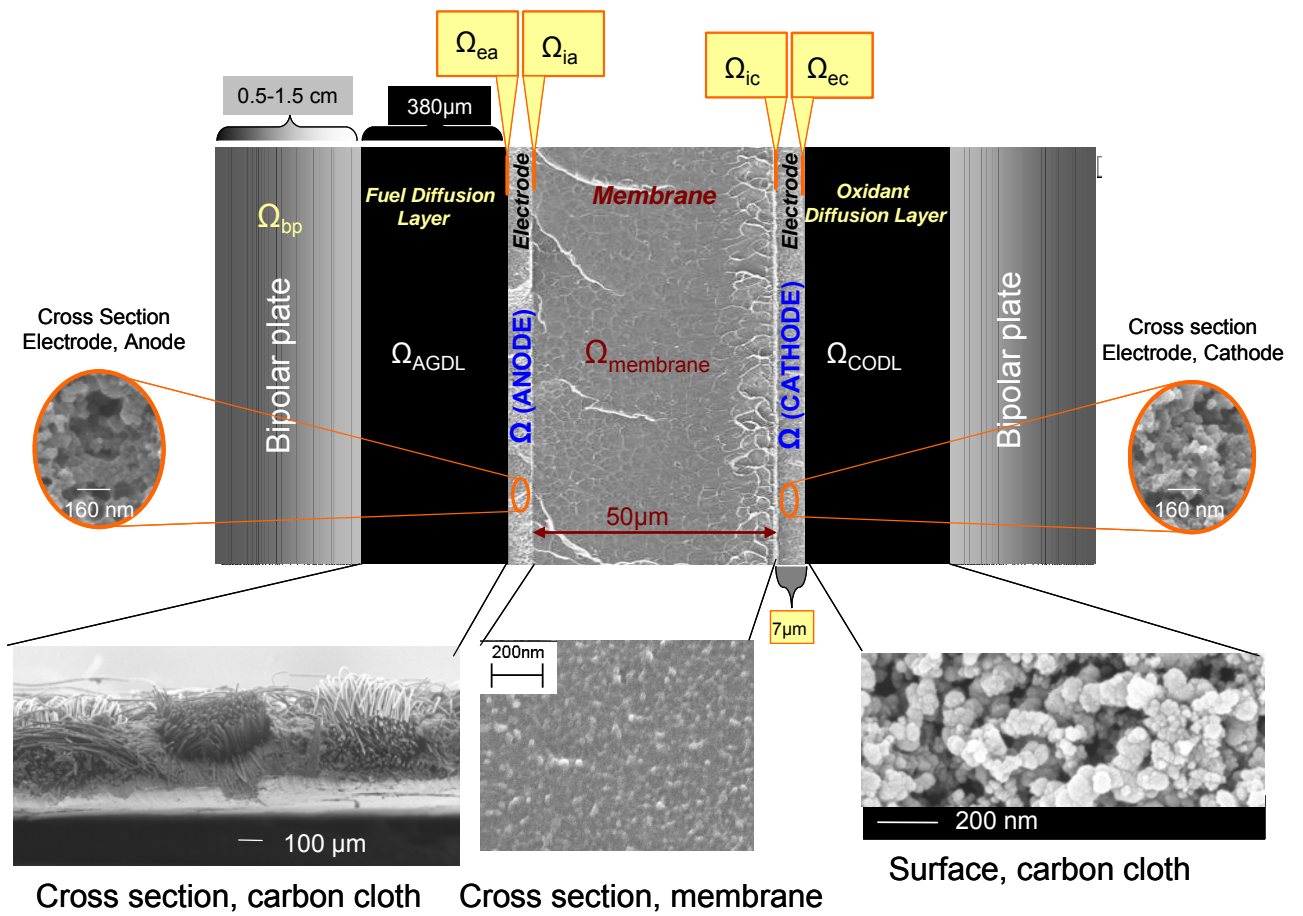


**Figure 5.8** The components of the membrane electrode assemblies

## 5.4 Results and Discussion

Direct nucleophilic polycondensation was used to synthesize several series of high molecular weight partially fluorinated disulfonated poly(arylene ether sulfone) and nitrile copolymers. Controlling the basic proton exchange membrane parameters such as water uptake and proton conductivity are key issues for proton exchange membrane fuel cells. For example, water uptake was traditionally controlled as a function of disulfonation (proton conducting sites). The challenge is to control the membrane parameters at the same level of disulfonation for the same kind of copolymer. Hence, a series of partially fluorinated copolymers at various level of fluorination as mol percent were synthesized to achieve that goal. However, disulfonation was kept constant at 35 mol percent which produced enough proton conductivity with tunable water uptake for partially fluorinated copolymers. The 4,4'-biphenol and 4,4'-hexafluoroisopropylidene diphenol were used together to obtain a series of partially fluorinated copolymers at the same level of disulfonation. The chemical structure of disulfonated poly(arylene ether benzonitrile) copolymer and partially fluorinated system can be seen in Figure 5.9.

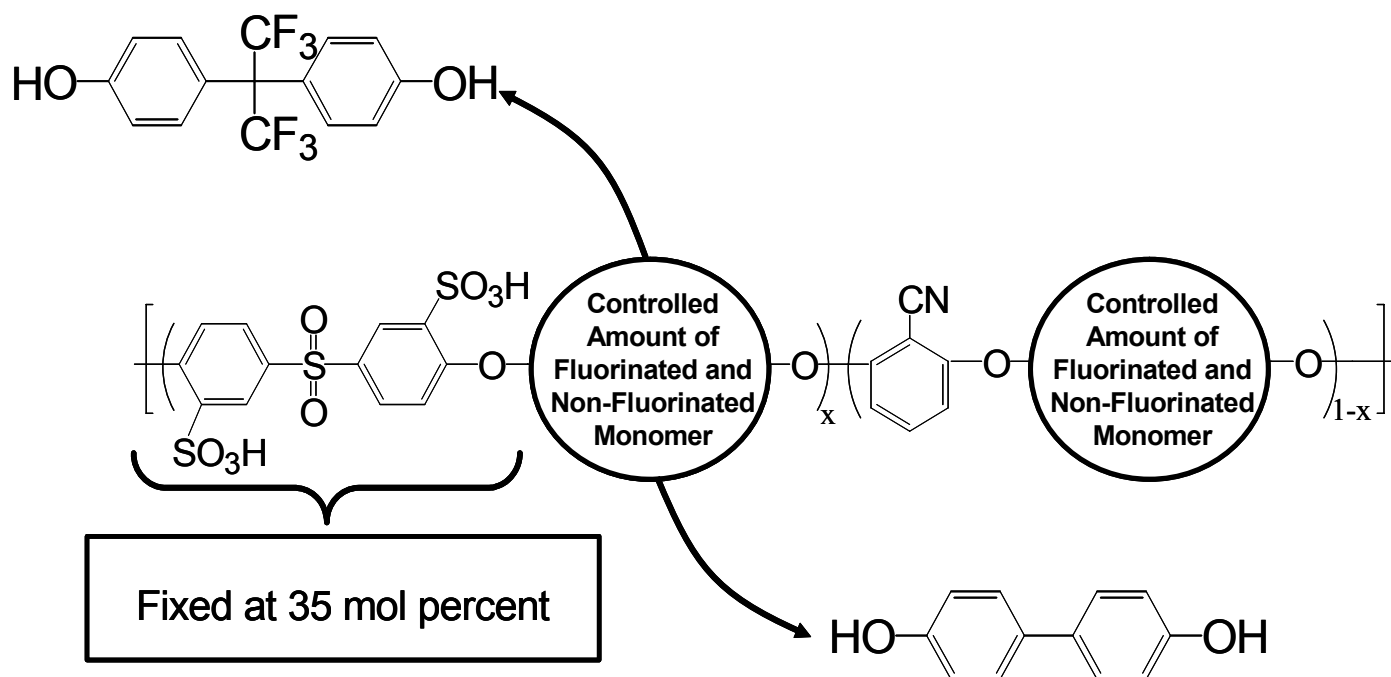
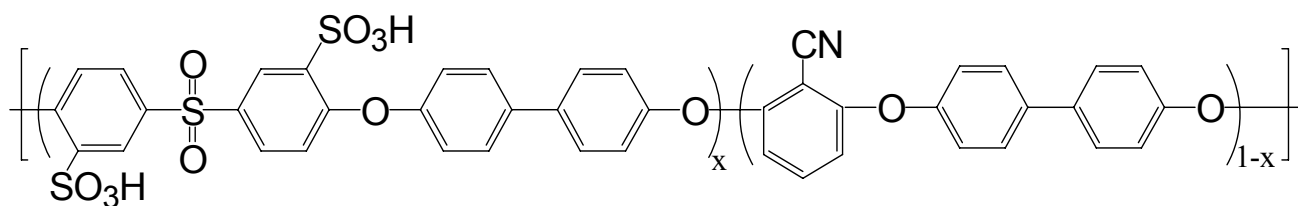


**Figure 5.9** Chemical structure of (a) 35 mol percent disulfonated poly(arylene ether benzonitrile) and (b) 35 mol percent disulfonated partially fluorinated poly(arylene ether benzonitrile)

The synthetic route for partially fluorinated systems (Figure 5.10) was quite similar to synthesis of both statistical poly(arylene ether sulfone) and poly(arylene ether benzonitrile) copolymers which have been previously synthesized, including a 4 h dehydration step and copolymerization for about 16 h. Total 100 mol percent of bisphenol (biphenol + 6F) was used and 6F was varied from 0 mol percent to 100 mol percent. (For example, when 25 mol percent biphenol was used, 75 mol percent 6F was added to copolymerization reaction to maintain total 100 mol percent bisphenol (biphenol + 6F) which was incorporated into copolymer backbone).

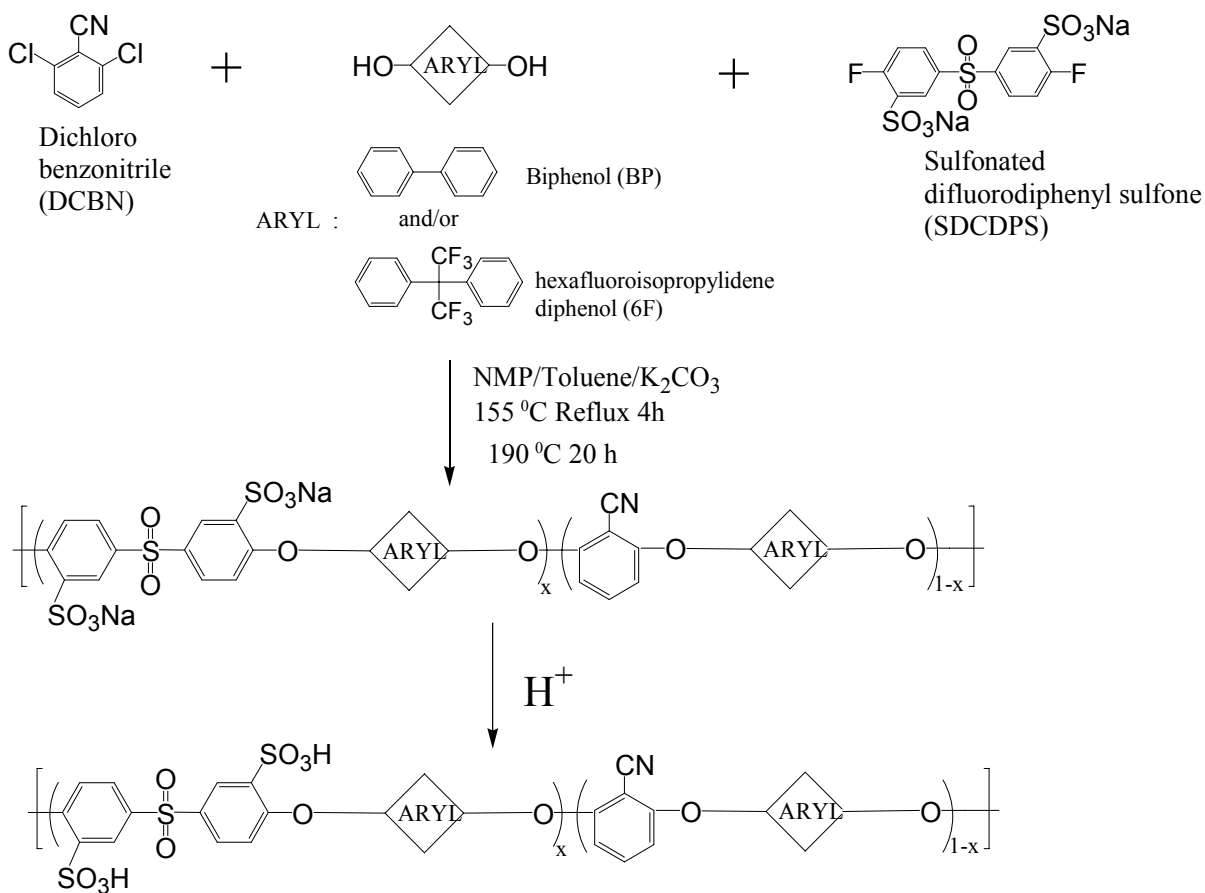


**Figure 5.10** Synthesis of partially fluorinated disulfonated poly(arylene ether benzonitrile) statistical copolymers

Intrinsic viscosities of the partially fluorinated 35 mol percent disulfonated poly(arylene ether benzonitrile copolymers) are presented in Table 5.1. Measurements were done in NMP at 30 °C, and a low molecular weight salt (0.05M LiBr) was used to prevent the polyelectrolyte effect. Otherwise, sulfonated copolymers always produced higher intrinsic viscosity than its non-sulfonated analogue. The high intrinsic viscosities were consistent with the generation of tough and ductile films.

Table 5.1 Intrinsic viscosity and 5 weight percent weight loss temperatures series of partially fluorinated copolymers at 35 mol percent disulfonation (Measurements were performed in 0.05 M LiBr containing NMP solution

<b>Copolymers</b>	<b>Intrinsic Viscosity (dL/g)</b>	<b>5 weight percent weight loss temperatures (°C) acid forms (by TGA)</b>
PAEB35 (35mol percent disulfonated poly(arylene ether benzonitrile)	1.2	350
6F25CN35 (25 mol percent 6F incorporated, 35 mol percent disulfonated poly(arylene ether benzonitrile)	1.1	
6F50CN35 (50 mol percent 6F incorporated, 35 mol percent disulfonated poly(arylene ether benzonitrile)	1.2	
6F75CN35 (75 mol percent 6F incorporated, 35 mol percent disulfonated poly(arylene ether benzonitrile)	1.5	400
6F100CN35 (100 mol percent 6F incorporated, 35 mol percent disulfonated poly(arylene ether benzonitrile)	1.4	

The proton NMR reveals that all monomers were successfully incorporated into the copolymer chain (Figure 5.11). A new peak observed with the fluorination at about 7.45 ppm. This peak was used for monitoring 6F incorporation. The peak for biphenol at about 7.7 ppm was decreased as 6F incorporation. The chemical structure was confirmed with proton NMR (Cosy NMR). The 6F incorporation at the same level of disulfonation was resulted with the different membrane properties which will be presented in this study. The high intrinsic viscosities of the copolymers proved that 6F incorporation was stoichiometric as designed.

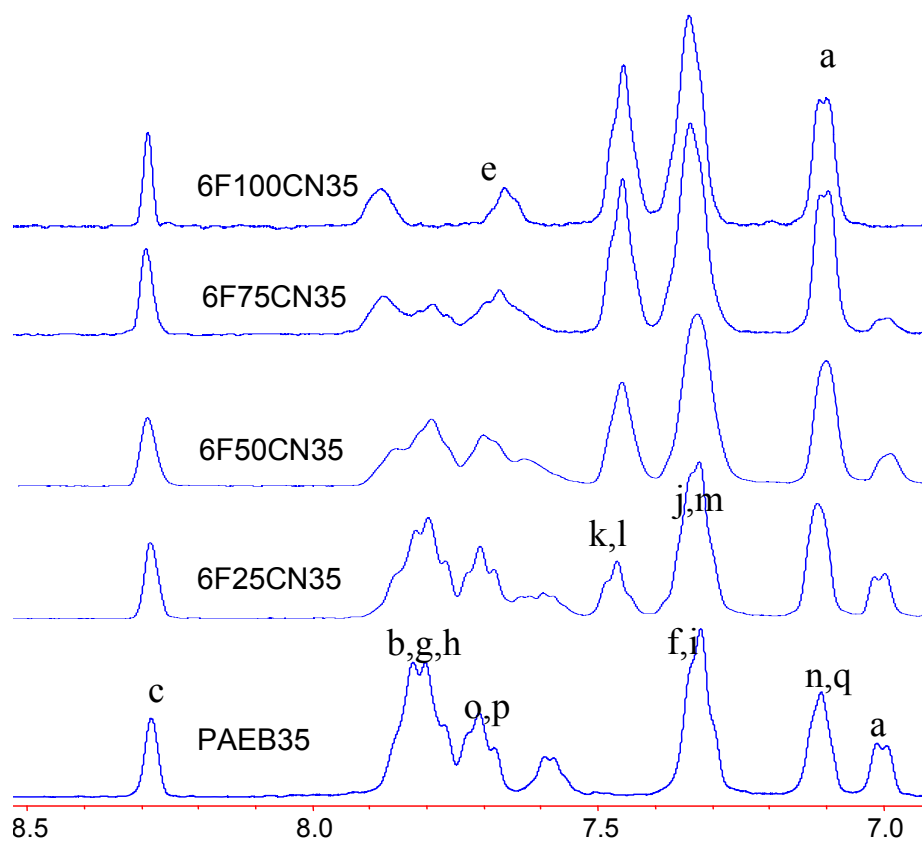
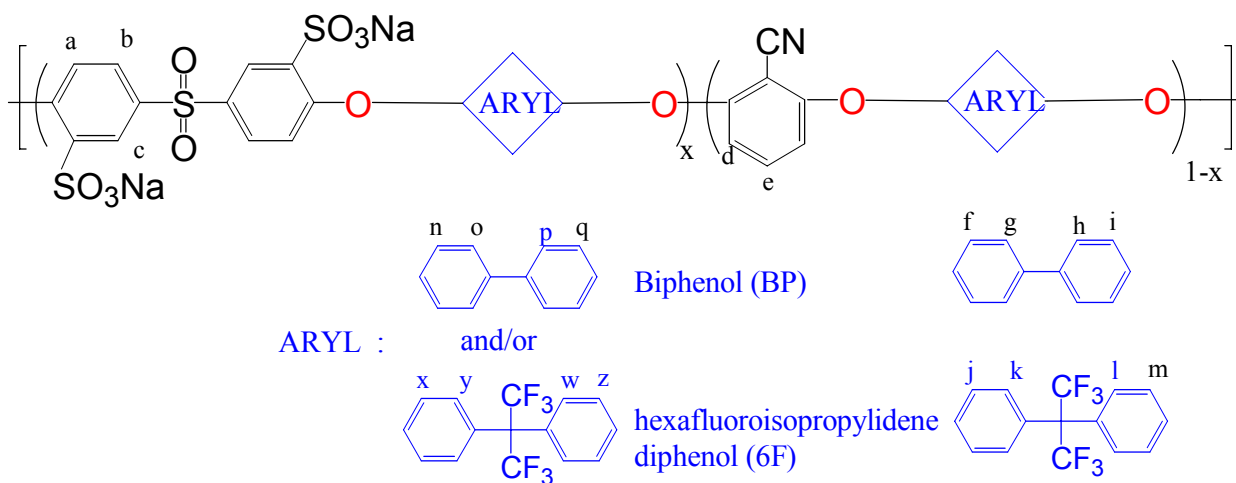


**Figure 5.11** Proton NMR of partially fluorinated copolymer series

The copolymers showed good thermooxidative stabilities (Figure 5.12). The five percent weight loss temperature for acid form of PAEB35, 6F25CN35 and 6F50CN35 was 350°C. Thermooxidative stability was increased with increasing fluorination and the five percent weight loss temperature reached up to 400 °C for 6F75CN35 and 6F75CN35, which is more than enough for 120 °C fuel cell operation.

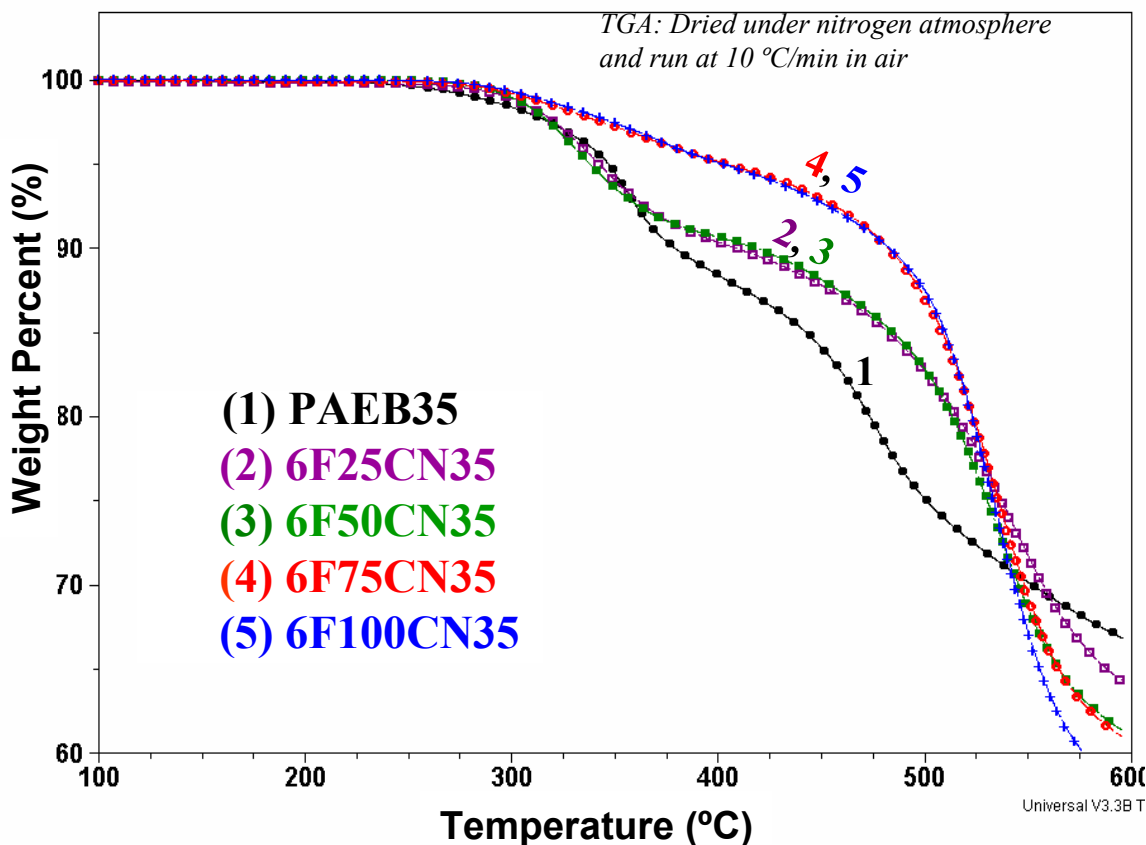


**Figure 5.12** Influence of partial fluorination on thermooxidative stability of acid form of PAEB copolymers (10 °C/min in air)

#### **5.4.1 Membrane Properties of a Series of Partially Fluorinated Copolymers**

A series of partially fluorinated copolymers at the same level of disulfonation resulted with tunable membrane characteristics as discussed below.

##### **5.4.1.1 Water Uptake of the Copolymer Membranes**

The series of partially fluorinated copolymers at the same level of disulfonation produced a gradual decrease in water uptake. Water uptake of 35 mol percent disulfonated copolymers were decreased from 40 to 24 weight percent with increasing fluorination (Figure 5.13). Water management including all water activities of the membrane electrode assemblies (electro-osmotic drag of water, diffusion of water, produced water from cell current and water cross-over methanol oxidation) is related with the adsorbed water and types of adsorbed water ( free water, loosely and tightly bound water)<sup>23</sup>. The free water in the perfluorinated ionomer membranes was higher compared to hydrocarbon type ionomer membranes. For example, the higher free water content enhances the electro-osmotic drag causing cathodic flooding. Although higher water content increases the protonic activity, unfortunately it also activates the methanol cross-over which results with loss of fuel, reduced fuel efficiency, reduced cathode voltage and excess thermal load on the cell.

---

<sup>23</sup> Kim, Y.S.; Dong, L.; Hickner, M.A.; Glass, T.E.; Webb, V.; McGrath, J.E., *Macromolecules* 2003, 36,6281

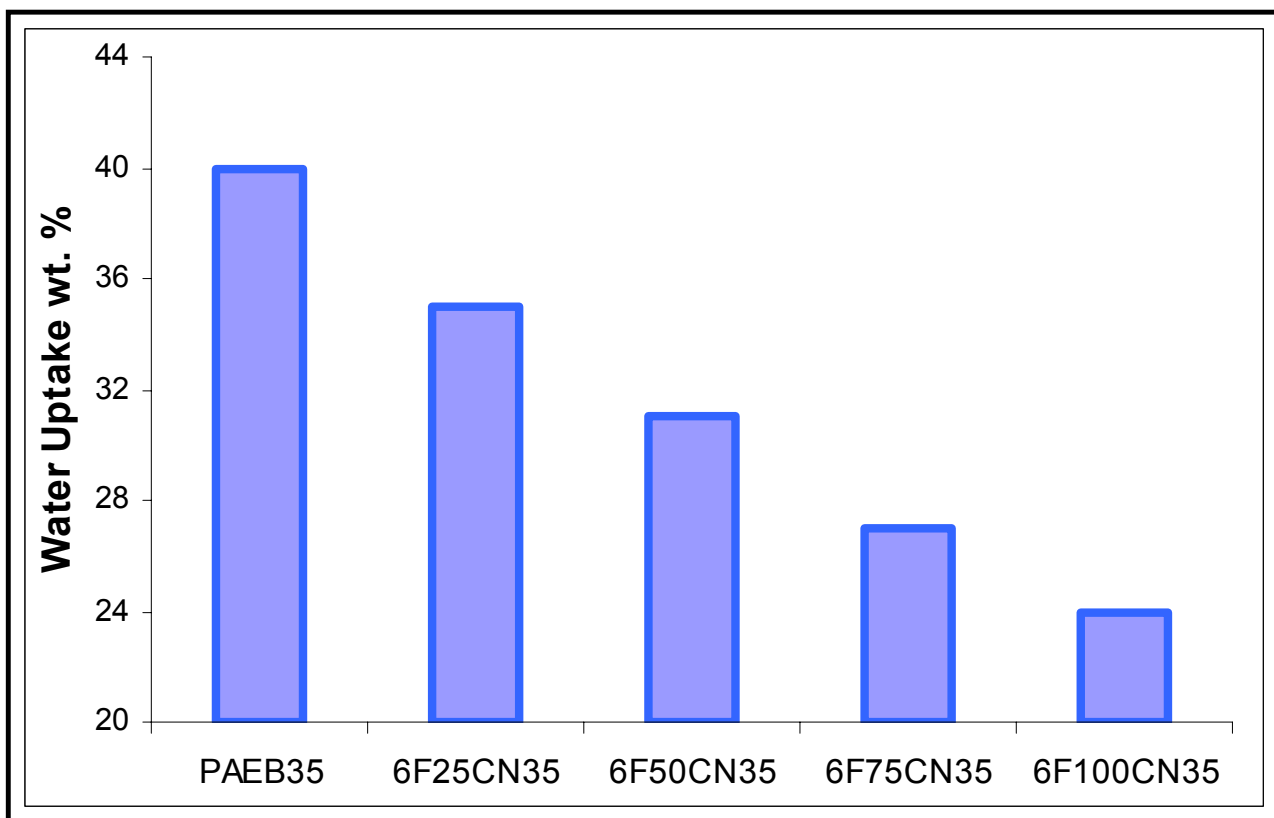


**Figure 5.13** Water uptake (weight percent) for a series of partially fluorinated disulfonated poly(arylene ether benzonitrile) statistical copolymers; degree of partial fluorination was achieved as mol percent from 25 to 100

#### 5.4.1.2 Ion Exchange Capacities of the Copolymer Membranes

Varying the ion content of the membrane can control both its water uptake and conductivity. While it is desirable to maximize the conductivity of the membrane by increasing its ion content (decreasing equivalent weight), other physical properties must be considered. Too many ionic groups will cause the membrane to swell excessively with water, which compromises mechanical integrity and durability. Hence controlling the water uptake at the same level of disulfonation brings several advantages on the basis of the water management. However, the ion exchange capacity was tended to decrease with increasing mol percent fluorination due to the high molecular weight of 4,4'-hexafluoroisopropylidene diphenol (6F) comonomer compare to biphenol. As the 6F was incorporated into polymer backbone, the ion exchange capacity was reduced from 1.87 to 1.33 mequiv/g (Figure 5.14). One can notice that the ion exchange capacity was decreased about less than 30 percent. However the water uptake was controlled up to 40 percent.

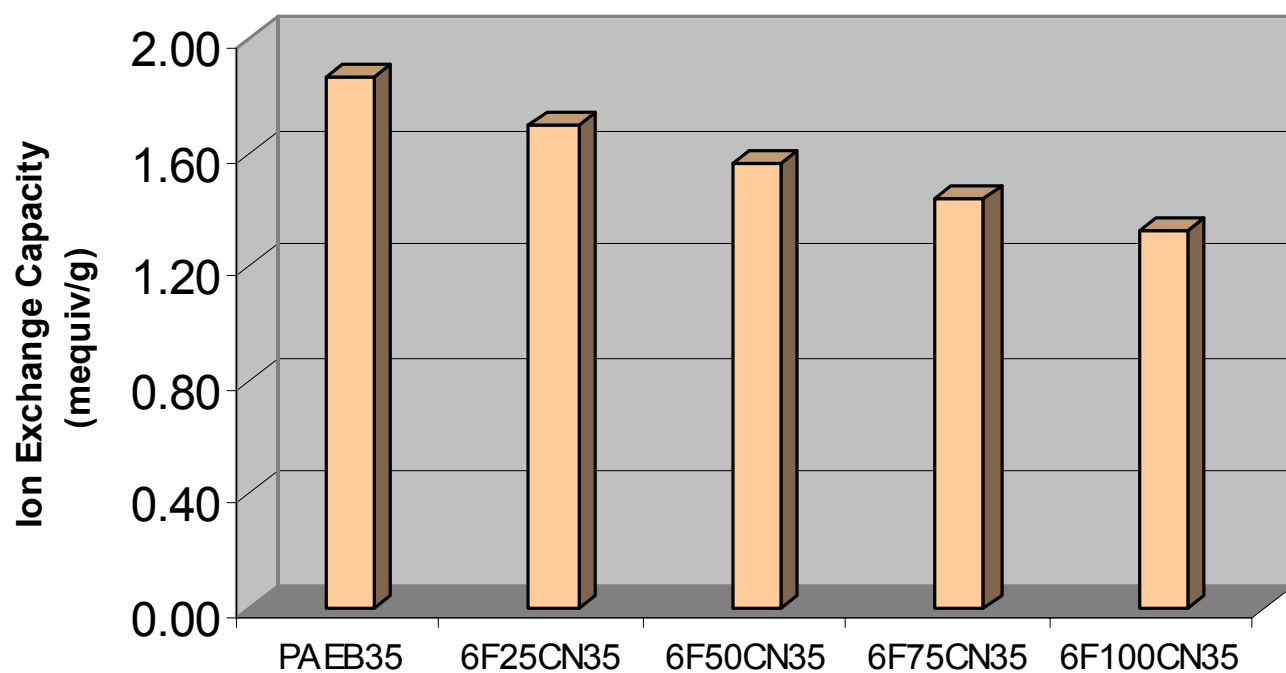


**Figure 5.14** The ion exchange capacity of a series of partially fluorinated disulfonated poly(arylene ether benzonitrile) statistical copolymers; degree of partial fluorination was achieved as a mole percent from 25 to 100

### 5.4.1.3 Proton Conductivity of the Copolymer Membranes

The 30 percent decrease in ion exchange capacity resulted in a decrease in the proton conductivity from 90 mS/cm to 70 mS/cm (Figure 5.15). The overall change in proton conductivity was about 22 percent. This decrease was not a draw back for the series. Since, proton conductivities along the series of copolymers were high enough for fuel cell applications.

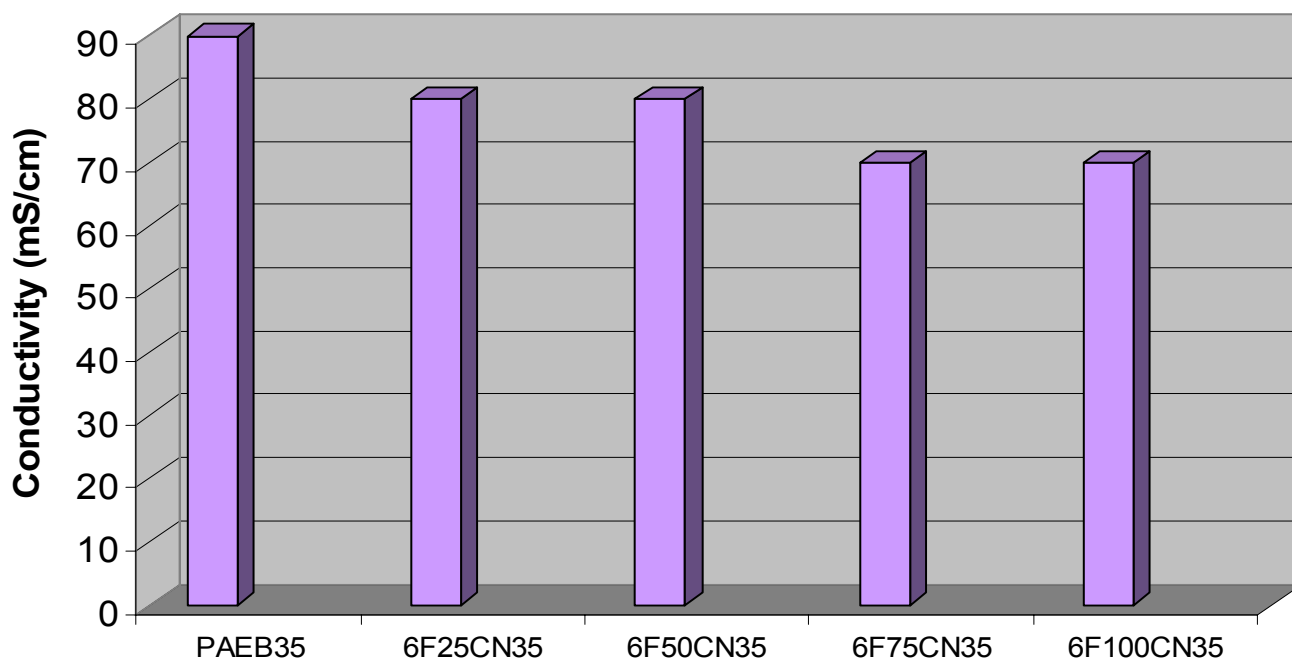


**Figure 5.15** The proton conductivities of a series of partially fluorinated disulfonated poly(arylene ether benzonitrile) statistical copolymers; degree of partial fluorination was achieved as mol percent from 25 to 100

As a result, the water uptake of the partially fluorinated copolymer series was controlled without losing much of the proton conductivities. Table 5.2 summarizes the overall effect, including how much (as percent) these membrane properties can be controlled. One can notice that for each 1 percent change in water uptake, 0.7 percent change in IEC and only 0.55 percent change in proton conductivity was observed.

Table 5.2 The basic membrane characteristics were demonstrated as tunable membrane parameters

Property	Water Uptake	Ion Exchange Capacity (IEC)	Proton Conductivity
Percent change	40	29	22
Percent change per water uptake	1.0	0.72	0.55

#### 5.4.1.4 Lambda Number

The lambda value ( $\lambda$ ) indicates the number of water molecules absorbed per sulfonic acid groups and can be expressed as;

$$\lambda_w = \frac{(mass_{wet} - mass_{dry}) / MW_{H_2O}}{IEC \times mass_{dry}} = \frac{Water\ Uptake(w)}{IEC \times MW_{H_2O}} \quad \text{Equation 5.11}$$

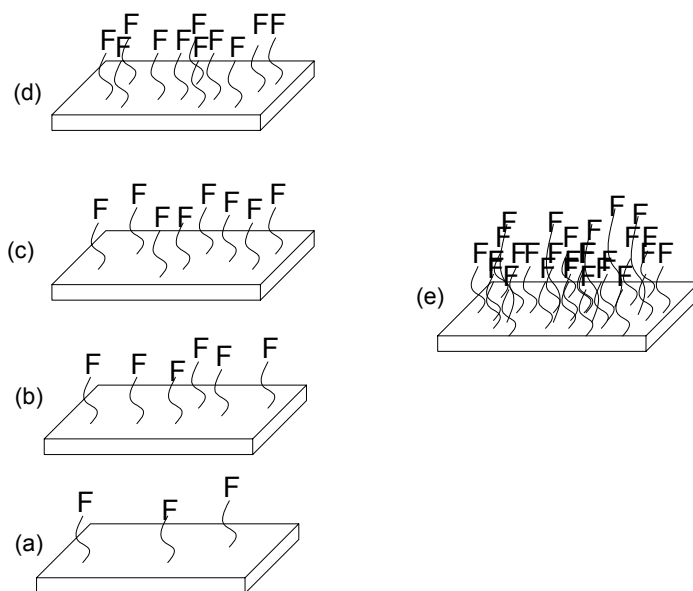
where,  $MW_{H_2O}$  is the molecular weight of water (18.01 g/mol), and IEC is the ion exchange capacity of the dry copolymer in equivalents per gram. The lambda number like proton conductivity scales with the ion exchange capacity. However the decreasing water uptake for the series with increasing fluorination stabilized the lambda value close to be close Nafion™, which was also good for water management (Table 5.3).

Table 5.3 Lambda numbers for the non fluorinated partially fluorinated copolymer series and Nafion™ ionomer

Copolymer	Weight based $\lambda$ number (H <sub>2</sub> O/SO <sub>3</sub> )
PAEB35	11.9
6F25CN35	11.4
6F50CN35	11.0
6F75CN35	10.4
6FCN35	10.0
Nafion™	11.5

#### 5.4.1.5 Surface Characteristics and XPS Data

XPS data showed that the surface fluorine of the solution-cast membranes increased with increasing mol percent fluorination. The fluorine atomic ratio was used to demonstrate the surface fluorination. The air side was found to have significant fluorine enrichment compare to glass side, which had higher free surface free energy. The surface fluorine as an atomic percent was either higher or close to its theoretically calculated bulk concentration. Hence, it was concluded that most of the fluorine was on the surface. This was a result of self assembly of the fluorine atoms on the surface, which was also controlled by the degree of fluorination (Figure 5.16 and Table 5.4). One can notice that the Nafion™ surface had much higher fluorine enrichment, providing better adhesion and lower HFR with the catalyst layer prepared Nafion™ dispersion.



**Figure 5.16** Surface fluorine enrichment of the series of partially fluorinated copolymers and Nafion™ 112. The number of fluorine was based on XPS data (air sides). a.

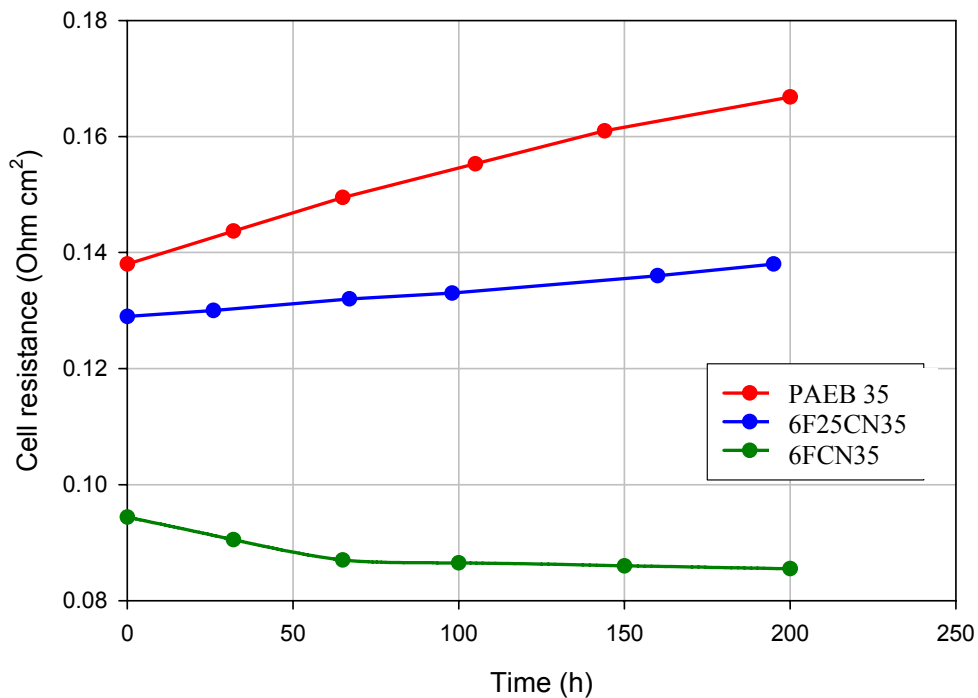
6F25CN35, b. 6F50CN35, c. 6F75CN35, d. 6FCN35, e. Nafion™ 112

Table 5.4 Surface fluorine atomic percentages of the partially fluorinated acid form copolymer series compared with Nafion™

Copolymer	Surface	Fluorine Atomic Percentages	Bulk Fluorine
6F25CN35	Air	5.1	4
	Glass	3.3	
6F50CN35	Air	11	9
	Glass	6.3	
6F75CN35	Air	15	13
	Glass	9.4	
6FCN35	Air	22	18
	Glass	14	
Nafion™ 112	NA	57	60

### 5.4.2 MEA Characteristics

It is proposed that the surface fluorine has two important roles which directly affect the initial and long term performance of the fuel cell. Surface fluorine lowers the contact resistance at catalyst layer membrane interface. Since the catalyst layer made of Nafion™ bonded electrode which is high in fluorine and provide better adhesion when both surface of the catalyst layer and membrane has similar chemical nature. The so-called cell equation also contains an ohmic polarization term which scales with the membrane specific resistivity and interfacial contact resistance at catalyst layer–membrane interface. Hence any results which reduces this resistance would increase the cell performances. The cell resistances were higher and unstabilized for non fluorinated copolymers. However it was lowered and stabilized with partial fluorination (Figure 5.17).



**Figure 5.17** Cell resistance was lowered and stabilized with partial fluorination

### 5.4.3 Fuel Cell Tests

The partially fluorinated copolymers were evaluated for both initial and long term direct methanol fuel cell performance tests principally at LANL.

#### 5.4.3.1 Initial Direct Methanol Fuel Cell Tests

The initial direct methanol fuel cell performances of partially fluorinated copolymers and comparison with their non fluorinated analogues and also with Nafion™ 112 are presented in Figure 5.18. One can notice that the initial cell performances increased with increasing mol percent fluorination, possibly due to the interfacial effect. The half voltage current density was minimum of a 200 mA/cm<sup>2</sup> and reached to 250 mA/cm<sup>2</sup> for the copolymer series of poly(arylene ether benzonitrile).

Regardless of the level of fluorination, all the copolymer series showed better cell performance than Nafion™ 112. The stiff aromatic backbone produces a more closed structure preventing fuel/oxidant permeability, whereas Nafion™ with its fluorocarbon backbone results its higher methanol permeability. Related permeability data for copolymers having similar thickness were compared with Nafion™ 112 (Figure 5.19).

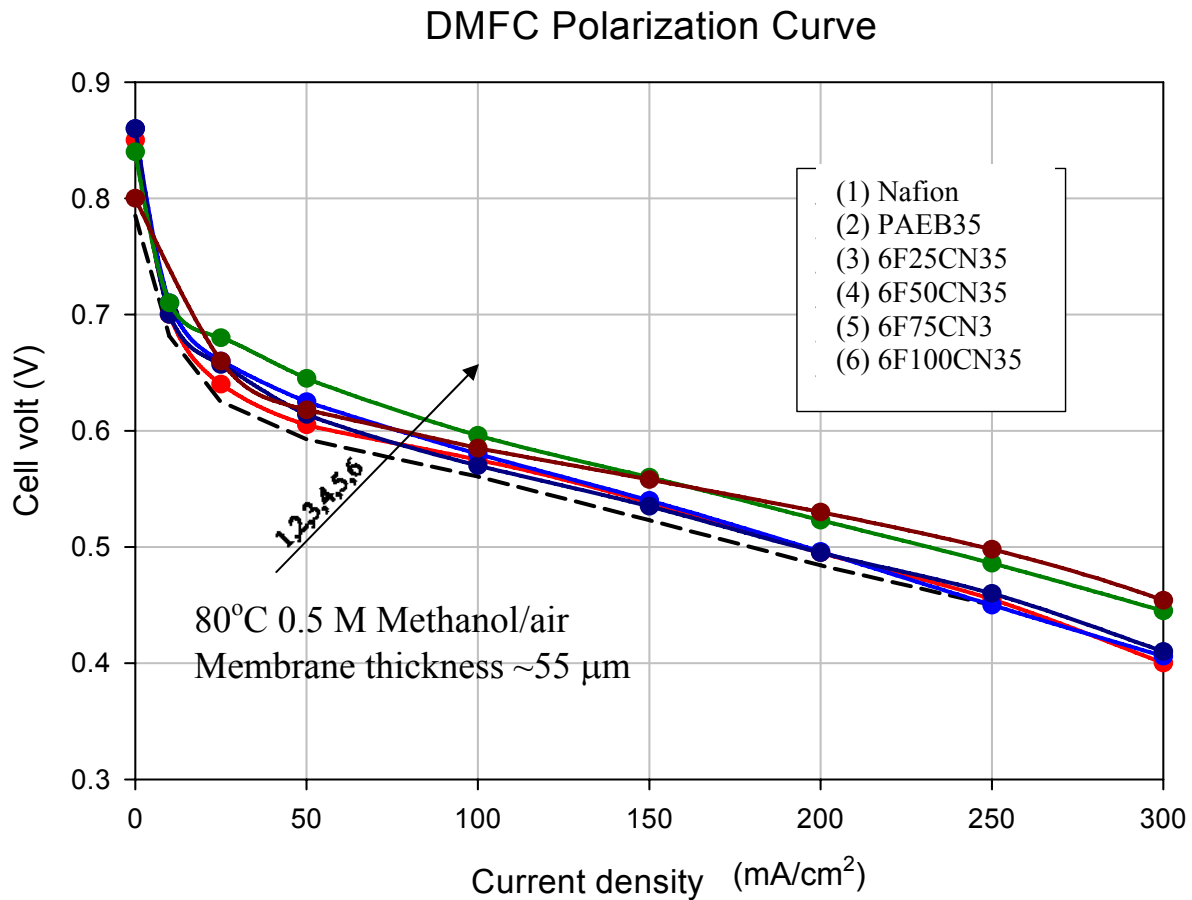


**Figure 5.18** Initial cell performances were improved with partial fluorination

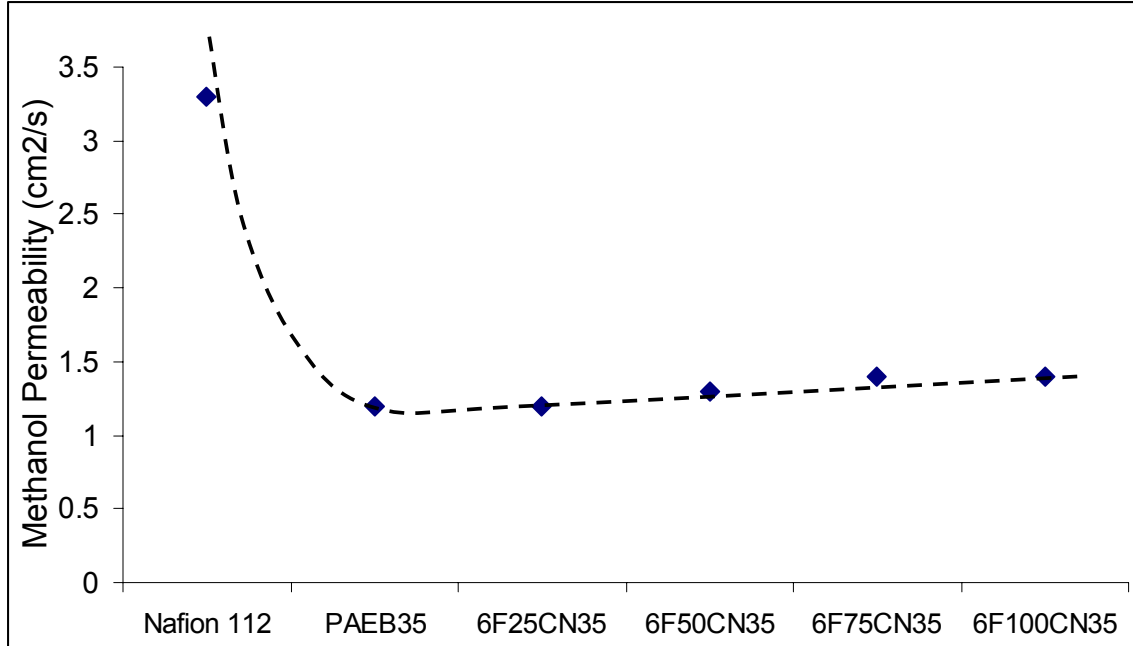


**Figure 5.19** Methanol permeabilities of stiff hydrocarbon type copolymer membrane series including 35 mol percent disulfonated poly(arylene ether benzonitrile) copolymer membrane and 35 mol percent disulfonated partially fluorinated (from 25 to 100 mol percent) poly(arylene ether benzonitrile) copolymer membrane, and perfluorinated ionomer membrane (Nafion™ 112) ; Nafion™ 112 showed much higher methanol permeability compare to any of the poly(arylene ether benzonitrile) copolymers

Figure 5.20 provides some important issues to obtain better fuel cell performance. Hence one can adjust these features to improve performance characteristics of the fuel cell. In addition to these factors, durability issues which include delamination of the catalyst layer, mechanical deformation of the membrane, etc. should also be considered.

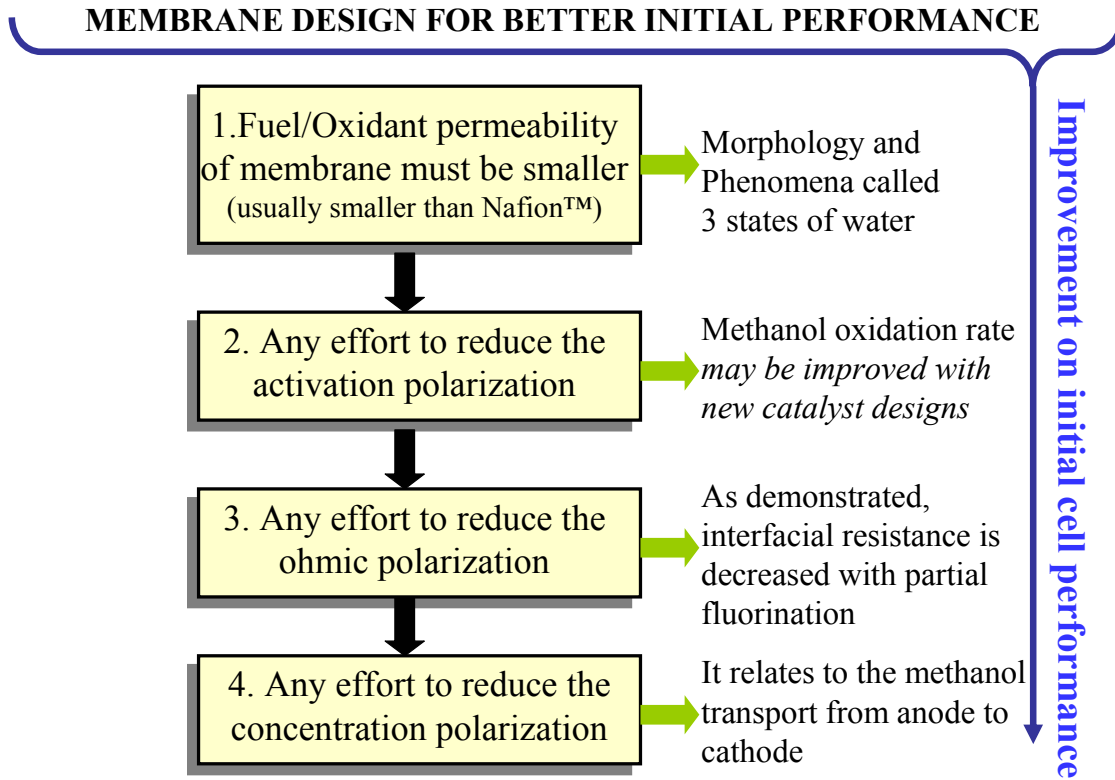


**Figure 5.20** Several important terms which directly affect the initial direct methanol fuel cell performances

Among these parameters first one is very crucial. The fully aromatic copolymer membranes show distinct differences to perfluorinated Nafion™ ionomer membranes. The well-known hydrophobic/hydrophilic micro-phase separation of Nafion™ ionomers is due to the its flexible more hydrophobic fluorinated backbone and more acidic side chains compare to the aromatic copolymer membranes. However, this distinct morphology effect likely relates to different states of the water in the copolymer

structure. (There were three different types of water in ionomer types of the polymerstructure; 1.Non-freezing water: Water that is strongly bound to the polymer chain and has a role in effective glass transition reduction (plasticization), 2.Freezable loosely bound water: Water that is weakly bound to the polymer chain or interacts weakly with nonfreezing water and displays relatively broad melting endotherms, 3.Free water: Water that is not intimately bound to the polymer chain and behaves like bulk water showing sharp melting point at 0 °C)<sup>23</sup>. The amount free water in Nafion™ membrane was higher than that in the aromatic hydrocarbon membrane. It was then concluded that a relatively large fraction of water in aromatic hydrocarbon membranes exists in a bound state, which can hinder transport. The lower permeability and electro-osmotic drag of these aromatic hydrocarbon copolymer membranes were also related this higher content of quantitative amount of bound water. The other parameters can be improved as suggested in Figure 5.19.

### 5.4.3.2 Long Term Direct Methanol Fuel Cell Tests

Partial fluorination also improved the longer term performances (200 h)\* as well as initial DMFC performances (Figure 5.22a and Figure 5.22b). This effect was mainly attributed to the decrease in water uptake with increasing fluorination. It has been proposed that the water uptake of a membrane was the critical factor for its long term performance. Interfacial delamination between electrode layer and membrane occurred when their water uptake values were not close to each other. Hence, the water uptake depression with increasing fluorine content decreased the dimensional mismatch between the electrodes and the membrane (Figure 5. 21).

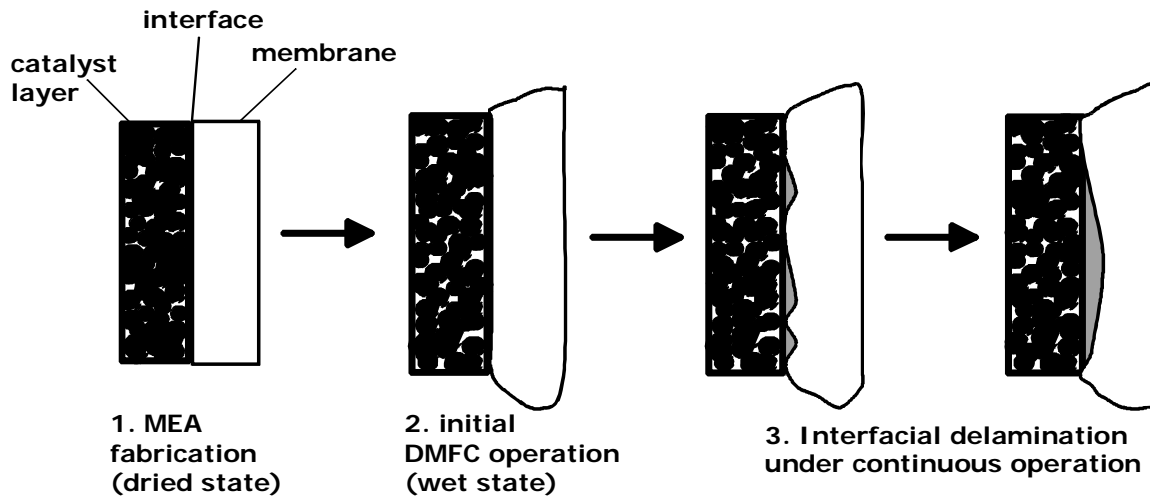


**Figure 5.21** Proposed interfacial delamination mechanism under continuous operation:

Water Uptake of membrane and catalyst layer should be similar to reduce the dimensional mismatch between the membrane and catalyst layer

\* Dr. Y.S. Kim has now shown membrane performance of > 3000 hour at 80 °C.

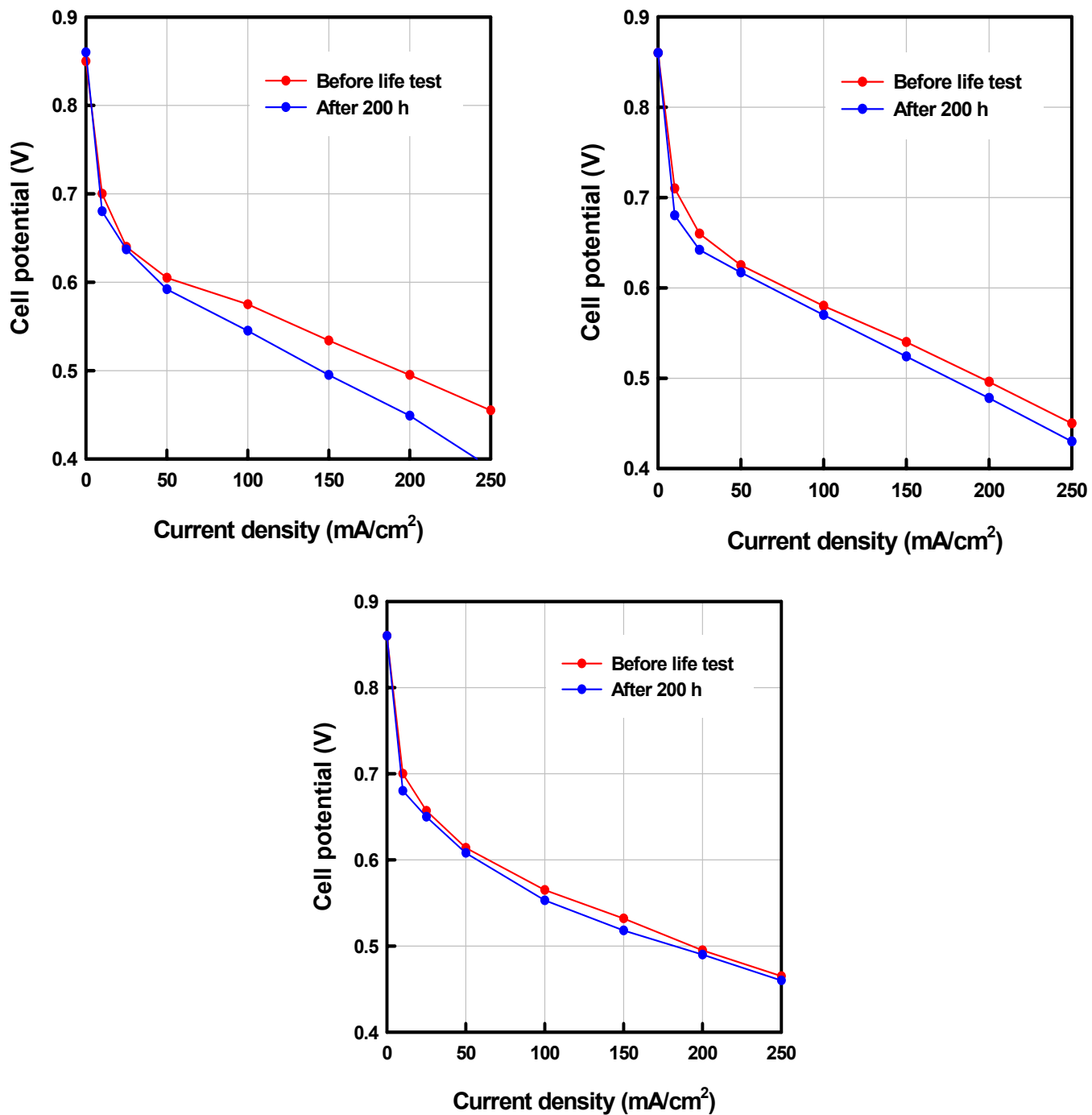


**Figure 5.22 a.** Initial and 200 h DMFC performances of copolymer membrane series (PAEB 35, 6F25CN35, 6F50CN35); Partial fluorination improved the long term performances

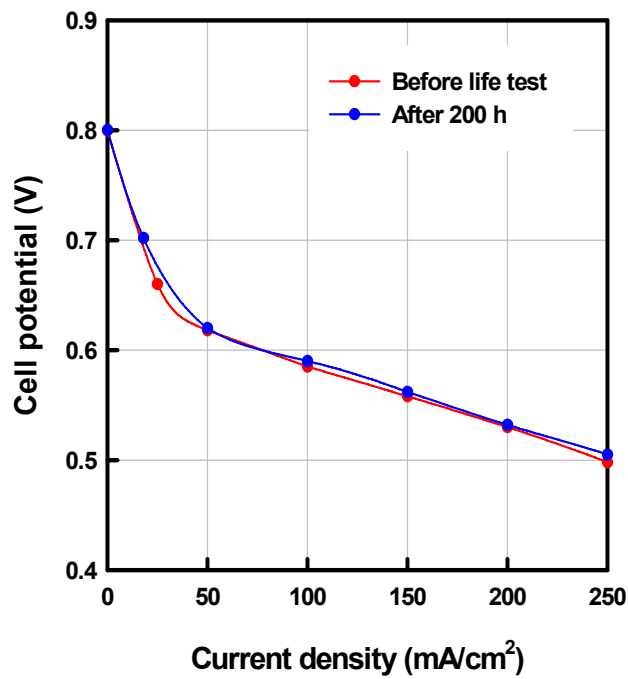
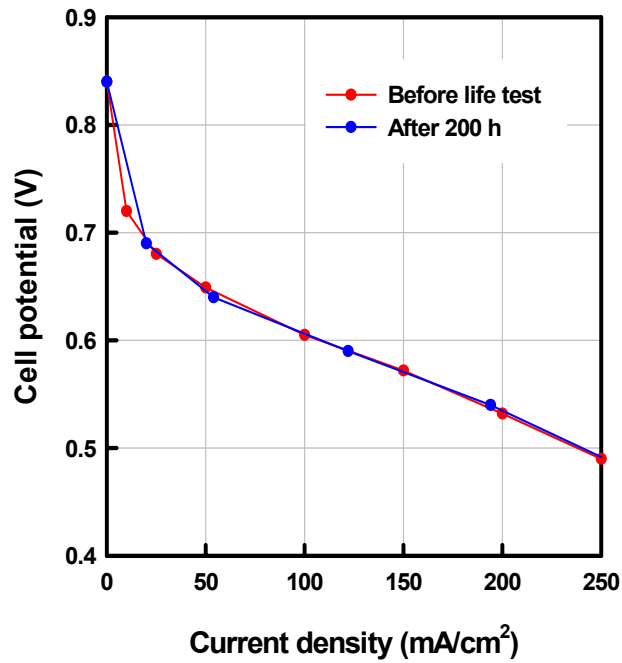


**Figure 5.22 b.** Initial and 200 h DMFC performances of copolymer membrane series (6F75CN35, 6FCN35): Partial fluorination improved the long term performances

Beside the durability issues, the most common parameters for better initial DMFC performance should also be considered for long term DMFC performances. Another follow-up was depicted to obtain better long term DMFC performances (Figure 5.23).

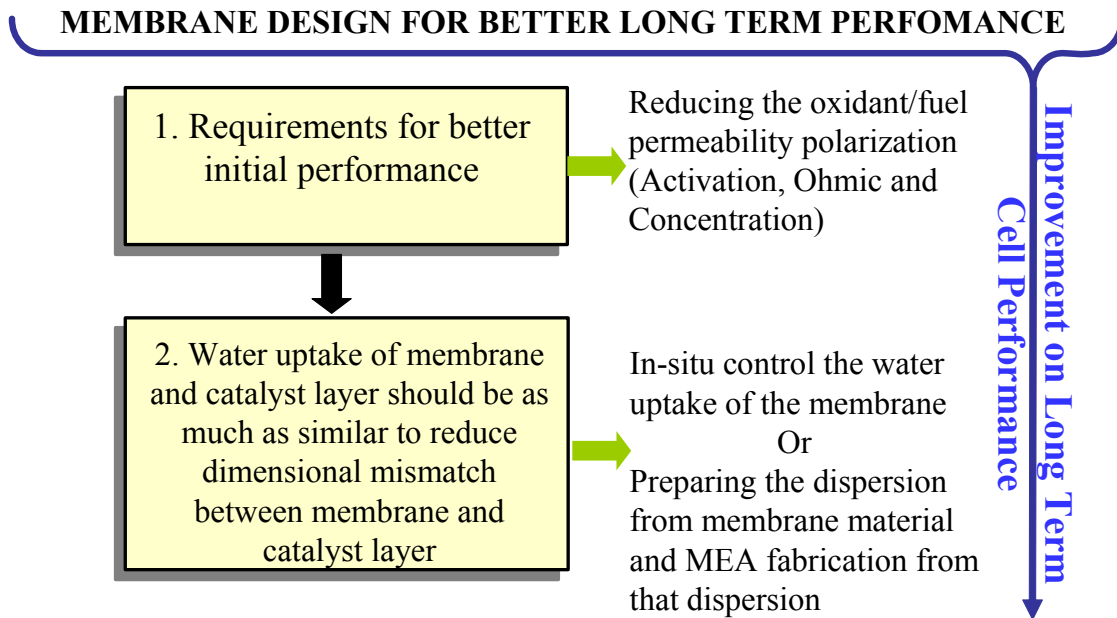


**Figure 5.23** The important terms which directly affect the long term direct methanol fuel cell performances

#### 5.4.4 Volume-based Proton Exchange Membrane Characteristics

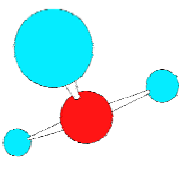
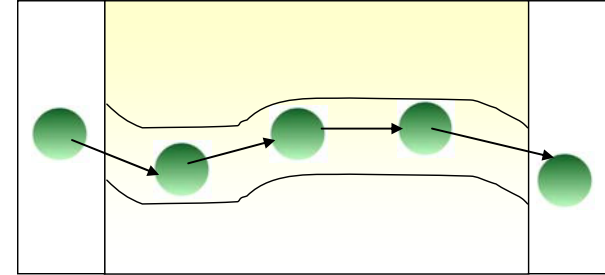
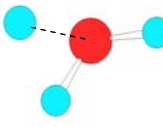
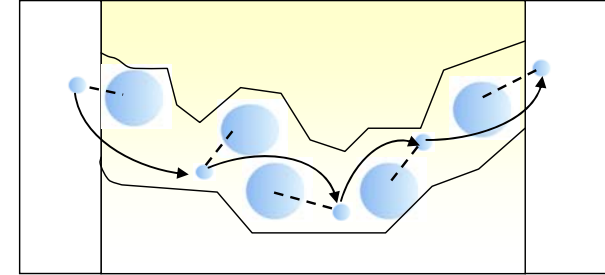
The factors influencing structure-property relationships have been limited to a very narrow range of variables and these properties have not been extended to the interpretation of observed fuel cell performance. Hence, the volume-based membrane parameters was developed which might better reflect the structure-property relationships than weight based parameters. For example, there are two major possibly proton conductive mechanisms, namely Vehicle<sup>24</sup> and Grotthuss<sup>25</sup>. One can notice that both mechanisms actually work based on the volume increment (Figure 5.24). Hence proton conductivity is likely a function of tunneling of either protons or hydronium ions.

Volume-based membrane characteristics were obtained by measuring the density of the membranes. Copolymer density was measured from a known membrane dimension and weight after drying at 75°C for 2 h.

---

<sup>24</sup> Kreuer, K.D.; Weppner, W.; Rabenau, A., *Angew. Chem. Int. Ed. Engl.* 1982 21, 208

<sup>25</sup> van Grotthuss, C.J.D., *Ann. Chim.*, 58, 54, 1806

Conductivity Mechanisms	Chemical Structure	Equivalent Structure	Model
<p><b>1. Vehicle</b></p> <p>Vehicle and proton are together as hydronium ion</p>	 <p><math>H_3O^+</math> ion is formed</p>		 <p>Electrode      Membrane      Electrode</p>
<p><b>2. Grotthuss</b></p> <p>Vehicle is water and proton transport occurs via hydrogen bonding</p>	 <p>Proton is in the vehicle (water). Vehicle and proton is connected by hydrogen bonding</p>		 <p>Electrode      Membrane      Electrode</p>

**Figure 5.24** Volume based membrane parameters might better reflect the structure-property relationship than weight based parameters; for example, proton conductivity or methanol permeability is such parameter directed through the membrane then requires of volume increment

#### 5.4.4.1 Volume Based Water Uptake

The volume based water uptake was calculated according to equation 5.12.

$$\text{Water uptake (WU) (vol.\%)} = (W_{wet} - W_{dry}) / (W_{dry} / \delta) \times 100 \quad \text{Equation 5.12}$$

where  $W_{wet}$  and  $W_{dry}$  are the weights of the wet and dry membranes, respectively;  $\delta$  is the membrane density in the dry state.

As noted in Table 5.5, Nafion™ ionomer is much denser than the poly (arylene ether benzonitrile copolymers). This could be advantages for aromatic hydrocarbon copolymer membranes on the basis of process economics. The fuel cell stacks from aromatic hydrocarbon copolymer membranes would also be lighter than fuel cell stacks based on Nafion™ ionomer.

The decreasing trend in the water uptake with increasing mol percent partial fluorination did not change with volume-based conversion. However, the volume based water uptake for 6F75CN35 and 6FCN35 copolymer membranes were similar to Nafion™ ionomer.

Table 5.5 Volume based water uptakes of copolymer series (compared with Nafion™)

Copolymer	Density (g/cm <sup>3</sup> )	Water uptake (wt%)	Water uptake (vol%)
PAEB35	1.33	40	67
6F25CN35	1.34	35	60
6F50CN35	1.36	31	52
6F75CN35	1.40	27	40
6FCN35	1.41	24	34
Nafion™112	2.01	19	38

#### 5.4.4.2 Volume Based Ion Exchange Capacity

A volume based IEC was obtained by multiplying the membrane density by  $IEC_w$  given in below;

$$IEC_v = IEC_w \times \delta \quad \text{Equation 5.13}$$

Unlike the weight based ion exchange capacity (IEC values Nafion™ were up to 2 times higher), the volume based ion exchange capacity of the Nafion™ was comparable with the partially fluorinated copolymer series (especially for the 6F75CN35 and 6FCN35). One can conclude that the volume based parameters of Nafion™ were closer to our copolymer series than what we observed with weight based parameters. This also proves the importance of the lower methanol permeability for expecting higher fuel cell performance.

Table 5.6 Volume based ion exchange capacities of the copolymer series (compared with Nafion™)

Copolymer	Density (g/cm <sup>3</sup> )	IEC <sub>w</sub> (meq/g)	IEC <sub>v</sub> (meq/cm <sup>3</sup> )
PAEB35	1.33	1.87	2.49
6F25CN35	1.34	1.70	2.29
6F50CN35	1.36	1.56	2.12
6F75CN35	1.40	1.44	1.98
6FCN35	1.40	1.33	1.86
Nafion™	2.01	0.92	1.93

#### 5.4.4.3 Selectivity and Relative Selectivity of the Membrane Electrode Assembly

Selectivity or relative selectivity (selectivity compare to Nafion™) of these membrane electrode assemblies can be calculated by following equation;

$$\alpha = \frac{l}{HFR \times \zeta_{\text{lim},m}} \quad \text{Equation 5.14}$$

where  $l$  is the thickness of the membrane, HFR is high frequency resistance,  $\zeta_{\text{lim},m}$  is electro-osmotic drag corrected methanol cross-over.

and relative selectivity can be expressed as;

$$\text{relative selectivity} = \frac{\alpha_{MEA}}{\alpha_{Nafion}} \quad \text{Equation 5.15}$$

where  $\alpha_{MEA}$  is selectivity of any MEA,  $\alpha_{Nafion}$  is selectivity of Nafion™

The following data (Table 5.6) was used to calculate both selectivity and relative selectivities of MEAs based on our copolymer series and Nafion™ ionomer and the results are presented in Table 5.7.

Table 5.7 Several MEA properties of copolymer series which were compared with Nafion™

Membrane Electrode Assembly	Thickness (micrometer)	High Frequency Resistance (HFR)	Methanol Cross-over Current
PAEB35	55	0.15	65
6F25CN35	55	0.13	63
6F50CN35	55	0.12	71
6F75CN35	55	0.11	89
6FCN35	51	0.1	77
Nafion™	51	0.07	190

Neither selectivities nor the relative selectivities of these membrane electrode assemblies did not resembled the observed fuel cell performances. Since the MEA conductivities were decreased with increasing mol percent fluorination and the methanol permeabilities were almost constant. However, our copolymer series showed better selectivity than Nafion™.

In order to draw a reasonable selectivity, the effect of water uptake (either volume or weight based) should be considered. Since the water uptake of the membranes were the important parameters observed for obtaining higher performance. Hence, the selectivity and relative selectivity was normalized with their water uptake using the following equation.

$$\text{Water uptake corrected (relative) selectivity} = \frac{(\text{relative}) \text{ selectivity}}{\text{Water uptake}} \quad \text{Equation 5.16}$$

Table 5.8 Selectivity, relative selectivity and water uptake corrected selectivity of MEA s based on our copolymer series and Nafion™ ionomer

Membrane Electrode Assembly	Selectivity	Relative selectivity	Water uptake (volume %)	Water uptake corrected selectivity	Water uptake corrected relative selectivity
PAEB35	0.056	1.5	53	0.0011	1.1
6F25CN35	0.067	1.8	47	0.0014	1.4
6F50CN35	0.065	1.7	42	0.0015	1.5
6F75CN35	0.056	1.5	38	0.0015	1.5
6FCN35	0.066	1.7	34	0.0019	1.9
Nafion™	0.038	1.0	38	0.0010	1.0

The relative selectivity of the Nafion™ is taken as unity. One can conclude that our copolymer showed higher selectivity than Nafion™ membrane. However, as stated previously relative selectivity data fluctuates and does not reflect the DMFC performance data. Hence a new interpretation where we consider the water uptake to be reciprocal function of the relative selectivity was introduced to better correlate the relative selectivity with the performance data. The relative selectivity (from Equation 5.15) and water uptake corrected relative selectivity (from Equation 5.16) were compared in Figure 5.25.

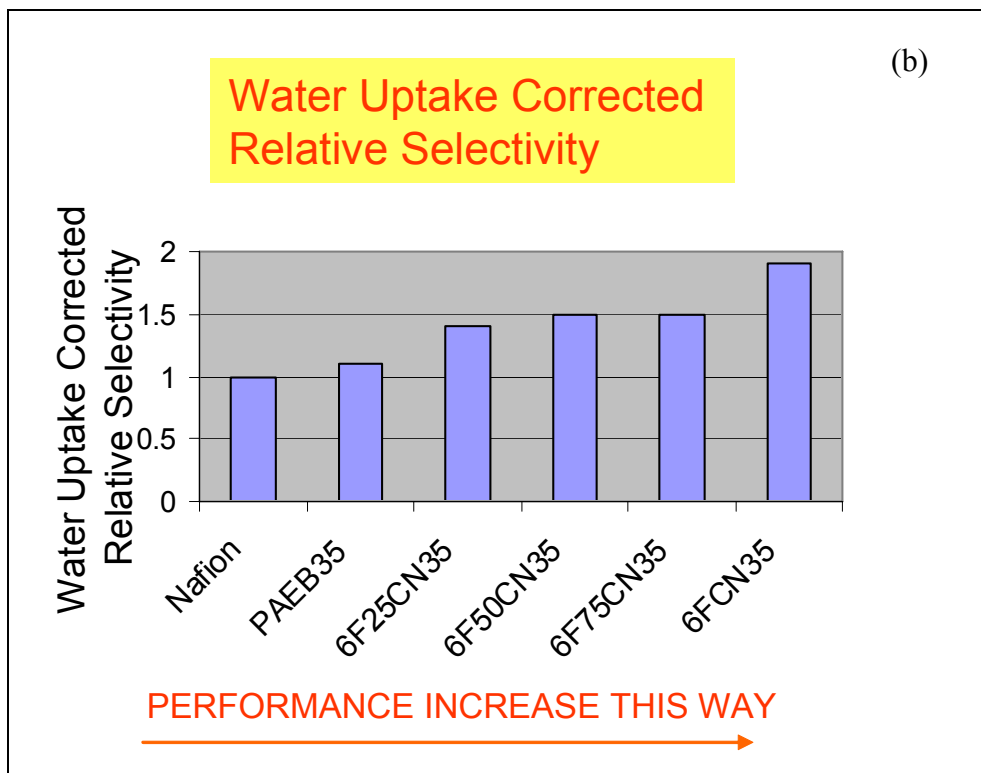
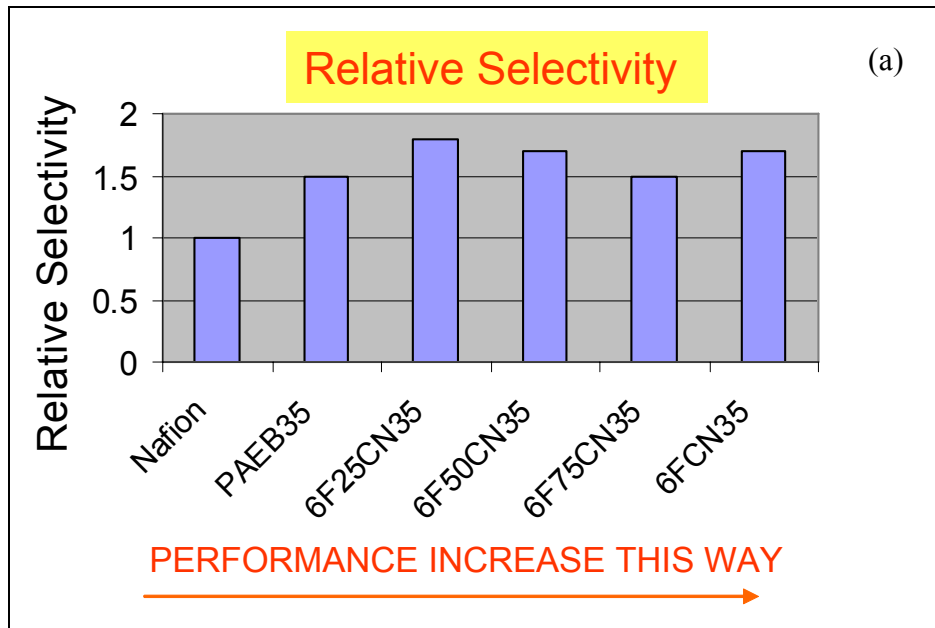


**Figure 5.25** a. Relative selectivity of the membranes, b. Water uptake corrected relative selectivity which better correlates structure-property-performance relations

## **5.5 Conclusions**

The benzonitrile-containing, thermally stable, ductile, high molecular weight partially fluorinated disulfonated copolymers were successfully synthesized. These copolymers showed better initial and long term performances than Nafion™ 112 due to their lower methanol permeabilities. The basic PEM properties such as water uptake, proton conductivity, methanol permeability, etc. were actually shown to allow for tunable properties. The partial fluorination has two important effects on a proton exchange membrane and/or membrane electrode assembly; it reduces the cell resistance and also lowers the water uptake of membrane. The former is important for initial performance, while the latter is crucial for long term performance. The delamination due to the large water uptake differences between catalyst layer (electrode) and the membrane in the membrane electrode assembly was proposed. Volume-based parameters of our copolymer series were similar to that of Nafion™ ionomer. Structure-property-performance relation was established when the water uptake corrected relative selectivity (or selectivity) was introduced.

## **5.6 Acknowledgement**

The University authors would like to thank the National Science Foundation “Partnership for Innovation” Program (HER-0090556), the Department of Energy (DE-FC36-01G01086) and the Army Research Laboratory for support of this research effort.

The LANL authors thank to US Department of Energy through Hydrogen, Fuel Cells and Infrastructure Technology Program.

---

## CHAPTER 6

### Structure-Property-Performance Relationships of Sulfonated Poly(Arylene Ether Sulfone)s as a Polymer Electrolyte for Fuel Cell Applications

---

Taken from:

Kim, Yu S.; Einsla, B.; Sankir, M.; Harrison, W.; Pivovar, B. S., **Submitted to Polymer 2006.**

## 6.1 Abstract

This article focuses on structure-property-performance relationships of directly copolymerized sulfonated polysulfone polymer electrolyte membranes. The chemical structure of the biphenol-based disulfonated polysulfone random copolymers was systematically alternated by introducing fluorine moiety or other polar functional groups such as benzonitrile or phenyl phosphine oxide in the copolymer backbone. AC impedance measurements of the polymer electrolyte membranes indicated that fluorine incorporation increased proton conductivity, while polar functional group incorporation decreased conductivity. Likewise, other properties such as water uptake and ion exchange capacity are impacted by the incorporation of fluorine moiety or polar groups. These properties are critically tied with H<sub>2</sub>/air and direct methanol fuel cell performance. We have rationalized fuel cell performance of these selected copolymers in light of structure-property relationships, which gives useful insight for the development and application of next generation polymer electrolytes.

## 6.2 Introduction

During the last two decades, extensive efforts have been made to develop alternative hydrocarbon-based polymer electrolyte membranes in order to overcome the drawbacks of the current widely used perfluorosulfonic acid Nafion™<sup>1,2,3</sup>. However, structure-property-performance relationships for hydrocarbon-based polymer electrolyte membranes (PEMs) have remained relatively unstudied. The lack of understanding in this area stems not only from insufficient data for alternative polymer electrolytes, but also due to difficulties in interpreting cross-influencing properties, such as ion exchange capacity (IEC), water uptake, morphology, acidity of sulfonic acid group, etc. Nevertheless, a few attempts have been made from limited experimental variations. Most established structure-property relationships of hydrocarbon-based PEMs are based on the effects of IEC (or relatedly, degree of sulfonation or equivalent weight). Several literature references have reported that the proton conductivity, methanol permeability and water swelling within a family of copolymers were found to be proportional to the IEC and often observed an abrupt increase at some specific IEC where a percolation limit occurred<sup>4,5,6</sup>. Cross-linking has also been investigated as a factor that influences structure-property relationships. Kerres and his coworkers reported that (either covalent or ionic) crosslinked copolymers showed significantly reduced water swelling behavior without significant proton-conductivity loss<sup>7,8</sup>. Additional structural effects include

---

<sup>1</sup> O. Savadogo, *J. New Mater. Electrochem. Sys* 1, 1998, 47

<sup>2</sup> J. Roziere, D. J. Jones, *Annu. Rev. Mater. Res.* 33, 2003, 503

<sup>3</sup> M. Hickner, H. Ghassemi, Y. S. Kim, B. Einsla, J. E. McGrath, *Chemical Review* 2004, 104, 4587-4612

<sup>4</sup> S. M. J. Zaidi, S. D. Mikhailenko, G. P. Robertson, M. D. Guiver, S. Kaliaguine, *J. Membr. Sci.* 2000, 173, 17

<sup>5</sup> Y. S. Kim, L. Dong, M. A. Hickner, B. S. Pivovar, J. E. McGrath, *Polymer* 2003, 44, 5729

<sup>6</sup> Y. A. Elabd, E. Napadensky, J. M. Sloan, D. M. Crawford, C. W. Walker, *J. Membr. Sci.* 2003, 217, 227

<sup>7</sup> J. Kerres, A. Ullrich, F. Meier, T. Haring, *Solid State Ionics* 1999, 125, 243

bulkiness of polymer components and backbone stiffness. The independent research groups of Litt and Watanabe reported that polyimide membranes having bulky functional group (increased free volume) exhibited higher proton conductivity, particularly under low humidity conditions<sup>9,10</sup>. The work of Guiver<sup>11</sup> and our own<sup>12</sup> research group, on the other hand, showed that more rigid backbones restricted proton/methanol transport and water swelling. For example, rigid polyimide produced higher barrier properties than flexible polyimide or polysulfone membranes. These examples represent a few studies that investigate structure-property relationships in PEMs; however, the factors influencing structure-property relationships have been limited to a very narrow range of variables and these properties have not been extended to the interpretation of observed fuel cell performance.

In this paper we extend the study of structure-property relationships by examining, chemical and structural effects of different chemical structural variations on hydrocarbon based polymer electrolytes properties, and their impact on the observed fuel cell performance.

As mentioned earlier, acid content (IEC, equivalent weight or degree of (di)sulfonation) is the chemical effect that has been the most highly reported. We begin by presenting the effect of disulfonation level within the polymers studied and relating

---

<sup>8</sup> J. Kerres, A. Ullrich, T. Haring, M. Baldauf, U. Gebhardt, W. Preidel, *J. New Mater. Electrochem. Sys.* 2000, 3, 229

<sup>9</sup> M. H. Litt, Y. Zhang, R. F. Savinell, J. S. Wainright, *Polym. Prepr.* 1999, 40, 480

<sup>10</sup> K. Miyatake, H. Zhou, H. Uchida, M. Watanabe, *Chem. Comm.* 2003, 3, 368

<sup>11</sup> P. Xing, G. P. Robertson, M. D. Guiver, S. D. Mikhaileuko, S. Kaliaguine, *Macromolecules* 2004, 37, 7960

<sup>12</sup> M. Hickner, B. S. Pivovar, *Fuel Cells* 2005, 5, 213

observed behavior to that in the literature. We then move to the effects of fluorine incorporation in the copolymer backbone. The effect of fluorination is a subject that has been presented in comparative studies between perfluorosulfonic acid (ca. Nafion™) and hydrocarbon copolymers,<sup>13,14</sup> but not within similar polymer families at varying degrees of fluorination as presented here. The other structural variable investigated is polar group incorporation. Polar groups have been previously investigated due to their exceptional ability to disperse high conductive inorganic additives<sup>15,16</sup>. In this paper, we focus on the effect of polar group on observed properties without the incorporation of additives.

As a baseline material, we chose biphenol-based disulfonated polysulfones (BP). In order to introduce fluorine moiety, the biphenol monomer was replaced with hexafluoro (6F) bisphenol A. This partially substituted system can serve as a link between perfluorosulfonic acid (wholly-fluorinated) and wholly aromatic hydrocarbon copolymers (non-fluorinated). For polar group incorporation, the diphenylsulfone monomer was replaced with either benzonitrile or *tri*-phenyl phosphine oxide (PPO). Because these polymers are made from disulfonated monomers, disulfonation level can be modified independently within any given family. These substitution patterns have allowed us to systematically investigate the role of acid group, fluorine and polar group incorporation on structure-property-performance relationships.

---

<sup>13</sup> K. D. Kreuer, *J. Memb. Sci.* 2001 185, 29

<sup>14</sup> G. Alberti, M. Casciola, L. Massinelli, B. Bauer *J. Memb. Sci.* 2001, 185, 73

<sup>15</sup> S. Wang, H. Zhuang, M. Sankarapandian, H. K. Shobha, Q. Ji, A. R. Shultz, J. E. McGrath, *Polym. Prepr.* 2000, 41, 1350

<sup>16</sup> M. Hill, B. R. Einsla, Y. S. Kim, J. E. McGrath, Division of Fuel Chemistry 228<sup>th</sup> ACS National Meeting, Philadelphia, PA, 2004

Among fuel cell related properties, we primarily focus on water uptake, number of water molecules per sulfonic acid site, proton conductivity and methanol permeability drawing comparisons between polymers of similar IEC. Other important factors such as morphology and the state of water within the polymer are also discussed based on previously reported studies. Finally, these properties are related to PEM fuel cell performance and discussed with aspects of molecular design and application of future generation polymer electrolytes in mind.

### 6.3 Experimental

Figure 6.1 shows the chemical structure and sample code for the protonated form of disulfonated poly(arylene ether) copolymers used in this study. All copolymers used in this study were kindly supplied by the research group of Prof. James McGrath at Virginia Polytechnic and State University, where the copolymers were synthesized by nucleophilic substitution polycondensation of sulfonated aromatic dihalides, one of three aromatic dihalides and one of two structurally distinct bisphenols i.e. biphenol A and hexafluoro bisphenol A in *N*-methylpyrrolidionone (NMP)<sup>17,18,19,20,21,22</sup>. This direct copolymerization gave precise control over degree of disulfonation with random copolymerization due to ether-ether exchange reactions. Since the synthesized polysulfones were initially in the sodium sulfonate form, they were converted into acid form by the boiling of cast membranes in 0.5 M sulfuric acid for 1.5 h, followed by 1.5 h of excess acid extraction in boiling deionized water<sup>23</sup>. Intrinsic viscosity of these copolymers was in the range of 1.2-1.6 dL/g in NMP at 30 °C, and generally increased with IEC (or degree of disulfonation) and molecular weight. The relative molecular weight of these copolymers was in the range of 25,000-50,000 g/mol by GPC.

---

<sup>17</sup> H. K Shobha, G. R. Smalley, M. Sankarapandian, J. E. McGrath, *Polym. Pripr.* 2000, 41, 180

<sup>18</sup> F. Wang, M. Hickner, Q. Ji, W. Harrison, J. Mecham, T. A. Zawodzinski, J. E. McGrath, *Macromol. Symp.* 2000, 175, 387

<sup>19</sup> F. Wang, M. Hickner, Y. S. Kim, T. A. Zawodzinski, J. E. McGrath, *J. Memb. Sci.*, 197, 231 (2002)

<sup>20</sup> W.L. Harrison, F. Wang, J. Mecham, V. Bhanu, M. Hill, Y. S. Kim, J. E. McGrath, *J. Polym. Sci. Part A: Polym. Chem.* 2003, 41, 2264

<sup>21</sup> M. J. Sumner, W. L. Harrison, R. M. Weyers, Y. S. Kim, J. E. McGrath, J. S. Riffle, A. Brink, M. H. Brink, *J. Memb. Sci.* 2004, 239, 199

<sup>22</sup> W. Harrison, M. Hickner, Y. S. Kim, J. E. McGrath, *Fuel Cells*, 2005,5, 201

<sup>23</sup> Y. S. Kim, F. Wang, M. Hickner, S. MaCartney, Y. T. Hong, T. A. Zawodzinski, J. E. McGrath, *J. Polym. Sci. Part B: Polym. Phys.* 2003, 41, 2816

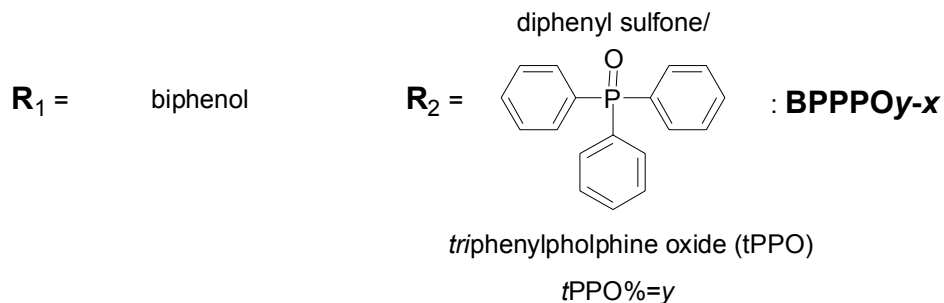
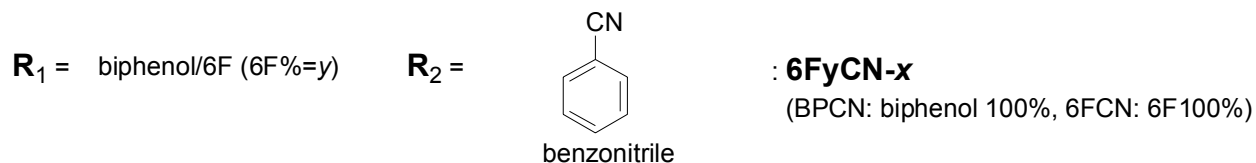
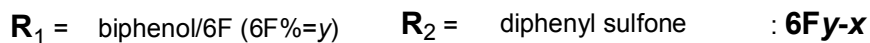
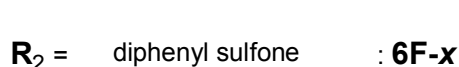
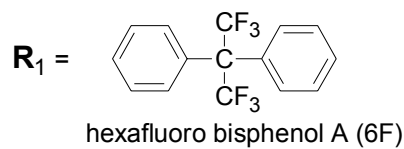
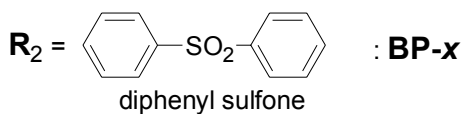
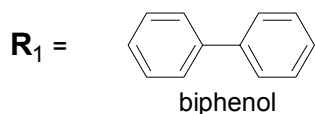
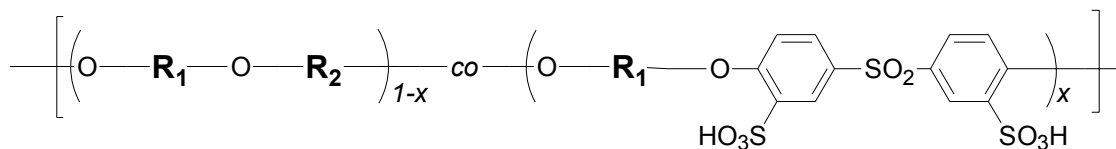


**Figure 6.1** Chemical structure of disulfonated poly(arylene ether sulfone) copolymers where the letter *x* in abbreviation refers to the sulfonation percentage of a disulfonated monomer

Water uptake was measured after drying the membrane in acid form at 100 °C under vacuum overnight. The dried membrane was immersed in water at 30 °C and periodically weighed on an analytical balance until a constant water uptake weight was obtained. The weight and volume based water uptake is reported as a percentage using the following equations:

$$\text{water absorption (\%)} = (W_{\text{wet}} - W_{\text{dry}}) / W_{\text{dry}} \times 100 \quad \text{Equation 6.1}$$

$$\text{Water uptake (WU) (vol.\%)} = (W_{\text{wet}} - W_{\text{dry}}) / (W_{\text{dry}} / \delta) \times 100 \quad \text{Equation 6.2}$$

where  $W_{\text{wet}}$  and  $W_{\text{dry}}$  are the weights of the wet and dry membranes, respectively;  $\delta$  is the membrane density in the dry state.

Due to the molecular weight variation of monomer building blocks, the IEC of different copolymers changed even at the same degree of disulfonation. We used calculated a weight based IEC ( $\text{IEC}_w$ ) from the copolymer structure, which were typically 5-10 % higher than the experimental value measured from nonaqueous potentiometric titration<sup>19,20</sup>. The typical range of  $\text{IEC}_w$  studied was 1.12 to 1.87 meq/g. All  $\text{IEC}_w$  are reported on the basis of the dry polymer. Copolymer density was measured from a known membrane dimension and weight after drying at 75 °C for 2 h. A volume based IEC ( $\text{IEC}_v$ ) was then obtained by multiplying the membrane density to  $\text{IEC}_w$ . This calculation resulted in  $\text{IEC}_v$  (dry) based on the dry membrane density. An  $\text{IEC}_v$  (wet) was then also calculated based on water uptake measurements using the following equation:

$$IEC_V(wet) = IEC_V(dry)/(1 + 0.01 \times WU) \quad \text{Equation 6.3}$$

The data are presented in terms of each IEC, and the importance of each is discussed in detail later. All membranes, cast from dimethylacetamide solution (10 % w/v), were transparent and had favorable tough/ductile characteristics, durable over several thousand hours under fuel cell conditions<sup>24</sup>.

Proton conductivity was measured using a Solatron 1260 impedance analyzer over the frequency range of 10 Hz - 1 MHz, using a reported procedure<sup>19</sup>.

Membrane electrode assemblies (MEAs) were prepared for fuel cell testing from cast membranes. MEAs were prepared from standard catalyst inks using unsupported Pt-Ru catalyst for anode and Pt catalyst for cathode following protocols from our laboratory<sup>25</sup>. The geometric active cell area was 5 cm<sup>2</sup>. The anode and cathode catalyst loading was approximately 10 and 6 mg/cm<sup>2</sup>, respectively.

Limiting methanol crossover currents through the membrane in a cell were measured to estimate the methanol permeability of PEMs. For the data reported here, 0.5 M methanol solution was fed to one side of the 5 cm<sup>2</sup> cell, while humidified nitrogen at 500 sccm and ambient pressure was supplied to the other side. The methanol permeation flux was determined from the limiting current density resulting from

---

<sup>24</sup> Y. S. Kim, B. S. Pivovar, *Advances in Materials for Proton Exchange Membrane Fuel Cell Systems*, Abs. No 35, Pacific Grove, CA, Feb. 20-23, 2005

<sup>25</sup> S.C. Thomas, X. M. Ren, S. Gottesfeld, P. Zelenay, *Electrochimica Acta*. 2002, 47, 22, 3741

transport-controlled methanol electro-oxidation at the other side of the cell using a potential step experiment<sup>26</sup>. Methanol permeability was calculated from following equation;

$$\text{Methanol permeability (cm}^2\text{/s)} = (\xi \times t) / (6F \times c) \quad \text{Equation 6.4}$$

where,  $\xi$  is the methanol crossover limiting current (A/cm<sup>2</sup>);  $t$  is the wet membrane thickness (cm);  $F$  is the Faraday constant (s·A·mol);  $c$  is the methanol feed concentration (mol/cm<sup>3</sup>)

---

<sup>26</sup> X. Ren, T. E. Springer, and S. Gottesfeld, *J. Electrochem. Soc.*, 2000, 147, 92

## 6.4 Results and Discussion

### 6.4.1 Effect of Disulfonation Level

The most common chemical variation of polymer electrolytes has been that of varying acid group content (IEC, equivalent weight or degree of (di)sulfonation). In this study, we first report fuel cell relevant properties of three classes of polymers (BP, 6F and 6FCN) as a function of disulfonation level, see Table 6.1. The data in Table 6.1 are consistent with those reported in other studies of sulfonation level within a family of copolymers<sup>19,20,21</sup>. For example, the water uptake, the number of waters per sulfonic acid site ( $\lambda$ ), and proton conductivity all increase within a copolymer family as a function of disulfonation level (or IEC). While this data is useful for those interested in the application of specific membranes for improved fuel cell performance, these trends are very predictable and serve little interest in the investigation of chemical and structural effects. However, they do serve as an appropriate baseline for investigating the impact of fluorine and polar group incorporation discussed in the following sections.

### 6.4.2 Effect of Fluorine Moiety

In order to investigate the effect of fluorine moiety in sulfonated copolymers, the properties of hexafluoro bisphenol A based poly(arylene ether sulfone) (6F-*x*) and copolymers of biphenol and hexafluoro bisphenol A (6FyBP-35) were compared with those of biphenol based poly(arylene ether sulfone) (BP-*x*). Structural differences between these copolymers were shown in Figure 6.1, and are as follows: 6F replaced the biphenol link of BP with 6F bisphenol A; 6FyBP-35 changed the mole ratio of 6F

bisphenol A to biphenol where degree of disulfonation was fixed at 35% (for example, 6F10BP-35 is a random copolymer containing 90% of the biphenol monomer and 10% of the 6F bisphenol A). Further complicating matters in the naming scheme used, copolymers that contain 100% of a specific monomer can be related to their partially substituted analogues (for example, BP-35 and 6F-35 are equivalent to 6F0BP-35 and 6F100BP-35, respectively). In order to simplify interpretation of the data, alternative (equivalent) names for polymers are often given within tables.

Table 6.2 shows the density, IEC, water uptake and proton conductivity of the copolymers tested as a function of fluorination level. The only chemical differences within these copolymer families are the relative ratio of the 6F bisphenol A group to the biphenol group. While the changes observed in properties can not wholly be attributed to fluorination, due to structural differences between bisphenol A and biphenol; the system presented here was chosen because of significantly more experience with the homopolymers of BP and 6F. Additionally, we believe that the factors dominating performance reported here have more to do with fluorination than structural differences, because an earlier study of biphenol, bisphenol A and 6F bisphenol A based polymers showed modest property changes for the hydrocarbon based membranes (biphenol versus bisphenol A), but significant property changes for the partially fluorinated system (6F bisphenol A)<sup>27</sup>. Therefore, we feel justified presenting the observed property differences in terms of fluorine content, and believe that differences due to chemical structure are secondary in this specific comparison.

---

<sup>27</sup> W. L. Harrison, F. Wang, M. A. Hickner, Y. S. Kim, M. Hill, T. A. Zawodzinski, J. E. McGrath, *Polymer* submitted

The data in Table 6.2 show that water uptake,  $\lambda$  and proton conductivity decrease in a systematic way with increasing fluorine content for both the 6F and 6FCN family of copolymers at similar disulfonation levels. However when water uptake of these copolymers (BP-*x* and 6F-*x*, and partially substituted 6F<sub>y</sub>BP-35 copolymers) are plotted as a function of IEC<sub>w</sub> (Figure 6.2a), the data show almost no dependence on polymer chemistry, exhibit a clear trend of increasing water uptake with IEC<sub>w</sub>, and are consistent with other directly copolymerized polysulfones having bisphenol A or hydroquinone units in the backbone<sup>20</sup>. These data exhibit a deflection point at 1.55 meq/g where water uptake increases substantially faster with IEC<sub>w</sub>, similar to that reported for other systems in the literature and related to a percolation threshold.<sup>19,20,28</sup>

Based on the data presented in Figure 6.2a, one might argue chemistry plays little role in water uptake. However, using IEC<sub>w</sub> for screening polymer properties, although common, is problematic. Choosing any weight normalized quantity (IEC<sub>w</sub> or water uptake (wt%)) as a basis for comparison adds importance to the density of the polymer and creates differences between hydrocarbon (lower density) and fluorinated (higher density) polymers based on mass that are not expected to affect fuel cell relevant properties. While polymer density does affect water uptake (wt%); in general, choosing quantities that are weighted by volume rather than mass serve a more reasonable comparison basis. This stems from the fact that changes in length scale (reflected in volume measurements) are expected to directly impact observed properties (i.e. conductivity and permeability) and changes in mass of the polymer are not.

---

<sup>28</sup> B. R. Einsla, Y. S. Kim, M. A. Hickner, Y. T. Hong, M. L. Hill, B. S. Pivovar, J. E. McGrath, *J. Memb. Sci.* 2005, 255, 141

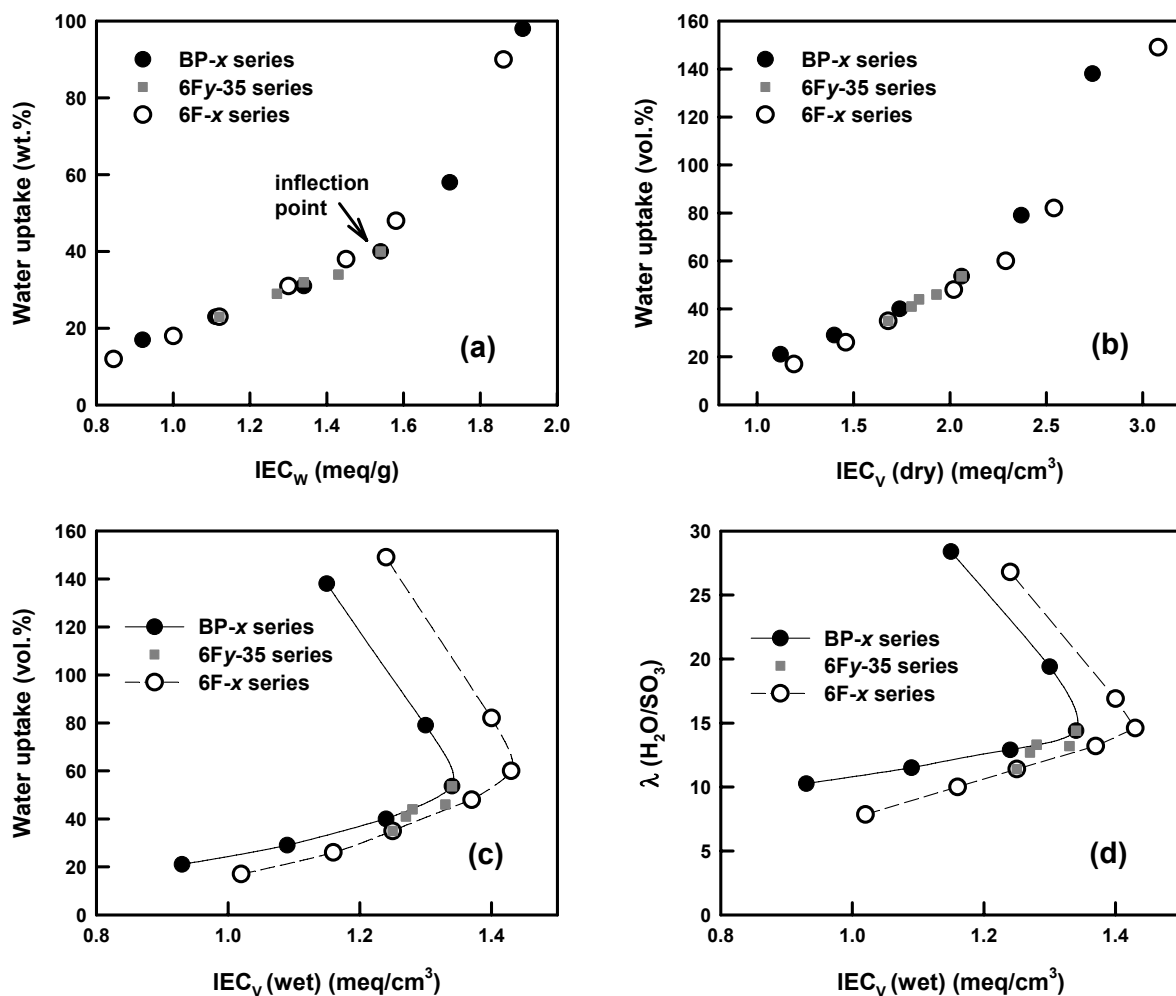


**Figure 6.2** Effect of fluorine incorporation on membrane water uptake as a function of (a)  $IEC_w$ , (b)  $IEC_v$  (dry), (c)  $IEC_v$  (wet), and (d) number of water molecules associated with sulfonic acid group ( $\lambda$ ) as a function of  $IEC_v$  (wet)

When  $IEC_w$  is changed to  $IEC_v$  (still on a dry polymer basis –  $IEC_v$  (dry)) and water uptake (wt%) is changed to water uptake (vol%), modest changes result as shown

in Figure 6.2b. The volume normalized data in Figure 6.2b follow the same trends as the weight normalized data in Figure 6.2a, except a clear trend to slightly decreased water uptake based on fluorination is discernable between the BP and 6F polymers. Incidentally, if a weight based water uptake were used in Figure 6.2b, although still small, a larger gap between the fluorinated and non-fluorinated polymers is evident due to the lower density of the hydrocarbon membrane.

While the changes in water uptake shown in Figure 6.2b are small, much more significant differences due to fluorination are apparent when considering  $IEC_V$  on a wet basis, see Figure 6.2c. In this case the fluorinated copolymer (6F) shows much lower water uptake at a given  $IEC_V$  (wet). Both the fluorinated and non-fluorinated copolymers exhibit an inflection point at high  $IEC_V$  (wet) where a percolation threshold is reached and substantially increased water uptake results in lowering of  $IEC_V$  (wet). Although, this inflection point happens at a much higher  $IEC_V$  (wet) for the fluorinated polymer. The controlled fluorine content 6FyBP-35 system shows the expected trend of tending from the non-fluorinated (BP- $x$ ) to fluorinated (6F- $x$ ) system as a function of fluorine substitution. The trends in water uptake shown in Figure 6.2c are even larger for  $\lambda$  as a function of  $IEC_V$  (wet), Figure 6.2d. This is because at the same water uptake,  $IEC_V$  (wet) is much larger for the fluorinated copolymer than non-fluorinated copolymer. Figures 6.2c and 6.2d show the clear importance of fluorine moieties on water uptake.

We have used  $IEC_V$  (wet) as a basis for comparison because it reflects the concentration of ions within the polymer matrix under hydrated (operationally relevant)

conditions. While other aspects such as morphology and specific chemical interactions are important and will be discussed later, when considering IEC, Figure 6.2 shows the clear risks of using mass normalized or dry polymer IECs as a basis for comparison. For this reason we will use  $IEC_V$  (wet) and water uptake (vol%) within the rest of this paper. Even though,  $IEC_W$  is the most easily obtained and most often reported IEC.

While water uptake has a strong influence on fuel cell related properties, it is proton conductivity that is the property of primary importance for fuel cell applications. The effects of incorporation of fluorine moiety are also very apparent when considering proton conductivity. Figure 6.3 shows the proton conductivity of the selected copolymers as a function of  $IEC_V$ . Again, significant differences result in comparing fluorinated and non-fluorinated polymers. At a given  $IEC_V$  the fluorinated system (6F) exhibited significantly higher conductivity except for disulfonation levels above the inflection point. These copolymers are of relatively little use in fuel cells as they swell significantly and have poor mechanical properties. For polymers with reasonable mechanical properties, fluorinated polymers exhibit significant advantages. The proton conductivities of the controlled fluorine content 6FyBP-35 series, like the water uptakes shown in Figure 6.2, changed in a predictable, systematic fashion as the level of fluorine moiety increased.

In order to isolate the effects of fluorine moiety, data in Tables 6.1 & 6.2 was interpolated to give conductivity, water uptake and  $\lambda$  at a fixed  $IEC_V$  (1.28 meq/cm<sup>3</sup>). The proton conductivity, water uptake and  $\lambda$  are reported as a function of atomic fluorine

composition for different copolymers in Figure 6.4. The data in Figure 6.4 clearly show that conductivity increases with fluorine composition at this fixed IEC<sub>v</sub>. Interestingly, although proton conductivity was shown to increase significantly with water uptake and  $\lambda$  within a family of copolymers (Table 6.1), the conductivity of copolymers at fixed IEC<sub>v</sub> increased with decreasing  $\lambda$  and water uptake, in part due to the increasing level of disulfonation at fixed IEC<sub>v</sub>.

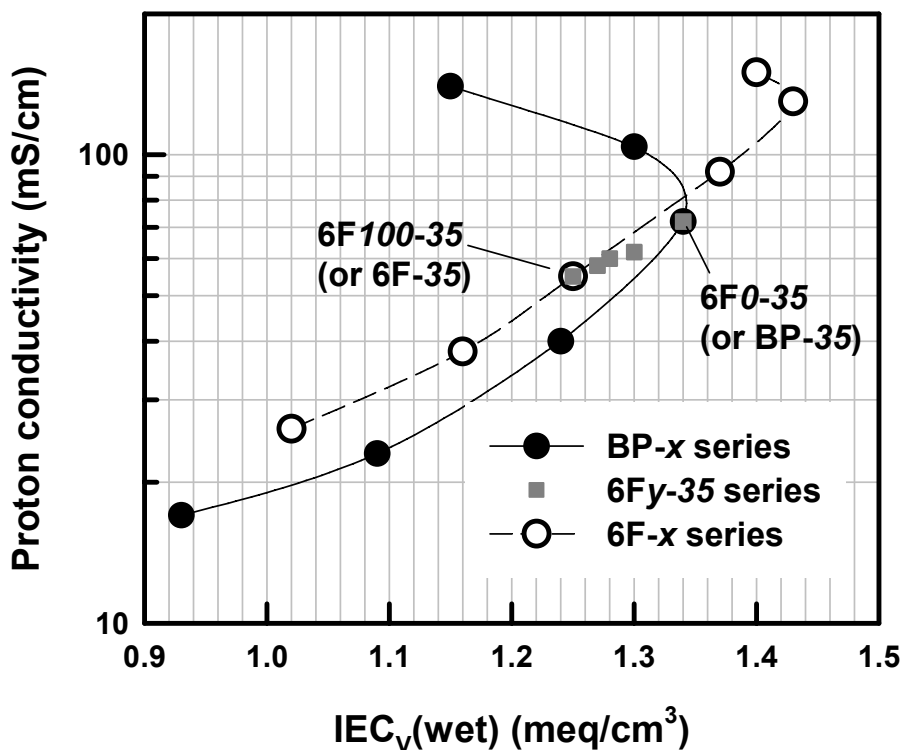


**Figure 6.3** Effect of fluorine incorporation on proton conductivity as a function of IEC<sub>v</sub> (wet)

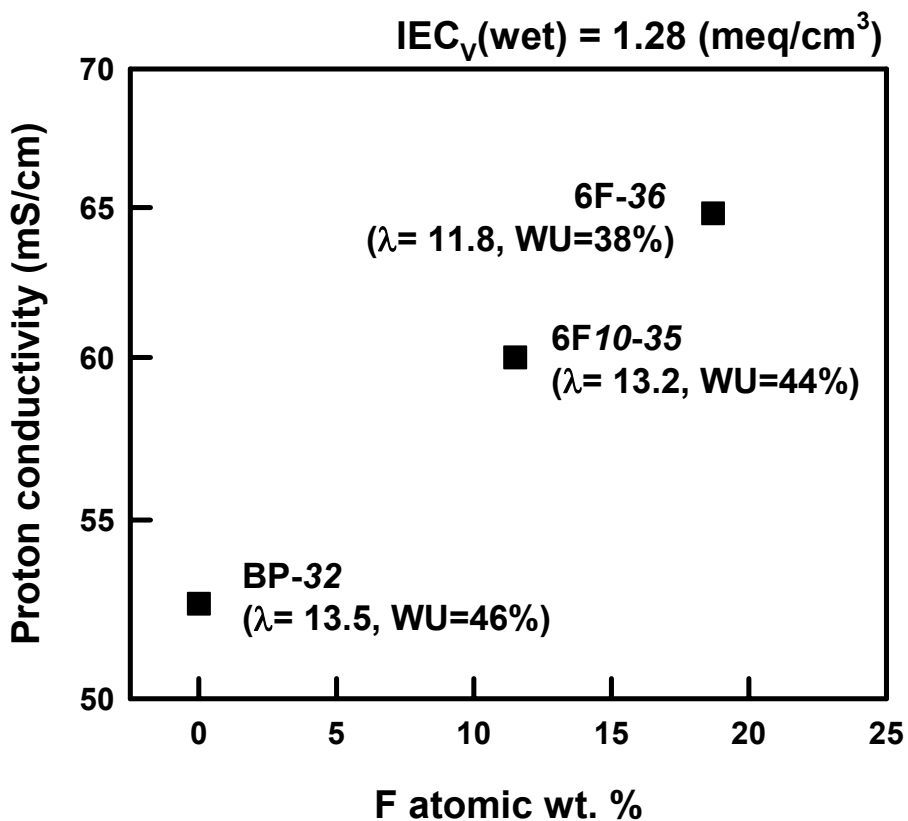


**Figure 6.4** Effect of fluorine incorporation on conductivity at a fixed  $IEC_V(\text{wet})$

Based on the data presented in Figures 6.3 and 6.4, phase separation or morphological differences between the selected copolymers appears to be driven by fluorine incorporation. Sulfonated copolymers have hydrophilic (sulfonated) and hydrophobic (aromatic, non-sulfonated and/or fluorinated) segments, which are prone to phase separate. When hydrophobic fluorine moiety is incorporated into the copolymer backbone, it can increase the hydrophobicity of those backbone segments and induce a greater degree of phase separation leading to more distinct and more strongly

hydrophilic/hydrophobic phases. Increased phase separation likely leads to changes in tortuosity and the state of water within these polymers, a topic reported previously in the literature for these materials<sup>12,13,29</sup>. These literature references also support increased phase separation with increasing fluorine content by increased free-water measurements made by differential scanning calorimetry and <sup>1</sup>H pulse nuclear magnetic resonance. Shorter conduction pathways and increased free water content due to increased phase separation are likely the driving forces behind the increased conductivity with increasing fluorine content shown in Figure 6.4.

### 6.4.3 Effect of Polar Functional Group

The effect of incorporation of two different polar groups in either the BP or 6F series: 1) benzonitrile (CN) and 2) phenyl phosphine oxide (PPO) group were explored. For benzonitrile group incorporation, the diphenylsulfone unit was completely replaced with benzonitrile in the 6F series (versus 6FCN) or BP-35 (versus BPCN-35). For the PPO series diphenylsulfone was partially replaced with benzonitrile for BP-35 or BP-40 (versus BPPPOy-35 or 40). Both benzonitrile and PPO groups are known to be strongly polar and have strong interactions with other polar groups (i.e. hydrogen bonding)<sup>30,31,32,33,34</sup>. The benzonitrile group has a large dipole moment (ca. 4.18D) and a large polarizability, which is capable of forming a stable complex with water molecules.

---

<sup>29</sup> Y. S. Kim, L. Dong, M. Hickner, T. E. Glass, J. E. McGrath, *Macromolecules* 2003, 36, 17, 6281

<sup>30</sup> B. Brutschy, *Chem. Rev.* 2000, 100, 3891

<sup>31</sup> E. S. Kryachko, M. T. Nguyen, *J. Chem. Phys.* 2001, 115, 833

<sup>32</sup> S. Wang, H. Zhuang, H. K. Shobha, T. E. Glass, M. Sankarapandian, Q. Ji, A. R. Shultz, J. E. McGrath, *Macromolecules* 2001, 34, 8051

<sup>33</sup> M. C. Etter, S. M. Reutzel, *J. Am. Chem. Soc.* 1991, 113, 2586

<sup>34</sup> R. Langner, G. Zundel, *J. Phys. Chem.* 1995, 99, 12214

Hydrogen bonding with benzonitrile and its strength in the presence of water molecules has been detected and measured by various analytical tools such as microwave, high resolution UV and infrared spectroscopy<sup>30,31</sup>. These studies indicate that water molecules bind to benzonitrile from the side, in-plane to the aromatic ring via two hydrogen bonds. The PPO group, on the other hand, is known to exhibit strong hydrogen bonding with other functional groups including hydroxyl,<sup>32</sup> imide,<sup>33</sup> and sulfonic and phosphoric acid<sup>34</sup>.

The density, IEC, water uptake,  $\lambda$ , and proton conductivity for selected copolymers as a function of polar group incorporation are summarized in Table 6.3. The data for water uptake are shown in Figure 6.5a and 6.5b as a function of IEC<sub>V</sub> for benzonitrile and PPO containing copolymers, respectively. In comparing benzonitrile containing polymers (6FCN) to analogous polymers without benzonitrile (6F), water uptake was found to decrease in a significant manner (~25%) at any given IEC<sub>V</sub> for the benzonitrile containing polymers. BPPPO<sub>y</sub> also showed lower water uptake than the non-functionalized system (i.e. BP) and the degree of decreasing water uptake was more significant with higher PPO composition. These results indicate that polar groups such as benzonitrile and PPO play a significant role in reducing water uptake. This observation is consistent with other copolymers having specific interactions that suppress membrane swelling under hydrating conditions.

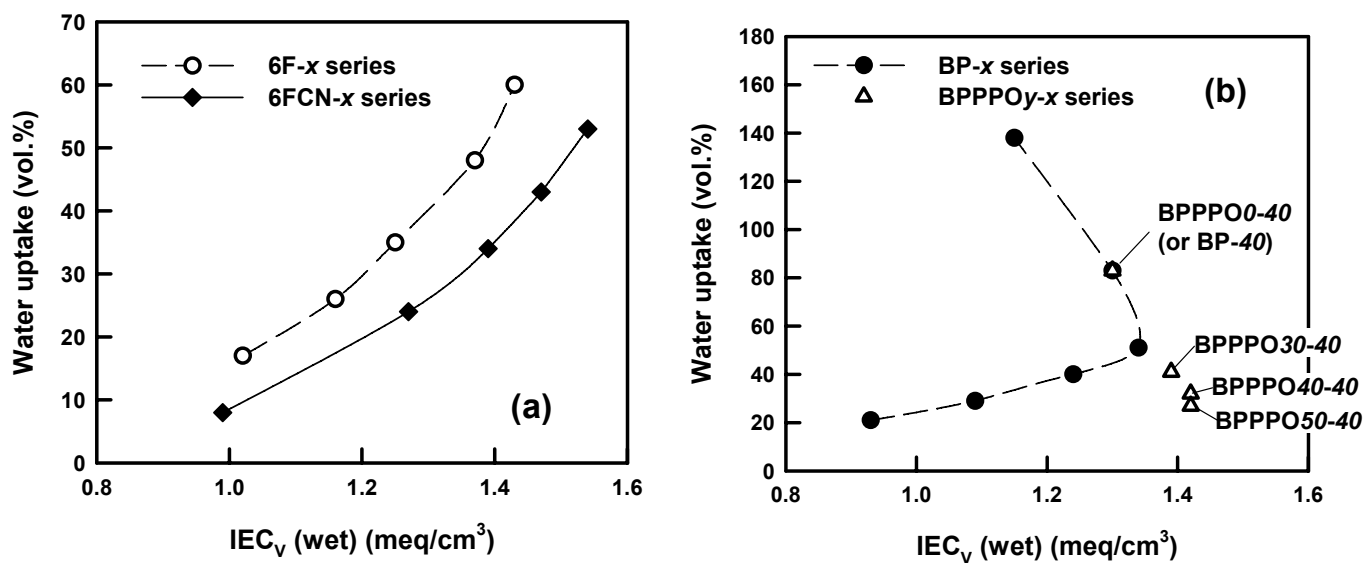


**Figure 6.5** Effect of (a) benzonitrile and (b) PPO polar group incorporation on membrane water uptake

The proton conductivity of these copolymers as a function of IEC<sub>V</sub> is shown in Figure 6.6. Almost immediately apparent is the similarity between Figures 6.5 and 6.6. The qualitative similarity between Figures 6.5 and 6.6 is a reflection of the role of water on proton conduction in these copolymers. Proton transport in polymer electrolytes relies on water to ionize acid sites and provide mobility (conductivity) for the proton. For the two polar groups investigated here, it appears that their primary impact is in preventing water uptake.

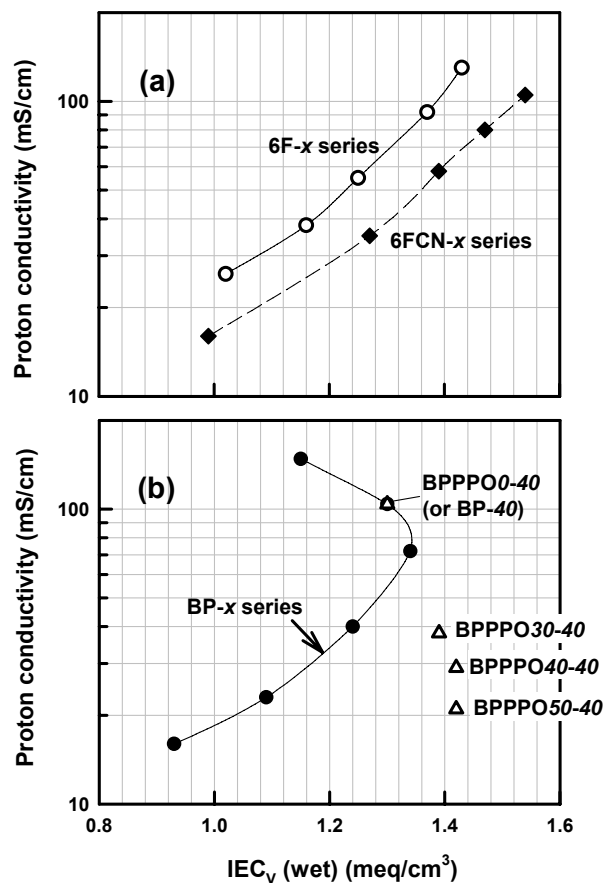


**Figure 6.6** Effect of (a) benzonitrile and (b) PPO polar group incorporation on membrane proton conductivity

These effects are isolated in Figure 6.7 where the effects of PPO group incorporation at roughly the same IEC<sub>v</sub> (~1.4 meq/cm<sup>3</sup>) are plotted as a function of proton conductivity. Values of water uptake (WU) and  $\lambda$  have been added to Figure 6.7 in order to discuss trends. There is a clear trend in this data toward decreasing conductivity with increasing PPO group incorporation. The water uptake and  $\lambda$  of these polymers also decrease with increasing PPO content. While these trends are unsurprising as they have been shown for many polymer electrolytes as a function of sulfonation level (such as those shown in Table 6.1); they run counter to those reported in Figure 6.4 for

the effects of fluorine incorporation. Whereas fluorine incorporation exhibited trends suggesting increased phase separation, the data for PPO group incorporation suggest its primary role is that of water exclusion, although specific interactions with other polymeric moieties like sulfonic acid cannot be ruled out based on this data. Interestingly, Roy et al. demonstrated that PPO containing polysulfones had higher free water fraction compared to BP control using pressurized DSC and pulse field gradient NMR experiments<sup>35</sup>. This result is surprising due to the lower water uptake of the PPO containing polysulfones and suggests that the role of PPO within the polymer framework is more complicated than simple water exclusion and its specific interactions are also important.

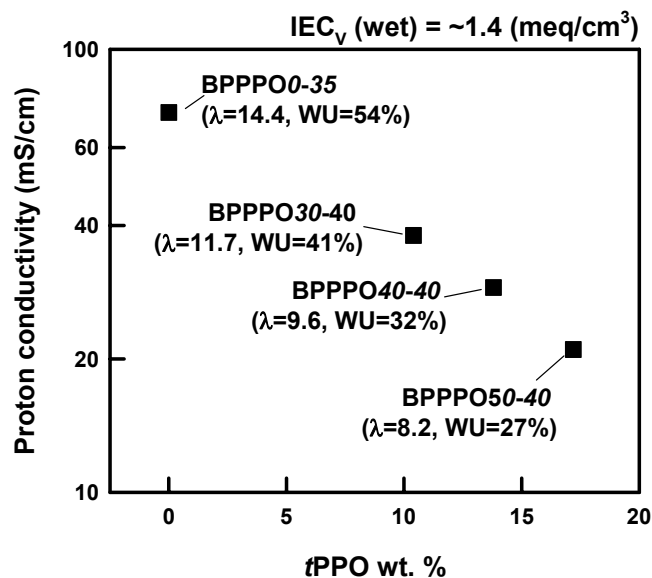


**Figure 6.7** Effect of PPO incorporation on proton conductivity at a fixed  $IEC_v(\text{wet})$

<sup>35</sup> A. Roy, M. Hickner, T. Glass, J. E. McGrath, Advances in Materials for Proton Exchange Membrane Fuel Cell Systems, Abs. No 55-II, Pacific Grove, CA, Feb. 20-23, 2005.

While decreasing conductivity is a shortcoming of polar group incorporation, polar group incorporation may lead to advantages in mechanical properties, decreased membrane-electrode interfacial resistance or in direct methanol fuel cells (DMFCs) due to decreased methanol crossover. Methanol permeability is directly related to methanol crossover, and selectivity (the ratio of proton conductivity to methanol permeability) has been put forward as a qualitative basis for evaluating the potential of a polymer as an electrolyte in DMFCs<sup>36</sup>. Table 6.4 contains data for the proton conductivity, methanol permeability and selectivity of selected copolymers at different degrees of polar group incorporation. Nafion™ has been added to Table 6.4 for comparison purposes because it is the standard membrane used in DMFCs, in spite of its poor selectivity. For the polymers listed in Table 6.4, all have lower conductivity than Nafion™. However, methanol permeability of these other copolymers is also significantly decreased, resulting in better selectivity for each of the alternative polymers presented. In comparing the effects of polar group incorporation, it is apparent that PPO incorporation although significantly lowering methanol permeability offers no improvement in selectivity compared to the base BP copolymers. The incorporation of benzonitrile, on the other hand, leads to the most selective copolymer (BPCN-35) presented in Table 6.4. Both the fluorinated (BP) and non-fluorinated polymers (6F) show increases in selectivity with benzonitrile incorporation. The addition of PPO or benzonitrile in these systems of polymers has significantly different effects and shows the importance of not only polar character, but the nature of interactions with specific polar groups.

---

<sup>36</sup> B. S. Pivovar, Y. Wang, E. L. Cussler, *J. Memb. Sci.* 1999, 154, 155

It is worth noting that the incorporation of fluorine moiety into the copolymer backbone, although found to be advantageous for proton conduction, results in lower selectivity as shown in Table 6.4. This result is in agreement with increased phase separation proposed during our discussion of the effect of fluorine incorporation.

#### **6.4.4 Impact on Fuel Cell Performance**

The final step required in drawing a link between structure, property and performance within these copolymers is to evaluate fuel cell performance. It is straightforward that higher membrane conductivity reduces the ohmic resistance of fuel cells and thus improves performance. Figure 6.8 compares the H<sub>2</sub>/air fuel performance of structure-modified membranes at similar IEC<sub>v</sub> and membrane thickness. The fuel cell was operated under same operating conditions (i.e. cell temperature, catalyst loading, reactant stoichiometry, back pressure, etc).

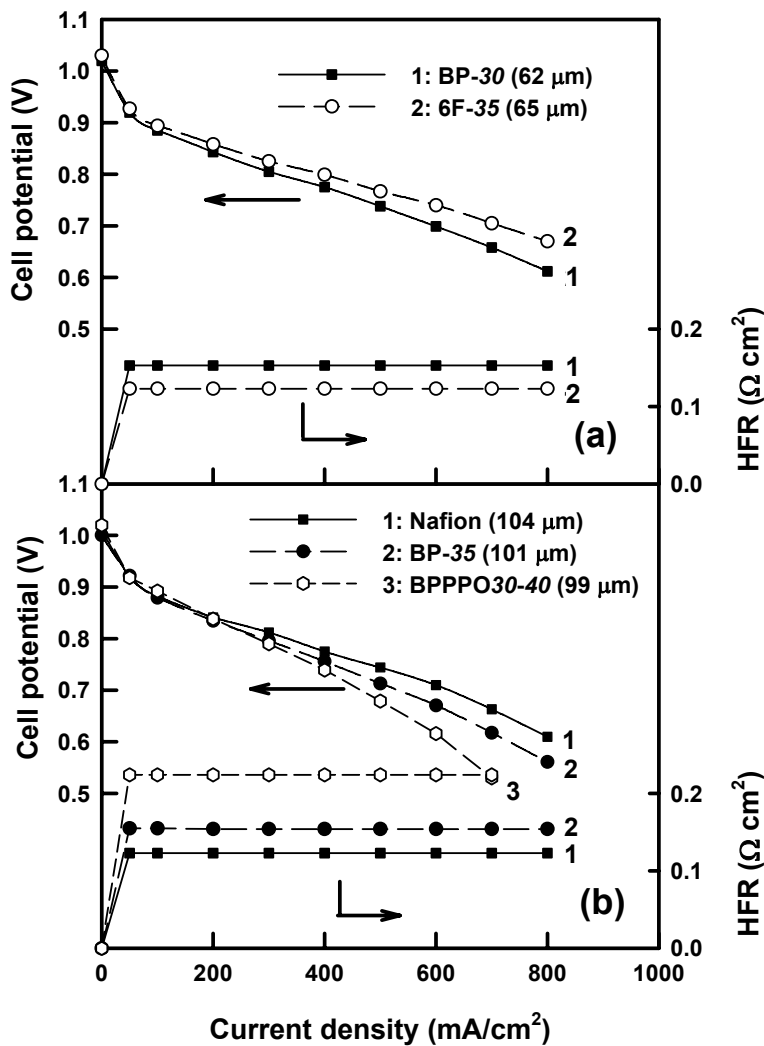


**Figure 6.8** Effect of (a) fluorine and (b) PPO incorporation on H<sub>2</sub>/air fuel cell performance at 80°C; IEC<sub>v</sub> (wet) values of membranes for (a) and (b) were fixed at 1.25 and 1.35 meq/cm<sup>3</sup>, respectively

Figure 6.8a showed that 6F copolymer exhibited superior performance due to decreased ohmic losses reflect in its lower high frequency resistance (HFR) compared to

the BP control. The HFR for BP was  $15.3 \text{ m}\Omega\cdot\text{cm}^2$  which was approximately 25 % higher than that of 6F counterpart ( $12.3 \text{ m}\Omega\cdot\text{cm}^2$ ). This HFR difference qualitatively agreed well with the free-standing membrane conductivity reported in Table 6.1. Figure 6.8b compares a PPO containing membrane with a BP control and Nafion™. The BPPPO membrane had a higher HFR and thus poorer performance than BP control. For hydrogen fuel cells, one could conclude that fluorine incorporation give advantageous effect while PPO group incorporation adversely impacted on fuel cell performance due to changes in proton conductivity.

Thus far, we have focused only on conductivity and not on aspects of mechanical robustness or membrane-electrode interfacial compatibility. While membrane conductivity (or lower cell resistance) increases with IEC, increasing IEC is usually accompanied by greater membrane water uptake. Higher water uptake results in poorer mechanical properties and potential electrode compatibility issues. Previous research indicated that increased water uptake of membrane resulted in increased membrane-electrode interfacial delamination and significant performance degradation<sup>37,38</sup>. In these regards, we could expect advantages from both fluorine and polar group incorporation.

Additionally, the copolymers presented demonstrate improved selectivity compared to Nafion™ and would be expected to be better electrolytes in DMFCs. This is particularly true at high methanol feed concentrations (> 2M) where the effects of methanol crossover are amplified. Figure 6.9 demonstrates DMFC performance of BPPPO30-40, BP-35 and Nafion™.

---

<sup>37</sup> Y. S. Kim, B. S. Pivovar, Abstract 1073, The Electrochemical Society Meeting Abstracts, Orlando, FL, Oct. 12-16, 2003, manuscript submitted in *J. Electrochem. Soc.*

<sup>38</sup> Y. S. Kim, M. J. Sumner, W.L. Harrison, J. Riffle, J. E. McGrath, B. S. Pivovar, Abstract 1012, The Electrochemical Society Meeting Abstracts, Orlando, FL, Oct. 12-16, 2003, manuscript submitted in *J. Electrochem. Soc.*

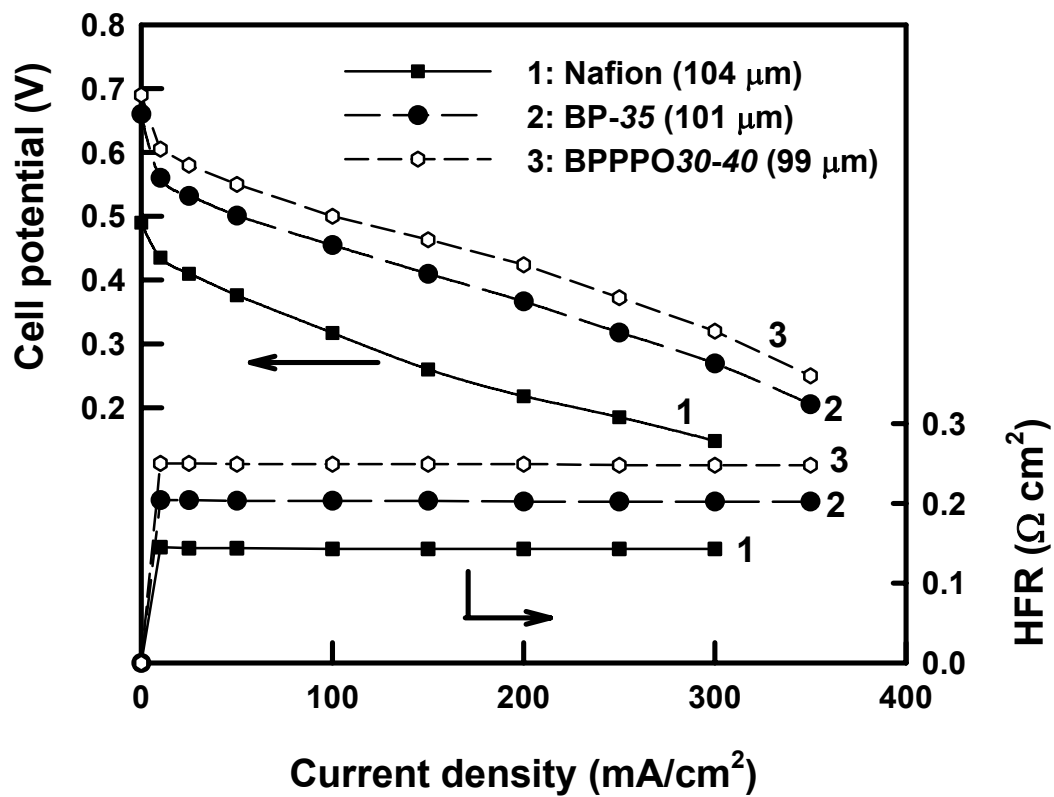


**Figure 6.9** Effect of PPO incorporations on high methanol concentration feed (5 M)

DMFC performance at 80°C; IEC<sub>v</sub> (wet) value of membranes was fixed at 1.35 meq/cm<sup>3</sup>

Nafion™ at a 5 M methanol feed concentration. Although the cell resistance of BPPPO30-40 was much greater than BP-35 and Nafion™, the fuel cell performance of BPPPO30-40 was superior. This result reflects the fact that copolymers having polar group incorporation can significantly suppress methanol transport, of particular use in high methanol feed concentration DMFCs. Further efforts in tailoring sulfonated polysulfone properties using fluorine and polar group moieties are being pursued<sup>39</sup>.

---

<sup>39</sup> Y. S. Kim, M. J. Sumner, W. L. Harrison, J. S. Riffle, J. E. McGrath, B. S. Pivovar, *J. Electrochem. Soc.* 2004, 151, A2150

Table 6.1 Effect of degree of sulfonation on density, IEC, water uptake and proton conductivity

Copolymer	Density (g/cm <sup>3</sup> )	IEC <sub>w</sub> (meq/g)	IEC <sub>v</sub> (dry) (meq/cm <sup>3</sup> )	IEC <sub>v</sub> (wet) (meq/cm <sup>3</sup> )	Water uptake (wt%)	Water uptake (vol%)	$\lambda$ (H <sub>2</sub> O/SO <sub>3</sub> )	Proton conductivity (mS/cm)
BP-20	1.22	0.92	1.12	0.93	17	21	10.2	16
BP-25	1.26	1.11	1.40	1.09	23	29	11.5	23
BP-30	1.30	1.34	1.74	1.24	31	40	12.9	40
BP-35	1.34	1.54	2.06	1.34	40	54	14.4	72
BP-40	1.38	1.72	2.37	1.30	60	83	19.4	104
BP-45	1.41	1.92	2.74	1.15	98	138	28.4	140
6F-25	1.42	0.85	1.19	1.02	12	17	7.8	26
6F-30	1.46	1.00	1.46	1.16	18	26	10.0	38
6F-35	1.50	1.12	1.68	1.25	23	35	11.4	55
6F-40	1.54	1.30	2.02	1.37	31	48	13.2	92
6F-45	1.58	1.45	2.29	1.43	38	60	14.6	130
6FCN-20	1.30	0.82	1.07	0.99	6	8	4.1	16
6FCN-30	1.36	1.16	1.58	1.27	18	24	8.6	35
6FCN-35	1.40	1.33	1.86	1.39	24	34	10.0	58
6FCN-40	1.44	1.46	2.10	1.47	30	43	11.4	80
6FCN-45	1.46	1.61	2.35	1.54	36	53	12.4	105

Table 6.2 Effect of fluorine moiety on density, IEC, water uptake and proton conductivity

Copolymer	Density (g/cm <sup>3</sup> )	IEC <sub>w</sub> (meq/g)	IEC <sub>v</sub> (dry) (meq/cm <sup>3</sup> )	IEC <sub>v</sub> (wet) (meq/cm <sup>3</sup> )	Water uptake (wt%)	Water uptake (vol%)	λ (H <sub>2</sub> O/SO <sub>3</sub> )	Proton conductivity (mS/cm)
6F0-35 (BP-35)	1.34	1.54	2.06	1.34	40	54	14.4	72
6F10-35	1.34	1.43	1.93	1.30	36	48	14.0	62
6F30-35	1.37	1.34	1.84	1.28	32	44	13.3	60
6F50-35	1.42	1.27	1.80	1.27	29	41	12.7	58
6F100-35 (6F-35)	1.50	1.12	1.68	1.25	23	35	11.4	55
6F0CN-35 (BPCN-35)	1.33	1.87	2.49	1.50	40	67	11.9	78
6F25CN-35	1.34	1.70	2.29	1.43	35	60	11.4	70
6F50CN-35	1.36	1.56	2.12	1.40	31	52	11.0	65
6F75CN-35	1.40	1.44	1.98	1.41	27	40	10.4	62
6F100CN-35 (6FCN-35)	1.40	1.33	1.86	1.39	24	34	10.0	58

Table 6.3 Effect of polar group on density, IEC<sub>w</sub>, water uptake and proton conductivity

Copolymer	Density (g/cm <sup>3</sup> )	IEC <sub>w</sub> (meq/g)	IEC <sub>v</sub> (dry) (meq/cm <sup>3</sup> )	IEC <sub>v</sub> (wet) (meq/cm <sup>3</sup> )	Water uptake (wt%)	Water uptake (vol%)	λ (H <sub>2</sub> O/SO <sub>3</sub> )	Proton conductivity (mS/cm)
BP-35	1.34	1.54	2.06	1.34	40	54	14.4	72
BPCN-35 (6F0CN-35)	1.33	1.87	2.49	1.63	40	53	11.9	78
6F-30	1.46	1.00	1.46	1.16	18	26	10.0	38
6FCN-30	1.36	1.16	1.58	1.27	18	24	8.6	35
6F-35	1.50	1.12	1.68	1.25	23	35	11.4	55
6FCN-35	1.40	1.33	1.82	1.39	24	34	10.0	58
6F-40	1.54	1.30	2.02	1.37	31	48	13.2	92
6FCN-40	1.44	1.46	2.10	1.47	30	43	11.4	80
6F-45	1.58	1.45	2.29	1.43	38	60	14.6	130
6FCN-45	1.46	1.61	2.35	1.54	36	53	12.4	105
BPPPO0-35 (BP-35)	1.34	1.54	2.06	1.34	40	54	14.4	72
BPPPO30-35	1.35	1.40	1.89	1.40	26	35	10.3	35
BPPPO0-40 (BP-40)	1.38	1.72	2.37	1.30	60	83	19.4	104
BPPPO30-40	1.25	1.57	1.97	1.39	33	41	11.7	38
BPPPO40-40	1.19	1.56	1.87	1.42	27	32	9.6	29
BPPPO50-40	1.16	1.55	1.80	1.42	23	27	8.2	21

Table 6.4 Methanol permeability and selectivity of selected copolymers

copolymer	<i>t</i> PPO (or benzonitrile) content (wt.%)	Proton conductivity (mS/cm)	Methanol permeability $\times 10^6$ (cm <sup>2</sup> /s)	Selectivity $\times 10^{-2}$ (S m/s)
BPPPO50-40	17.2	21	0.55	3.8
BPPPO40-40	13.8	29	0.67	4.3
BPPPO30-35	12.4	35	0.82	4.3
BPPPO30-40	10.5	38	1.02	3.7
BPCN-35	(17.2)	78	1.44	5.4
6FCN-35	(14.1)	58	1.32	3.6
6F-35	0	55	1.66	3.3
BP-35	0	72	1.55	4.7
BP-40	0	104	2.20	4.7
Nafion™	0	111	4.20	2.6

## **6.5 Conclusions**

Structure-property-performance relationships of directly copolymerized disulfonated poly(arylene ether sulfone) random copolymers were investigated. The polysulfone membrane incorporated with hexafluoro bisphenol A (6F) showed decreased water uptake compared to non-fluorinated polysulfones (BP) while conductivity increased at a similar IEC, attributed to a greater degree of phase separation. The polysulfone membranes incorporated with polar groups such as benzonitrile and PPO, on the other hand, showed decreased water uptake, conductivity and methanol permeability. Increased conductivity of the fluorine incorporated system improved fuel cell performance by reducing cell resistance, while polar group incorporation adversely impacted the fuel cell performance by lowering conductivity. Improvements in selectivity and DMFC performance, at high methanol feed concentration, were shown for all alternative copolymers tested.

## **6.6 Acknowledgments**

Expressed appreciation to the U.S. Department of Energy and the Defense Advanced Research Project Agency (DARPA) for support. Research group of Drs. James E. McGrath and Judy Riffle (Virginia Polytechnic and State University) for supply of polysulfone copolymers.

---

## CHAPTER 7

### Overall Conclusions

---

This dissertation has focused on disulfonated poly(arylene ether sulfone) random copolymer membranes to better understand the structure-property and structure-property-performance relationships.

The synthesis and characterization of the important comonomer (3,3'-disulfonated 4,4'-dichlorodiphenyl sulfone) which provides the proton conductivity when incorporated into the mechanically and thermally stable copolymer backbone was investigated. The one-step process developed could be a very important crucial starting point for commercialization efforts.

The synthesis and structural characterization of nitrile functional disulfonated poly(arylene ether sulfone) was also demonstrated. The copolymers were synthesized at various levels of disulfonation with or without fluorine containing monomers. The membrane characteristics of these copolymers were evaluated to better understand the structure-property relationship of these copolymers. The dynamic modulus of these stiff

chains at various levels of disulfonation was much higher than Nafion™, which is a desired parameter for long term operation, particularly at elevated temperatures

Heteropolyacid nanocomposites based on these copolymers were developed potentially for higher temperature proton exchange membrane fuel cells.

The basic PEM properties such as water uptake, proton conductivity, methanol permeability, etc. were actually shown to allow for tunable properties. Direct methanol fuel cell performances (DMFC) was much better than commercial Nafion™, probably due to less fuel/oxidant permeability. Surface properties of the membranes were also demonstrated as an important parameter in performance tests. The interfacial resistance and water uptake of the membranes could be adjusted by copolymer composition. This allowed improvement in both initial and long term performance tests, by lowering the interfacial resistance and water uptake. Water uptake was an important parameter that influenced the structural durability of membrane electrode assemblies. The delamination due to the large water uptake differences between catalyst layer (electrode) and the membrane in the membrane electrode assembly was proposed.

Finally, structure-property-performance relation of directly copolymerized disulfonated poly(arylene ether sulfone) random copolymers was illustrated. They were demonstrated as strong candidate for proton exchange membrane fuel cells in this dissertation.

---

## CHAPTER 8

### Suggested Future Research

---

The disulfonated polysulfone copolymers always resulted in with lower fuel/oxidant permeability compare to Nafion™. However, the large water dependence of the proton conductivity of copolymers makes these membranes limited at higher temperature applications. Our group and others are blending these copolymers with inorganic proton conductors to produce reasonable proton conductivity at higher temperatures. Additionally, next generation copolymers such as multiblock copolymers and crosslinked systems were being investigated by our group, since the current random copolymers do not produce very well defined ionic clusters. New transport characteristics might improve membrane performance at higher temperatures. Multiblock systems have potential to produce nanophase-separated morphologies. However, the multiblock systems still may have rotational barriers due to their stiff back bone which may prevent the ionic clustering. One suggestion could be to use short side chain branching which is attached to the sulfonic acid. Even in this situation the persistence length would remain similar (might be little shorter) because of the high rotational barrier of the back bone. This discussion is also applicable for the crosslinked systems.

With this perspective, one suggestion is to use multiblock system with shorter length of flexible backbone. This could increase the conformational entropy which may enhance the ionic clustering and reduce the persistence length. The hydrolytic stability would be poor, when siloxanes were utilized. However, this idea is not restricted with siloxanes, other flexible oligomers such as the perfluoroethers might be utilized to overcome stability issues.

## **Vita**

Mehmet SANKIR was born in Ankara, Türkiye. He joined the highest ranking university, Middle East Technical University in Türkiye, and received both M.S. and B.S. in Chemistry. He completed both industrial chemistry and polymer chemistry programs during his B.S. education. He is interested in physical chemistry. He studied electrically conductive polymers in his M.S. In fall of 2001, he enrolled at Virginia Polytechnic Institute and State University to pursue his PhD. He studied polymer science and engineering in the Macromolecular Science and Engineering program at Virginia Tech under the guidance of Prof. J.E. McGrath during his doctoral degree. He studied synthesis and characterizations of proton exchange membrane materials for fuel cells in his PhD. He presented his studies at various national meetings. He will continue his studies at Virginia Tech as a post doctoral research associate.